EISSN: 2687-4482

ABCResearch

Archives of Basic and Clinical Research

Official Journal of the Erzincan Binali Yıldırım University School of Medicine

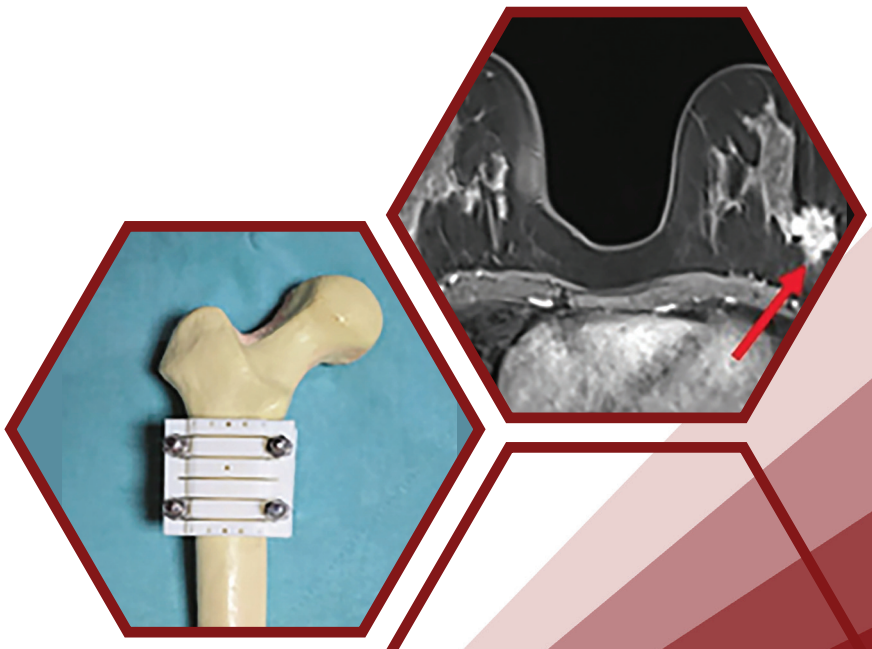

galenos Publishing House

abcresearch.net

Volume 8
Issue 1
January 2026

ABCResearch

Please refer to the journal's webpage (**https://abcresearch.net/**) for "**Journal Policies**" and "**Instructions**".

The editorial and publication process of the Archives of Basic and Clinical Research are shaped in accordance with the guidelines of the **ICMJE, WAME, CSE, COPE, EASE**, and **NISO**. The journal is in conformity with the Principles of Transparency and Best Practice in Scholarly Publishing.

Archives of Basic and Clinical Research is indexed in **CNKI, DOAJ, TUBITAK Ulakbim TR Index, EBSCO**, and **TurkMedline**.

The journal is published online.

Owner: Erzincan Binali Yıldırım University

Responsible Manager: Mecit Kantarcı

Publisher Contact

Address: Molla Gürani Mah. Kaçamak Sk. No: 21/1 34093 İstanbul, Türkiye

Phone: +90 (530) 177 30 97 / +90 (539) 307 32 03

E-mail: info@galenos.com.tr/yayin@galenos.com.tr

Web: www.galenos.com.tr

Publisher Certificate Number: 14521

Publication Date: January 2026

E-ISSN: 2687-448

International scientific journal published quarterly.

ABCResearch

Editorial Board

ABCResearch

Contents

Research Articles

Contents

ABCResearch

Arch Basic Clin Res 2026;8(1):1-6
DOI: 10.4274/ABCR.2025.25395

Research Article

Diagnostic Effectiveness of Ischiofemoral Space and Quadratus Femoris Distance Measurements in Ischiofemoral Impingement Syndrome

Merve Kolak[1], Volkan Kızılgöz[2], Mehmet Burak Gökgöz[3], Mukadder Sunar[1]

[1]Department of Anatomy, Erzincan Binali Yıldırım University Faculty of Medicine, Erzincan, Türkiye
[2]Department of Radiology, Erzincan Binali Yıldırım University Faculty of Medicine, Erzincan, Türkiye
[3]Department of Orthopedics and Traumatology, Erzincan Binali Yıldırım University Faculty of Medicine, Erzincan, Türkiye

Cite this article as: Kolak M, Kızılgöz V, Gökgöz MB, Sunar M. Diagnostic effectiveness of ischiofemoral space and quadratus femoris distance measurements in ischiofemoral impingement syndrome. *Arch Basic Clin Res*. 2026;8(1):1-6.

ORCID IDs of the authors: M.K. 0009-0000-5796-233X, V.K. 0000-0003-3450-711X, M.B.G. 0000-0003-0758-5382, M.S. 0000-0002-6744-3848.

ABSTRACT

Objective: To ascertain whether measurements of the quadratus femoris and ischiofemoral intervals obtained on pelvic magnetic resonance imaging (MRI) examinations are useful for diagnosing ischiofemoral impingement (IFI) syndrome.

Methods: MRIs of 178 patients (104 females and 74 males) were reinterpreted bilaterally for signal changes on T2-weighted sequences in the ischiofemoral space (IFS) and quadratus femoris space (QFS), indicating IFI. Receiver operating characteristic (ROC) curves were plotted for each measurement parameter, and the corresponding area under the curve (AUC) values were reported. A *P* value of less than 0.05 was considered to indicate a significant difference, and the results were assessed at the 95% confidence level.

Results: There was no significant difference in age between females and males ($P = 0.064$). Radiologically, 17.7% of all participants were diagnosed with IFI. Significant differences were observed between IFS and obturator femoris space values by gender, with both values being significantly lower in women. A higher percentage of patients testing positive for IFI was observed in women compared with men. In the ROC analysis conducted according to IFS, the AUC was 0.840. The highest value of sensitivity × specificity was 21.29 mm. The sensitivity at this value was 0.676. The specificity at this value was 0.857. In the ROC analysis using QFS, the AUC was 0.856. The highest value of (sensitivity × specificity) was 16.17 mm. The sensitivity at this value was 0.765. The specificity at this value was 0.794.

Conclusion: The results of the current study indicated a significant relationship between the IFS and QFS measurements and IFI. These intervals showed a significant negative correlation with age. This study also identified important cut-off values for IFS and QFS intervals that indicate IFI, with relatively high sensitivity and specificity.

Keywords: Pelvic anatomy, ischiofemoral impingement, ischiofemoral space, quadratus femoris space, magnetic resonance imaging

INTRODUCTION

The posterior hip is a crucial area where pain can arise from conditions such as osteoarthritis, sacroiliac joint disorders and piriformis syndrome. Ischiofemoral impingement (IFI) syndrome, caused by narrowing of the space between the medial aspect of the lesser trochanter and the lateral aspect of the ischial tuberosity, is a neglected cause of posterior hip pain.[1] The ischiofemoral space (IFS) is bounded medially by the ischial tuberosity and laterally by the lesser trochanter of the femur.[2] The posteromedial surface of the iliopsoas tendon or the lesser trochanter and the superolateral surface of the hamstring tendons define the quadratus femoris space (QFS), which is the narrowest space through which the quadratus femoris muscle (QFM) passes.[3] Originating from the inferolateral margin of the

Corresponding author: Merve Kolak, **E-mail:** mervekolak@hotmail.com

Received: November 20, 2025 **Accepted:** December 9, 2025 **Publication Date:** January 26, 2026

ischium, the QFM inserts onto the posteromedial aspect of the proximal femur at the quadrate tubercle on the posterior intertrochanteric ridge. It stabilizes the femoral head in the acetabulum and acts as a strong external rotator and adductor of the thigh[4] within the acetabulum and functions as a strong external rotator and adductor of the thigh.

Magnetic resonance imaging (MRI) is an important diagnostic tool, most frequently used in the evaluation of IFI, because of its multiplanar imaging, high resolution, lack of ionizing radiation, and superiority over other radiological methods in demonstrating soft tissues and soft-tissue edema.[5] Utilizing MRI of the hip allows us to identify a reduced distance between the lesser trochanter and the ischial tuberosity, as well as abnormal signal intensity of the QFM.[3]

This study aims to determine the diagnostic effectiveness of ischiofemoral interval and quadratus femoris interval measurements obtained from pelvic MRI examinations for IFI.

To the best of our knowledge, few studies have investigated IFI syndrome. Therefore, this study aimed to determine the effectiveness of IFS and QFS measurements obtained from pelvic MRI for the diagnosis of IFI. We hypothesize that patients with IFI will have significantly lower IFS and QFS values than patients without IFI, and that these measurements will provide significant diagnostic discrimination for IFI in receiver operating characteristic (ROC) analysis.

MATERIALS AND METHODS

This retrospective cross-sectional study was approved by the Institutional Ethics Committee of Erzincan Binali Yıldırım University Institutional Ethics Committee (decision no.: 2025-09/01, session: 09, date: 15.05.2025). After approval, all patients who had undergone pelvic MRI at our institution between November 1, 2024, and June 18, 2025 (n=202) reassessed for the IFS intervals. After obtaining approval, all patients who underwent pelvic MRI at our hospital between November 1, 2024, and June 18, 2025 (n=202) were reassessed for IFS intervals. All pelvic measurements were performed using the institutional hospital's picture archiving and communication system. To examine patients with complete bone maturation, those younger than 18 years (n=5) were excluded from the study. In order to examine patients with complete bone maturation, both male and female patients over 18 years of age were included. Patients younger than 18 years of age (n=5) were excluded from the study. Additionally, the patients whose orthopaedic examination results could not be obtained or whose images were unsuitable for evaluation because of technical flaws or artifacts were excluded (n=19). Additionally, patients whose orthopedic examination results were unavailable or whose images were unsuitable for evaluation due to technical flaws or artifacts (n=19) were excluded. After exclusions, 104 women and 74 men, a total of 178 patients, were reinterpreted bilaterally for measurements and signal changes indicating IFI.

MAIN POINTS

- Ischiofemoral space (IFS) and quadratus femoris space (QFS) measurements using pelvic magnetic resonance imaging showed significant indicator for the diagnosis of Ischiofemoral impingement (IFI) syndrome.
- Women exhibited lower IFS and QFS measurements and a higher IFI rate; the overall incidence of IFI within the study population was 17.7%.
- Sensitivity/specificity were 0.676/0.857 for IFS and 0.765/0.794 for QFS at the optimal thresholds.

MRI

Technical Parameters of Pelvic MRI

A 1.5-Tesla MR scanner (Magnetom Aera; Siemens Healthineers, Erlangen, Germany) was used to perform pelvic MRI. All patients were examined in the supine position, and the imaging procedure was performed using standard (15-channel) abdominal coils. The turbo spin echo MR sequences for the pelvic imaging with relevant technical parameters [Time of repetition (TR), time of echo (TE), number of excitations (NEX), field of view, slice thickness (ST), voxel size (VS)] were listed for all sequences as follows: Coronal plane T2-weighted imaging (TR: 3660 ms, TE: 66 ms, NEX: 1, ST: 4 mm, VS: 0.7 x 0.7 x 4 mm), coronal plane T1-weighted imaging (TR: 504 ms, TE: 21 ms, NEX: 2, ST: 4 mm, VS: 1.4 x 1.4 x 4 mm), axial plane fat saturated proton density (TR: 2920 ms, TE: 34 ms, NEX: 2, ST: 5 mm VS: 1.3 x 1.3 x 5 mm), axial plane T1-weighted imaging (TR: 714 ms, TE: 11 ms, NEX: 2, ST: 5 mm, VS: 5 mm), fat saturated axial plane T1-weighted imaging (TR: 677 ms, TE: 11 ms, NEX: 2 mm, ST: 5 mm, VS: 0.6 x 0.6 x 5 mm).

Measurement Technique

The ischiofemoral bone-to-bone distance and the distance between the lesser trochanter of the femur and the lateral borders of the hamstring tendons can be readily measured on axial images. Therefore, the axial planes were used to perform the measurements. The IFS is defined as the shortest distance between the lateral cortex of the ischial tuberosity and the medial cortex of the lesser trochanter. The QFS was measured as the shortest distance through which the QFM passes, bounded by the superolateral surface of the hamstring tendons and the lesser trochanter. The IFS is defined as the shortest distance between the lateral cortex of the ischial tuberosity and the medial cortex of the lesser trochanter. The QFS was measured as the shortest distance through which the QFM could pass and was bounded by the superolateral surface of the hamstring tendons and the lesser trochanter. The ischiofemoral (bone-to-bone) space and the bone-to-quadriceps femoris tendon space can be readily estimated on axial images. Therefore, axial planes were used for measurements. T1 sequences were used for these measurements because of their superiority in defining regional anatomy and delineating cortical borders (Figure 1). Proton-weighted T2 sequences were used to assess signal changes in the QFM (Figure 2).[3] After measuring the IFS and QFS distances, the presence of a signal increase in the QFS muscle on the T2 sequence was assessed. IFI was considered positive in those with a signal increase and negative in those without a signal increase.

Statistical Analysis

All statistical analyses were performed using IBM SPSS Statistics for Windows, version 22.0 (IBM Corp., Armonk, NY, USA). Descriptive statistics are presented as frequency, percentage, mean, standard deviation, median, and minimum-maximum values. In the normality analysis, Kolmogorov-Smirnov tests were performed. An Independent Samples t-test was used to compare female and male groups with respect to IFS and QFS values. This test was also used to analyze the statistical significance of differences between the patient and normal groups in the IFS and QFS measurements. The correlations of these two measurements with age were analyzed using Spearman's rho. IFS and QFS values were also analyzed using chi-square tests to calculate sensitivity and specificity to indicate the presence of IFI. The chi-square test was used for binary analyses of categorical data. ROC curves were used to estimate the area under the curve (AUC) for each measured parameter. Results were evaluated at a 95% confidence level, and a *P* value of < 0.05 was considered to indicate statistical significance.

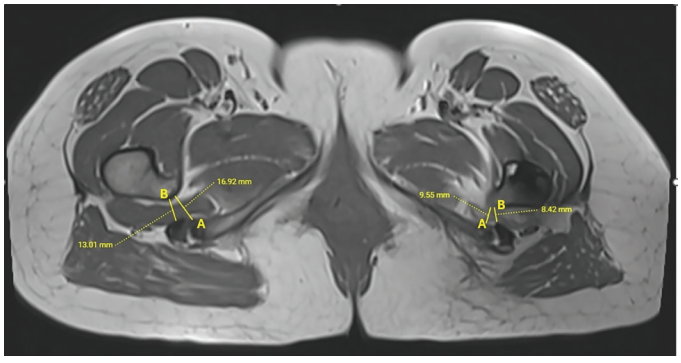

Figure 1. IFS and QFS intervals measuremet on T1 sequence. A) Ischiofemoral space (IFS), B) quadratus femoris space (QFS).

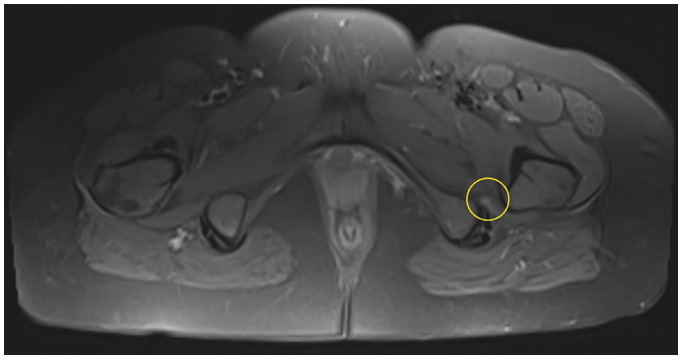

Figure 2. On the PDW (proton density-weighted) sequence, increased signal intensity was observed in the quadratus femoris muscle compared with the contralateral side. Note the narrow QFS interval.

QFS, quadratus femoris space.

RESULTS

Among the participants, 58.4% were female and 41.6% male, with a mean age of 48.51 (16.10). There was no significant age difference between females and males (*P* = 0.064). Radiologically, 17.7% of the total participants were diagnosed as IFI. Significant differences in IFS and OFS values were observed between genders, with both values lower in women (Table 1).

A higher percentage of positive patients was observed in women compared to men for IFI. (*P* < 0.05, Table 2).

A significant but very weak negative correlation was found between age and the IFS value (*r* = -0.146, *P* = 0.006). A weak, negative, and statistically significant correlation was found between age and the QFS value (*r* = -0.255, *P* < 0.0001). A very weak negative correlation between age and the IFS value (*r* = -0.146, *P* = 0.006) and a weak negative correlation between age and the QFS value (*r* = -0.255, *P* < 0.0001) were observed.

In the ROC analysis conducted using IFS, the AUC was 0.840. (Figure 3). The highest cut-off value of (sensitivity x specificity) was 21.285 21,29 mm. The sensitivity at this value was 0.676. The specificity at this value was 0.857.

In the ROC analysis conducted according to QFS, the AUC was 0.856 (Figure 4). The highest cut-off value of (sensitivity × specificity) was 16.17 mm. The sensitivity at this value was 0.765. The specificity at this value was 0.794 (Table 3).

DISCUSSION

Hip discomfort following hip surgery or trauma may be caused by IFI; however, this condition is relatively rare. Nevertheless, only one documented instance of IFI without a history of lower extremity trauma or surgery has been reported.[6] Although the exact origin of IFI is unknown, there are both congenital and acquired causes. Osteoarthritis resulting in superior and medial migration of the femur, valgus deformity requiring intertrochanteric osteotomy, and intertrochanteric fractures involving the lesser trochanter are some acquired causes.

Table 1. The IFS and QFS Measurement Results Regarding to the Genders and the Presence of IFI

	Group	
	IFS	**QFS**
Gender		
F (n=208)	21.52 (7.0806)[a]	18.81 (7.36)[a]
M (n=148)	25.68(7.6933)[b]	22.76 (8.12)[b]
IFI		
N (n=293)	24.86(6.99)[a]	22.1213 (7.44)[a]
P (n=63)	15.7786 (5.75)[b]	12.6846 (4.90)[b]

[a,b]: Different letters in the same column indicate statistically different (*P* < 0.05).

F, female; M, male; N, negative; P, positive; IFI, ischiofemoral impingement; IFS, ischiofemoral space; QFS, quadratus femoris space.

Table 2. The percentages of Positive and Negative Patients for Each Gender Group and for the Total Population of the Study

	Gender			
IFI	**Female**	**Male**	**Total**	***P* value**
Negative	163 (78.4%)	130 (87.8%)	293 (82.3%)	**0.021***
Positive	45 (21.6%)	18 (12.2%)	63 (17.7%)	
Total	208 (100%)	148 (100%)	356 (100%)	

* Pearson's chi-square test indicated that gender was significantly associated with IFI (ischiofemoral impingement). The *P* value indicated that the proportion of positive patients among females was significantly higher than that among males.
IFI, Ischiofemoral impingement.

Table 3. Results of ROC analysis based on IFS and QFS mesurements (Asymptotic 95% Confidence Interval)

Model Name	Sensitivity	Specificity	Sensitivity × Specificity	AUC
IFS	0.676	0.857	21.285	0.840
QFS	0.765	0.794	16.17	0.856

[(IFS, Lower bound: 0,788; Upper bound: 0,891) and QFS Lower bound: 0,809; Upper bound: 0,904].
IFS, ischiofemoral space; QFS, quadratus femoris space; AUC, area under the curve; ROC, receiver operating characteristic.

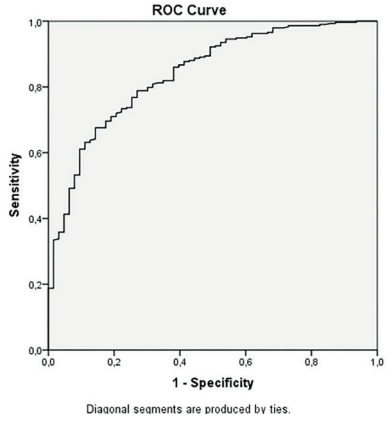

Figure 3. ROC curve analysis of raw data from available hip IFS measurements (n=178) yielded an AUC of 0.840 (95% confidence interval: 0.788-0.891).

ROC, receiver operating characteristic; IFS, ischiofemoral space; AUC, area under the curve.

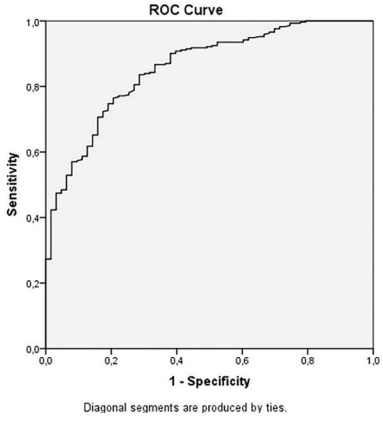

Figure 4. ROC curve analysis from raw data of available hip QFS measurements; n=178, AUC=0.856 (95% confidence interval 0.809-0.904).

ROC, receiver operating characteristic; QFS, quadratus femoris space; AUC, area under the curve.

Ischiofemoral narrowing can have a congenital or positional origin, independent of any acquired bone abnormalities.[6] According to reports, IFI can be identified on hip MRI by constriction of the quadratus femoris and IFS.[7] This paper aims to evaluate the accuracy of IFI diagnosis from pelvic MRI exams utilizing the quadratus femoris and ischiofemoral interval measures. The purpose of this article is to assess how well pelvic MRI examinations that use the ischiofemoral and quadratus femoris interval measurements diagnose IFI syndrome.

Our findings support this hypothesis. Patients diagnosed with IFI syndrome showed significantly smaller IFS and QFS measurements on pelvic MRI compared with those without IFI. Moreover, ROC curve analysis demonstrated that both intervals provided meaningful diagnostic discrimination, indicating that reduced IFS and QFS values are useful imaging markers for identifying IFI in routine pelvic MRI evaluations.

Our study was designed as a retrospective, cross-sectional analysis of images from patients who underwent hip and pelvic MRI for various reasons, particularly hip pain, and these images were re-evaluated according to radiological IFI criteria. The degree of hip flexion and rotation during the MRI may substantially affect these measurements. Additionally, the QF space should be assessed, even though the majority of IFI literature focuses on narrowing of the (bony) IF space. Functionally, impingement of the QF muscle against the lesser trochanter may result from a lateralized and widened hamstring origin, particularly during hip external rotation and extension.[8,9] We also evaluated both spaces.

In practical terms, a meta-analysis of 27 studies in individuals with IFI provides useful cutoff points for detecting space narrowing on standard hip MRI. A total of six articles, including their respective institutional series but excluding case reports and reviews were evaluated for QFS and IFS. A. Singer et al.'s[10] meta-analysis reports that the T1W axial sequence cut-off value for the QFS is < 10 mm (sensitivity 79%, specificity 74%, accuracy 77%), and for the IFS ≤ 15 mm (sensitivity 77%, specificity 81%, accuracy 74%). In our study the T1W axial sequence cut-off value for the IFS is 21,285 mm (sensitivity

67,6%, specificity 85.7%) and for the QFS is 16,17 (sensitivity 76,5%, specificity 79,4%). In our study, the T1W axial sequence cut-off values were 21.29 mm for the IFS (sensitivity 67.6%, specificity 85.7%) and 16.17 mm for the QFS (sensitivity 76.5%, specificity 79.4%).[3,6,10-13]

It has been proposed that IFI syndrome is gender-related because females' ischial tuberosities are farther apart, which reduces the ischiofemoral distance.[7,11,13,14] Sussman et al.[15] found that female cadavers exhibited altered ischial angulation and increased intertuberous diameter, which may explain the greater prevalence of IFI syndrome in females. In our study, we observed that the incidence of IFI was higher in women.[16] According to the majority of studies, IFI is more prevalent in adults. However, we observed a low but significant negative correlation between age and the IFS and QFS values.[8]

Study Limitations

This study has several limitations that should be discussed before analyzing the results. First, our study was retrospective. Since IFI findings were not prospectively evaluated clinically or radiologically in these studies, some cases of IFI may have been missed during the period examined. Second, the definition of pain characteristics for IFI is unclear. Specificity would likely be increased if this type of pain were clinically significant and accompanied by an abnormal QF MRI appearance and narrowing of the IFI and/or QFS. More specific definitions of hip pain associated with IFI have recently been presented; however, larger studies are needed to confirm their sensitivity and specificity profiles.[13,17] Considering the various hip positioning protocols that can be used during MRI, researchers have suggested imaging through the arc of femoral rotation to locate the point where the IFS and QFS are narrowest. To provide a constant hip posture, internal rotation was used. Considering the various hip positioning protocols during MRI, researchers have suggested imaging throughout the arc of femoral rotation to identify the point where the IFS and QFS are narrowest. In our study, internal rotation was applied to maintain a consistent hip posture.[3,7,11,14] However, recent research has revealed notable alterations in the IF gap brought on by hip flexion or rotation,[18-20] with the shortening between the ischium and lesser trochanter becoming particularly noticeable during hip external rotation.[8] We obtained MRIs of our patients in the neutral, supine position. Further studies are needed to determine the effect of position on IFI diagnosis. Because the measurements were made by consensus between a radiologist and an anatomist, double-blinding was not feasible. This may have increased the risk of bias in the measurement results due to interaction between observers.

CONCLUSION

IFI syndrome is an extra-articular compressive phenomenon caused by a narrowing between the ischium and the proximal femur in native hips. The results of the current study indicated the significant relationship between the IFS and QFS measurements and IFI syndrome. These intervals showed a significant and negative correlation regarding age. This study also revealed important cut-off values for IFS and QFS intervals indicating IFI with relatively high sensitivity and specificity values. Including these study results, a meticulous meta-analysis that gathers other research focusing on the same interval measurements would be useful to better understand and specify the threshold values that indicate IFI.

Ethics

Ethics Committee Approval: This retrospective cross-sectional study was approved by the Institutional Ethics Committee of Erzincan Binali Yıldırım University (decision no.: 2025-09/01, session: 09, date: 15.05.2025).

Informed Consent: Since our study was designed as a retrospective radiological study, it did not require a patient consent form.

Footnotes

Author Contributions

Concept Design – M.K.,V.K.; Data Collection or Processing – M.K.,V.K.; Analysis or Interpretation – M.K.,V.K., M.B.G., M.S.; Literature Review – M.K., M.B.G., M.S.; Writing, Reviewing and Editing – M.K.,V.K., M.B.G., M.S.

Declaration of Interests: The authors declare that they have no conflicts of interest.

Funding: The authors declare that this study has received no financial support.

REFERENCES

1. Stafford GH, Villar RN. Ischiofemoral impingement. *J Bone Joint Surg Br*. 2011;93(10):1300-1302. [CrossRef]
2. Barros AAG, Dos Santos FBG, Vassalo CC, Costa LP, Couto SGP, Soares ARDG. Evaluation of the ischiofemoral space: a case-control study. *Radiol Bras*. 2019;52(4):237. [CrossRef]
3. Torriani M, Souto SC, Thomas BJ, Ouellette H, Bredella MA. Ischiofemoral impingement syndrome: an entity with hip pain and abnormalities of the quadratus femoris muscle. *AJR Am J Roentgenol*. 2009;193(1):186-190. [CrossRef]
4. Aung HH, Sakamoto H, Akita K, Sato T. Anatomical study of the obturator internus, gemelli and quadratus femoris muscles with special reference to their innervation. *Anat Rec*. 2001;263(1):41-52. [CrossRef]
5. Akça A, Şafak KY, İliş ED, Taşdemir Z, Baysal T. Ischiofemoral impingement: assessment of MRI findings and their reliability. *Acta Ortop Bras*. 2016;24(6):318-321. [CrossRef]
6. Ali AM, Whitwell D, Ostlere SJ. Case report: imaging and surgical treatment of a snapping hip due to ischiofemoral impingement. *Skeletal Radiol*. 2011;40(5):653-656. [CrossRef]
7. Patti JW, Ouellette H, Bredella MA, Torriani M. Impingement of lesser trochanter on ischium as a potential cause for hip pain. *Skeletal Radiol*. 2008;37(10):939-941. [CrossRef]
8. Torriani M. Ischiofemoral impingement syndrome in 2024: updated concepts and imaging methods. *Magn Reson Imaging Clin N Am*. 2025;33(1):63-73. [CrossRef]

9. Xing Q, Feng X, Wan L, Cao H, Bai X, Wang S. MRI measurement assessment on ischiofemoral impingement syndrome. *Hip Int*. 2023;33(1):119-125. [CrossRef]

10. Singer AD, Subhawong TK, Jose J, Tresley J, Clifford PD. Ischiofemoral impingement syndrome: a meta-analysis. *Skeletal Radiol*. 2015;44(6):831-837. [CrossRef]

11. Tosun O, Algin O, Yalcin N, Cay N, Ocakoglu G, Karaoglanoglu M. Ischiofemoral impingement: evaluation with new MRI parameters and assessment of their reliability. *Skeletal Radiol*. 2012;41(5):575-587. [CrossRef]

12. Hatem MA, Palmer IJ, Martin HD. Diagnosis and 2-year outcomes of endoscopic treatment for ischiofemoral impingement. *Arthroscopy*. 2015;31(2):239-246. [CrossRef]

13. Bredella MA, Azevedo DC, Oliveira AL, et al. Pelvic morphology in ischiofemoral impingement. *Skeletal Radiol*. 2015;44(2):249-253. [CrossRef]

14. Ali AM, Teh J, Whitwell D, Ostlere S. Ischiofemoral impingement: a retrospective analysis of cases in a specialist orthopaedic centre over a four-year period. *Hip Int*. 2013;23(3):263-268. [CrossRef]

15. Sussman WI, Han E, Schuenke MD. Quantitative assessment of the ischiofemoral space and evidence of degenerative changes in the quadratus femoris muscle. *Surg Radiol Anat*. 2013;35(4):273-281. [CrossRef]

16. Erol S, Ataş AE. Evaluation of ischiofemoral and quadratus femoris spaces, quadratus femoris muscle signal in ischiofemoral impingement syndrome by magnetic resonance imaging. *Genel Tip Dergisi*. 2025;35(1):91-96. [CrossRef]

17. Backer MW, Lee KS, Blankenbaker DG, Kijowski R, Keene JS. Correlation of ultrasound-guided corticosteroid injection of the quadratus femoris with MRI findings of ischiofemoral impingement. *AJR Am J Roentgenol*. 2014;203(3):589-593. Erratum in: *AJR Am* J Roentgenol. 2014;203(5):1156. [CrossRef]

18. Hatem M, Martin RL, Nimmons SJ, Martin HD. Frequency of ischiofemoral space discrepancy when comparing magnetic resonance images of distinct institutions for the same patient. *Proc (Bayl Univ Med Cent)*. 2020;34(2):242-246. [CrossRef]

19. Johnson AC, Hollman JH, Howe BM, Finnoff JT. Variability of ischiofemoral space dimensions with changes in hip flexion: an MRI study. *Skeletal Radiol*. 2017;46(1):59-64. [CrossRef]

20. Vicentini JRT, Martinez-Salazar EL, Simeone FJ, Bredella MA, Palmer WE, Torriani M. Kinematic MRI of ischiofemoral impingement. *Skeletal Radiol*. 2021;50(1):97-106. [CrossRef]

ABCResearch

Arch Basic Clin Res 2026;8(1):7-19
DOI: 10.4274/ABCR.2025.25386

Research Article

Venetoclax-Ibrutinib Combinations as First-Line Therapy in Chronic Lymphocytic Leukemia: A Meta-Analysis of Randomized Controlled Trials with GRADE Approach

Lokman Hekim Tanrıverdi[1], Ahmet Sarıcı[2]

[1]Department of Medical Pharmacology, İnönü University Faculty of Medicine, Malatya, Türkiye,
[2]Division of Hematology, Department of Internal Medicine, İnönü University Faculty of Medicine, Malatya, Türkiye

Cite this article as: Tanrıverdi LH, Sarıcı A. Venetoclax-ibrutinib combinations as first-line therapy in chronic lymphocytic leukemia: a meta-analysis of randomized controlled trials with GRADE approach. *Arch Basic Clin Res*. 2026;8(1):7-19.

ORCID IDs of the authors: L.H.T. 0000-0003-4263-5234, A.S. 0000-0002-5916-0119.

ABSTRACT

Objective: Chronic lymphocytic leukemia (CLL) treatment has shifted from chemoimmunotherapy to targeted agents. Venetoclax and ibrutinib, which act through complementary mechanisms, have shown promise in achieving deep remissions. Their combination may enhance efficacy, but pooled evidence from randomized trials is lacking.

Methods: We systematically searched CENTRAL, MEDLINE, PubMed, Web of Science, and Scopus through April 1, 2025, for phase II/III randomized controlled trials (RCTs) comparing venetoclax-ibrutinib based combinations to standard regimens in treatment-naive CLL. Outcomes included progression-free survival (PFS) at predefined time points, overall survival (OS), undetectable measurable residual disease (uMRD) in blood and bone marrow, and safety. Risk ratios (RRs) were synthesized using inverse-variance weighted random-effects models.

Results: Four RCTs (n=1.343; CAPTIVATE, GLOW, GAIA-CLL13, and FLAIR were eligible. Venetoclax-ibrutinib combinations significantly prolonged PFS at 12 months [RR 1.10; 95% confidence interval (CI) 1.05-1.15], 24 months (RR 1.21; 95% CI 1.15-1.28), 36 months (RR 1.27; 95% CI 1.14-1.42), and 48 months (RR 1.47; 95% CI 1.18-1.84), with attenuation at 60 months (RR 1.74; 95% CI 0.88-3.43), when the effect was no longer statistically significant. Rates of uMRD were higher in peripheral blood (RR 1.55, 95% CI 1.35-1.79) and in bone marrow (RR 2.15, 95% CI 1.37-3.38). OS at 36 months was similar between groups (RR, 1.05; 95% CI, 0.93-1.17). Safety outcomes were broadly comparable, though diarrhea (RR 2.10) and hypertension (RR 2.86) were more frequent with venetoclax-ibrutinib. Subgroup analysis revealed a transient 24-month PFS benefit in patients with unmutated immunoglobulin heavy chain variable.

Conclusion: Venetoclax-ibrutinib combinations significantly improve disease control in first-line CLL, achieving higher uMRD and sustained PFS benefits without compromising safety.

Keywords: Venetoclax, ibrutinib, chronic lymphocytic leukemia, progression-free survival, meta-analysis

INTRODUCTION

Chronic lymphocytic leukemia (CLL) is the most common adult leukemia in Western countries, characterized by the accumulation of mature clonal B cells in the peripheral blood (PB), bone marrow, and lymphoid tissues. Although the disease course is heterogeneous, many patients eventually require therapy, and historically, chemoimmunotherapy with fludarabine, cyclophosphamide, and rituximab or bendamustine-based regimens represented standard first-line approaches.[1]

CLL treatment has shifted from chemoimmunotherapy to targeted agents that disrupt key pathogenic pathways.[2] Among these, the Bruton's tyrosine kinase inhibitor ibrutinib and the B-cell lymphoma-2 (BCL-2) inhibitor venetoclax have each demonstrated durable remissions as monotherapy in CLL. The combination of ibrutinib and venetoclax is supported by a

Corresponding author: Lokman Hekim Tanrıverdi, **E-mail:** lokmanhekim.tanriverdi@inonu.edu.tr

Received: October 6, 2025 **Accepted:** November 17, 2025 **Publication Date:** January 26, 2026
Revision Requested: October 20, 2025

strong biological rationale. The lymph node microenvironment provides CLL cells with protective signals from T cells, natural killer cells, macrophages, endothelial cells, and stromal cells, which collectively promote CLL cell survival and suppress immune responses.[3,4] B-cell receptor (BCR) activation and cluster of differentiation 40 (CD40)-CD40 ligand interactions upregulate antiapoptotic proteins such as B-cell lymphoma-extra large (BCL-XL) and myeloid cell leukemia-1 (MCL-1),[5] while Toll-like receptor stimulation and CD40 overexpression reduce sensitivity to venetoclax.[6,7] Furthermore, loss of the tumor-suppressor microRNAs miR-15a/miR-16-1 leads to aberrant upregulation of BCL-2 and impaired apoptosis.[8]

Preclinical studies also reinforce this synergy. *Ex vivo* drug profiling showed that ibrutinib-treated CLL cells became more venetoclax-sensitive through reductions in MCL-1 and BCL-XL.[9,10] BH3 profiling confirmed increased BCL-2 dependence, and *in vivo* models demonstrated cooperative activity with distinct effects on proliferative versus quiescent CLL subpopulations.[11] Together, these findings highlight that combining these agents, as suggested by National Comprehensive Cancer Network guideline v3.2024,[12] exploits complementary mechanisms: ibrutinib inhibits tumor cell proliferation, mobilizes malignant cells from their protective niches in the lymphoid organs into the circulation, and impairs BCR signaling, while venetoclax induces apoptosis by inhibiting BCL-2.[1] This strategy promises minimal residual disease (MRD) negativity and improved progression-free survival (PFS).[12]

We conducted a meta-analysis to evaluate the efficacy, safety, and tolerability of venetoclax-ibrutinib combinations (VIC) in treatment-naive CLL patients.

MATERIAL AND METHODS

This study was a systematic review and meta-analysis of previously published studies and did not involve human participants directly; therefore, ethics committee approval and informed consent were not required.

MAIN POINTS

- Venetoclax-ibrutinib combinations (VIC) significantly improved progression-free survival (PFS) versus standard regimens across multiple time points—12 months [Risk ratio (RR) 1.10; 95% confidence interval (CI) 1.05-1.15], 24 months (RR 1.21; 95% CI 1.15-1.28), 36 months (RR 1.27; 95% CI 1.14-1.42), 48 months (RR 1.47; 95% CI 1.18-1.84)—with attenuation at 60 months (RR 1.74; 95% CI 0.88-3.43).
- Undetectable minimal residual disease was achieved more frequently with VIC, both in peripheral blood (RR 1.55; 95% CI 1.35-1.79) and in bone marrow (RR 2.15; 95% CI 1.37-3.38).
- Safety profiles were comparable, with no significant differences in serious adverse events (RR 1.10; 95% CI 0.74-1.62) or deaths (RR 0.70; 95% CI 0.22-2.29).
- Both the doublet (venetoclax + ibrutinib) and the triplet (venetoclax + ibrutinib + obinutuzumab) regimens yielded comparable efficacy for 36-month PFS [RR 1.28 (1.12-1.46) versus 1.26 (1.05-1.51)].

Eligibility criteria

We included randomized controlled trials (RCTs) (parallel-group, phase II or III) enrolling adults with previously untreated CLL that compared venetoclax-ibrutinib-based combinations against chemoimmunotherapy or other targeted regimens.

Information Sources

We searched Cochrane CENTRAL, Ovid MEDLINE, PubMed, Web of Science, and Scopus from database inception through April 1, 2025. No language restrictions were applied.

Search Strategy

The search combined controlled vocabulary and free-text terms for "venetoclax-," "ibrutinib-," and "CLL-," adapted to each database.

Study Selection

Two reviewers independently screened titles and abstracts, and then the full texts of potentially eligible records, using prespecified criteria. Discrepancies were resolved by consensus. Reasons for exclusion at full-text review were documented and summarized in the PRISMA flow diagram (Figure 1).

Data Collection Process

Two reviewers independently extracted data using a piloted form. Extracted items included trial characteristics (design, phase, setting, sample size), patient features (age, comorbidity status, genomic risk including immunoglobulin heavy chain variable (IGHV), del(17p)/tumor protein 53 (TP53) when

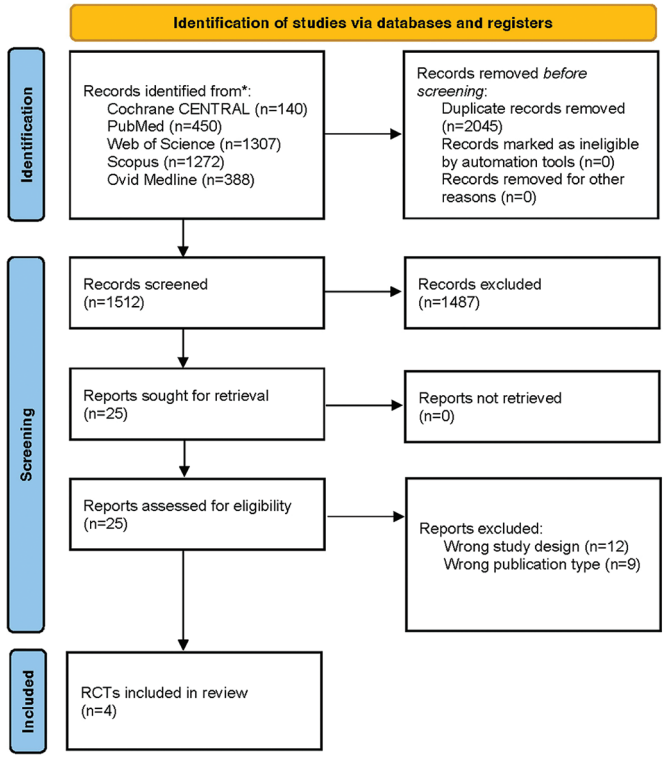

Figure 1. Flow diagram of literature search.

RCT, randomized controlled trial.

reported), intervention details (drug(s), dosing, treatment duration, MRD-guided versus fixed-duration strategy), comparator regimens, outcome definitions and assessment schedules, follow-up duration, and effect estimates for all outcomes. Any disagreements were resolved through discussion.

Study Outcomes

The primary efficacy outcome was PFS at 36 months; secondary outcomes included landmark PFS at additional time points (12, 24, 48, and 60 months, as available), overall survival (OS), undetectable minimal residual disease (uMRD) in PB and/or bone marrow, treatment discontinuation due to adverse events (AEs), serious AEs, infection outcomes, and selected AEs of special interest (e.g., diarrhea, hypertension). Trials of relapsed/refractory disease, non-randomized trials, single-arm trials, and trials in pediatric populations were excluded.

Definitions and Outcome Measures

PFS and OS were used as defined by each trial. When time-to-event hazard ratios (HRs) were unavailable at a given landmark time, we abstracted aggregate data at prespecified time points for binary outcomes and calculated risk ratios (RRs). uMRD was accepted as defined in each trial (typically < 10^{-4} by flow cytometry or next-generation sequencing) and was abstracted separately for PB and bone marrow, when available. Safety outcomes followed trial-reported grading (e.g., Common Terminology criteria for Adverse Events version used in each study).

Statistical Analysis

For dichotomous outcomes (e.g., landmark PFS, uMRD, AEs), we calculated RRs with 95% confidence intervals (CIs). For rare events, the Mantel-Haenszel method, with a continuity correction when required.[13] For time-to-event outcomes with available HRs, we planned to synthesize log HRs and their standard errors. Primary analyses used inverse-variance-weighted random-effects models. Between-study variance (τ^2) was estimated with the Paule-Mandel method[14], and statistical heterogeneity was quantified using I^2. Planned sensitivity analyses included fixed-effect models; exclusion of studies at high risk of bias (RoB); and leave-one-out analyses. When ≥ 10 studies were available for an outcome, we planned to explore small-study effects via funnel plots and Egger's test; with fewer studies, we did not formally assess publication bias and instead interpreted pooled results with caution. All analyses were conducted in R (version 4.5.1; www.r-project.org; R Foundation for Statistical Computing, Vienna, Austria), using the validated meta and metafor packages.http://www.r-project.org/

RoB Assessment

The RoB for each included randomized controlled trial was independently assessed by two reviewers using the Cochrane RoB 2 tool[15], evaluating five domains: (1) randomization process, (2) deviations from intended interventions, (3) missing outcome data, (4) measurement of the outcome, and (5) selection of the reported result. Any disagreements were resolved through discussion. The overall RoB judgment for each trial was determined in accordance with the Cochrane Handbook for Systematic Reviews of Interventions, version 6.5.

Assessing of Certainty of Evidence

The certainty of the evidence for the primary outcome (PFS at 36 months) was evaluated using the Grading of Recommendations, Assessment, Development, and Evaluation approach, considering RoB, inconsistency, indirectness, imprecision, and publication bias as described in our prior study.[16] Evidence was rated as high, moderate, low, or very low.

Subgroup Analysis

A priori subgroups, contingent on data availability, included IGHV mutational status (mutated versus unmutated) and regimen composition (venetoclax + ibrutinib doublet versus venetoclax + ibrutinib + anti-CD20 triplet). Additional exploratory subgroups (age- or comorbidity-defined populations, MRD-guided vs fixed-duration strategies, and comparator category) were also considered.

Assessment of Reporting Bias and Study Registration

Because this was a synthesis of published randomized trials with ≤ 10 studies per outcome, formal statistical tests for small-study effects were generally not applicable.

RESULTS

Four RCTs (n=1343) met eligibility criteria: CAPTIVATE[17], global study of venetoclax and obinutuzumab in previously untreated CLL (GLOW)[18], global assessment of ibrutinib and venetoclax in previously untreated CLL (GAIA-CLL13)[19], and frontline therapy with ibrutinib, venetoclax and rituximab (FLAIR)[20]; three of which explored venetoclax + ibrutinib[17,18,20], while one explored venetoclax + ibrutinib + obinutuzumab (Table 1).[19]

Study Characteristics

CAPTIVATE evaluated fixed-duration venetoclax-ibrutinib in patients age < 70 years (median age 58). After a 3-cycle ibrutinib lead-in followed by 12 cycles of combination therapy, 75% of patients achieved undetectable MRD in PB, and 68% of patients achieved undetectable MRD in bone marrow. One-year disease-free survival in the confirmed uMRD group was 95% with placebo and 100% with ibrutinib; PFS rates were ≥ 95% at approximately 30 months' follow-up compared with placebo.[17]

GLOW compared fixed-duration venetoclax-ibrutinib with chlorambucil–obinutuzumab in older and/or comorbid patients (median age 71 years). At 27.7 months, PFS favored venetoclax-ibrutinib (HR 0.216; 95% CI, 0.13-0.36; $P < 0.001$). The estimated 30-month PFS rates were ~80% with venetoclax-ibrutinib versus ~36% with chlorambucil-obinutuzumab, consistent across subgroups. Sustained uMRD in blood was achieved in 84.5% versus 29.3%.[18]

GAIA-CLL13 enrolled 926 fit patients without TP53 aberrations and randomized them to chemoimmunotherapy, venetoclax–rituximab, venetoclax–obinutuzumab, or venetoclax-obinutuzumab-ibrutinib. At three years, PFS was 90.5% with venetoclax-obinutuzumab-ibrutinib (HR for disease progression

or death, 0.32; 97.5% CI, 0.19-0.54; $P < 0.001$) and 87.7% with venetoclax-obinutuzumab (HR for disease progression or death, 0.42; 97.5% CI, 0.26-0.68; $P < 0.001$), compared with chemoimmunotherapy. The venetoclax-rituximab arm (80.8%) did not significantly outperform chemoimmunotherapy. The triple regimen venetoclax-ibrutinib-obinutuzumab yielded the highest uMRD rate (92.2%).[19]

FLAIR randomized 523 previously untreated patients eligible for fludarabine, cyclophosphamide, rituximab (FCR) to MRD-guided venetoclax-ibrutinib or FCR. At a median follow-up of 43.7 months, venetoclax-ibrutinib strongly reduced the risk of disease progression or death (HR, 0.13; 95% CI, 0.07-0.24; $P < 0.001$). By five years, 65.9% of patients had bone marrow uMRD, and 92.7% had PB uMRD.[20]

RoB

The overall RoB was low for Kater et al.,[18] of some concern for Wierda et al.[17] and Eichhorst et al.,[19], and high for Munir et al.[20] (Figure 2).

Table 1. Study Characteristics of the Included Trials

Study (year)	Trial / registration	Design	Setting	Population	n	Intervention	Comparator	Primary end point(s)
Wierda et al.[17]	CAPTIVATE; NCT02910583	Phase II RCT	46 sites across 6 countries	Age ≥ 18 to < 70 y with previously untreated CLL/SLL	149	Leadin ibrutinib × 3 cycles, then 12 cycles ibrutinib + venetoclax	Placebo or Ibrutinib	1year diseasefree survival in confirmed uMRD population
Kater et al.[18]	GLOW; NCT03462719	Phase 3, open-label RCT	67 sites across 14 countries	Previously untreated CLL, older or 18 to 64 years of age with comorbidities	211	Ibrutinib 420 mg qd ×3 lead-in cycles, then 12 cycles of ibrutinib + venetoclax	Obinutuzumab + chlorambucil	IRC assessed PFS (time from randomization to progression or death from any-cause)
Eichhorst et al.[19]	GAIA-CLL13; NCT02950051; EudraCT 2015-004936-36	Phase 3, open-label RCT	159 sites in 9 European countries and Israel	Previously untreated, fit CLL; ECOG 0-2	460	Venetoclax 400 mg qd for 10 cycles after 5 wk ramp-up; Ibrutinib 420 mg qd starting C1D1; Obinutuzumab per label; 12 cycles total with MRD guided	Chemoimmunotherapy (FCR for ≤ 65 y or bendamustine-rituximab for > 65 y); 6 × 28 day cycles	uMRD in peripheral blood at month 15 and PFS (time from randomization to progression or death)
Munir et al.[20]	FLAIR; ISRCTN01844152; EudraCT 2013-001944-76	Phase 3, open-label RCT	96 sites in United Kingdom	Previously untreated CLL/SLL; considered fit for FCR	523	Ibrutinib 420 mg qd for 8 weeks, then add venetoclax (ramp up to 400 mg qd)	FCR every 28 days × 6 cycles	PFS (time from randomization to progression or all-cause death)

CLL, chronic lymphocytic leukemia; SLL, small lymphocytic lymphoma; uMRD, undetectable minimal residual disease; RCT, randomized controlled trial; FCR, fludarabine-cyclophosphamide-rituximab; ECOG, Eastern Cooperative Oncology Group; IRC, independent review committee; PFS, progression-free survival; qd, once daily; C1D1, cycle 1 day 1; wk, week; MRD, minimal residual disease; GLOW, global study of venetoclax and obinutuzumab in previously untreated CLL; GAIA-CLL, global assessment of ibrutinib and venetoclax in previously untreated CLL; FLAIR, frontline therapy with ibrutinib, venetoclax and rituximab.

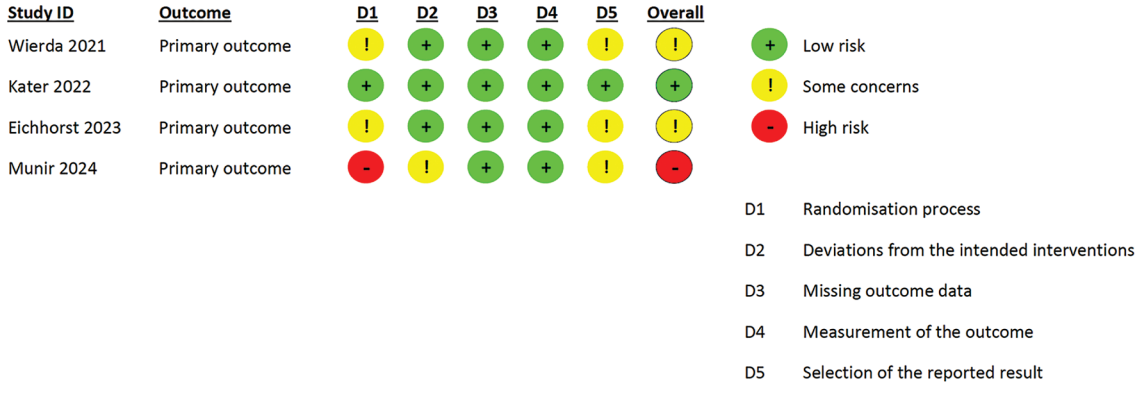

Figure 2. Risk of bias assessment of the included trials per each primary outcome.

Primary and Secondary Efficacy Outcomes

VIC significantly prolonged PFS compared to controls at early timepoints: month 12 (RR 1.10; 95% CI, 1.05-1.15), month 24 (RR 1.21; 95% CI, 1.15-1.28), month 36 (RR 1.27; 95% CI, 1.14-1.42; moderate certainty of evidence), and month 48 (RR 1.47; 95% CI, 1.18-1.84) (Table 2), but not at month 60 (RR 1.74; 95% CI, 0.88-3.43) (Figure 3).

MRD negativity was more frequent with VIC in peripheral blood (RR 1.55; 95% CI, 1.35-1.79) and in bone marrow (RR 2.15; 95% CI, 1.37-3.38) (Figure 4). OS at 36 months was similar between groups (RR 1.05; 95% CI, 0.93-1.17).

Safety and Tolerability Outcomes

Compliance and safety outcomes were generally comparable (Table 3). Rates of withdrawal due to AEs (RR 1.29; 95% CI, 0.43-3.87), of any serious AEs (RR 1.10; 95% CI, 0.74-1.62), of pneumonia (RR 0.86; 95% CI, 0.22-3.30), of upper respiratory tract infection (RR 0.75; 95% CI, 0.24-2.33), and of death (RR 0.70; 95% CI, 0.22-2.29) did not differ significantly. However, VIC was associated with an increased risk of diarrhea (RR 2.10; 95% CI, 1.00-4.40) and hypertension (RR 2.86; 95% CI, 1.26-6.49).

Subgroup Analysis

Subgroup analyses by IGHV mutational status are presented in Supplementary Figures S1-S5. At most time points (12, 36, 48, and 60 months), no statistically significant interaction was detected between IGHV mutational status and the effect of regimens containing venetoclax and ibrutinib on PFS. However, at 24 months, there was evidence of a differential treatment effect, with patients harboring unmutated IGHV deriving a greater relative benefit than those with mutated IGHV (P for interaction < 0.1).

In an additional subgroup analysis stratified by VIC regimen composition, venetoclax plus ibrutinib (RR, 1.28; 95% CI, 1.12-1.46) and venetoclax plus ibrutinib plus obinutuzumab (RR, 1.26; 95% CI, 1.05-1.51) yielded comparable relative benefits for the primary outcome. This indicates that the addition of obinutuzumab to venetoclax-ibrutinib did not substantially alter efficacy in terms of PFS at 36 months, consistent with the absence of significant subgroup interaction.

Furthermore, we performed additional subgroup analyses for the primary outcome of PFS at 36 months by management strategy (specifically, fixed-duration versus MRD-guided venetoclax–ibrutinib regimens; Figure S6) and by overall RoB classification of the included RCTs (Figure S7). The pooled estimates demonstrated similar effect sizes between the two management strategies. The RRs for both analyses were consistent with the main analysis, and the test for subgroup differences yielded P = 0.9074, indicating no statistically significant interaction for management type or RoB classification.

DISCUSSION

No previous meta-analysis had been published on this topic. However, Wen et al.[21] conducted a network meta-analysis (NMA) evaluating first-line treatment strategies for CLL using a frequentist approach and incorporating 30 RCTs (n=12,818) across chemotherapy, chemoimmunotherapy, and targeted regimens. Inclusion criteria encompassed treatment-naive adults with CLL or small lymphocytic lymphoma requiring therapy per the International Workshop on CLL guidelines; eligible trials were phase II/III RCTs reporting PFS, OS, objective response, uMRD, or AEs. The authors conducted comprehensive database searches, applied Cochrane risk-of-bias assessments, and used frequentist NMA with P-scores to rank regimens, complemented by subgroup analyses stratified by age, comorbidities, IGHV status, and cytogenetic features. PFS of acalabrutinib-obinutuzumab in the overall population was found to be statistically superior to that of all chemotherapy-free regimens and chemoimmunotherapies, except for ibrutinib-venetoclax and MRD-guided ibrutinib-venetoclax regimens. Specifically, acalabrutinib-obinutuzumab demonstrated significant benefit compared with ibrutinib (HR = 0.19; 95% CI, 0.12-0.32), zanubrutinib (HR = 0.23; 95% CI, 0.13-0.43), obinutuzumab-venetoclax (HR = 0.34; 95% CI, 0.22-0.53), and ibrutinib-obinutuzumab (HR = 0.56; 95% CI, 0.32-0.98). Both ibrutinib-venetoclax (HR = 0.53; 95% CI, 0.32-0.87) and MRD-guided ibrutinib-venetoclax (HR = 0.43; 95% CI, 0.22-0.85) yielded superior PFS compared with obinutuzumab-venetoclax.[21] Furthermore, they reported that zanubrutinib consistently exhibited the most favorable safety profile, with significantly fewer grade ≥ 3 AEs than were observed with acalabrutinib, acalabrutinib-obinutuzumab, ibrutinib-obinutuzumab, ibrutinib-venetoclax, and obinutuzumab-venetoclax. Acalabrutinib also demonstrated lower rates of severe toxicity compared with ibrutinib-obinutuzumab, ibrutinib-venetoclax, and obinutuzumab-venetoclax. The triplet regimen obinutuzumab-ibrutinib-venetoclax was associated

Table 2. Summary of Findings on Progression-free Survival at 36 Months for VIC Compared to Control Regimens

Outcome no of participants (studies)	Relative effect (95% CI)	Anticipated absolute effects (95% CI)			Certainty
		Control	VIC	Difference	
Progression-free survival at 36 months assessed with: as defined by each trial follow-up: range 38.8 months to 43.7 months no of participants: 970 (2 RCTs)	RR 1.27 (1.14 to 1.42)	50.7%	64.4% (57.8 to 72)	13.7% more (7,1 more to 21,3 more)	⨁⨁⨁◯ Moderate[a]

[a]Risk of bias: Downgraded one levels as Munir[20] were at high RoB due to randomization process and Eichhorst[19] was at some concerns of RoB in the randomisation process and selection of the reported results.
CI, confidence interval; RR, risk ratio; RoB, risk of bias; RCT, randomized controlled trial; VIC, venetoclax-ibrutinib combinations.

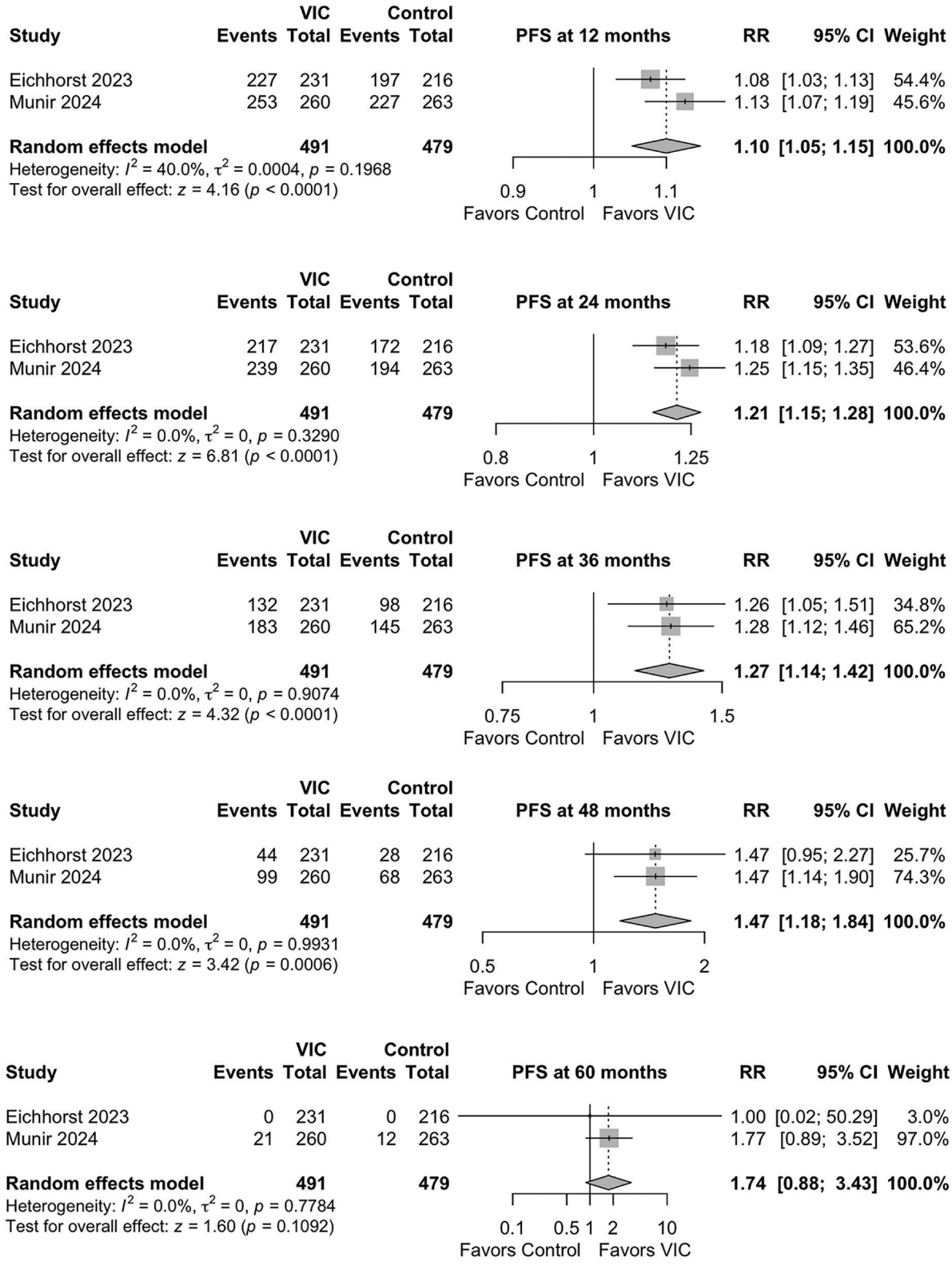

Figure 3. Forest plots of progression-free survival (PFS) during follow-up.

VIC, venetoclax-ibrutinib combinations; RR, risk ratio; CI, confidence interval.

Table 3. Effects of Venetoclax-ibrutinib Combinations on Safety and Tolerability Outcomes

Outcomes	Number of studies	Number of participants	Pooled effect size RR (95% CI)	*P* value	I-square (%)
Overall survival at 36 months	2	970	1.05 (0.93; 1.17)	0.44	71
Death	4	1212	0.70 (0.22; 2.29)	0.56	51
Diarrhea	4	1212	2.10 (1.00; 4.40)	0.49	94
Hypertension	4	1212	2.86 (1.26; 6.49)	0.01	77
Pneumonia	3	1149	0.86 (0.22; 3.30)	0.83	48
Upper respiratory infections	3	1149	0.75 (0.24; 2.33)	0.61	91
Serious or severe AEs	3	1149	1.10 (0.74; 1.62)	0.64	89
Withdrawal due to AEs	3	1162	1.29 (0.43; 3.87)	0.64	67

AEs, adverse events; RR, risk ratio; CI, confidence interval.

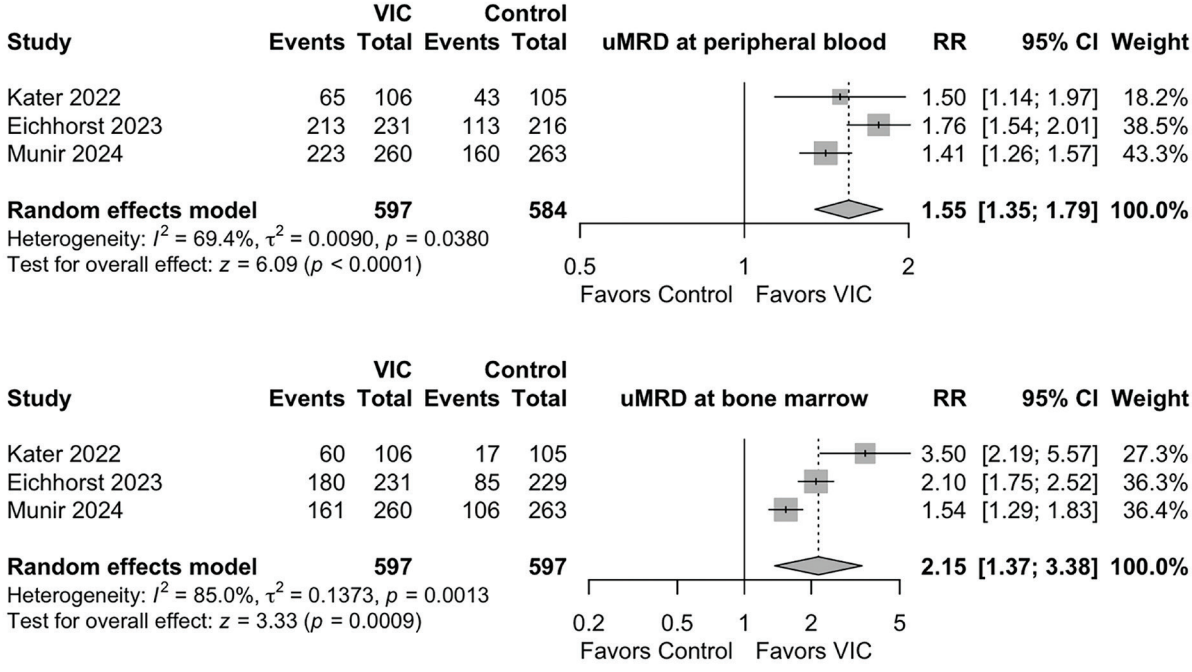

Figure 4. Forest plots of undetected minimal residual disease rates in peripheral blood and bone marrow.

VIC, venetoclax-ibrutinib combinations; uMRD, undetectable minimal residual disease; RR, risk ratio; CI, confidence interval.

with increased dose reductions (> 20%) and treatment discontinuations, whereas ibrutinib-venetoclax carried a higher risk of grade ≥ 3 diarrhea than acalabrutinib, ibrutinib, acalabrutinib-obinutuzumab, and obinutuzumab-venetoclax. Neutropenia rates, both overall and grade ≥ 3, were lowest with zanubrutinib and highest with obinutuzumab-venetoclax. Notably, they found that ibrutinib-venetoclax showed a significantly lower incidence of neutropenia compared with obinutuzumab-venetoclax (any grade: odds ratios (OR) 0.50; 95% CI, 0.26-0.98; grade ≥ 3: OR 0.50; 95% CI, 0.26-0.97).[21]

While the NMA by Wen et al.[21] provides valuable network-level insights by incorporating 30 RCTs and enabling indirect comparisons across diverse regimens, its findings must be interpreted with caution. Notably, the exclusion of the CAPTIVATE trial[17], a pivotal study of venetoclax-ibrutinib with MRD-guided discontinuation, may have introduced bias by underrepresenting key data on time-limited VIC therapy. Moreover, the reliance on indirect comparisons can amplify heterogeneity from varying trial populations and designs. In contrast, our meta-analysis synthesized direct, head-to-head evidence. Additionally, we assessed detailed landmark PFS outcomes at 12, 24, 36, and 48 months that the NMA did not address.

A recently published Bayesian NMA[22] restricted to physically fit, untreated CLL patients synthesized RCTs of first-line targeted regimens (venetoclax, obinutuzumab, ibrutinib, and their combinations) and analyzed PFS and uMRD negativity in PB [MRD(-)PB]. Searches spanned MEDLINE, Embase,

and CENTRAL. The authors found no statistically significant differences between regimens in PFS; however, ibrutinib-rituximab and venetoclax-obinutuzumab-ibrutinib ranked highest according to the surface under the cumulative ranking curves (PFS: 91% and 83% at matched follow-up; 75% and 74% at the longest follow-up). For uMRD in peripheral blood, venetoclax-obinutuzumab-ibrutinib was significantly superior to other targeted options, with large OR; for example, in comparisons with the most similar follow-up: vs. venetoclax-rituximab, OR 10.58 (95% CI 5.46-22.38); vs. venetoclax-obinutuzumab, OR 2.21 (95% CI 1.04-4.94); vs. ibrutinib-rituximab, OR 127.8 (95% CI 59.24-295.77); and vs. ibrutinib-venetoclax, OR 9.43 (95% CI 3.43-27.06).[22]

Our meta-analysis synthesizes direct head-to-head evidence exclusively from RCTs of VIC (with or without obinutuzumab) in untreated patients and quantifies landmark PFS at 12, 24, 36, 48, and 60 months, rather than relying solely on the longest follow-up or on indirect comparisons. We found that VIC significantly prolonged PFS at 12-48 months (RRs 1.10-1.47), with attenuation at 60 months; increased uMRD rates in blood and bone marrow; and revealed no meaningful difference in PFS at 36 months between venetoclax-ibrutinib [RR 1.28 (1.12-1.46)] and venetoclax-obinutuzumab-ibrutinib [RR 1.26 (1.05-1.51)]. In IGHV-defined subgroups, only the 24-month signal favored unmutated IGHV (pinteraction < 0.1). Although all trials applied the standard 10^{-4} threshold, minor methodological differences—such as the use of next-generation sequencing versus flow cytometry, and varying sampling schedules (fixed versus MRD-guided)—may introduce subtle heterogeneity. However, because the sensitivity thresholds were harmonized and concordance between blood and marrow uMRD has been shown to be high, these differences are unlikely to have meaningfully impacted the pooled uMRD estimates in this meta-analysis.

That the study[22] concludes that venetoclax-ibrutinib and venetoclax-obinutuzumab-ibrutinib are among the most effective therapies for prolonging PFS aligns with our observation that triplet therapy is highly efficacious. Importantly, our results extend the literature by demonstrating, with direct evidence, that the doublet (venetoclax-ibrutinib) also achieves robust PFS benefits in untreated CLL, and that adding obinutuzumab did not materially change 36-month PFS in our pooled RCT data. Moreover, to our knowledge, our study is the first meta-analysis built solely on direct randomized evidence on VIC in the frontline setting and the first to provide granular, time-anchored PFS estimates at 12, 24, 36, 48, and 60 months, which can inform shared decision-making regarding time-limited strategies.

Study Limitations

Limitations include heterogeneity in comparator arms (chemoimmunotherapy vs. targeted combinations) and variability in outcomes due to differing definitions and timelines of efficacy endpoints across trials. Nevertheless, the consistent PFS benefit and favorable safety profile support incorporating VIC as a standard frontline option. Although the included RCTs differed in comparator regimens (chemoimmunotherapy vs. targeted agents), subgroup analysis by comparator type could not be performed due to the limited number of studies reporting the primary outcome. This variability should therefore be considered when interpreting the pooled results. Finally, because there is a lack of published systematic reviews and meta-analyses on this subject, we were unable to compare our findings with other studies.

CONCLUSION

Our analysis showed that VIC provides superior disease control compared with established regimens in first-line treatment of CLL, particularly by achieving prolonged PFS and sustained MRD negativity. The inclusion of both fit and older patients across trials strengthens the generalizability of these results.

Ethics

Ethics Committee Approval: This study was a systematic review and meta-analysis of previously published studies and did not involve human participants directly; therefore, ethics committee approval and informed consent were not required.

Acknowledgment

Preliminary results of this study were presented at 11th Society of Hematologic Oncology Türkiye Meeting, April 27-28, 2024, İstanbul and the abstract was published at the Clinical Lymphoma Myeloma and Leukemia.

Footnotes

Author Contributions

Concept Design – L.H.T., A.S.; Data Collection or Processing – L.H.T., A.S.; Analysis or Interpretation – L.H.T., A.S.; Literature Review – L.H.T., A.S.; Writing, Reviewing and Editing – L.H.T., A.S.

Declaration of Interests: The authors declare no conflict of interest regarding the publication of this paper.

Funding: The authors declare no financial support or funding.

REFERENCES

1. Hallek M. Chronic lymphocytic leukemia: 2025 update on the epidemiology, pathogenesis, diagnosis, and therapy. *Am J Hematol*. 2025;100(3):450-480. [CrossRef]
2. Fresa A, Innocenti I, Tomasso A, et al. Treatment sequencing in chronic lymphocytic leukemia in 2024: where we are and where we are headed. *Cancers (Basel)*. 2024;16(11):2011. [CrossRef]
3. Herishanu Y, Katz BZ, Lipsky A, Wiestner A. Biology of chronic lymphocytic leukemia in different microenvironments: clinical and therapeutic implications. *Hematol Oncol Clin North Am*. 2013;27(2):173-206. [CrossRef]
4. Haselager MV, Kater AP, Eldering E. Proliferative signals in chronic lymphocytic leukemia; what are we missing? *Front Oncol*. 2020;10:592205. [CrossRef]
5. Timofeeva N, Jain N, Gandhi V. Ibrutinib and venetoclax in combination for chronic lymphocytic leukemia: synergy in practice. *Blood Neoplasia*. 2024;1(3):100034. [CrossRef]

6. Kielbassa K, Haselager MV, Bax DJC, et al. Ibrutinib sensitizes CLL cells to venetoclax by interrupting TLR9-induced CD40 upregulation and protein translation. *Leukemia*. 2023;37(1):1268-1276. [CrossRef]
7. Thijssen R, Slinger E, Weller K, et al. Resistance to ABT-199 induced by microenvironmental signals in chronic lymphocytic leukemia can be counteracted by CD20 antibodies or kinase inhibitors. *Haematologica*. 2015;100(8):e302-e306. [CrossRef]
8. Pekarsky Y, Balatti V, Croce CM. BCL2 and miR-15/16: from gene discovery to treatment. *Cell Death Differ*. 2018;25(1):21-26. [CrossRef]
9. Deng J, Isik E, Fernandes SM, Brown JR, Letai A, Davids MS. Bruton's tyrosine kinase inhibition increases BCL-2 dependence and enhances sensitivity to venetoclax in chronic lymphocytic leukemia. *Leukemia*. 2017;31(10):2075-2084. [CrossRef]
10. Cervantes-Gomez F, Lamothe B, Woyach JA, et al. Pharmacological and protein profiling suggests venetoclax (ABT-199) as optimal partner with ibrutinib in chronic lymphocytic leukemia. *Clin Cancer Res*. 2015;21(16):3705-3715. [CrossRef]
11. Lu P, Wang S, Franzen CA, et al. Ibrutinib and venetoclax target distinct subpopulations of CLL cells: implication for residual disease eradication. *Blood Cancer J*. 2021;11(2):39. [CrossRef]
12. Wierda WG, Brown J, Abramson JS, et al. Chronic lymphocytic leukemia/small lymphocytic lymphoma, version 2.2024, NCCN Clinical Practice Guidelines in Oncology. *J Natl Compr Canc Netw*. 2024;22(3):175-204. [CrossRef]
13. Higgins JP, Thompson SG, Spiegelhalter DJ. A re-evaluation of random-effects meta-analysis. *J R Stat Soc Ser A Stat Soc*. 2009;172(1):137-159. [CrossRef]
14. Higgins JP, Thompson SG. Quantifying heterogeneity in a meta-analysis. *Stat Med*. 2002;21(11):1539-1558. [CrossRef]
15. Sterne JAC, Savović J, Page MJ, et al. RoB 2: a revised tool for assessing risk of bias in randomised trials. *BMJ*. 2019;366:l4898. [CrossRef]
16. Tanriverdi LH, Aksan F, Aroniadis O, Monzur F. S1P Receptor modulators improve clinical outcomes in ulcerative colitis: a stratified meta-analysis by prior biological use, corticosteroid exposure, and disease characteristics. *J Clin Gastroenterol*. 2025. [CrossRef]
17. Wierda WG, Allan JN, Siddiqi T, et al. Ibrutinib plus venetoclax for first-line treatment of chronic lymphocytic leukemia: primary analysis results from the minimal residual disease cohort of the randomized phase II CAPTIVATE study. *J Clin Oncol*. 2021;39(34):3853-3865. [CrossRef]
18. Kater AP, Owen C, Moreno C, et al. Fixed-duration ibrutinib-venetoclax in patients with chronic lymphocytic leukemia and comorbidities. *NEJM Evid*. 2022;1(7):EVIDoa2200006. [CrossRef]
19. Eichhorst B, Niemann CU, Kater AP, et al. First-line venetoclax combinations in chronic lymphocytic leukemia. *N Engl J Med*. 2023;388(19):1739-1754. [CrossRef]
20. Munir T, Cairns DA, Bloor A, et al. Chronic lymphocytic leukemia therapy guided by measurable residual disease. *N Engl J Med*. 2024;390(4):326-337. [CrossRef]
21. Wen T, Sun G, Jiang W, Steiner K, Bridge S, Liu P. Comparing the efficacy and safety of first-line treatments for chronic lymphocytic leukemia: a network meta-analysis. *J Natl Cancer Inst*. 2025;117(2):322-334. [CrossRef]
22. Stożek-Tutro A, Reczek M, Kawalec P. Efficacy and safety of first-line targeted therapies in physically fit patients with chronic lymphocytic leukemia: a systematic review and network meta-analysis. *Clin Ther*. 2025;47:e12-e20. [CrossRef]

Supplementary Figures

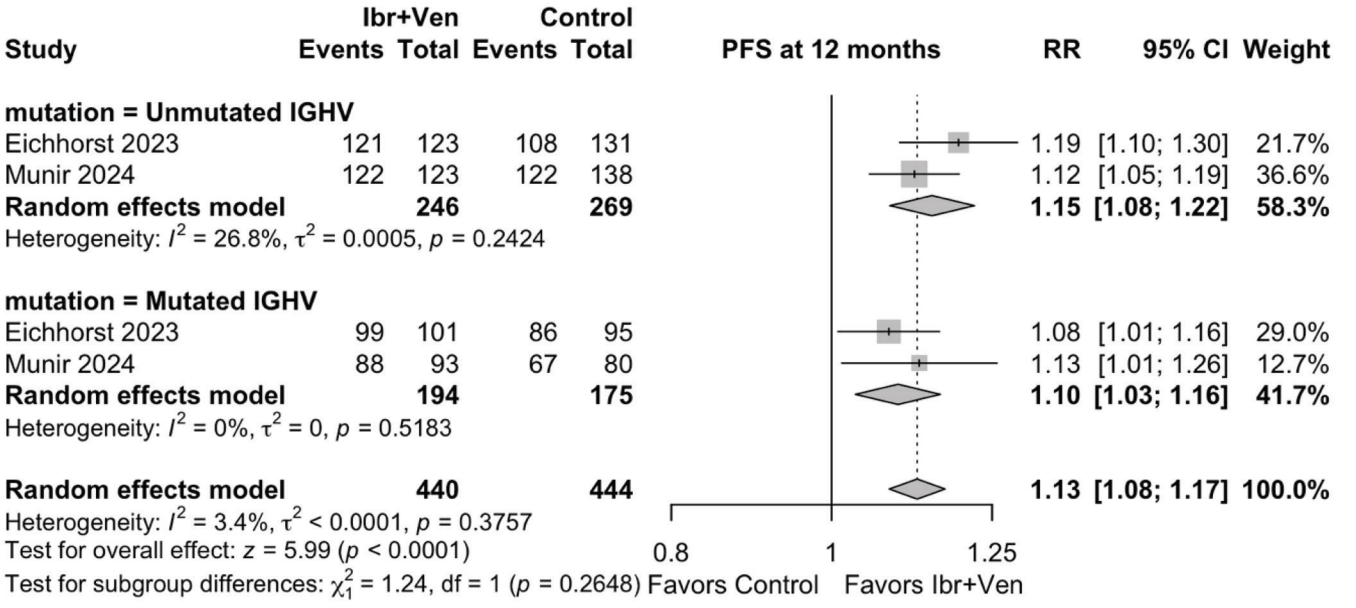

Figure S1. Subgroup analyses of progression-free survival at 12 months by IGHV mutation status.

RR, risk ratio; PFS, progression-free survival; CI, confidence interval; IGHV: immunoglobulin heavy chain variable.

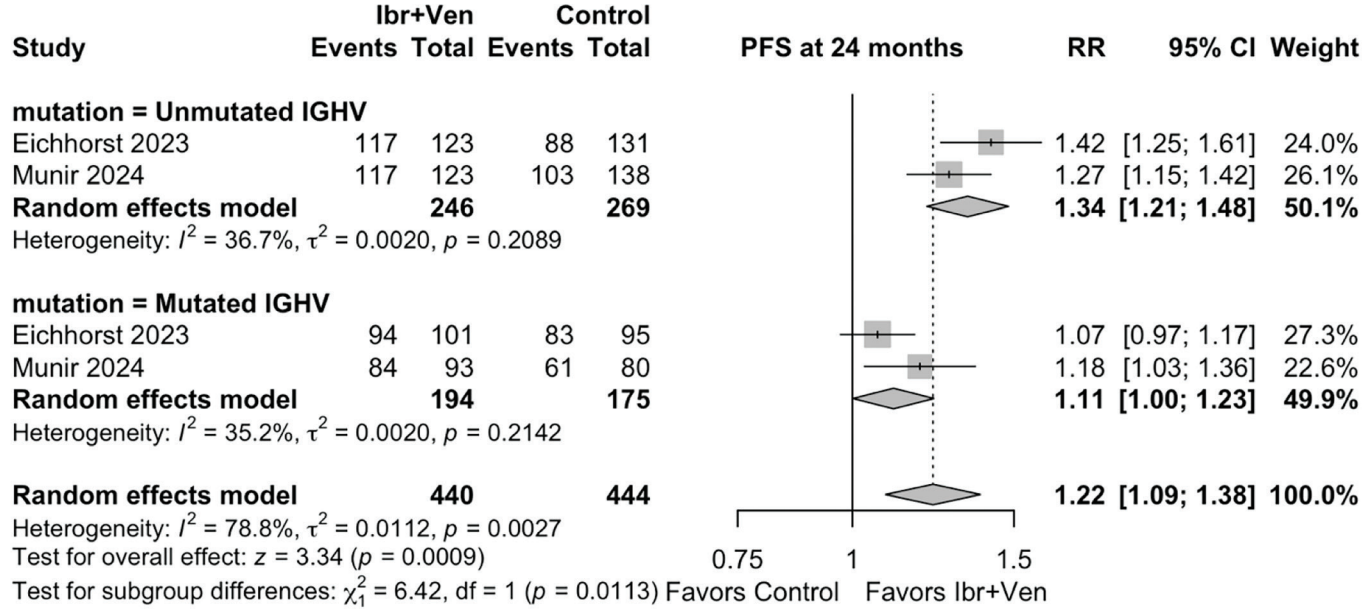

Figure S2. Subgroup analyses of progression-free survival at 24 months by IGHV mutation status.

RR, risk ratio; PFS, progression-free survival; CI, confidence interval; IGHV: immunoglobulin heavy chain variable.

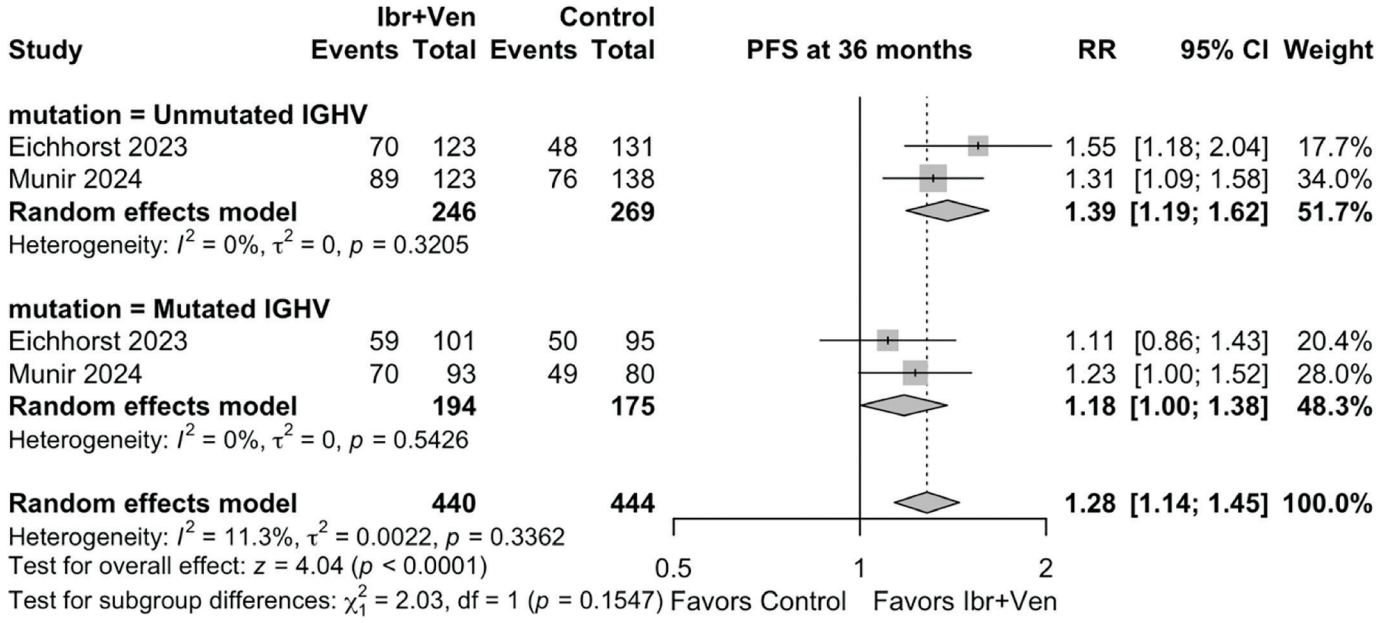

Figure S3. Subgroup analyses of progression-free survival at 36 months by IGHV mutation status.

RR, risk ratio; PFS, progression-free survival; CI, confidence interval; IGHV: immunoglobulin heavy chain variable.

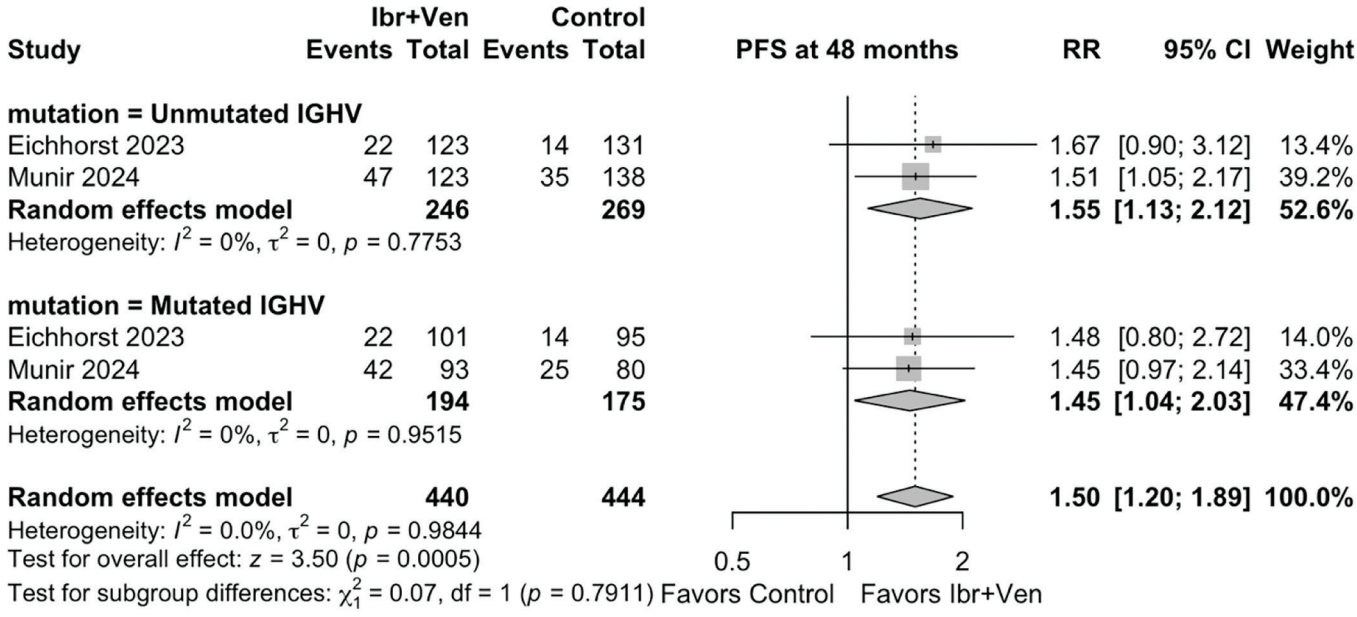

Figure S4. Subgroup analyses of progression-free survival at 48 months by IGHV mutation status.

RR, risk ratio; PFS, progression-free survival; CI, confidence interval; IGHV: immunoglobulin heavy chain variable.

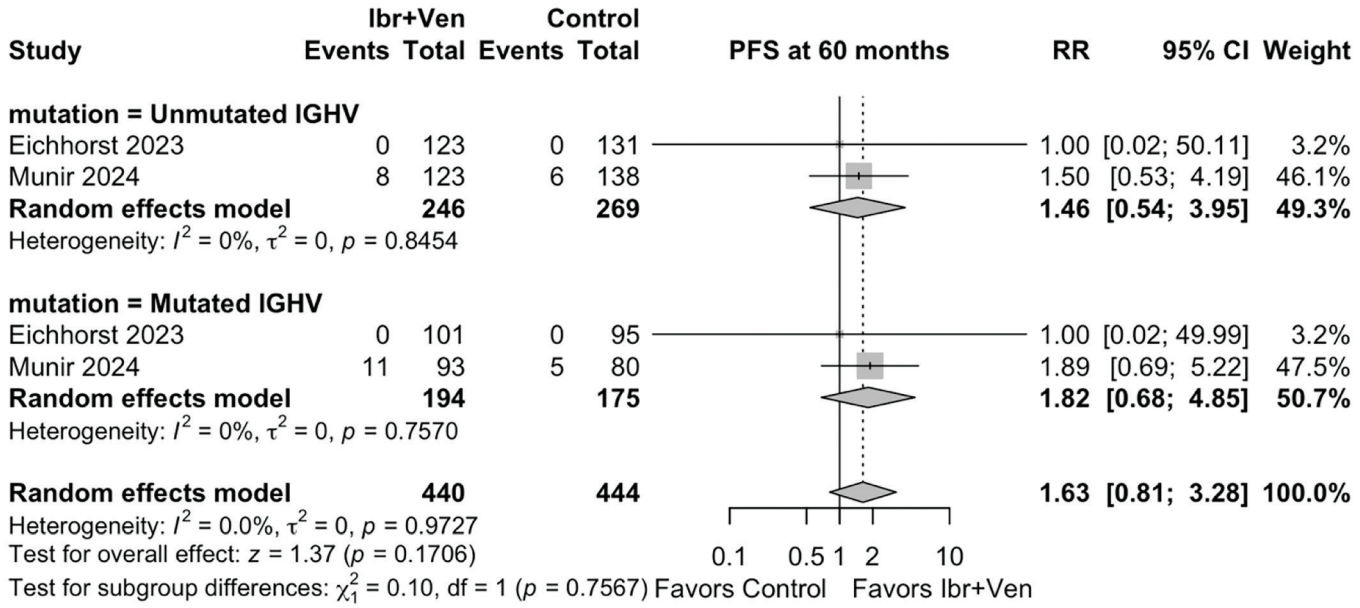

Figure S5. Subgroup analyses of progression-free survival at 60 months by IGHV mutation status.

RR, risk ratio; PFS, progression-free survival; CI, confidence interval.

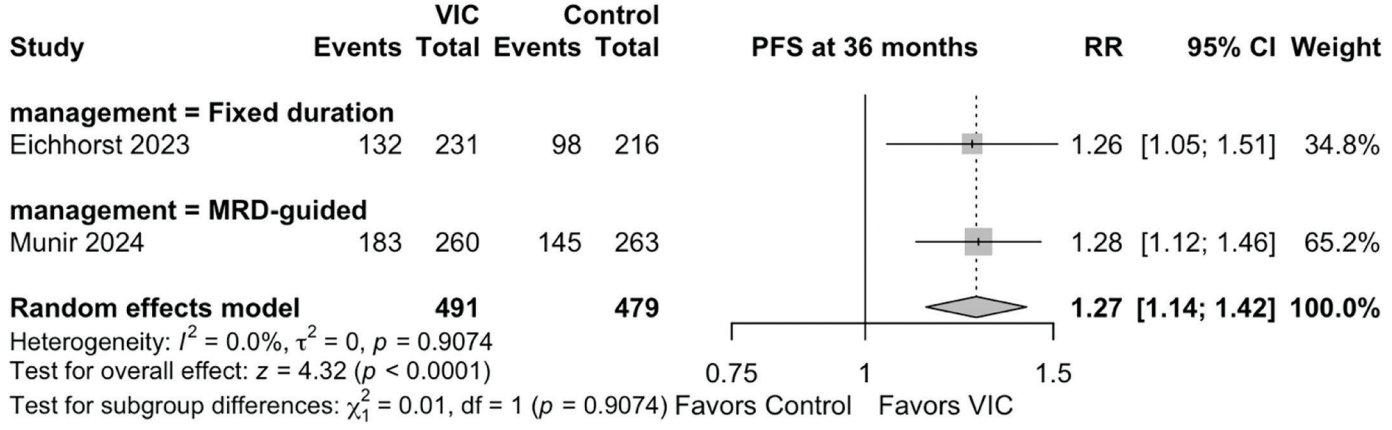

Figure S6. Subgroup analyses of progression-free survival at 36 months by type of management.

RR, risk ratio; PFS, progression-free survival; VIC, venetoclax-ibrutinib combinations.

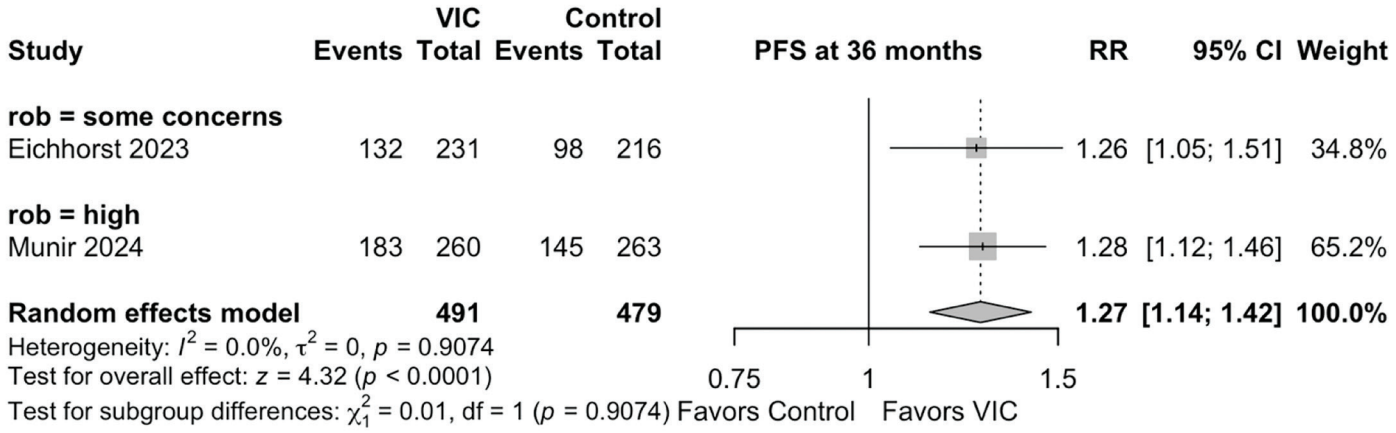

Figure S7. Subgroup analyses of progression-free survival at 36 months by type of risk of bias.

RR, risk ratio; PFS, progression-free survival; VIC, venetoclax-ibrutinib combinations.

ABCResearch

Arch Basic Clin Res 2026;8(1):20-26
DOI: 10.4274/ABCR.2025.25358

Research Article

Investigation of Sensitivity and Specificity of Biochemical Markers for Cardiac Contusion due to Blunt Chest Trauma

Yasin Bilgin[1], Fatih Mehmet Sarı[1], Bekir Elma[2], Mücahit Emet[3], Funda Öz[4]

[1]Department of Emergency Medicine, Erzincan Binali Yıldırım University Faculty of Medicine, Erzincan, Türkiye
[2]Department of Thoracic Surgery, Gaziantep University Faculty of Medicine, Gaziantep, Türkiye
[3]Freelance Emergency Medicine Specialist, İstanbul, Türkiye
[4]Department of Thoracic Surgery, Erzincan Binali Yıldırım University Faculty of Medicine, Erzincan, Türkiye

Cite this article as: Bilgin Y, Sarı FM, Elma B, Emet M, Öz F. Investigation of sensitivity and specificity of biochemical markers for cardiac contusion due to blunt chest trauma. *Arch Basic Clin Res*. 2026;8(1):20-26.

ORCID IDs of the authors: Y.B. 0000-0002-1582-223X, F.M.S. 0009-0007-7022-3751, B.E. 0000-0001-5083-8088, M.E. 0000-0003-2752-8270, F.Ö. 0000-0002-1224-0226.

ABSTRACT

Objective: There remains a significant need for precise biomarkers to diagnose cardiac contusion. The objective of this study is to examine the diagnostic significance of cardiac myosin-binding protein-C (cMyBP-C) in thoracic injuries, including cardiac contusion.

Methods: The inclusion criteria were patients who consented to take part, were over 18 years of age, had sustained severe blunt chest injuries, were admitted within 24 hours post-injury, had their blood samples taken within the first 2 hours of admission, and had at least one of the following injuries: sternal, rib, or left scapular fractures; hemothorax, pneumothorax, pulmonary contusion, traumatic asphyxia, or pneumomediastinum. Troponin I levels ≥ 0.04 ng/mL, measured within 2 hours of admission, are considered the gold standard for diagnosing cardiac contusion. Serum troponin-I concentrations were assessed using an immunochemical technique. Serum cMyBP-C concentrations were measured using an enzyme-linked immunosorbent assay.

Results: Participants included 85 patients, with 59 men (69.4%) and a mean age of 48.6 ± 20.8 years (range: 18-84 years). Among them, 18 individuals (21.2%) experienced cardiac contusion. No significant difference was observed in cMyBP-C levels between the cardiac contusion group and the other group (17.7 ± 18.6 vs. 14 ± 15.3, $P = 0.328$). Receiver operating characteristic analysis revealed that the discriminative performance of cMyBP-C in distinguishing contusion was not statistically significant. In this analysis, the area under the curve for cMyBP-C was 0.575 ± 0.077 (95% confidence interval, 0.425-0.726; $P = 0.328$), indicating poor discriminative ability and a lack of statistically significant diagnostic value for contusion.

Conclusion: While cMyBP-C holds theoretical promise as a cardiomyocyte-specific biomarker, our findings suggest that its current diagnostic performance may be limited in the context of blunt cardiac contusion. Further studies with larger cohorts and refined detection methods are warranted to clarify its clinical utility.

Keywords: Blunt thoracic trauma, cardiac contusion, cardiac myosin binding protein

Corresponding author: Yasin Bilgin, **E-mail:** dr.ysn.blgn@gmail.com

Received: August 18, 2025
Revision Requested: November 10, 2025
Last Revision Received: November 10, 2025
Accepted: November 13, 2025
Publication Date: January 26, 2026

INTRODUCTION

Blunt thoracic trauma and its complications are important causes of trauma-related mortality.[1] Blunt cardiac injuries that develop after blunt thoracic trauma are associated with higher mortality than other organ and system injuries.[2] Forceful impact, rapid deceleration, and crush injuries, when they do not penetrate the chest or heart, are common causes of blunt cardiac trauma. Blunt cardiac injuries can lead to various complications, including myocardial contusion; rupture of the cardiac chambers; dissection, thrombosis, or both of the coronary arteries; and disruption of heart valves.[3] Myocardial contusion is the most common type of blunt cardiac injury (BCI); its incidence is primarily reported in autopsy series because the location and mechanism of injury influence survival.[4] The prevalence of myocardial contusion in individuals with blunt thoracic trauma ranges from 0% to 76%, depending on the diagnostic criteria utilized.[5] Myocardial contusion is an emergency condition requiring prompt recognition and diagnosis. However, the variable nature of the symptoms and the anxiety experienced by the patient after trauma make diagnosis difficult. Although direct chest radiography, multidetector computed tomography (CT), electrocardiography (ECG), cardiac biomarkers, transthoracic or transesophageal echocardiography (TEE), magnetic resonance imaging, focused assessment with sonography in trauma, and nuclear imaging are all used for diagnosis, definitive diagnosis can only be made by direct inspection of the damaged myocardium.[3,6]

ECG is the initial approach for identifying myocardial contusion because it is rapid, simple, inexpensive, and non-invasive. Studies report varying rates of ECG findings such as ST-segment elevation or depression, T-wave inversion, arrhythmias (atrial fibrillation, atrial flutter, supraventricular tachycardia, and premature ventricular complexes), and intraventricular conduction abnormalities, in patients with myocardial contusion.[5] However, its value in diagnosing contusion is controversial. ECG alone has low sensitivity and specificity; both measures improve when findings are supported by cardiac biomarkers.[7,8]

MAIN POINTS

- Electrocardiography (ECG) and a single troponin-I test are insufficient to diagnose blunt cardiac contusion (BCI); neither test alone provides diagnostic accuracy, particularly in the early stages of trauma assessment.
- Serial measurements of cardiac enzymes combined with ECG monitoring improve diagnostic reliability: Repeated troponin-I testing over time, alongside ECG follow-up, enhances diagnostic sensitivity and supports more accurate identification of BCI.
- Troponin-I remains the primary biomarker for BCI, but benefits from serial protocolized testing: Although troponin-I is essential, its diagnostic power increases when it is incorporated into structured testing intervals.
- There is a need for more sensitive biomarkers like cardiac myosin-binding protein-C, until such markers are validated, a multimodal approach is preferable. Emerging markers show promise, but current best practice involves using multiple diagnostic tools over time for optimal management.

Monitoring cardiac biomarkers—creatine kinase (CK), CK-myocardial band (MB) (CK-MB), troponin I (Tn-I), and troponin T is the most widely used method for diagnosing cardiac contusion in emergency services.[9,10] Following trauma, overall CK levels are often high, and CK-MB levels may also be increased. However, these markers are also elevated in severe damage to skeletal muscle, the diaphragm, the liver, or the intestine, in addition to cardiac injury, limiting their utility and reliability. Troponin-I, which is more specific to the myocardium, is a better indicator of myocardial damage[11] than CK-MB and troponin-T. Additionally, high-sensitivity cardiac troponin (hs-cTn) tests are used for the early diagnosis of acute myocardial injury.[11,12] However, its application in the identification of BCI is not definitive, and it provides no additional information compared with the ECG.[3] The usability of methods such as TEE, nuclear imaging, and dual CT is limited due to difficult access, operator dependence, and trauma-related complications. Additionally, insufficient data exist regarding the safety of their use in cardiac contusions.[13,14]

Following cardiac contusion, pathological findings such as intramyocardial hemorrhage, edema, and necrosis of myocardial cells are observed. Because cardiomyocyte damage can be examined histopathologically only in postmortem cases, the need for biomarkers with high sensitivity and specificity persists. While the degradation of thin filament proteins found in cardiac sarcomeres, including cardiac Tn-I and cardiac troponin T, has been used as a marker of cardiac damage, the degradation patterns of thick filament proteins such as titin, myosin, and cardiac myosin-binding protein C (cMyBP-C) and the consequent contractile dysfunction have not been thoroughly examined.[15] The cardiac-specific sarcomere-binding protein cMyBP-C regulates heart structure and function, and has been shown to increase after tissue damage due to myocardial infarction.[16] Additionally, cMyBP-C has been suggested as a cardiomyocyte-specific biomarker and may measure cardiomyocyte damage more accurately than hs-cTn.[17,18] It is recognized for its potential diagnostic and prognostic significance for the treatment of acute coronary syndromes.[16,19] This protein may be a biochemical marker of damage in myocardial contusion.

This study was designed to examine the use of cMyBP-C as an adjunct or alternative to Tn-I in the detection of cardiac contusion.

MATERIAL AND METHODS

Population of the Study

This study was conducted prospectively in the Emergency Department of Atatürk University Faculty of Medicine between September 2015 and June 2016. Eighty-five consecutive patients aged 18 years or older who presented to the emergency department with blunt chest trauma were included in the study. Patients with blunt chest trauma and their relatives who met the study criteria were included in the study group after obtaining their consent. This study was deemed ethically

appropriate by the Atatürk University Non-Interventional Clinical Research Ethics Committee (session number 6, dated 17.09.2015; decision number 03). It was deemed compliant with the ethical rules by the Atatürk University.

Patients were deemed eligible to participate in the study if they met all of the following criteria: were over the age of 18; were admitted to our emergency department within the first 24 hours after the trauma; had high-energy blunt chest trauma (e.g., assault, falls from heights, motor vehicle accidents in- or outside the vehicle, animal attacks, crushing, or being struck by objects); had at least one of the following findings: rib fracture, sternal fracture, hemothorax, pneumothorax, traumatic asphyxia, pulmonary contusion, pneumomediastinum, or left scapular fracture; and had blood drawn for examination within the first 2 hours after presenting to our emergency department.

The study exclusion criteria were as follows: patients who did not agree to participate in the study (n=13); who were under the age of 18; who reported chest pain that started at least 6 hours before the trauma (n=5); who were suspected of having acute coronary syndrome (n=4); who had a history of rhythm disturbance, congestive heart failure, cardiac surgery, chronic renal failure, or cancer (n=7); and who did not have any of the following findings after thoracic trauma: rib fracture, sternum fracture, hemothorax, pneumothorax, traumatic asphyxia, pulmonary contusion, pneumomediastinum, or left scapula fracture (n=92).

Marker Accepted in the Study for Cardiac Contusion Diagnosis

A Tn-I level of 0.04 ngmL or higher at initial presentation to the emergency department (within the first 2 hours) was considered indicative of cardiac contusion. Serum Tn-I levels were measured by the immunochemical method (Beckman Coulter UniCel DxI 600, USA). The measurement (reference) range of the Tn-I kit used was 0.01-40 ng/mL.

Data Collection

After clinical evaluation and stabilization, patients who met the above criteria underwent assessment for cardiac contusion using ECG and troponin measurement. In addition to the ECG and troponin I levels measured in patients with suspected cardiac contusion as part of the routine trauma protocol in the emergency department, and after obtaining consent from the patients or their relatives, blood was drawn from these patients into biochemistry tubes to measure their cMyBP-C levels. The samples were centrifuged at 4000 rpm for 15 minutes at +4°C within 1 hour of collection and stored at -80°C in a deep freezer. The storage periods in the deep freezer varied between 10 days and 24 months.

Data on patients' demographic characteristics (such as age and gender), cause and time of trauma, time of hospital admission, known diseases, vital signs, ECG findings on arrival, cardiac troponin levels, and accompanying traumas were recorded. Serum cMyBP-C levels were measured using the enzyme-linked immune sorbent assay (ELISA) method using the ''Human CMyBP-C Binding Protein (MYCBP) ELISA Kit'' (Bioassay Technology Laboratory, lot no:20151123, China) according to the manufacturer's instructions. Concentrations were calculated using the ELISA reader's KC Junior software (Bio-Tek Inc.). The intra-assay coefficient of variation (CV) of the MYCBP kit is below 8% and the inter-assay CV is below 10%.

Statistical Analysis

Statistical analyses were performed using the SPSS software package (Version 22.0; IBM Corp., Armonk, NY, USA). Continuous variables were presented as median (min-max) and/or mean ± standard deviation (SD), whereas categorical variables were expressed as frequencies and percentages. The normality of the data distribution was evaluated using the Shapiro-Wilk test, and the homogeneity of variances was assessed using Levene's test.

For comparisons between two independent groups, the Student's t-test was applied to normally distributed variables, whereas the Mann-Whitney U test was used for non-normally distributed variables. Categorical variables were compared using the chi-square (χ^2) test.

A receiver operating characteristic (ROC) curve analysis was performed to assess the diagnostic performance of cMyBP-C for predicting the presence of a contusion. The area under the ROC curve (AUC) was calculated, together with its standard error and 95% confidence interval (CI). A P value < 0.05 was considered statistically significant.

RESULTS

A total of 85 patients, 59 (69.4%) of whom were male, were included in the study. As the gold standard, a troponin I level of 0.04 ng/mL or higher at initial admission to the emergency department (within the first 2 hours) was considered diagnostic of cardiac contusion. According to this gold standard, 18 patients (21.2%) had cardiac contusion. Patient characteristics, vital signs, and Glasgow Coma Scale (GCS) are summarized in Table 1.

The mean age was 48.1 ± 21.4 years in the cardiac contusion (-) group and 50.6 ± 18.7 years in the cardiac contusion (+) group. However, this difference was not statistically significant (P = 0.649). The proportion of males was 71.6% in the cardiac contusion (-) group and 61.1% in the cardiac contusion (+) group. There was also no significant difference in gender distribution (P = 0.389). The median (min-max) of systolic blood pressure in the contusion (+) group was 117 (64-180), and the mean (Mean ± SD) was 116.3 ± 25.4, which was lower than the mean in the contusion (-) group. However, this difference was not statistically significant (P =0.070). Nevertheless, a tendency toward decreased blood pressure was observed in the presence of cardiac contusion.

Diastolic blood pressure was also lower in the contusion (+) group (69.1 ± 20.4), but this difference was not statistically significant (P = 0.138). The mean pulse in the contusion (+) group was 93.6 ± 24.6, and in the (-) group was 86.9 ± 15.1. However, this difference was also not statistically significant (P = 0.285). No significant differences were observed between the two groups for respiratory rate, fever, and oxygen saturation (P = 0.833, 0.396, and 0.935, respectively). The mean ± SD and

median (min-max) of GCS in the contusion (+) group were 11.7 ± 5.5 and 15 (3-15), respectively; in the contusion (-) group, they were 14.2 ± 2.7 and 15 (3-15), respectively. This indicates that cardiac contusion reduces GCS, although this reduction was not statistically significant (P = 0.058).

ECG Findings

When the ECGs collected in our study were examined, normal sinus rhythm was detected in 50 of the 85 patients (58.8%). The most common pathological finding was sinus tachycardia, observed in 18 patients (21.2%). Table 2 lists the ECG changes observed in the patients, ordered by frequency.

Analysis of cMyBP-C According to Troponin-I

The median (min–max) and mean cMyBP-C values in cardiac contusion (+) patients are higher than those in cardiac contusion (-) patients. However, no statistically significant difference was detected (Table 3).

Diagnostic Value of cMyBP-C in Detecting Cardiac Contusion

According to the ROC analysis, the discriminatory power of CMyBP-C levels for the diagnosis of contusion was not statistically significant (AUC = 0.575; SE = 0.077; 95% CI: 0.425-0.726; P = 0.328). The obtained AUC was close to 0.5, indicating that the CMyBP-C had limited diagnostic value for detecting contusion (Figure 1).

Table 1. The Characteristics of the Population

Characteristics	Total n=85	Cardiac contusion (-) n=67	Cardiac contusion (+) n=18	*P*
Age*	48.6 ± 20.8	48.1 ± 21.4	50.6 ± 18.7	0.649
Male*	59 (69.4%)	48 (71,6%)	11 (61.1%)	0.389
Systolic blood pressure**				
Median (min-max)	122 (64-191)	123 (80-191)	117 (64-180)	0.070
Mean ± SD	126.1 ± 23.7	128.7 ± 22.7	116,3 ± 25,4	
Diastolic blood pressure*	75.2 ± 14.6	76.9 ± 12.3	69.1 ± 20.4	0.138
Pulse*	88.4 ± 17.6	86.9 ± 15.1	93.6 ± 24.6	0.285
Respiratory rate**				
Median (min-max)	17 (10-38)	17 (10-34)	17 (12-38)	0.833
Mean ± SD	16.9 ± 3.8	16.8 ± 3.2	17.4 ± 5.8	
Fever*	36.2 ± 0.52	36.2 ± 0.53	36.1 ± 0.52	0.396
Oxygen saturation**				
Median (min-max)	93 (68-100)	93 (70-99)	93.5 (68-100)	0.935
Mean ± SD	92 ± 5.5	92.1 ± 5.2	91.5 ± 6.9	
GCS**				
Median (min-max)	15 (3-15)	15 (3-15)	15 (3-15)	0.058
Mean ± SD	13.6 ± 3.6	14.2 ± 2.7	11.7 ± 5.5	

P value of < 0.05 was considered statistically significant. *According to the Student's *t*-test, **according to the Mann-Whitney U test was used.
GSC, Glasgow Coma Scale; SD, standard deviation.

Table 2. ECG Changes of the Patients

ECG findings	n (85)	%
Normal sinus rhythm	50	58.8
Sinus tachycardia	17	20
T (-) in the anterior	5	5.9
Early repolarization	3	3.5
Ventricular extra beat	3	3.5
Sinus bradycardia	2	2.4
Sinus arrhythmia	2	2.4
Right bundle branch block	2	2.4
Atrial fibrillation	1	1.2

ECG, electrocardiography.

Table 3. Mean Levels of cMyBP-C in Cardiac Contusion Negative and Positive Patients

Feature	Cardiac contusion (-) n=(67)	Cardiac contusion (+) n=(18)	*P**	Total
cMyBP-C Median (min-max) Mean ± SD	7.2 (1.6-56.1) 14 ± 15.3	9 (3.6-55.9) 17.7 ± 18.6	0,328	7.3 (1.6-56.1) 14.8 ± 16

*P value of < 0.05 was considered statistically significant according to Mann-Whitney U test.
cMyBP-C, cardiac myosin-binding protein-C; SD, standard deviation.

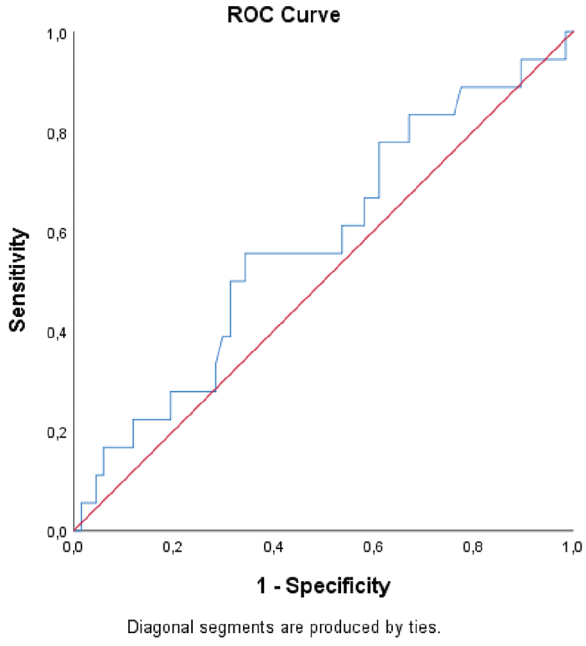

Figure 1. ROC value of cMyBP-C in determining cardiac contusion.

ROC, receiver operating characteristic; cMyBP-C, cardiac myosin-binding protein-C.

DISCUSSION

Cardiac contusion is an important and insidious injury that is often overlooked in trauma patients, is difficult to diagnose, and can affect morbidity and mortality. Despite numerous studies on cardiac contusions, are no universally accepted diagnostic criteria for trauma patients admitted to emergency departments. The cMyBP-C protein is crucial for cardiac contraction. It is thought that the concentration of this protein may increase in the blood early after cardiac contusion due to cellular damage. Therefore, in this study investigating the sensitivity and specificity of biochemical markers in cardiac contusion caused by blunt chest trauma, cMyBP-C levels were examined in patients who had troponin (+) and were considered to have cardiac contusion.

Troponin and CK-MB are initial screening tools used to detect cardiac injury. The increased sensitivity and specificity relative to creatine phosphokinase-MB are due to the presence of serum cardiac troponins, which are regulatory contractile proteins exclusive to heart muscle cells and absent from skeletal muscle. When the cardiac muscle is damaged, membrane integrity is disrupted, leading to the release of cardiac troponins into the bloodstream. Troponin is considered invaluable in the diagnosis of heart damage; positive serum cardiac troponins accurately diagnose cardiac contusion, whereas negative serum troponins strongly indicate the absence of disease.[14] Among the markers used to detect myocardial damage to date, Tn-I is a more specific marker for detecting cardiac contusion.[5]

Nonetheless, it is important to acknowledge that considerable cardiac damage may occur without significant troponin elevation. Studies have also reported that patients with initially normal Tn-I who showed increases after 24 hours were positive for BCI, and it has been suggested that troponin release may reflect secondary ischemic insults—hemorrhage or shock—rather than direct myocardial contusion in severely injured patients.[7] Another study demonstrated that patients receiving pre-hospital norepinephrine treatment had notably higher troponin levels, and that these levels are significantly associated with mortality in patients with BCI.[20] The study, which evaluated the precision of diagnostic assessments for identifying BCI and reviewed the literature over an extended period, reported that Tn-I had a sensitivity of 64.4% and a specificity of 84.1%. Also, ECG demonstrated a sensitivity of 55.1% and a specificity of 84.5% in the same study. However, when both ECG and Tn-I are positive, the diagnostic sensitivity for BCI is reduced. Conversely, when only one test is positive, sensitivity increases while specificity decreases. A normal ECG combined with a normal Tn-I level is highly effective in excluding BCI.[14]

In our study of 85 patients with blunt chest trauma, Tn-I values measured at initial presentation (< 2 hours) were elevated in 18 (21.2%). In light of all this literature, we accepted it as the gold-standard diagnostic test and considered Tn-I (+) patients to have cardiac contusion.

The ECG is a simple, rapid, non-invasive, and crucial diagnostic tool for detecting BCI in patients with recent chest trauma. However, the value of ECG changes in diagnosing cardiac contusion remains highly controversial. The ECG after a BCI may be normal or exhibit abnormalities.[9] ECG abnormalities may result from catecholamine release provoked by traumatic stress. However, lung pathologies, existing coronary artery disease, hypovolemia, abnormal arterial blood gases, serum electrolyte and pH disturbances, and changes in vagal tone may also cause changes on the ECG. The type of disturbance in BCI depends on the injured portion of the heart.[21] Because the left ventricle has greater myocardial mass, ECG findings primarily reflect its electrical activity, making the test relatively insensitive to right ventricular involvement. Mild right ventricular contusions may produce only nonspecific ECG changes, whereas more severe

injury may lead to a transient right bundle branch block.[22] For these reasons, the reliability of the ECG alone for the diagnosis of cardiac contusion is debatable. In this study, ECG abnormalities were detected in 35 (41.2%) of 85 patients. In many studies, the most common ECG abnormalities were ST-segment and T-wave changes, and supraventricular tachycardias.[5,23] In our study, we detected sinus tachycardia as the most common ECG abnormality.

During tachycardia, stimulation of β-adrenergic receptors activates intracellular signaling pathways that enhance myocardial contractility. In this context, phosphorylation of cMyBP-C, a cardiac-specific sarcomeric regulatory protein, enhances contractile efficiency by modulating the structural and functional dynamics of the myocardium. Importantly, cMyBP-C is released into the circulation when cardiomyocytes are injured; studies in both rats and humans with acute myocardial infarction (MI) have demonstrated that plasma cMyBP-C levels rise significantly within the first hour post-infarction—before any detectable increase in Tn-I—supporting its role as a rapid, cardiomyocyte-specific biomarker.[16,18,24] Moreover, cMyBP-C has been shown to correlate closely with infarct size and is highly specific for cardiac injury, potentially outperforming high-sensitivity troponins in early MI detection.[17,19]

In contrast, when we examined patients with blunt myocardial injury, we found that—despite its mechanistic plausibility—plasma cMyBP-C levels did not increase significantly in Tn-I–positive cases. In this context, cMyBP-C phosphorylation under adrenergic stress may facilitate contractility; however, its release kinetics and the sensitivity of current assays limit its diagnostic utility in the setting of blunt trauma. Possible explanations include (1) degradation fragments that are rapidly cleared or present at concentrations below assay detection thresholds, (2) non-infarct-mediated mechanisms (e.g., increased proteolysis without full cardiomyocyte necrosis), and (3) confounding hemodynamic factors that alter cMyBP-C release independently of direct myocyte injury. Although cMyBP-C is a promising early biomarker in ischemic MI—where its plasma rise precedes detection by conventional troponin assays—its role in blunt cardiac contusion remains uncertain. Future research involving larger cohorts, serial time-point sampling, and more sensitive immunoassays may yet reveal a complementary role for cMyBP-C within a multimodal biomarker panel alongside troponin and ECG.

Study Limitations

Limitations of our study include its single-center design, modest sample size, and the exclusion of 12 patients who succumbed acutely to severe trauma, which may have skewed the true incidence and spectrum of BCI. Moreover, the absence of a universally agreed biomarker cut-off for cMyBP-C and the heterogeneity of our ECG and enzyme measurement intervals may have attenuated our ability to detect subtle patterns.

CONCLUSION

Neither an ECG nor a single troponin-I measurement provides a definitive diagnosis of blunt cardiac contusion. Rather, a combination of serial cardiac enzyme sampling and ECG monitoring enhances diagnostic accuracy. Troponin-I remains the cornerstone biomarker for BCI; its diagnostic sensitivity can be improved by protocolized serial testing. The search for additional, more sensitive markers, such as cMyBP-C, continues, but until a consensus emerges, a multimodal, time-dependent diagnostic approach offers the best strategy for identifying and managing cardiac contusions in trauma patients.

Ethics

Ethics Committee Approval: This study was deemed ethically appropriate by the Atatürk University Non-Interventional Clinical Research Ethics Committee (session number 6, dated 17.09.2015; decision number 03).

Informed Consent: Patients with blunt chest trauma and their relatives who met the study criteria were included in the study group after obtaining their consent.

Acknowledgments

This study, titled "Investigation of the Sensitivity and Specificity of Biochemical Markers for Cardiac Contusion Due to Blunt Chest Trauma," was approved by the Atatürk University Department of Emergency Medicine as a specialist thesis by Dr. Yasin Bilgin, under the supervision of Assoc. Prof. Dr. Mücahit Emet.

Footnotes

Author Contributions

Concept Design – Y.B., M.E.; Data Collection or Processing – Y.B., B.E.; Analysis or Interpretation – Y.B., M.E.; Literature Review - Y.B., F.M.S., M.E.; Writing, Reviewing and Editing – Y.B., F.M.S., B.E., M.E., F.Ö.

Declaration of Interests: The authors declare that they have no conflicts of interest.

Funding: The authors declare that this study has received no financial support.

REFERENCES

1. Dogrul BN, Kiliccalan I, Asci ES, Peker SC. Blunt trauma related chest wall and pulmonary injuries: an overview. *Chin J Traumatol.* 2020;23(3):125-138. [CrossRef]
2. Huis In 't Veld MA, Craft CA, Hood RE. Blunt cardiac trauma review. *Cardiol Clin*. 2018;36(1):183-191. [CrossRef]
3. Galvagno SM Jr, Nahmias JT, Young DA. Advanced Trauma Life Support® Update 2019: management and applications for adults and special populations. *Anesthesiol Clin*. 2019;37(1):13-32. [CrossRef]
4. El-Qawaqzeh K, Anand T, Richards J, et al. Predictors of mortality in blunt cardiac injury: a nationwide analysis. *J Surg Res.* 2023;281:22-32. [CrossRef]
5. Van Lieshout EMM, Verhofstad MHJ, Van Silfhout DJT, Dubois EA. Diagnostic approach for myocardial contusion: a retrospective evaluation of patient data and review of the literature. *Eur J Trauma Emerg Surg*. 2021;47(4):1259-1272. [CrossRef]

6. Lee C, Jebbia M, Morchi R, Grigorian A, Nahmias J. Cardiac trauma: a review of penetrating and blunt cardiac injuries. *Am Surg.* 2025;91(3):423-433. [CrossRef]
7. Emet M, Akoz A, Aslan S, Saritas A, Cakir Z, Acemoglu H. Assessment of cardiac injury in patients with blunt chest trauma. *Eur J Trauma Emerg Surg.* 2010;36(5):441-447. [CrossRef]
8. Sade R, Kantarci M, Ogul H, et al. The feasibility of dual-energy computed tomography in cardiac contusion imaging for mildest blunt cardiac injury. *J Comput Assist Tomogr.* 2017;41(3):354-359. [CrossRef]
9. Norton MJ, Stanford GG, Weigelt JA. Early detection of myocardial contusion and its complications in patients with blunt trauma. *Am J Surg.* 1990;160(6):577-581. [CrossRef]
10. Sağlam Gürmen E, Tulay CM. Attention: cardiac contusion. *Ulus Travma Acil Cerrahi Derg.* 2022;28(5):634-640. [CrossRef]
11. Elma B, Mammadov R, Süleyman H, et al. The effect of rutin on experimentally induced acute heart contusion in rats: Biochemical and histopathological evaluation. *Ulus Travma Acil Cerrahi Derg.* 2022;28(8):1073-1081. [CrossRef]
12. Saenger AK, Beyrau R, Braun S, et al. Multicenter analytical evaluation of a high-sensitivity troponin T assay. *Clin Chim Acta.* 2011;412(9-10):748-754. [CrossRef]
13. Emet M, Saritemur M, Altuntas B, et al. Dual-source computed tomography may define cardiac contusion in patients with blunt chest trauma in ED. *Am J Emerg Med.* 2015;33(6):865.e1-e3. [CrossRef]
14. Kyriazidis IP, Jakob DA, Vargas JAH, et al. Accuracy of diagnostic tests in cardiac injury after blunt chest trauma: a systematic review and meta-analysis. *World J Emerg Surg.* 2023;18(1):36. [CrossRef]
15. Govindan S, McElligott A, Muthusamy S, et al. Cardiac myosin binding protein-C is a potential diagnostic biomarker for myocardial infarction. *J Mol Cell Cardiol.* 2012;52(1):154-164. [CrossRef]
16. Kozhuharov N, Wussler D, Kaier T, et al. Cardiac myosin-binding protein C in the diagnosis and risk stratification of acute heart failure. *Eur J Heart Fail.* 2021;23(5):716-725. [CrossRef]
17. Kaier TE, Twerenbold R, Puelacher Cet al. Direct comparison of cardiac myosin-binding protein c with cardiac troponins for the early diagnosis of acute myocardial infarction. *Circulation.* 2017;17;136(16):1495-1508. Epub 2017;26. Erratum in: *Circulation.* 2017;19;136(25):e469. [CrossRef]
18. Marjot J, Liebetrau C, Goodson RJ, et al. The development and application of a high-sensitivity immunoassay for cardiac myosin-binding protein C. *Transl Res.* 2016;170:17-25.e5. [CrossRef]
19. Kuster DW, Cardenas-Ospina A, Miller L, et al. Release kinetics of circulating cardiac myosin binding protein-C following cardiac injury. *Am J Physiol Heart Circ Physiol.* 2014;306(4):H547-H556. [CrossRef]
20. Kalbitz M, Pressmar J, Stecher J, et al. The role of troponin in blunt cardiac injury after multiple trauma in humans. *World J Surg.* 2017;41(1):162-169. [CrossRef]
21. Yousef R, Carr JA. Blunt cardiac trauma: a review of the current knowledge and management. *Ann Thorac Surg.* 2014;98(3):1134-1140. [CrossRef]
22. Scagliola R, Seitun S, Balbi M. Cardiac contusions in the acute care setting: Historical background, evaluation and management. *Am J Emerg Med.* 2022;61:152-157. [CrossRef]
23. Biffl WL, Fawley JA, Mohan RC. Diagnosis and management of blunt cardiac injury: What you need to know. *J Trauma Acute Care Surg.* 2024;96(5):685-693. [CrossRef]
24. Marjot J, Kaier TE, Martin ED, et al. Quantifying the release of biomarkers of myocardial necrosis from cardiac myocytes and intact myocardium. *Clin Chem.* 2017;63(5):990-996. [CrossRef]

ABCResearch

Arch Basic Clin Res 2026;8(1):27-34
DOI: 10.4274/ABCR.2025.25364

Research Article

Diagnostic Value of Initial Laboratory Parameters in Predicting Hemothorax among Adult Patients with Isolated Blunt Thoracic Trauma Presenting to the Emergency Department: A Retrospective Observational Study

Veysi Siber[1], Sinan Özdemir[2], Serdal Ateş[3], Zafer Beşer[1], Hatice Kübra Siber[4], Meryem Sara Dayan[1], Ahmet Burak Erdem[1]

[1]Clinic of Emergency Medicine, University of Health Scienes Türkiye, Ankara Etlik City Hospital, Ankara, Türkiye
[2]Clinic of Emergency Medicine, Düzce Atatürk State Hospital, Düzce, Türkiye
[3]Clinic of Emergency Medicine, University of Health Sciences Türkiye, Ankara Training and Research Hospital, Ankara, Türkiye
[4]Department of Family Medicine, Reyhanlı District Health Directorate, Hatay, Türkiye

Cite this article as: Siber V, Özdemir S, Ateş S, et al. Diagnostic value of initial laboratory parameters in predicting hemothorax among adult patients with isolated blunt thoracic trauma presenting to the emergency department: a retrospective observational study. *Arch Basic Clin Res.* 2026;8(1):27-34.

ORCID IDs of the authors: V.S. 0000-0003-2856-8303, S.Ö. 0000-0001-7396-0529, S.A. 0000-0003-2224-2134, Z.B. 0000-0001-6373- 8588, H.K.S. 0009-0008-2947-3932, M.S.D. 0009-0008-1580-6492, A.B.E. 0000-0002-3618-6252.

ABSTRACT

Objective: Hemothorax is a serious complication of blunt thoracic trauma requiring early recognition. While computed tomography (CT) is the diagnostic gold standard, imaging delays in unstable patients necessitate alternative early markers. This study evaluated the predictive value of initial laboratory parameters in adult patients with isolated blunt thoracic trauma.

Methods: This retrospective study included adults with isolated blunt thoracic trauma presenting to a tertiary emergency department between March 1, 2023, and March 1, 2024. Based on CT findings, patients were categorized as hemothorax-positive or hemothorax-negative. Demographic data, admission laboratory results, and outcomes were extracted from the hospital information system. Laboratory variables included complete blood count, platelet indices, venous blood gas analysis, lactate, and coagulation parameters. Group comparisons were conducted to assess the associations between these variables and the presence of hemothorax.

Results: A total of 414 patients were evaluated (median age: 55 years; 69.8% male). Hemothorax was identified in 171 patients (41.3%) based on chest CT. Compared with the non-hemothorax group, the hemothorax group had significantly higher median white blood cell counts ($P = 0.027$), lymphocyte counts ($P = 0.032$), and serum lactate levels ($P < 0.001$), whereas venous pH values were significantly lower ($P < 0.001$).

Conclusion: Elevated white blood cell, lymphocyte count, lactate levels, and decreased venous pH at admission may help predict hemothorax in isolated blunt chest trauma, especially when imaging is delayed. Platelet indices showed no diagnostic utility.

Keywords: Blunt trauma, hemothorax, lactic acid, lymphocyte, emergency service, hospital

Corresponding author: Veysi Siber, **E-mail:** veysiber.ss@gmail.com

Received: August 13, 2025
Revision Requested: November 4, 2025
Last Revision Received: September 22, 2025
Accepted: December 2, 2025
Publication Date: January 26, 2026

INTRODUCTION

Thoracic trauma is a significant contributor to trauma-related morbidity and mortality worldwide, accounting for roughly 10-15% of trauma cases presenting to emergency departments (EDs).[1,2] Blunt thoracic trauma commonly results from mechanisms such as motor vehicle collisions, falls from a height, and physical assault, with mortality rates ranging from 10% to as high as 60%.[3] Hemothorax, which occurs as a consequence of blunt thoracic trauma, is characterized by the accumulation of blood in the pleural cavity and, if not promptly diagnosed, may lead to severe impairments in respiratory mechanics, gas exchange, and hemodynamic stability.[4,5]

The diagnosis of hemothorax should involve an integrated assessment of clinical findings, radiologic imaging, and laboratory parameters.[6] Although chest computed tomography (CT), a routinely used imaging modality, can accurately identify the presence and extent of hemothorax, the need for early clinical decision-making before imaging highlights the potential role of laboratory markers.[7,8] In particular, complete blood count (CBC) parameters, lactate levels, blood gas findings, and coagulation tests may assist in predicting both hemodynamic status and possible pleural pathologies in trauma patients.[9]

In trauma populations, lactate levels are widely recognized as markers of tissue hypoperfusion and have been associated with increased mortality.[10] Moreover, growing evidence suggests that hematologic markers such as platelet indices [mean platelet volume (MPV), platelet distribution width (PDW), platelet large cell ratio (P-LCR)] may reflect the inflammatory response and thrombotic tendency following trauma.[11] However, the predictive value of these parameters in identifying hemothorax remains unclear. Within this framework, assessing the relationship between initial ED laboratory findings and the occurrence of hemothorax is crucial for early risk stratification and for guiding optimal treatment decisions.

This study sought to determine the diagnostic utility of initial laboratory parameters for predicting hemothorax in adult patients with isolated blunt thoracic trauma presenting to the ED.

MAIN POINTS

- Higher admission white blood cell and lymphocyte counts are significantly associated with the presence of hemothorax in adults with isolated blunt thoracic trauma. Increased serum lactate levels and decreased venous pH values may serve as early biochemical indicators for diagnosing hemothorax.
- Platelet indices (mean platelet volume, platelet distribution width, platelet–large cell ratio) showed no significant diagnostic value in predicting the presence of hemothorax.
- In situations where imaging may be delayed, these laboratory parameters can provide early risk stratification and support clinical decision-making.

MATERIAL AND METHODS

Study Design and Setting

This retrospective observational study, conducted at a single center, was reported in accordance with the Strengthening the Reporting of Observational Studies in Epidemiology guidelines to ensure methodological transparency and completeness. It incorporated both descriptive and analytical components. Ethical approval was granted by the Clinical Research Ethics Committee of University of Health Scienes Türkiye, Ankara Etlik City Hospital (approval no.: AEŞH-BADEK-2024-307, date: 03.04.2024), and the study adhered to the principles outlined in the Declaration of Helsinki. As all data were anonymized, the requirement for informed consent was waived.

Participants

Adults aged 18 years or older who presented to the ED with isolated blunt thoracic trauma between March 1, 2023, and March 1, 2024, were enrolled. Based on chest CT results, relevant specialist consultations, and clinical assessments, patients were classified as hemothorax-positive or hemothorax-negative.

Exclusion criteria

- Pregnant patients,
- Active external bleeding,
- Cases with documented liver or splenic laceration,
- Penetrating thoracic trauma,
- Receiving anticoagulant therapy,
- Concomitant bleeding from other organ systems,
- A known pre-existing hematologic disorder (e.g., thrombocytopenia, myelodysplastic syndrome, leukemia),
- Underwent major surgery within the past month,
- Missing laboratory or imaging data,
- Patients whose medical records could not be accessed or whose diagnoses were uncertain.

Data Collection Process

All study data were retrospectively retrieved from the Hospital Information Management System. Medical records of all eligible patients were reviewed individually using protocol numbers matched to patient identifiers; however, no personal identifying information was recorded in the study file. The data collection process was conducted in the following order:

1. Patient Selection:

All adult patients aged over 18 years who presented to the ED trauma unit during the study period were screened. Among these, patients with thoracic trauma were identified. Only those with a confirmed diagnosis of isolated blunt thoracic trauma, based on discharge summaries, consultation notes, CT reports, and final diagnoses, were included.

2. Imaging Evaluation:

CT reports of all thoracic trauma patients were reviewed, and those with a documented diagnosis of hemothorax were identified. The diagnosis was based on radiology reports that

explicitly stated "hemothorax." Patients without hemothorax constituted the comparison group.

3. Clinical Data Collection:

The following demographic and clinical variables were recorded for each patient using a standardized data collection form:

- Age and sex
- Comorbidities (hypertension, diabetes mellitus, chronic obstructive pulmonary disease, chronic kidney disease)
- Trauma-related clinical findings and injuries (rib fracture, sternal fracture, pneumothorax, need for blood transfusion)
- Requirement for tube thoracostomy
- Disposition from the ED [discharge, ward admission, intensive care unit (ICU) admission]
- Mortality data based on 24-hour and 30-day outcomes

4. Collection of Laboratory Parameters:

For all patients, initial laboratory results obtained at ED admission were documented. These parameters were grouped as follows:

- **CBC:**
  - White blood cell (WBC) count, red blood cell count, and hemoglobin (Hb) level, hematocrit, neutrophils, lymphocytes, monocytes
  - Mean corpuscular volume, mean corpuscular Hb
  - Platelet count (PLT), MPV
  - PDW,
  - P-LCR
- **Blood Gas and Coagulation Tests:**
  - pH, base excess, lactate level
  - International normalized ratio

5. Data Entry and Quality Control:

All data were entered by two independent researchers. A 10% random sample was selected for cross-checking to ensure accuracy. Cases with incomplete or inconsistent data were excluded from the analysis.

6. Data Classification:

Patients were classified into two primary groups according to the presence of hemothorax confirmed by chest CT imaging:

- Hemothorax-positive group
- Hemothorax-negative group

Statistical Analysis

Statistical analyses were conducted using Jamovi software (version 2.5.7). Categorical variables were presented as frequencies and percentages. Continuous variables with a normal distribution were presented as mean ± SD, while those without a normal distribution were presented as medians with interquartile ranges [(IQR); 25^{th}-75^{th} percentiles]. The distribution of continuous variables was assessed using the Kolmogorov-Smirnov test and histogram evaluation. Group comparisons for categorical data were performed using the chi-square test or Fisher's exact test. For continuous variables with a normal distribution, the either Student's t-test or Welch's t-test was applied, depending on variance homogeneity as assessed by Levene's test. Non-normally distributed continuous variables were compared using the Mann-Whitney U test. In subgroup analyses, Bonferroni correction was applied to adjust *P* values. A *P* value < 0.05 was considered statistically significant.

RESULTS

During the study period, 12.561 adult patients presented to the ED trauma unit. Of these, 11,764 were excluded for not meeting the criteria for isolated thoracic trauma. As a result, 797 patients were evaluated for eligibility. Following application of the exclusion criteria, 383 additional patients were excluded for the following reasons: pregnancy (n=16), active external bleeding (n=41), penetrating thoracic trauma (n=37), bleeding involving other organ systems (n=157), ongoing anticoagulant therapy (n=11), missing laboratory or imaging data (n=113), and known pre-existing hematologic disorders (n=8). After applying all exclusion criteria, 414 patients were eligible and included in the final analysis (Figure 1).

The study cohort comprised 414 adult patients with isolated blunt thoracic trauma. The mean age was 54.2 ± 19.5 years and males accounted for 69.8% of the population. The most common comorbidities were hypertension (13.5%) and diabetes mellitus (4.1%) (Table 1).

Laboratory analyses at the time of ED admission revealed a median WBC count of 12.0 × 10^9/L (IQR: 8.8-15.7), a Hb level of 13.2 g/dL (IQR: 11.8-14.9), and a mean PLT of 246 ± 82 × 10^9/L. The median venous lactate level was 2.1 mmol/L (IQR: 1.4-3.1), and venous pH was 7.39 (IQR: 7.34-7.42). The base deficit was -0.4 mmol/L (IQR: -0.5 to -0.3), suggesting a mild metabolic disturbance in a subset of the cohort (Table 1).

Regarding traumatic thoracic findings, hemothorax was observed in 171 patients (41.3%), rib fractures in 171 patients (41.3%), and pneumothorax in 65 patients (15.7%). Chest tube placement was performed in 51 patients (12.3%), and 28 (6.8%) received blood transfusions (Table 1).

Regarding clinical outcomes, 57.2% of patients (n=237) required admission to the ICU, while 28.5% were admitted to general wards and 14.3% were discharged from the ED. The 30-day mortality rate was 2.4% (n=10) (Table 1).

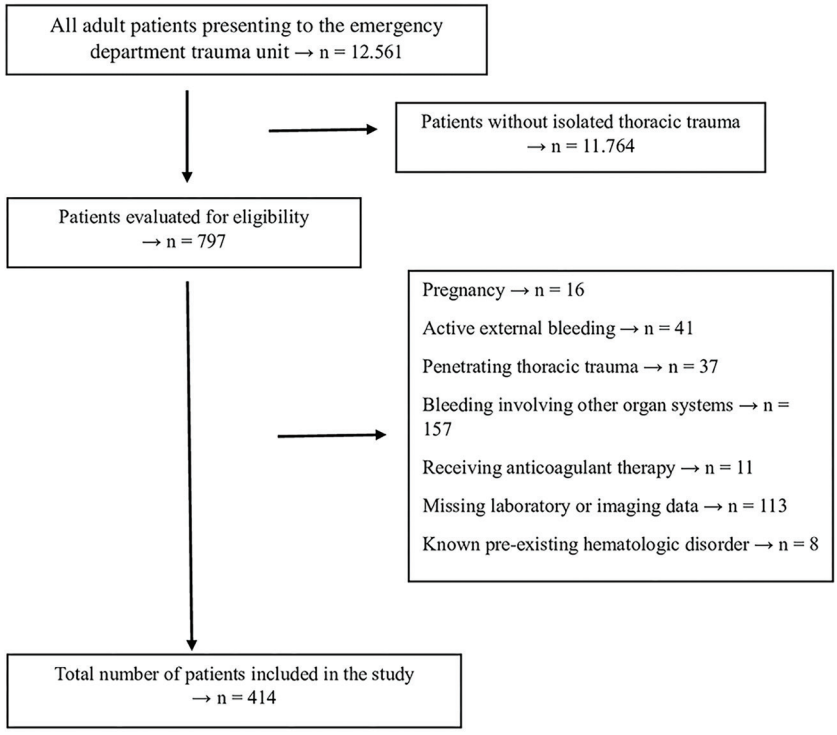

Figure 1. Patient flow diagram

Table 1. Distribution of Patients' Demographic Characteristics, Comorbidities, Laboratory Parameters, and Clinical Findings

	n=414
Age, years, mean ± SD	54.2 ± 19.5
Sex, n (%)	
Male	289 (69.8 %)
Female	125 (30.2 %)
Comorbidities, n (%)	
Hypertension	56 (13.5 %)
Diabetes mellitus	17 (4.1 %)
Chronic kidney disease	2 (0.5 %)
Chronic kidney disease	1 (0.2 %)
Laboratuar parametreleri, median (IQR 25-75) / mean ± SD	
WBC, 10^9/L	12.0 (8.8-15.7)
RBC, 10^{12}/L	4.5 (4.1-5.0)
Hemoglobin, g/dL	13.2 (11.8-14.9)
Hematokrit, %	41 (37-45)
MCV, fL	90 (87-93)
MCH, pg	29 (28-31)
Platelet, 10^9/L	246 ± 82
MPV, fL	10.5 ± 0.9
Neutrophil, 10^9/L	8.7 (5.9-12.8)
Lymphocyte, 10^9/L	1.8 (1.1-2.9)
Monocyte, 10^9/L	0.74 (0.55-0.98)
PDW, %	12.0 ± 2.0
RDW, %	13.2 (12.7-14.3)
PLCR, %	28.5 ± 7.4
Venous blood pH, -	7.39 (7.34-7.42)
Base excess, mmol/L	0.4 (0.3-0.5)
Lactate, mmol/L	2.1 (1.4-3.1)
INR, -	1.05 (0.99-1.14)
Thoracic injuries, n (%)	
Hemothorax	171 (41.3 %)
Pneumothorax	65 (15.7 %)
Rib fracture	171 (41.3 %)
Sternal fracture	8 (1.9 %)
Chest tube requirement	51 (12.3 %)
Blood transfusion requirement	28 (6.8 %)
Emergency department disposition, n (%)	
Discharged from the emergency department	59 (14.3 %)
Admitted to the ward	118 (28.5 %)
Admitted to the ICU	237 (57.2 %)
30-day mortality, n (%)	10 (2.4 %)

WBC, white blood cell; RBC, red blood cell; MCV, mean corpuscular volume; MCH, mean corpuscular hemoglobin; MPV, mean platelet volume; PDW, platelet distribution width; RDW, red cell distribution width; PLCR, platelet large cell ratio; INR, international normalized ratio; ICU, intensive care unit; SD, standard deviation.

Comparative Analysis Based on Hemothorax Status

When patients were grouped according to the presence of hemothorax, statistically significant differences were observed in several clinical and laboratory variables (Table 2).

Hypertension was significantly more prevalent among patients with hemothorax than in those without ($P < 0.001$). Among laboratory parameters, WBC was elevated in the hemothorax group [(12.5 (IQR: 9.2-17.2) $\times 10^9$/L vs. 11.7 (IQR: 8.6-14.6) $\times 10^9$/L; $P = 0.027$] and lymphocyte count was also higher [2.1 (IQR: 1.2-3.0) $\times 10^9$/L vs. 1.6 (IQR: 1.1-2.2) $\times 10^9$/L; $P = 0.032$]. In contrast, venous blood pH was significantly lower in the hemothorax group [7.37 (IQR: 7.33-7.41) vs. 7.40 (IQR: 7.36-7.43), $P < 0.001$]. Lactate levels were significantly elevated in patients with hemothorax [2.3 mmol/L (IQR 1.6-3.4) vs. 1.8 mmol/L (IQR 1.3-2.8); $P < 0.001$] (Table 2).

Table 2. Association Between Patients' Demographic Characteristics, Comorbidities, Laboratory Parameters, and Clinical Findings and the Presence of Hemothorax

	Hemothorax		*P* value
	Present (n=171)	**Absent (n=243)**	
Age, years, mean ± SD	53.8 ± 18.8	54.5 ± 19.9	0.752[1]
Sex, n (%)			
Male	127 (74.3%)	162 (66.7%)	0.097[2]
Female	44 (25.7%)	81 (33.3%)	
Comorbidities, n (%)			
Hypertension	40 (23.4%)	16 (6.6%)	**< 0.001[2]**
Diabetes mellitus	9 (5.3%)	8 (3.3%)	0.320[2]
Laboratory, median (IQR 25-75) / mean ± SD			
WBC, 10^9/L	12.5 (9.2-17.2)	11.7 (8.6-14.6)	**0.027[3]**
RBC, 10^{12}/L	4.5 (4.0-4.9)	4.5 (4.1- 5.0)	0.753[3]
Hemoglobin, g/dL	13.4 (11.8-15.0)	13.1 (11.8-14.9)	0.695[3]
Hematokrit, %	41 (37-45)	41 (37-45)	0.793[3]
MCV, fL	91 (88-93)	90 (87-93)	0.109[3]
MCH, pg	30 (29-31)	29 (28-30)	0.137[3]
Platelet, 10^9/L	240 ± 67	251 ± 91	0.194[1]
MPV, fL	10.5 ± 0.8	10.4 ± 1.0	0.371[1]
Neutrophil, 10^9/L	9.4 (6.1-15.0)	8.3 (5.8-11.3)	0.062[3]
Lymphocyte, 10^9/L	2.1 (1.2-3.0)	1.6 (1.1-2.2)	**0.032[3]**
Monocyte, 10^9/L	0.74 (0.57-1.04)	0.74 (0.54-0.95)	0.221[3]
PDW, %	12.1 ± 1.9	12.0 ± 2.1	0.573[1]
RDW, %	13.2 (12.7-14.0)	13.2 (12.8-14.6)	0.225[3]
PLCR, %	28.9 ± 6.9	28.2 ± 7.8	0.289[1]
Venous blood pH,	7.37 (7.33-7.41)	7.40 (7.36-7.43)	**< 0.001[3]**
Base excess, mmol/L	0.4 (0.3-0.6)	0.3 (0.3-0.5)	0.188[3]
Lactate, mmol/L	2.3 (1.6-3.4)	1.8 (1.3-2.8)	**< 0.001[3]**
INR, -	1.05 (1.00-1.14)	1.05 (0.98-1.13)	0.762[3]
Thoracic injuries, n (%)			
Pneumothorax	54 (31.6%)	11 (4.5%)	**< 0.001[2]**
Rib fracture	134 (78.4%)	37 (21.6%)	**< 0.001[2]**
Sternal fracture	4 (2.3%)	4 (1.6%)	0.723[4]
Chest tube requirement	47 (27.5 %)	4 (1,6%)	**< 0.001[2]**
Blood transfusion requirement	28 (6.8 %)	0	
Emergency department disposition, n (%)			
Discharged from the emergency department	7 (4.1%)	5 (21.4%)	
Admitted to the ward	19 (11.1%)	99 (40.7%)	**< 0.001[2]**
Admitted to the ICU	145 (84.8%)	92 (37.9%)	
30-day mortality, n (%)	9 (5.3%)	1 (0.4%)	**0.002[4]**

[1]Independent Samples t-test, , [2]chi-square test, [3]Mann-Whitney U test, [4]Fisher's Exact test. WBC, white blood cell; RBC, red blood cell; MCV, mean corpuscular volume; MCH, mean corpuscular hemoglobin; MPV, mean platelet volume; PDW, platelet distribution width; RDW, red cell distribution Width, PLCR, platelet large cell ratio; INR, international normalized ratio; ICU, intensive care unit; SD, standard deviation.

Regarding thoracic injuries, pneumothorax (31.6% vs. 4.5%, *P* < 0.001), rib fractures (78.4% vs. 21.6%, *P* < 0.001), chest tube placement (27.5% vs. 1.6%, *P* < 0.001), and blood transfusion (16.4% vs. 0%, *P* < 0.001) occurred significantly more often in the hemothorax group (Table 2).

A significant association was found between ED disposition and hemothorax status (*P* < 0.001 by chi-square test). Subgroup analysis showed that patients admitted to the ICU differed significantly from both discharged patients and those admitted to the general ward (both *P* < 0.001), whereas no significant difference was observed between the discharged and general ward groups (*P* > 0.005). Furthermore, 30-day mortality was markedly higher in the hemothorax group than in the non-hemothorax group (5.3% vs. 0.4%, *P* = 0.002) (Table 2).

Additionally, in the subgroup analysis of patients with hemothorax (Table 3), non-survivors (n=9) had higher WBC and lymphocyte counts, higher lactate levels, and lower venous pH compared with survivors. Pneumothorax, sternal fracture, and the need for blood transfusion were also observed more frequently in this group. These findings indicate that both laboratory parameters and specific clinical injury characteristics are associated with 30-day mortality.

Table 3. The Relationship Between Demographic Characteristics, Comorbidities, Laboratory Parameters, and Clinical Findings of Patients with Hemothorax and the Presence of Mortality

	Mortality		*P* value
	Yes (n=9)	**No (n=162)**	
Age, years, mean ± SD	62.0 ± 18.2	53.4 ± 18.8	0.183[1]
Sex, n (%)			
Male	5 (55.6%)	122 (75.3%)	0.238[2]
Female	4 (44.4%)	40 (24.7%)	
Comorbidities, n (%)			
Hypertension	1 (11.1%)	39 (24.1%)	0.687[2]
Diabetes mellitus	1 (11.1%)	8 (4.9%)	0.393[2]
Laboratory, median (IQR 25-75) / mean ± SD			
WBC, 10^9/L	18.2 (17.6-24.4)	12.1 (8.8-16.4)	**0.027[3]**
RBC, 10^{12}/L	4.0 (3.8-4.5)	4.6 (4.1-5.0)	0.753[3]
Hemoglobin, g/dL	11.4 (9.9-12.6)	13.6 (11.8-15.0)	0.695[3]
Hematokrit, %	37 (34-40)	41 (37- 45)	0.793[3]
MCV, fL	89 (88-91)	91 (87-94)	0.109[3]
MCH, pg	28 (27-29)	30 (29-31)	0.137[3]
Platelet, 10^9/L	251 ± 53	240 ± 68	0.194[1]
MPV, fL	10.4 ± 0.8	10.5 ± 0.9	0.371[1]
Neutrophil, 10^9/L	15.5 (14.3-18.1)	9.0 (6.0-13.8)	0.062[3]
Lymphocyte, 10^9/L	3.7 (2.5-5.2)	2.1 (1.2-2.8)	**0.032[3]**
Monocyte, 10^9/L	0.83 (0.55-1.07)	0.74 (0.57-1.03)	0.221[3]
PDW, %	12.2 ± 1.8	12.1 ± 1.9	0.573[1]
RDW, %	14.1 (13.2-17.2)	13.1 (12.7-13.9)	0.225[3]
PLCR, %	28.6 ± 6.6	29.0 ± 7.0	0.289[1]
Venous blood pH,	7.26 (6.82-7.33)	7.38 (7.34-7.41)	**< 0.001[3]**
Base excess, mmol/L	0.5 (0.3-0.8)	0.4 (0.3-0.6)	0.188[3]
Lactate, mmol/L	7.5 (4.1-8.2)	2.2 (1.6-3.3)	**< 0.001[3]**
INR, -	1.24 (1.18-1.55)	1.05 (0.99-1.14)	0.762[3]
Thoracic injuries, n (%)			
Pneumothorax	6 (66.7%)	48 (29.6%)	**0.029[2]**
Rib fracture	8 (88.9%)	126 (77.8%)	0.686[2]
Sternal fracture	2 (22.2%)	2 (1.2%)	**0.014[2]**
Chest tube requirement	5 (55.6%)	42 (25.9%)	0.117[2]
Blood transfusion requirement	6 (66.7%)	22 (13.6%)	**< 0.001[2]**
Emergency department disposition, n (%)			
Discharged from the emergency department	0	7 (4.3%)	
Admitted to the ward	1 (11.1%)	18 (11.1%)	
Admitted to the ICU	8 (88.9%)	137 (84.6%)	

[1]Independent Samples t-test, [2]Fisher's exact test, [3]Mann-Whitney U test; WBC, white blood cell; RBC, red blood cell; MCV, mean corpuscular volume; MCH, mean corpuscular hemoglobin; MPV, mean platelet volume; PDW, platelet distribution width; RDW, red cell distribution width; PLCR, platelet large cell ratio, INR, international normalized ratio; ICU, intensive care unit; SD, standard deviation.

DISCUSSION

This study assessed the ability of initial laboratory parameters to predict hemothorax in adult patients presenting to the ED with isolated blunt thoracic trauma. The findings demonstrated that WBC count, lactate level, venous pH, and lymphocyte count were significantly associated with the presence of hemothorax. In contrast, traditional platelet indices such as MPV, PDW, and P-LCR did not demonstrate significant diagnostic value.

Blunt thoracic trauma can lead to various intrathoracic and extrathoracic complications, with hemothorax being among the most severe and life-threatening complications.[12,13] In hemothorax, blood accumulation within the thoracic cavity can mechanically limit respiratory function, impair oxygenation, and reduce systemic perfusion, thereby accelerating clinical deterioration.[6] Early diagnosis and intervention may reduce the need for invasive procedures and improve clinical outcomes. Although chest CT is considered the gold standard for diagnosing hemothorax, it may be delayed in hemodynamically unstable patients. Therefore, the contribution of laboratory parameters assessed prior to CT becomes particularly valuable in early clinical decision-making.[14,15]

In the present study, WBC levels and lymphocyte counts were significantly elevated in the hemothorax group (P = 0.027 and P = 0.032, respectively). This may reflect the systemic inflammatory response and activation resulting from trauma-induced tissue injury. Consistent with our results, previous studies have reported that elevated WBC and lymphocyte counts in the acute phase of trauma are associated with greater clinical severity and increased risk of complications.[16,17] These results suggest that CBC parameters may assist in the early identification of traumatic hemothorax. The clinical relevance of these parameters becomes particularly evident in cases where imaging is delayed or patients are hemodynamically unstable. At admission to the ED, patients presenting with elevated WBC and lymphocyte counts, increased lactate levels, and decreased pH are more likely to have a hemothorax. Such patients should be prioritized for expedited imaging, closely monitored, and considered for early tube thoracostomy if necessary. In this way, laboratory findings may serve not only as diagnostic adjuncts but also as tools for clinical prioritization.

Increased intrathoracic pressure due to hemothorax can restrict lung expansion, disrupt the ventilation-perfusion balance, and consequently lead to impaired tissue oxygenation and lactate accumulation.[18] Consistent with this pathophysiological mechanism, our study showed significantly higher lactate levels in the hemothorax group (median: 2.3 mmol/L vs. 1.8 mmol/L; P < 0.001). This observation supports previous reports highlighting lactate as a prognostic marker of hypoperfusion and systemic inflammation in trauma patients.[19,20]

Venous pH levels were also significantly lower in the hemothorax group (P < 0.001). This decrease may reflect both respiratory acidosis due to ventilation-perfusion mismatch and metabolic acidosis resulting from hypoperfusion secondary to hemorrhage. Previous studies have demonstrated that the pH level serves as an early prognostic marker in trauma-induced hemorrhagic shock.[21,22]

However, no statistically significant differences in the platelet indices MPV, PDW, and P-LCR were observed between the hemothorax and control groups. Although these parameters have previously been shown to reflect hematologic dynamics and microcirculatory responses following trauma in various patient populations,[23,24] our findings suggest that they did not demonstrate sufficient diagnostic performance to predict hemothorax among patients with isolated thoracic trauma. This discrepancy may be attributed to factors such as sample selection, timing of laboratory measurements, or coexisting systemic variables.

Study Limitations

This study has certain limitations. Primarily, its retrospective, single-center nature may have introduced selection bias and limited the ability to draw causal inferences. Additionally, potential confounding variables such as prehospital interventions, the mechanism and severity of the trauma, and patients' baseline coagulation status were not included in the analysis. Moreover, time-dependent changes in laboratory parameters were not evaluated; this aspect may serve as a valuable focus for prospective studies.

CONCLUSION

This study demonstrates that WBC count, lactate level, pH, and lymphocyte count may serve as significant predictors of hemothorax in patients presenting with isolated blunt thoracic trauma. In contrast, platelet indices did not appear to have discriminative value in this patient population. These findings contribute to identifying supportive laboratory markers for early risk stratification and clinical decision-making in the ED setting.

Ethics

Ethics Committee Approval: This study was designed as a single-center, retrospective, descriptive observational analysis. Ethical approval was obtained from the Clinical Research Ethics Committee of University of Health Scienes Türkiye Ankara Etlik City Hospital (approval no.: AEŞH-BADEK-2024-307, date: 03.04.2024).

Informed Consent: Retrospective study. Permission was obtained from hospital management to collect study data from the Information Management System.

Acknowledgments

We would like to express our sincere gratitude to Mr. Selim Doğan for his valuable technical support and dedicated contributions throughout the study.

Footnotes

Author Contributions

Concept Design – V.S., S.Ö., A.B.E.; Data Collection or Processing – V.S., S.A., Z.B., H.K.S., M.S.D.; Analysis or Interpretation – S.Ö., S.A.; Literature Review – V.S., S.A., Z.B., H.K.S., M.S.D.; Writing, Reviewing and Editing – V.S., A.B.E.

Declaration of Interests: The authors declared no conflicts of interest.

Funding: No funding.

REFERENCES

1. Battle C, Hutchings H, Lovett S, et al. Predicting outcomes after blunt chest wall trauma: development and external validation of a new prognostic model. *Crit Care*. 2014;18:R98. [CrossRef]
2. Ziegler DW, Agarwal NN. The morbidity and mortality of rib fractures. *J Trauma*. 1994;37 (6):975-979. [CrossRef]
3. Ali S, Kumar A, Kumar R, et al. Prediction of outcomes of chest trauma using chest trauma scoring system at a rural tertiary health-care facility. *Saudi J Health Sci*. 2024;13:42-48. [CrossRef]
4. Dogrul BN, Kiliccalan I, Asci ES, Peker SC. Blunt trauma related chest wall and pulmonary injuries: An overview. *Chin J Traumatol*. 2020;23(3):125-138. [CrossRef]
5. Fattori S, Reitano E, Chiara O, Cimbanassi S. Predictive factors of ventilatory support in chest trauma. *Life (Basel)*. 2021;11(11):1154. [CrossRef]
6. Beyer CA, Ruf AC, Alshawi AB, Cannon JW. Management of traumatic pneumothorax and hemothorax. *Curr Probl Surg*. 2025;63:101707. [CrossRef]
7. Baseer A, Noor N, Aman N, Qureshi AN. Utilizing un-enhanced chest computed tomography screening for blunt trauma surgery decisions. *Cureus*. 2024;16(9):e69590. [CrossRef]
8. Trupka A, Waydhas C, Hallfeldt KK, Nast-Kolb D, Pfeifer KJ, Schweiberer L. Value of thoracic computed tomography in the first assessment of severely injured patients with blunt chest trauma: results of a prospective study. *J Trauma*. 1997;43(3):405-411. [CrossRef]
9. Băetu AE, Mirea LE, Cobilinschi C, Grințescu IC, Grințescu IM. Hemogram-based phenotypes of the ımmune response and coagulopathy in blunt thoracic trauma. *J Pers Med*. 2024;14(12):1168. [CrossRef]
10. Guyette F, Suffoletto B, Castillo JL, Quintero J, Callaway C, Puyana JC. Prehospital serum lactate as a predictor of outcomes in trauma patients: a retrospective observational study. *J Trauma*. 2011;70(4):782-786. [CrossRef]
11. Thomas KA, Rassam RMG, Kar R, et al. Trauma patients have reduced ex vivo flow-dependent platelet hemostatic capacity in a microfluidic model of vessel injury. *PLoS One*. 2024;19(7):e0304231. [CrossRef]
12. Chen Q, Huang G, Li T, et al. Insights into epidemiological trends of severe chest injuries: an analysis of age, period, and cohort from 1990 to 2019 using the Global Burden of Disease study 2019. *Scand J Trauma Resusc Emerg Med*. 2024;32(1):89. [CrossRef]
13. Adal O, Tareke AA, Bogale EK, et al. Mortality of traumatic chest injury and its predictors across sub-saharan Africa: systematic review and meta-analysis, 2024. *BMC Emerg Med*. 2024;24(1):32. [CrossRef]
14. Gilbert RW, Fontebasso AM, Park L, Tran A, Lampron J. The management of occult hemothorax in adults with thoracic trauma: a systematic review and meta-analysis. *J Trauma Acute Care Surg*. 2020;89(6):1225-1232. [CrossRef]
15. Zeiler J, Idell S, Norwood S, Cook A. Hemothorax: a review of the literature. *Clin Pulm Med*. 2020;27(1):1-12. [CrossRef]
16. Hasjim BJ, Grigorian A, Stopenski S, et al. Moderate to severe leukocytosis with vasopressor use is associated with increased mortality in trauma patients. *J Intensive Care Soc*. 2022;23(2):117-123. [CrossRef]
17. Rau CS, Kuo SC, Tsai CH, et al. Elevation of white blood cell subtypes in adult trauma patients with stress-ınduced hyperglycemia. *Diagnostics (Basel)*. 2023;13(22):3451. [CrossRef]
18. Carlino MV, Guarino M, Izzo A, et al. Arterial blood gas analysis utility in predicting lung injury in blunt chest trauma. *Respir Physiol Neurobiol*. 2020;274:103363. [CrossRef]
19. Sadrzadeh SM, Talebzadeh V, Mousavi SM, et al. Prognostic value of lactate levels in trauma patients' outcomes in emergency department. *Bull Emerg Trauma*. 2025;13:32-36. [CrossRef]
20. Alshiakh SM. Role of serum lactate as prognostic marker of mortality among emergency department patients with multiple conditions: a systematic review. *SAGE Open Med*. 2023;11:20503121221136401. [CrossRef]
21. Corral Torres E, Hernández-Tejedor A, Millán Estañ P, et al. Prognostic value of metabolic parameters measured by first responders attending patients with severe trauma: associations with the New Injury Severity Score and mortality. *Emergencias*. 2023;35(2):90-96. [CrossRef]
22. Werner M, Bergis B, Leblanc PE, et al. Femoral blood gas analysis, another tool to assess hemorrhage severity following trauma: an exploratory prospective study. *Scand J Trauma Resusc Emerg Med*. 2023;31(1):31. [CrossRef]
23. Palabiyik O, Tomak Y, Acar M, et al. Relationship between platelet indices and red cell distribution width and short-term mortality in traumatic brain injury with 30-day mortality. *Rev Assoc Med Bras (1992)*. 2023;69(1):18-23. [CrossRef]
24. Schofield H, Rossetto A, Armstrong PC, et al. Immature platelet dynamics are associated with clinical outcomes after major trauma. *J Thromb Haemost*. 2024;22(4):926-935. [CrossRef]

ABCResearch

Arch Basic Clin Res 2026;8(1):35-39
DOI: 10.4274/ABCR.2025.25373

Research Article

The Relationship Between Allergic Reactions and Serum Erythropoietin Levels: A New Biomarker Candidate in Allergic Reactions

Fatih Mehmet Sarı[1], Yasin Bilgin[1], Haticetül Kübra Sarı[2], Mücahit Emet[3]

[1]Department of Emergency Medicine, Erzincan Binali Yıldırım University Faculty of Medicine, Erzincan, Türkiye
[2]Freelance Dermatology Specialist, Erzincan, Türkiye
[3]Freelance Emergency Medicine Specialist, İstanbul, Türkiye

Cite this article as: Sarı FM, Bilgin Y, Sarı HK, Emet M. The relationship between allergic reactions and serum erythropoietin levels: a new biomarker candidate in allergic reactions. *Arch Basic Clin Res*. 2026;8(1):35-39.

ORCID IDs of the authors: F.M.S. 0009-0007-7022-3751, Y.B. 0000-0002-1582-223X, H.K.S. 0000-0003-1885-973X, M.E. 0000-0003-2752-8270.

ABSTRACT

Objective: This study aimed to compare serum erythropoietin (EPO) levels in patients admitted to the emergency department with allergic reactions who were clinically diagnosed with urticaria, angioedema, or anaphylaxis, and to evaluate the diagnostic value of EPO as a potential biomarker.

Methods: The study was conducted prospectively in the Emergency Department of Atatürk University between 2013 and 2016. A total of 156 patients diagnosed with urticaria, angioedema, or anaphylaxis were included. Serum EPO levels from blood samples taken at admission were analyzed using the enzyme-linked immunosorbent assay method. Relationships between vital signs, clinical symptoms, and EPO levels were statistically evaluated.

Results: No significant difference in serum EPO levels was observed among the urticaria (41.7%), angioedema (35.9%), and anaphylaxis (24.4%) groups (P = 0.799). However, patients with uvular edema had significantly higher EPO levels (6.5 ± 1.6 vs. 6.0 ± 1.7 mIU/mL; P = 0.027). In the anaphylaxis group, oxygen saturation and blood pressure were significantly lower, whereas pulse rate and respiratory rate were significantly higher.

Conclusion: EPO levels alone are not sufficient for differential diagnosis of acute allergic reactions. However, when assessed alongside specific symptoms, such as uvular edema, EPO may reflect the severity of the inflammatory response and serve as a potential biomarker. Multicenter studies including tissue-level analyses are needed to better understand the role of EPO in allergic inflammation.

Keywords: Anaphylaxis, angioedema, erythropoietin, hypoxia, urticaria

INTRODUCTION

Allergic reactions are common clinical presentations in emergency departments and often require prompt intervention. These reactions typically manifest in three major forms: urticaria, angioedema, and anaphylaxis. Urticaria is characterized by well-demarcated, erythematous, and often pruritic plaques on the skin, usually resolving spontaneously. Angioedema involves swelling of deeper tissues and is frequently observed in periorbital, perioral, or oropharyngeal regions. Anaphylaxis, on the other hand, is a rapidly developing hypersensitivity reaction following allergen exposure, potentially life-threatening and characterized by systemic inflammatory responses that may impair the respiratory, circulatory, or gastrointestinal systems.[1,2]

Corresponding author: Fatih Mehmet Sarı, **E-mail:** drfmsari@gmail.com

Received: September 10, 2025 **Accepted:** October 16, 2025 **Publication Date:** January 26, 2026
Revision Requested: October 10, 2025

Because of the symptomatic overlap among these clinical entities, differential diagnosis often relies solely on patient history and physical examination. However, this approach may lead to diagnostic uncertainty and delays, particularly in cases of mild anaphylaxis, adversely affecting treatment and prognosis.[3] Indeed, a retrospective study reported that only one in four patients who met the diagnostic criteria for anaphylaxis were correctly identified.[4] This underscores the need for objective biomarkers to aid in diagnosis.

Erythropoietin (EPO) is a glycoprotein hormone secreted by the kidneys in response to hypoxia, stimulating the proliferation of erythroid progenitor cells and enhancing erythropoiesis. During hypoxemia, EPO levels may increase by up to 5- to 8-fold, serving as a compensatory mechanism to improve oxygen delivery.[5] Recent experimental and clinical studies, however, have demonstrated that EPO exerts effects beyond hematopoiesis, particularly on inflammatory processes.

EPO may exert anti-inflammatory effects in immune cells such as macrophages and monocytes by suppressing the release of proinflammatory cytokines, including tumor necrosis factor alpha (TNF-α) and interleukin-6 (IL-6), and by inhibiting nuclear factor-κB (NF-κB) activation, thereby exerting immunomodulatory effects.[6,7] Through these mechanisms, EPO has been shown to reduce tissue damage in systemic inflammatory conditions such as sepsis, trauma, and myocardial ischemia.[8] Moreover, elevated EPO levels have been observed in conditions associated with oropharyngeal edema and hypoxia, suggesting a potential role in the inflammatory process.

Nevertheless, the literature on how EPO levels change in acute allergic reactions and whether these changes carry diagnostic significance remains limited. Existing studies have mainly focused on mast cell activation and tryptase levels, often neglecting the potential role of EPO as a biomarker. Given the variable degrees of hypoxia and inflammatory burden across urticaria, angioedema, and anaphylaxis, investigating the potential utility of EPO for differential diagnosis appears warranted.

In this study, we aimed to compare serum EPO levels among patients presenting to the emergency department with clinically diagnosed allergic reactions (urticaria, angioedema, or anaphylaxis) to evaluate its diagnostic utility in distinguishing these conditions. Additionally, we sought to examine the relationship between specific symptom clusters (e.g., uvular edema, dyspnea) and EPO levels to assess the potential contribution of this biomarker to clinical decision-making.

MAIN POINTS

- This study evaluated the association between serum erythropoietin (EPO) levels and allergic reactions in emergency department patients.
- Serum EPO levels did not differ significantly among patients with urticaria, angioedema, or anaphylaxis.
- Patients with uvular edema had significantly higher EPO levels compared with those without uvular edema.
- These findings indicate that EPO may contribute to the pathophysiology of airway involvement in allergic reactions.

Study Design and Population

This prospective study was conducted between June 2013 and January 2016 in the Department of Emergency Medicine at Atatürk University Faculty of Medicine. The study was approved by the Atatürk University Non-Interventional Clinical Research Ethics Committee prior to patient enrollment (decision no: 25, date: 02.05.2013). Subsequently, when the study was decided to be used as a thesis project, a second ethics committee approval was obtained in accordance with institutional regulations. Patients aged 18 years or older who presented to the emergency department with allergic reactions and were clinically diagnosed with urticaria, angioedema, or anaphylaxis were included. Written informed consent was obtained from all participants.

Exclusion criteria

The following patients were excluded:

- Those with known anemia, chronic renal failure, or liver disease
- Patients with a history of chronic obstructive pulmonary disease or asthma
- Patients with bone marrow disorders or active malignancy
- Those with other systemic diseases that could affect EPO levels

Diagnostic criteria and Patient Classification

- Patients were categorized into three groups based on clinical findings:
- Urticaria: Patients with skin lesions only
- Angioedema: Patients with skin and mucosal edema
- Anaphylaxis: Patients meeting the 2014 diagnostic criteria of the World Allergy Organization.[9]

Data Collection

Vital signs (blood pressure, heart rate, oxygen saturation, respiratory rate) and laboratory parameters [White blood cell, neutrophil, lymphocyte, eosinophil, basophil, red blood cell hemoglobin, hematocrit, mean corpuscular volume, mean corpuscular hemoglobin, mean corpuscular hemoglobin concentration, red cell distribution width, platelet, platelet distribution width, creatinine, and blood urea nitrogen] were recorded for each patient. Suspected allergens and clinical symptoms (such as pruritus, rash, uvular edema, and stridor) were documented using a standardized form.

Biochemical Analysis

Serum EPO levels were measured in blood samples collected on admission. After clotting, the samples were centrifuged and stored at -80 °C. Measurements were performed using the enzyme linked immune sorbent assay (ELISA) method (Human EPO Platinum ELISA Kit, eBioscience, Austria) in accordance with the manufacturer's protocol.

Statistical Analysis

Data were analyzed using SPSS version 22.0 (IBM Corp., Armonk, NY, USA). Continuous variables were expressed as mean ± standard deviation when normally distributed, or as median (min-max) when non-normally distributed; categorical variables were presented as percentages (%). The Kolmogorov-Smirnov test was used to assess normality. Comparisons among more than two groups were performed using one-way ANOVA for parametric variables and the Kruskal-Wallis test for non-parametric variables. Post-hoc analyses were conducted with the Bonferroni correction. Comparisons between two groups were made using the Independent-samples t-test or the Mann-Whitney U test, as appropriate. Categorical variables were compared using the chi-square test. Logistic regression was used to identify independent predictors. A *P* value of < 0.05 was considered statistically significant.

RESULTS

A total of 156 patients were included in the study. Of these, 41.7% (n=62) were diagnosed with urticaria, 35.9% (n=56) with angioedema, and 24.4% (n=38) with anaphylaxis. Among the participants, 45.5% (n=71) were male and 54.5% (n=85) were female. The mean age was 40.9 ± 17.1 years, with no significant age difference between genders ($P > 0.05$). Drugs were the most common cause of allergic reactions (38.2%) and were the leading cause in both males (39.4%) and females (37.6%). The distribution of probable allergens by gender is presented in Table 1.

Vital signs were compared among the three clinical groups using one-way ANOVA. Post-hoc Bonferroni analysis revealed that the anaphylaxis group had significantly lower systolic (111.0 ± 30.9 mmHg) and diastolic (67.2 ± 18.2 mmHg) blood pressure compared with both the urticaria and angioedema groups ($P = 0.004$ and $P < 0.001$, respectively). Additionally, the anaphylaxis group exhibited significantly higher heart and respiratory rates (heart rate: 94.8 ± 18.9 bpm; respiratory rate: 18.5 ± 5.0/min) ($P = 0.008$ and $P < 0.001$, respectively). Oxygen saturation was also significantly lower in the anaphylaxis group (93.3 ± 4.0%; $P = 0.003$). Details of vital signs are shown in Table 2.

Serum EPO levels were compared among the groups: urticaria (6.2 ± 1.7 mIU/mL), angioedema (6.2 ± 1.7 mIU/mL), and anaphylaxis (6.4 ± 1.7 mIU/mL), with no significant differences observed ($P = 0.799$). The results are summarized in Table 3.

In subgroup analyses, EPO levels did not differ significantly by drug allergy, food allergy, rash, or pruritus ($P > 0.05$). However, patients with uvular edema had significantly higher EPO levels (6.5 ± 1.6 mIU/mL) than those without edema (6.0 ± 1.7 mIU/mL; $P = 0.027$). The detailed subgroup comparisons are presented in Table 4.

Table 1. Probable Allergens by Gender

Etiology	Male n (%)	Female n (%)
Drugs	28 (39.4)	32 (37.6)
Idiopathic	26 (36.6)	25 (29.4)
Food	7 (9.9)	11 (12.9)
Insect bites	7 (9.9)	4 (4.7)
Cleaning products	1 (1.4)	1 (1.2)
Clothing	0 (0.0)	2 (2.4)
Infection	1 (1.4)	3 (3.5)
Other	0 (0.0)	5 (5.9)
Cold	1 (1.4)	0 (0.0)
Stress	0 (0.0)	2 (2.4)

Table 2. Vital Signs by Clinical Groups

Parameter	Urticaria (n=62)	Angioedema (n=56)	Anaphylaxis (n=38)	*P* value	Total (n=156)
Systolic BP (mmHg)	125.8 ± 18.9	123.7 ± 15.9	111.0 ± 30.9*	**0.004**	121.5 ± 22.2
Diastolic BP (mmHg)	77.8 ± 12.4	77.9 ± 10.9	67.2 ± 18.2*	**< 0.001**	75.3 ± 14.2
Heart rate (bpm)	87.8 ± 12.5	86.0 ± 10.4	94.8 ± 18.9*	**0.008**	88.9 ± 14.0
Oxygen saturation (%)	94.9 ± 2.4	95.1 ± 2.0	93.3 ± 4.0*	**0.003**	94.6 ± 2.8
Respiratory rate (/min)	16.3 ± 2.3	15.9 ± 1.5	18.5 ± 5.0*	**< 0.001**	16.7 ± 3.2

Values are presented as mean ± standard deviation (SD). Comparisons between clinical groups were performed using one-way ANOVA. Post-hoc analysis was conducted using the Bonferroni correction.
*: Statistically significant compared to the urticaria and angioedema group with the anaphylaxis group ($P < 0.05$).

Table 3. Serum Erythropoietin Levels by Clinical Groups

Parameter	Urticaria (n=62)	Angioedema (n=56)	Anaphylaxis (n=38)	*P* value
Erythropoietin (mIU/mL)	6.2 ± 1.7	6.2 ± 1.7	6.4 ± 1.7	0.799

Data are expressed as mean ± SD. Comparisons among groups were performed using one-way ANOVA.

Table 4. Comparison of Erythropoietin Levels in Subgroups

Parameter	Absent (n)	Mean ± SD (absent)	Present (n)	Mean ± SD (present)	*P* value
Drug allergy	96	6.2 ± 1.5	60	6.2 ± 2.0	0.749
Food allergy	139	6.2 ± 1.7	17	6.4 ± 1.5	0.695
Rash	30	5.8 ± 1.3	126	6.3 ± 1.7	0.159
Pruritus	60	6.1 ± 1.6	96	6.3 ± 1.7	0.467
Uvular edema	89	6.0 ± 1.7	67	6.5 ± 1.6	**0.027**

Values are presented as mean ± SD. Comparisons were made using Student's t-test.

DISCUSSION

In this study, serum EPO levels were examined in patients who presented to the emergency department with allergic reactions and were clinically diagnosed with urticaria, angioedema, or anaphylaxis. Our findings showed no significant differences in EPO levels among these three clinical conditions. However, the observation of significantly higher EPO levels in patients with uvular edema is noteworthy. This suggests that EPO may be involved not only in responses to hypoxic stimuli but also in inflammatory processes.

Anaphylaxis is a rapidly developing systemic hypersensitivity reaction that often affects the respiratory or circulatory systems and is life-threatening. During anaphylaxis, mast cells and basophils are activated via FcεRI receptors, leading to the release of histamine, tryptase, prostaglandin D2, and various cytokines. The resulting bronchoconstriction, vascular leakage, and vasodilation cause hypoxia, tachycardia, and hypotension.[9,10] In our study, patients with anaphylaxis exhibited significantly lower oxygen saturation, systolic and diastolic blood pressure, whereas their heart rate and respiratory rate were significantly higher. These findings confirm the presence of hypoxia and hemodynamic compromise.

EPO is a glycoprotein hormone secreted by the kidneys in response to hypoxia; it stimulates erythropoiesis. EPO production typically increases within several hours in response to low tissue oxygen tension. However, some studies have shown that EPO may also play a role in inflammatory processes. By exerting anti-inflammatory effects on macrophages and monocytes, EPO suppresses proinflammatory cytokines such as TNF-α and IL-6 and inhibits NF-κB activation, thereby providing immunomodulation.[6,7] With these properties, EPO has been considered a tissue-protective agent in conditions such as sepsis, myocardial ischemia, and trauma.[8]

Although no overall differences in EPO levels were found among clinical groups, the significantly higher levels observed in patients with uvular edema are noteworthy. The uvula, located in the upper airway, may be exposed to both mechanical and inflammatory stress. An experimental study demonstrated infiltration of cluster of differentiation 4 (CD4) and CD8+ T cells and macrophages into the uvular tissue, contributing to inflammation.[11] Such cellular infiltration may enhance local cytokine release, thereby stimulating EPO production.

The relationship between uvular edema and hypoxia may also trigger systemic EPO release. Reports in the literature indicate that EPO levels can increase five- to eightfold in hypoxic states.[5] However, the timing of this increase is critical. Some studies have indicated that EPO does not rise significantly within hours of acute hypoxia, suggesting that early serum measurements may not fully capture this response.[12] The absence of significant EPO elevation in the anaphylaxis group in our study may, therefore, be related to this physiological delay.

Interestingly, immune responses against EPO itself have been described, leading to allergic reactions. Cases of angioedema, urticaria, and even anaphylaxis associated with recombinant EPO and its derivatives have been reported.[13,14] These findings suggest that EPO may interact bidirectionally with the immune system, functioning both as a stimulus and as a target.

Our findings indicate that EPO levels alone are insufficient for distinguishing among urticaria, angioedema, and anaphylaxis. However, when evaluated alongside specific findings, such as uvular edema, they may have clinical relevance. This suggests the potential role of EPO as an inflammatory biomarker, although further histopathological and immunological studies at the tissue level are warranted.

Finally, it has been suggested that the anti-inflammatory effects of EPO require plasma levels above a certain threshold, which may be higher than the threshold needed for hematopoietic effects.[15] Thus, even if serum levels remain stable during acute inflammation, local tissue-level effects of EPO may persist.

Study Limitations

This study has several methodological and structural limitations. First, it was conducted at a single center with a relatively small sample size, which may limit the generalizability of the results. Additionally, molecular parameters, such as erythropoietin receptor (EPOR) expression and tissue-level EPO accumulation, could not be evaluated, leaving the tissue-level correlates of the observed serum differences unknown.

Furthermore, correlations with other inflammatory biomarkers, such as tryptase, histamine, and IL-6, were not examined, nor were mast cell density or IgE levels in urticarial lesions assessed. Finally, the study was conducted at a high-altitude center (1850 m), which may differ from other centers with respect to hypoxic stimuli.

Recommendations:

Large-scale, multicenter studies are recommended to more reliably evaluate the diagnostic value of serum EPO levels in allergic conditions.

Molecular parameters, such as tissue-level EPO expression, EPOR presence, and local cytokine profiles, should be investigated to clarify the role of EPO in allergic inflammation.

Evaluating EPO levels when specific symptoms are present, particularly uvular edema, may help predict clinical severity.

The timing of the EPO response to acute hypoxia should be examined further in detailed time-course studies in the context of allergic reactions.

Developing a biomarker panel incorporating acute-phase reactants such as histamine, tryptase, and IL-6 alongside EPO may improve the accuracy of the diagnosis of anaphylaxis in emergency settings.

CONCLUSION

This study is a pioneering analysis of the diagnostic value of serum EPO levels in patients with acute allergic reactions, such as urticaria, angioedema, and anaphylaxis. Our results revealed no significant differences in EPO levels among these three clinical conditions. However, the significantly higher EPO levels in patients with uvular edema suggest that this finding may serve as an indicator of systemic inflammatory activity.

Overall, EPO levels appear insufficient as a standalone biomarker for the differential diagnosis of allergic reactions. However, when assessed in conjunction with specific symptoms such as uvular edema, EPO may contribute to clinical decision-making. This finding implies that EPO elevation may reflect not only hypoxic responses but also inflammation-related processes.

In this context, uvular edema emerges as a clinically significant sign with dual implications: a risk of local airway obstruction and an indicator of the severity of systemic inflammation. The observed association between uvular edema and increased EPO levels suggests that uvular edema should be considered an active finding requiring careful evaluation in emergency departments, rather than a passive clinical observation.

Ethics

Ethics Committee Approval: The study was approved by the Atatürk University Non-Interventional Clinical Research Ethics Committee prior to patient enrollment (decision no: 25, date: 02.05.2013).

Informed Consent: Allergic patients who met the study criteria were included in the study group after verbal consent was obtained from themselves or their relatives.

Footnotes

Author Contributions

Concept Design – F.M.S., M.E.; Data Collection or Processing – F.M.S., H.K.S; Analysis or Interpretation – F.M.S., H.K.S., M.E.; Literature Review – F.M.S., Y.B., M.E.; Writing, Reviewing and Editing – F.M.S., Y.B., M.E.

Declaration of Interests: The authors declare no conflict of interest regarding the publication of this paper.

Funding: The authors declare no financial support or funding.

REFERENCES

1. Zuberbier T, Aberer W, Asero R, et al. The EAACI/GA²LEN/EDF/WAO guideline for the definition, classification, diagnosis and management of urticaria. *Allergy*. 2018;73(7):1393-1414. [CrossRef]
2. Cardona V, Ansotegui IJ, Ebisawa M, et al. World allergy organization anaphylaxis guidance 2020. *World Allergy Organ J*. 2020;13(10):100472. [CrossRef]
3. Campbell RL, Li JT, Nicklas RA, Sadosty AT; Members of the Joint Task Force; Practice Parameter Workgroup. Emergency department diagnosis and treatment of anaphylaxis: a practice parameter. *Ann Allergy Asthma Immunol*. 2014;113(6):599-608. [CrossRef]
4. Klein JS, Yocum MW. Underreporting of anaphylaxis in a community emergency room. *J Allergy Clin Immunol*. 1995;95(2):637-638. [CrossRef]
5. Suresh S, Rajvanshi PK, Noguchi CT. The many facets of erythropoietin physiologic and metabolic response. *Front Physiol*. 2020;10:1534. [CrossRef]
6. Nairz M, Sonnweber T, Schroll A, Theurl I, Weiss G. The pleiotropic effects of erythropoietin in infection and inflammation. *Microbes Infect*. 2012;14(3):238-246. [CrossRef]
7. Brines M, Cerami A. Erythropoietin-mediated tissue protection: reducing collateral damage from the primary injury response. *J Intern Med*. 2008;264(5):405-432. [CrossRef]
8. Jelkmann W. Proinflammatory cytokines lowering erythropoietin production. *J Interferon Cytokine Res*. 1998;18(8):555-559. [CrossRef]
9. Simons FE, Ardusso LR, Bilò MB, et al. World allergy organization guidelines for the assessment and management of anaphylaxis. *World Allergy Organ J*. 2011;4(2):13-37. [CrossRef]
10. Pier J, Bingemann TA. Urticaria, angioedema, and anaphylaxis. *Pediatr Rev*. 2020;41(6):283-292. [CrossRef]
11. Olofsson K, Hellström S, Hammarström ML. Human uvula: characterization of resident leukocytes and local cytokine production. *Ann Otol Rhinol Laryngol*. 2000;109(5):488-496. [CrossRef]
12. Bahlmann FH, de Groot K, Haller H, Fliser D. Erythropoietin: is it more than correcting anaemia? *Nephrol Dial Transplant*. 2004;19(1):20-22. [CrossRef]
13. Tahan F, Akar HH, Dursun I, Yilmaz K. Desensitization of darbepoetin-α: a case report. *Eur Ann Allergy Clin Immunol*. 2013;45(5):176-177. [CrossRef]
14. Alexandre AF, Ali M, Lawrence A, McKendrick J. Delayed-type hypersensitivity reaction due to epoetin-alfa in CKD: a therapeutic challenge. *J Am Soc Nephrol*. 2021;32:189.
15. Brines M, Grasso G, Fiordaliso F, et al. Erythropoietin mediates tissue protection through an erythropoietin and common beta-subunit heteroreceptor. *Proc Natl Acad Sci U S A*. 2004;101(41):14907-14912. [CrossRef]

ABCResearch

Arch Basic Clin Res 2026;8(1):40-46
DOI: 10.4274/ABCR.2025.25376

Research Article

Non-Motor Symptoms in Gabapentin Users: A Clinical Evaluation

Ceyda Tanoğlu[1], Alevtina Ersoy[2]

[1]Department of Neurology, Health Sciences University Türkiye, İzmir Tepecik Education and Research Hospital, İzmir, Türkiye
[2]Department of Neurology, Erzincan Binali Yıldırım University Faculty of Medicine, Erzincan, Türkiye

Cite this article as: Tanoğlu C, Ersoy A. Non-motor symptoms in gabapentin users: a clinical evaluation. *Arch Basic Clin Res*. 2026;8(1):40-46.

ORCID IDs of the authors: C.T. 0000-0002-4303-6797, A.E. 0000-0002-4968-0786.

ABSTRACT

Objective: Gabapentin is widely used for neuropathic pain, epilepsy, and other indications; however, its non-motor side effects remain understudied. This prospective, cross-sectional observational study aimed to evaluate non-motor symptoms in gabapentin users, assessed with the Non-Motor Symptom Scale (NMSS).

Methods: The Turkish version of the NMSS was administered once to 105 patients who had been receiving gabapentin for at least 120 days and to 107 demographically matched healthy controls at our Non-Motor Symptom Scale (NMSS) between January and December 2022. Exclusion criteria included neurodegenerative diseases, diabetes, psychiatric disorders, and thyroid dysfunction. Group comparisons were performed using independent samples t-tests for continuous variables and chi-square or Fisher's exact tests for categorical data.

Results: Gabapentin users had significantly higher total NMSS scores than controls (11.6 ± 5.56 vs. 6.03 ± 4.28, $P < 0.001$). Symptoms such as salivation, constipation, urgency, nocturia, pain, memory impairment, depression, anxiety, sexual dysfunction, orthostatic hypotension, daytime sleepiness, and leg edema were reported more frequently in the gabapentin group ($P < 0.05$).

Conclusion: Gabapentin use was associated with a higher frequency of non-motor symptoms, as assessed by the NMSS. This study suggests that the NMSS may serve as a structured tool for the systematic screening of non-motor symptoms in patients receiving gabapentin. Prospective studies with indication-matched controls and validated assessment tools are warranted to confirm these associations.

Keywords: Salivation, constipation, gabapentin, urinary incontinence, non-motor symptoms

INTRODUCTION

Gabapentin was first approved by the United States Food and Drug Administration in 1993 for the treatment of postherpetic neuralgia and epilepsy. The European Medicines Agency later approved the drug for the treatment of neuropathic pain. Beyond its approved indications, gabapentin is frequently prescribed off-label for migraine, trigeminal neuralgia, acute or chronic postoperative pain, relief of fibromyalgia symptoms, psychiatric disorders (such as anxiety and bipolar disorder), alcohol and opioid withdrawal syndromes, insomnia, restless legs syndrome (RLS), and pruritus associated with certain dermatological conditions.[1,2] Over the last decade, gabapentin prescriptions have quadrupled due to its broad indication profile and analgesic efficacy.[3] Correspondingly, reports of adverse effects—including sedation, dizziness, somnolence, ataxia, nystagmus, nausea, and vomiting—have increased.[4,5]

In our clinical practice, gabapentin-treated patients have reported subjective complaints such as hypersalivation, constipation, and sexual dysfunction. These symptoms are not routinely assessed in clinical practice. Although the Non-Motor Symptom Scale (NMSS) was originally developed for Parkinson's disease, we considered it the most structured and multidimensional tool available for systematically evaluating non-motor effects potentially associated with gabapentin use. The NMSS has also been applied in conditions such as idiopathic or isolated rapid eye movement (REM) sleep behavior

Corresponding author: Alevtina Ersoy, **E-mail:** alevtina_ersoy@hotmail.com

Received: September 26, 2025 **Accepted:** December 2, 2025 **Publication Date:** January 26, 2026
Revision Requested: October 20, 2025

disorder and essential tremor to explore non-motor domains beyond idiopathic Parkinson's disease.[6,7] However, to our knowledge, this is the first study employing the NMSS to assess medication-related non-motor adverse effects.

The NMSS provides a comprehensive assessment across multiple non-motor domains but evaluates only the presence of symptoms, not their severity. Although the NMSS was originally developed and validated for Parkinson's disease, we selected it for this study because gabapentin is known to affect several non-motor systems, including gastrointestinal, urinary, mood, and sleep functions. A structured tool capable of simultaneously screening a wide range of non-motor symptoms (NMS) was required; the NMSS was considered the most suitable instrument reported in the literature.

Gabapentin is widely used for neuropathic pain, epilepsy, and other indications, and is known to affect multiple non-motor domains, including gastrointestinal and urinary function, mood, and sleep. However, its non-motor side effects remain understudied and have not been systematically evaluated with structured instruments. Therefore, the aim of the present study was to assess NMS in patients using gabapentin, applying the NMSS as an exploratory screening tool.

MATERIAL AND METHODS

Patients aged 18-65 years who had been receiving gabapentin treatment for at least 120 consecutive days for various indications, including neuropathic pain, postherpetic neuralgia, and migraine prophylaxis, at the Mengücek Gazi Training and Research Hospital Neurology Outpatient Clinic between January 2022 and December 2022 were included in the study. Patients with incomplete clinical records, irregular medication use, or concurrent treatment with other anticonvulsants or antidepressants were excluded. Written informed consent was obtained from all participating patients, and the study protocol was approved by the Ethics Committee of Erzincan Binali Yıldırım University. Individuals with neurodegenerative or cardiovascular diseases, diabetes mellitus, primary gastrointestinal or genitourinary diseases, psychiatric conditions, or thyroid dysfunction were excluded. This was a prospective cross-sectional observational study. The NMSS was administered in person during routine outpatient visits by a trained neurologist. Demographic and clinical data, including medication use, gabapentin dosage, and comorbidities, were recorded contemporaneously using standardized forms and subsequently entered into the hospital database for analysis.

MAIN POINTS

- Patients receiving gabapentin reported significantly higher non-motor symptom scores compared with healthy controls, as assessed by the Non-Motor Symptom Scale (NMSS).
- Salivation, constipation, urinary urgency or nocturia, pain, memory impairment, depression, anxiety, sexual dysfunction, orthostatic hypotension, daytime sleepiness, leg edema, and sweating were significantly more frequent among gabapentin users.
- This study is the first to systematically assess non-motor symptoms in gabapentin users with the NMSS, highlighting a broad range of underrecognized complaints.
- The NMSS may serve as a structured tool for the systematic screening of non-motor symptoms in patients receiving gabapentin in routine clinical practice.
- Findings are exploratory, but suggest the need for prospective, indication-matched studies to confirm and clarify the associations between gabapentin and non-motor symptoms.

The Turkish-validated NMSS for Parkinson's disease was administered to gabapentin users and healthy controls. The control group consisted of age- and sex-matched healthy individuals who were not using gabapentin or any other medications affecting the central nervous system. All control participants were recruited from the same outpatient clinic to minimize selection bias. Potential confounding factors, such as diabetes mellitus, thyroid dysfunction, cardiovascular diseases, psychiatric disorders, or systemic inflammatory diseases, were explicitly excluded from both groups. Comorbidities were reviewed using detailed medical histories and current medication records to ensure comparability between groups. The NMSS consists of 30 yes/no items covering gastrointestinal, genitourinary, cardiovascular, attention/memory, perception, mood, and sleep domains. The items are scored as 1 (yes or presence) or 0 (no or absence).[8]

Patients with at least 120 days of gabapentin use were included because long-term adverse effects typically emerge after 3-4 months .[4,9]

Data were retrieved from Mengücek Gazi Training and Research Hospital's database. The study was approved by the Erzincan Binali Yıldırım University Clinical Research Ethics Committee (approval no.: 14/11, dated: 10.01.2022). The study was conducted in accordance with the ethical standards of the institutional research committee and with the Declaration of Helsinki (1964) and its later amendments.

Statistical Analysis

The sample size was determined based on a priori power analysis using G*Power version 3.1.9.7 (Heinrich Heine University Düsseldorf, Düsseldorf, Germany). The analysis indicated that a minimum sample size of 52 subjects was required. Additionally, a post-hoc power analysis indicated that the study had 99% power. Statistical analyses were performed using IBM SPSS Statistics for Windows, version 25.0 (IBM Corp., Armonk, NY, USA). The distributions of continuous variables were assessed for normality using the Shapiro-Wilk and Kolmogorov-Smirnov tests. Descriptive statistics were presented as mean ± standard deviation for continuous variables and as frequencies (n, %) for categorical variables. For comparisons of total NMSS scores between groups, the Independent samples t-test was applied. For categorical symptom data (yes/no responses), chi-square tests were used, with Fisher's exact test applied when expected cell counts were less than.[5] Correlation analyses were performed using Spearman's rho for non-normally distributed

variables. Spearman's rank correlation test was used to evaluate associations between daily gabapentin dose, age, and total NMSS scores within the gabapentin-treated group. A *P* value < 0.05 was considered statistically significant.

RESULTS

The study included 105 patients receiving gabapentin and 107 demographically matched healthy controls. The demographic characteristics of the groups are presented in Table 1. Statistical analysis revealed no significant differences between the groups in terms of sex or age ($P > 0.05$ for both). Indications for gabapentin use are listed in Table 2.

The NMSS was administered to patients receiving gabapentin treatment and to healthy controls. The total NMSS score was significantly higher in the gabapentin group than in the control group (11.6 ± 5.56 vs. 6.03 ± 4.28, $P < 0.001$). Item-based results are summarized in Table 3. Salivation, gastrointestinal, urinary, neuropsychiatric, and autonomic symptoms were significantly more frequent in the gabapentin group than in controls. Among gabapentin users, daily doses ranged from 200 to 1800 mg/day (median = 850 mg/day). No significant correlation was found between daily gabapentin dose and total NMSS score ($P = 0.21$). In contrast, age was positively correlated with the total NMSS score among gabapentin users ($P = 0.006$). No significant association between age and NMSS score was observed in the control group, likely due to minimal variability in non-motor symptom reporting.

DISCUSSION

In the present study, the total NMSS score was significantly higher in the gabapentin-user group than in the control group. To the best of our knowledge, this is the first study to evaluate NMS during gabapentin treatment using a structured screening tool. While many of the individual complaints observed in our cohort, such as constipation, salivation, and sexual dysfunction, have previously been reported as adverse effects of gabapentin, our study is novel in systematically assessing these symptoms with the NMSS in a relatively large sample of gabapentin-treated patients.

The novelty of our findings does not lie in identifying previously unrecognized side effects, but rather in providing a systematic overview of non-motor domains potentially affected by gabapentin. By applying the NMSS as a structured screening tool, we captured a wide range of symptoms often underreported in routine clinical practice, thereby providing a more comprehensive profile of gabapentin's tolerability. These results should be considered exploratory and hypothesis-generating, underscoring the need for future studies using validated adverse events or quality-of-life instruments to confirm and extend our observations.

Items 1, 3, 4, 5, 6, and 7 of the NMSS pertain to gastrointestinal dysfunction. In our cohort, excessive salivation and constipation were significantly more common among gabapentin-treated patients than among controls. Hypersalivation has a reported prevalence of 6%-15% in healthy individuals.[10], but no clinical studies have specifically investigated salivation during gabapentin treatment in humans. A feline study reported post-gabapentin hypersalivation, although it was unclear whether this was a pharmacological effect or related to stress or oral irritation from administration.[11]

There were no statistically significant differences between the groups regarding dysphagia or nausea/vomiting. Gabapentin has been shown to improve swallowing function after radiotherapy and head and neck surgery, likely by reducing neuropathic pain rather than through a direct effect on swallowing mechanics.[12] Although nausea and vomiting are recognized adverse effects of gabapentin[5], studies have also shown its effectiveness in the treatment of hyperemesis gravidarum. Conversely, one study reported no statistically significant effect of gabapentin on chemotherapy-related nausea and vomiting.[13,14] These divergent outcomes likely reflect differences in patient populations and treatment indications.

In the present study, the prevalence of constipation was significantly higher in the gabapentin-user group than in the control group. Constipation is a known side effect of gabapentin, generally of mild to moderate severity.[15] The mechanism remains unclear, but it may involve reduced neuronal excitability and decreased release of neurotransmitters such as glutamate and substance P. Paradoxically, gabapentin has been shown to alleviate symptoms in diarrhea-predominant irritable bowel syndrome by enhancing rectal compliance and reducing rectal sensitivity.[16]

No statistically significant differences were observed for fecal incontinence or tenesmus between the groups. A case series of four patients reported that gabapentin and pregabalin alleviated cancer-related tenesmus, although the evidence remains limited.[17] The differing results reported in the literature may reflect the use of gabapentin in diverse patient populations with varying indications.

Table 1. Comparison of Demographic Characteristics Between the Gabapentin and Control Groups

Characteristic	Gabapentin group (n=105)	Control group (n=107)	*P* value
Sex, n (%)			0.919
Female	67 (63.8%)	67 (62.6%)	
Male	38 (36.2%)	40 (37.4%)	
Age (years)			0.164
Mean ± SD	57.7 ± 11.8	55.7 ± 9.8	

SD, standard deviation.

Table 2. Indications for Gabapentin Use (n=105)

Indication	Number of patients	Percentage (%)
Lumbar disc herniation	25	23.8%
Polyneuropathy	19	18.1%
Restless leg syndrome	20	19.1%
Cervical disc herniation	18	17.1%
Trigeminal neuralgia	7	6.67%
Carpal tunnel syndrome	7	6.67%
Fibromyalgia	6	5.71%
Ulnar nerve lesion	3	2.86%

Urinary dysfunction is assessed by questions 8 and 9 of the NMSS. In the present study, urinary urgency and nocturia were significantly more frequent among gabapentin users. Case reports describe gabapentin-associated urinary incontinence, thought to result from inhibitory effects on bladder C-fiber afferents and reduced detrusor contractility.[18] In contrast, Chua et al.[19] demonstrated that gabapentin was effective in the treatment of overactive bladder. In the same study, gabapentin was more effective than solifenacin in treating nocturia, an effect attributed to hypothalamic inhibition of bladder activity. These discrepancies may reflect differential effects of gabapentin in individuals with and without underlying urinary symptoms.

Questions 2, 10, and 29 of the NMSS pertain to the sensory domain. No statistically significant difference in olfactory function was observed between the groups. Published studies on gabapentin's effect on olfaction are limited to cohorts with COVID-19: one study reported no change in olfaction, while another, with a very small sample size, reported subjective improvement.[20,21]

To the best of our knowledge, there are no studies addressing gabapentin's impact on gustatory function.

Despite gabapentin's well-established efficacy in pain management, reported pain complaints were significantly higher in the gabapentin group than in controls. We attribute this finding to the underlying indications for gabapentin, rather than to a nociceptive side effect.

Table 3. NMSS Findings Across Study Groups

Symptom	Gabapentin group (n=105)		Control group (n=107)		*P* value
	Yes	No	Yes	No	
1.Increased salivation	13 (12.4%)	92 (87.6%)	3 (2.8%)	104 (97.2%)	**0.009**
2.Loss of taste/smell	13 (12.4%)	92 (87.6%)	9 (8.4%)	98 (91.6%)	0.343
3.Difficulty swallowing	14 (13.3%)	91 (86.7%)	7 (6.5%)	100 (93.5%)	0.098
4.Nausea/vomiting	18 (17.1%)	87 (82.9%)	9 (8.4%)	98 (91.6%)	0.057
5.Constipation	41 (39%)	64 (61%)	25 (23.4%)	82 (76.6%)	**0.014**
6.Fecal incontinence	14 (13.3%)	91 (86.7%)	7 (6.5%)	100 (93.5%)	0.098
7.Tenesmus	48 (45.7%)	57 (54.3%)	48 (44.9%)	59 (55.1%)	0.901
8.Urgency	61 (58.1%)	44 (41.9%)	76 (71%)	31 (29%)	**0.049**
9.Nocturia	84 (80%)	21 (20%)	50 (46.7%)	57 (53.3%)	**< 0.001**
10.Pain	68 (64.8%)	37 (35.2%)	21 (19.6%)	86 (80.4%)	**< 0.001**
11Weight change	20 (19%)	85 (81%)	2 (1.9%)	105 (98.1%)	**< 0.001**
12.Memory impairment	57 (54.3%)	48 (45.7%)	36 (33.6%)	71 (66.4%)	**0.003**
13.Apathy	39 (37.1%)	66 (62.9%)	26 (24.3%)	81 (75.7%)	**0.043**
14.Hallucinations	21 (20%)	84 (80%)	2 (1.9%)	105 (98.1%)	**< 0.001**
15.Attention deficits	43 (41%)	62 (59%)	25 (23.4%)	82 (76.6%)	0.006
16.Depression	69 (65.7%)	36 (34.3%)	30 (28%)	77 (72%)	**< 0.001**
17.Anxiety	44 (41.9%)	61 (58.1%)	20 (18.7%)	87 (81.3%)	**< 0.001**
18.Reduced libido	58 (55.2%)	47 (44.8%)	33 (30.8%)	74 (69.2%)	**< 0.001**
19.Sexual dysfunction	57 (54.3%)	48 (45.7%)	24 (22.4%)	83 (77.6%)	**< 0.001**
20.Orthostatic hypotension	60 (57.1%)	45 (42.9%)	27 (25.2%)	80 (74.8%)	**< 0.001**
21.Falls	35 (33.3%)	70 (66.7%)	14 (13.1%)	93 (86.9%)	**< 0.001**
22.Daytime sleepiness	21 (20%)	84 (80%)	9 (8.4%)	98 (91.6%)	**0.016**
23.Difficulty initiating/maintaining sleep	50 (47.6%)	55 (52.4%)	45 (42.1%)	62 (57.9%)	0.415
24.Vivid dreams	33 (31.4%)	72 (68.6%)	18 (16.8%)	89 (83.2%)	**0.013**
25.REM sleep behavior disorder	28 (26.7%)	77 (73.3%)	14 (13.1%)	93 (86.9%)	**0.013**
26.Restless leg syndrome	63 (60%)	42 (40%)	26 (24.3%)	81 (75.7%)	**< 0.001**
27.Leg edema	48 (45.7%)	57 (54.3%)	9 (8.4%)	98 (91.6%)	**< 0.001**
28.Sweating	52 (49.5%)	53 (50.5%)	19 (17.8%)	88 (82.2%)	**< 0.001**
29.Diplopia	26 (24.8%)	79 (75.2%)	6 (5.6%)	101 (94.4%)	**< 0.001**
30.Delusions	22 (21%)	83 (79%)	4 (3.7%)	103 (96.3%)	**< 0.001**

REM, Rapid eye movement; NMSS, Non-Motor Symptom Scale.

Diplopia was also reported significantly more often by gabapentin users. One study noted an 8% incidence of diplopia with 2,400 mg/day gabapentin treatment.[22] The mechanism by which gabapentin causes diplopia is not known.

Items 12-17 and 30 of the NMSS capture neuropsychiatric and cognitive complaints. In our cohort, "yes" responses to these items were more frequent in the gabapentin group than in controls. Memory and attention disturbances were notably higher among gabapentin users. Forgetfulness has been reported in 20% of gabapentin users and may be related to reduced glutamate release or suppression of neuronal hyperactivity.[23]

Gabapentin's psychiatric effects are inconsistent across studies. While some trials found no psychotropic effects, others demonstrated anxiolytic effects; gabapentin has shown benefit as an adjunct in bipolar disorder.[24]

In several cases where gabapentin was initiated in patients already receiving psychotropic medications, hallucinations and agitation were reported. Additionally, a single case report described a patient without prior psychiatric history who developed hallucinations, suicidal ideation, and agitation after gabapentin administration. Gabapentin-associated psychiatric side effects may be linked to elevated extracellular glutamate or downregulation of serotonin receptors.[25] Variability in findings may reflect differences in psychiatric background across study populations.

Sexual dysfunction is assessed by questions 18 and 19 of the NMSS. Both low- and high-dose gabapentin have been implicated in sexual side effects, possibly due to its inhibitory effects on neurotransmission.[26,27] In the present study, decreased libido and erectile or sexual dysfunction occurred significantly more frequently among gabapentin users. Libido is governed by limbic system pathways, while erectile function is regulated by autonomic circuits. Decreased libido is more often linked to hormonal and psychiatric factors, whereas erectile dysfunction is more commonly associated with vascular and neurogenic causes. Dopamine supports both libido and erection.[28]

Questions 20 and 21 of the NMSS relate to cardiovascular autonomic function and falls. In our cohort, orthostatic hypotension and falls were significantly more common among gabapentin users than controls. Chen et al.[29] observed that microinjection of gabapentin into the nucleus tractus solitarii of hypertensive rats induced hypotension and bradycardia via the nitric oxide synthase pathway. Moreover, clinical studies have shown that gabapentin substantially increases the the risk of falls in older adults, independent of cognitive function.[30,31]

Weight loss is among the known side effects of gabapentin, although its mechanism remains unknown.[32] In the present study, complaints of weight loss were significantly more frequent in the gabapentin group than in controls.

Questions 22-26 of the NMSS assess sleep complaints. In our cohort, with the exception of items related to sleep initiation, scores for sleep-related NMS were significantly higher in the gabapentin group. Somnolence is a known adverse effect of gabapentin.[33] No studies have evaluated the association between gabapentin and REM sleep behavior disorder.

RLS complaints were significantly more common in the gabapentin group than in the control group. We attribute this finding not to a side effect of gabapentin but to its use in patients with RLS.

Leg edema is assessed by questions 27 of the NMSS. This complaint was significantly more frequent in the gabapentin group. Gabapentin-induced peripheral edema is thought to result from reduced vascular autoregulation and increased vascular permeability.[5,34]

Excessive sweating is assessed by questions 28 of the NMSS. In our cohort, this complaint was more frequently reported by gabapentin users. Although no studies have directly examined excessive sweating as a side effect, gabapentin has shown efficacy in treating menopausal and cancer-related sweating and hot flashes.[35,36] The discrepancy between our findings and previous reports may relate to the inclusion of hormonally unstable patients in those studies. Gabapentin's effect on sweating may involve modulation of hypothalamic calcium channels. Gabapentin binds to α2-δ subunits of voltage-gated calcium channels, modulating the release of several neurotransmitters. These pharmacological effects may contribute to the broad range of NMS observed in clinical use.[37]

Although many adverse effects of gabapentin have been described as dose-dependent[38], our findings did not demonstrate a significant association between daily dose and total NMSS score. Conversely, a positive correlation between age and non-motor symptom burden was observed among gabapentin users but not in the control group, suggesting that aging-related factors may play a more prominent role than dosage in the manifestation of non-motor adverse effects. These findings highlight the importance of considering patient age when evaluating non-motor side effects associated with gabapentin therapy.

These results should therefore be viewed as exploratory. While the NMSS is not a validated instrument in this population, its use enabled the detection of a broad range of complaints that are often underreported in daily clinical practice. Future studies with disease-specific adverse event or quality-of-life measures are required to confirm the clinical significance of these findings.

Study Limitations

There are several limitations to the present study. First, we applied the NMSS, originally developed and validated for Parkinson's disease. Although the scale has not been formally validated in non-Parkinson's populations, its multidimensional structure enabled us to systematically assess a broad spectrum of non-motor domains relevant to gabapentin therapy, including gastrointestinal, urinary, neuropsychiatric, and sleep-related symptoms. For this reason, we considered the NMSS an appropriate exploratory tool. Second, the NMSS does not encompass all possible NMS and functions only as a screening instrument rather than providing a detailed quantitative assessment. For instance, behavioral aspects such as medication misuse or dependence are not captured within the NMSS domains, despite emerging evidence suggesting that

gabapentinoids may have potential for dependence.[38] Third, as gabapentin dosage was neither tapered nor discontinued in this study, the reversibility of non-motor adverse effects could not be evaluated. Furthermore, serum iron and ferritin levels were not assessed; therefore, the potential contribution of iron deficiency to the higher frequency of RLS among gabapentin users could not be evaluated. Autonomic function tests were not performed; therefore, the possibility that some NMS (e.g., orthostatic hypotension, sweating abnormalities, constipation) may reflect autonomic involvement in patients with polyneuropathy cannot be excluded. Finally, the study's cross-sectional observational design precludes causal inference; the associations observed should be interpreted as correlational rather than causal. Prospective studies with indication-matched controls are warranted to confirm and further elucidate these associations.

CONCLUSION

In this study, patients receiving gabapentin reported a higher frequency of NMS, as assessed by the NMSS, compared with healthy controls. These findings suggest a potential association between gabapentin use and NMS. However, they should be interpreted with caution due to the exploratory use of the NMSS, the heterogeneity of clinical indications, and the cross-sectional design. Additionally, the NMSS may serve as a practical tool for the systematic screening of potential side effects in clinical settings. Prospective studies with indication-matched control groups and validated assessment tools are warranted to confirm and clarify these associations.

Ethics

Ethics Committee Approval: The study was approved by the Erzincan Binali Yıldırım University Clinical Research Ethics Committee (approval no.: 14/11, dated: 10.01.2022).

Informed Consent: Written informed consent was obtained from all participating patients.

Acknowledgments

The authors would like to thank those who assisted in collecting data.

Footnotes

Author Contributions

Concept Design – C.T., A.E.; Data Collection or Processing – C.T., A.E.; Analysis or Interpretation – C.T., A.E.; Literature Review – C.T., A.E.; Writing, Reviewing and Editing – C.T., A.E.

Declaration of Interests: The authors declare no conflict of interest regarding the publication of this paper.

Funding: The authors declare no financial support or funding.

REFERENCES

1. Athavale A, Murnion B. Gabapentinoids: a therapeutic review. *Aust Prescr.* 2023;46(4):80-85. [CrossRef]
2. Chincholkar M. Gabapentinoids: pharmacokinetics, pharmacodynamics and considerations for clinical practice. *Br J Pain.* 2020;14(2):104-114. [CrossRef]
3. Chan AYL, Yuen ASC, Tsai DHT, et al. Gabapentinoid consumption in 65 countries and regions from 2008 to 2018: a longitudinal trend study. *Nat Commun.* 2023;14(1):5005. [CrossRef]
4. Ri K, Fukasawa T, Yoshida S, Takeuchi M, Kawakami K. Risk of parkinsonism and related movement disorders with gabapentinoids or tramadol: a case-crossover study. *Pharmacotherapy.* 2023;43(2):136-144. [CrossRef]
5. Nwankwo A, Koyyalagunta D, Huh B, D'Souza RS, Javed S. A comprehensive review of the typical and atypical side effects of gabapentin. *Pain Pract.* 2024;24(8):1051-1058. [CrossRef]
6. Peng J, Wang L, Li N, Li J, Duan L, Peng R. Distinct non-motor features of essential tremor with head tremor patients. *Acta Neurol Scand.* 2020;142(1):74-82.[CrossRef]
7. Zang Y, Zhang H, Li Y, et al. Fatigue in patients with idiopathic/isolated rem sleep behavior disorder. *Brain Sci.* 2022;12(12):1728. [CrossRef]
8. Çankaya Ş, Altınayar S. Parkinson hastalarında motor olmayan bulguların NMSQ anketi kullanılarak değerlendirilmesi. *Ann Health Sci Res.* 2020;1:47-55.
9. Gomes T, Juurlink DN, Antoniou T, et al. Gabapentin, opioids, and the risk of opioid-related death: a population-based nested case-control study. *PLoS Med.* 2017;14(10):e1002396. [CrossRef]
10. Metta V, Chung-Faye G, Benamer TS, Mrudula R, Goyal V, Falup-Pecurariu C, et al. Hiccups, hypersalivation, hallucinations in Parkinson's disease: new insights, mechanisms, pathophysiology, and management. *J Pers Med.* 2023;13(5):711.[CrossRef]
11. Pankratz KE, Ferris KK, Griffith EH, Sherman BL. Use of single-dose oral gabapentin to attenuate fear responses in cage-trap confined community cats: a double-blind, placebo-controlled field trial. *J Feline Med Surg.* 2018;20(6):535-543.
12. Miller N, Noller M, Yang A, McCoul ED, Tolisano AM, Riley CA. Lesser known uses of γ-aminobutyric acid analogue medications in otolaryngology. *Laryngoscope.* 2022;132(5):954-964. [CrossRef]
13. Guttuso T Jr, Messing S, Tu X, et al. Effect of gabapentin on hyperemesis gravidarum: a double-blind, randomized controlled trial. *Am J Obstet Gynecol MFM.* 2021;3(1):100273. [CrossRef]
14. Kiani MH, Shayesteh AA, Ahmadzadeh A. An investigation into the effect of gabapentin capsules on the reduction of nausea and vomiting after chemotherapy in cancerous patients under platinum-based treatment. *J Family Med Prim Care.* 2019;8(6):2003-2007. [CrossRef]
15. Xu W, Dong H, Ran H, et al. Efficacy and safety of pregabalin and gabapentin for pruritus: a systematic review and meta-analysis. *J Pain Symptom Manage.* 2025;69(1):65-81. [CrossRef]
16. Lee KJ, Kim JH, Cho SW. Gabapentin reduces rectal mechanosensitivity and increases rectal compliance in patients with diarrhoea-predominant irritable bowel syndrome. *Aliment Pharmacol Ther.* 2005;22(10):981-988. [CrossRef]
17. Tagami K, Yoshizumi M, Inoue A, Matoba M. Effectiveness of gabapentinoids for cancer-related rectal and vesical tenesmus: report of four cases. *Indian J Palliat Care.* 2020;26(3):381-384. [CrossRef]
18. Rissardo JP, Caprara ALF. Gabapentin-associated urinary incontinence: a case verified by rechallenge. *Clin Neuropharmacol.* 2019;42(3):91-93. [CrossRef]
19. Chua ME, See MC 4th, Esmeña EB, Balingit JC, Morales ML Jr. Efficacy and safety of gabapentin in comparison to solifenacin succinate in adult overactive bladder treatment. *Low Urin Tract Symptoms.* 2018;10(2):135-142. [CrossRef]

20. Garcia JAP, Miller E, Norwood TG, et al. Gabapentin improves parosmia after COVID-19 infection. *Int Forum Allergy Rhinol.* 2023;13(6):1034-1036. [CrossRef]

21. Mahadev A, Hentati F, Miller B, et al. Efficacy of gabapentin for post-COVID-19 olfactory dysfunction: the GRACE randomized clinical trial. *JAMA Otolaryngol Head Neck Surg*. 2023;149(12):1111-1119. [CrossRef]

22. Wilson EA, Sills GJ, Forrest G, Brodie MJ. High dose gabapentin in refractory partial epilepsy: clinical observations in 50 patients. *Epilepsy Res*. 1998;29(2):161-166. [CrossRef]

23. Putzke JD, Richards JS, Kezar L, Hicken BL, Ness TJ. Long-term use of gabapentin for treatment of pain after traumatic spinal cord injury.*Clin J Pain*. 2002;18(2):116-121. [CrossRef]

24. Ahmed S, Bachu R, Kotapati P, et al. Use of gabapentin in the treatment of substance use and psychiatric disorders: a systematic Review. *Front Psychiatry*. 2019;10:228. [CrossRef]

25. Evrensel A, Ünsalver BÖ. Psychotic and depressive symptoms after gabapentin treatment. *Int J Psychiatry Med*. 2015;49(4):245-248. [CrossRef]

26. Calabrò RS. Gabapentin and sexual dysfunction: an overlooked and underreported problem? *Epilepsy Behav*. 2011;22(4):818. [CrossRef]

27. Kaufman KR, Struck PJ. Gabapentin-induced sexual dysfunction. *Epilepsy Behav*. 2011;21(3):324-326. [CrossRef]

28. Dean RC, Lue TF. Physiology of penile erection and pathophysiology of erectile dysfunction. *Urol Clin North Am*. 2005;32(4):379-395. [CrossRef]

29. Chen HH, Li YD, Cheng PW, et al. Gabapentin reduces blood pressure and heart rate through the nucleus tractus solitarii. *Acta Cardiol Sin*. 2019;35(6):627-633. [CrossRef]

30. Painter JT, Peng C, Burlette M, et al. The effect of concurrent use of opioids and gabapentin on fall risk in older adults. *J Pain Palliat Care Pharmacother*. 2024;38(4):327-333. [CrossRef]

31. Oh G, Moga DC, Fardo DW, Harp JP, Abner EL. The association of gabapentin initiation with cognitive and behavioral changes in older adults with cognitive impairment: a retrospective cohort study. *Drugs Aging*. 2024;41(7):623-632. [CrossRef]

32. Sabers A, Gram L. Newer anticonvulsants: comparative review of drug interactions and adverse effects. *Drugs*. 2000;60(1):23-33. [CrossRef]

33. Goa KL, Sorkin EM. Gabapentin. A review of its pharmacological properties and clinical potential in epilepsy. *Drugs*. 1993;46(3):409-427. [CrossRef]

34. Largeau B, Bordy R, Pasqualin C, et al. Gabapentinoid-induced peripheral edema and acute heart failure: a translational study combining pharmacovigilance data and in vitro animal experiments. *Biomed Pharmacother*. 2022;149:112807. [CrossRef]

35. Porzio G, Aielli F, Verna L, et al. Gabapentin in the treatment of severe sweating experienced by advanced cancer patients. *Support Care Cancer*.2006;14(4):389-391. [CrossRef]

36. Pandya KJ, Morrow GR, Roscoe JA, et al. Gabapentin for hot flashes in 420 women with breast cancer: a randomised double-blind placebo-controlled trial. *Lancet*. 2005;366 (9488):818-824. [CrossRef]

37. Perez Lloret S, Amaya M, Merello M. Pregabalin-induced parkinsonism: a case report. *Clin Neuropharmacol*. 2009;32(6):353-354. [CrossRef]

38. Tanoğlu C, Öcal R. Are gabapentinoids addictive? *Academic Journal of Neurology and Neurosurgery*. 2025 Mar 21;2(1):9-12. [CrossRef]

ABCResearch

Arch Basic Clin Res 2026;8(1):47-52
DOI: 10.4274/ABCR.2025.25392

Research Article

Predicting Breast Cancer Biomarker Expression with Diffusion-Weighted Magnetic Resonance Imaging

Kemal Buğra Memiş, Ayşe Sena Çelik, Muhammet Fırat Öztepe

Department of Radiology, Erzincan Binali Yıldırım University, Faculty of Medicine, Erzincan, Türkiye

Cite this article as: Memiş KB, Çelik AS, Öztepe MF. Predicting breast cancer biomarker expression with diffusion-weighted magnetic resonance imaging. *Arch Basic Clin Res*. 2026;8(1):47-52.

ORCID IDs of the authors: K.B.M. 0009-0007-6746-3906, A.S.Ç. 0009-0009-8860-4936, M.F.Ö. 0000-0002-1027-0915.

ABSTRACT

Objective: To evaluate the diagnostic performance of diffusion-weighted magnetic resonance imaging (DWI) and apparent diffusion coefficient (ADC) values in differentiating benign and malignant breast lesions, and to investigate correlations between ADC values and immunohistochemical (IHC) biomarkers (estrogen receptor, progesterone receptor, human epidermal growth factor receptor 2, Ki-67) as well as axillary lymph node status.

Methods: This retrospective study included 148 female patients (159 breast lesions) who underwent preoperative breast magnetic resonance imaging (MRI) between January 2022 and December 2024. DWI was performed using b values of 0 and 1000 s/mm^2, and mean ADC values were calculated from regions of interest placed within solid tumor areas. Histopathological and IHC analyses were used to classify lesions and molecular subtypes.

Results: Among the 159 lesions, 56 (35.2%) were malignant and 103 (64.8%) were benign. Malignant lesions exhibited significantly lower ADC values than benign ones (0.92×10^{-3} mm^2/s vs. 1.66×10^{-3} mm^2/s). The optimal ADC cut-off for malignancy was 1.24×10^{-3} mm^2/s, yielding 95.2% sensitivity and 89.1% specificity. Hormone receptor-positive tumors and lesions with high Ki-67 index showed lower ADC values. No significant correlation was found between ADC and human epidermal growth factor receptor 2 status. Triple-negative breast cancers demonstrated the highest ADC values among subtypes. ADC values of metastatic axillary lymph nodes were significantly lower than those of contralateral benign nodes (0.78×10^{-3} vs. 1.82×10^{-3} mm^2/s).

Conclusion: ADC values are effective in distinguishing malignant from benign breast lesions and provide non-invasive insights into tumor biology. Lower ADC values correlate with malignancy, hormone receptor positivity, proliferative activity, and metastatic nodal involvement. DWI is a reliable, non-contrast imaging biomarker that may enhance personalized evaluation of breast cancer.

Keywords: Apparent diffusion coefficient values, estrogen receptor, progesterone receptor, immunohistochemical biomarkers, lymph node metastasis

INTRODUCTION

Breast cancer is the most common malignancy among women worldwide and remains a leading cause of mortality. Accurate, non-invasive characterization of tumor biology is essential for early diagnosis and tailored treatment strategies. Magnetic resonance imaging (MRI), especially dynamic contrast-enhanced MRI, offers high sensitivity in lesion detection. However, due to the limitations associated with contrast agent use—such as nephrotoxicity and gadolinium retention—alternative, contrast-free imaging techniques have gained prominence. Among these, diffusion-weighted imaging (DWI) and the derived apparent diffusion coefficient (ADC) have emerged as promising tools for functional lesion characterization.[1,2]

DWI reflects the mobility of water molecules within tissues and provides indirect information about cellular density, stromal composition, and membrane integrity. Moreover,

Corresponding author: Kemal Buğra Memiş, **E-mail:** kemalbugramemis@gmail.com

Received: November 11, 2025 **Accepted:** December 2, 2025 **Publication Date:** January 26, 2026
Revision Requested: November 20, 2025

the quantitative evaluation of water diffusion is performed using ADC values derived from DWI. The ADC is expressed in square millimeters per second (mm^2/s) and is determined by quantifying signal attenuation on DWI acquired with at least two different b values. Malignant breast tumors typically demonstrate restricted diffusion and thus lower ADC values due to high cellularity, while benign lesions tend to exhibit higher ADC values.[3-6]

In addition to lesion characterization, DWI is increasingly investigated for its potential to reflect tumor molecular characteristics. Several studies suggest that ADC values may correlate with immunohistochemical (IHC) biomarkers such as estrogen receptor (ER), progesterone receptor (PR), human epidermal growth factor receptor 2 (HER2), and Ki-67, which are used to define tumor subtypes and aggressiveness.[7,8]

Moreover, axillary lymph node involvement, a key component in breast cancer staging and management, is also evaluated using DWI. By assessing the diffusion properties of lymph nodes, DWI may help distinguish between benign and metastatic nodes non-invasively.[9]

This study aims to comprehensively evaluate the diagnostic value of DWI-derived ADC measurements in differentiating benign and malignant breast lesions, to delineate their associations with major IHC biomarkers (ER, PR, HER2, Ki-67), and to determine their added utility in axillary staging through comparison of ADC values between metastatic ipsilateral and benign contralateral lymph nodes.

MATERIAL AND METHODS

Ethical Aspects

The study received ethical approval from the Clinical Research Ethics Committee at Erzincan Binali Yıldırım University (protocol number: EBYU-KAEK-2024-17-008-412224, date: 05.12.2024). All patients have provided written informed consent for their data to be included in the MRI studies database and used in scientific research.

Patient Selection

Patients who received breast MRI scans at our center from January 2022 to December 2024 were analyzed retrospectively. The inclusion criteria for our study were patients with masses identified in breast MRI for whom histological (obtained by needle biopsy and/or surgical intervention) sampling data were accessible, patients whose breast MRI reports were categorized as Breast Imaging Reporting and Data System (BI-RADS) 4/5/6, and patients with diagnostic-quality DWI and ADC images in breast MRI scans. Precautions were taken to ensure an interval of more than three weeks between the breast biopsy and the subsequent breast MRI scans.

Patients who did not have breast MRI before surgical excision were excluded from the study to avoid misinterpretations due to bleeding or postoperative changes. Patients for whom the results of the IHC biomarker and the histological examination could not be obtained were also excluded from the study. Furthermore, patients exhibiting only non-mass-like contrast enhancement on breast MRI and those for whom the lesion was undetectable on DWI images because of small lesion size or suboptimal image resolution were excluded from the study.

During the retrospective review of the targeted time frame, we identified 680 breast MRI scans performed at our center. Among these, 322 had breast lesions categorized as BI-RADS 4, 5, or 6. Seven patients with a history of breast surgery, 71 patients without histopathology and biomarker results, 67 patients exhibiting non-mass contrast enhancement, and 29 patients for whom quantitative analysis on DWI images was unfeasible were excluded from the study. Finally, this study included 148 female patients (Figure 1).

MAIN POINTS

- Apparent diffusion coefficient (ADC) values serve as a reliable non-invasive biomarker capable of precisely differentiating between benign and malignant breast lesions.
- Lower ADC values are substantially correlated with malignancy, hormone receptor positivity, and a high Ki-67 proliferation index.
- Metastatic axillary lymph nodes exhibit significantly reduced ADC values compared to benign nodes, underscoring the utility of diffusion-weighted imaging in axillary staging.

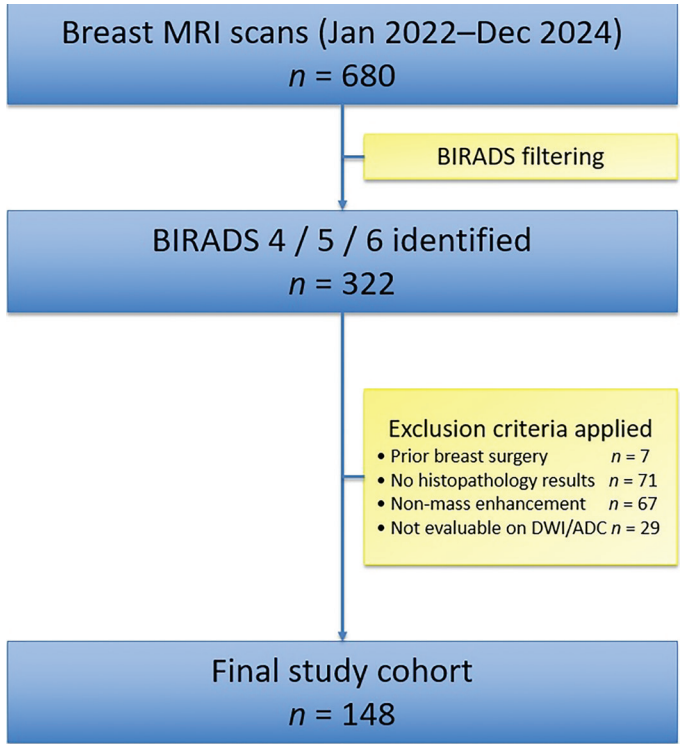

Figure 1. A flow chart illustrating the designation of the study cohort.

MRI, magnetic resonance imaging; BI-RADS, Breast Imaging Reporting and Data System. DWI, diffusion-weighted imaging; ADC, apparent diffusion coefficient

MRI Acquisition Protocol

A 1.5-T MRI scanner (Siemens Magnetom Aera, Erlangen, Germany) equipped with a dedicated 16-channel bilateral breast coil was used for all breast MRI examinations. Patients were positioned prone during imaging. The standardized protocol included 3D T1-weighted gradient-recalled echo sequences [repetition time (TR)/echo time (TE) = 20/4.5 ms; slice thickness = 3 mm] and T2-weighted fast spin-echo sequences (TR/TE = 4000/90 ms; slice thickness = 3 mm). For additional lesion characterization, an short tau inversion recovery sequence was acquired. DWI was performed using a single-shot echo-planar imaging technique with b-values of 0 and 1000 s/mm^2. The parameters for DWI included TR/TE = 5600/70 ms, field of view = 340 mm, slice thickness = 4 mm, and a matrix size of 128 × 128. ADC maps were automatically generated by the workstation software. All examinations adhered to a standardized institutional protocol.

Image Analysis

Image analysis was performed on a dedicated workstation (Syngo.via, Siemens Healthineers, Erlangen, Germany). The breast MRI scans of the study participants were evaluated by two radiologists. Observer A, with 10 years of experience, and Observer B, with 3 years of experience, jointly evaluated the MRI data sets without knowledge of the clinical and histopathological findings. Any disagreements among them were resolved by consensus. The recorded parameters included lesion size, morphological features (shape, margin, and internal architecture) according to the BI-RADS MRI lexicon, and DWI-signal intensity and ADC values obtained by placing a region of interest (ROI) within the solid portions of the lesion, carefully avoiding necrotic or cystic areas. At least three ROIs were placed, and the average ADC value was recorded. Additionally, ADC values of the most suspicious axillary lymph node on the ipsilateral side were measured in its cortical region. In these patients, the ADC value of the largest lymph node on the contralateral side was also recorded.

Histopathological and IHC Analysis

Histopathological evaluation was performed on tissue specimens obtained after biopsy or surgical resection, and tumors were classified as benign or malignant according to the World Health Organization criteria. IHC data analysis included assessment of ER and PR, with positivity defined as ≥ 1% nuclear staining. HER2 status was scored on a scale of 0-3+ in accordance with the American Society of Clinical Oncology/College of American Pathologists guidelines. The Ki-67 proliferation index was determined by calculating the percentage of positively stained nuclei.

Based on these results, tumors were categorized into molecular subtypes as follows: Luminal A (ER-positive and/or PR-positive, HER2-negative, and Ki-67 < 14%), Luminal B (ER-positive and/or PR-positive, HER2-negative or HER2-positive with Ki-67 ≥ 14%), HER2-enriched (ER-negative, PR-negative, and HER2-positive), and triple-negative breast cancer (TNBC); ER-negative, PR-negative, and HER2-negative).

Statistical Analysis

All statistical analyses were performed using IBM SPSS Statistics for Windows (version 25.0; IBM Corp., Armonk, NY, USA). Data normality was assessed using the Kolmogorov-Smirnov test. Continuous variables were expressed as mean ± standard deviation or median (range), and categorical variables as frequencies and percentages. The Mann-Whitney U test was applied to compare ADC values between benign and malignant lesions. The Wilcoxon test was applied to evaluate the differences in mean ADC values among molecular subtypes. The Bonferroni test was used as a post-hoc analysis. Spearman correlation coefficients were calculated to assess the relationships between ADC values and IHC biomarkers (ER, PR, HER2, Ki-67). Differences in ADC values between metastatic and benign lymph nodes were analyzed using the Mann-Whitney U test. Receiver operating characteristic (ROC) curve analysis was performed to determine optimal ADC cut-off values for differentiating malignancy, and the area under the curve, sensitivity, and specificity were calculated. A two-tailed *P* value < 0.05 was considered statistically significant.

RESULTS

A total of 159 breast lesions from 148 female patients were analyzed. The median age of our cohort was 48 years (range: 25-75 years). The median age of patients with malignant tumors was 52 years (range: 38-75), whereas that of patients with benign lesions was 42 years (range: 25-62). The median age of patients with malignant tumors was substantially greater than that of individuals with benign lesions ($P = 0.035$).

Among them, 56 lesions (35.2%) were malignant and 103 lesions (64.8%) were benign. Eight patients with multiple lesions underwent needle biopsies, all of which showed benign cytology. The mean tumor diameter of all the 159 breast masses assessed in the study was 28 ± 8.3 mm (range 5-70 mm). All 56 malignant breast tumors exhibited hyperintense signal features on DWI.

The histopathological distribution of malignant lesions included 6 cases of ductal carcinoma in situ (10.7%), 41 cases of invasive ductal carcinoma (73.2%), and 9 cases of invasive lobular carcinoma (16.1%).

When comparing the median ADC values of malignant lesions (0.92×10^{-3} mm^2/s) to those of benign lesions (1.66×10^{-3} mm^2/s), it was found that the malignant ones had significantly lower values ($P < 0.001$, Figure 2). ROC curve analysis indicated that the optimal ADC cut-off value for differentiating malignant from benign masses was 1.24×10^{-3} mm^2/s (sensitivity 95.2%, specificity 89.1%). Figure 3 illustrates a specific case of a malignant tumor.

Upon classifying malignant tumors into molecular subtypes according to IHC markers, we detected 6 (10.7%) luminal A tumors, 38 (67.9%) luminal B tumors, 4 (7.1%) HER2-enriched tumors, and 8 (14.3%) triple-negative tumors.

Hormone receptor-positive tumors exhibited a statistically significant reduction in median ADC value compared to hormone receptor-negative tumors (0.90×10^{-3} mm^2/s versus

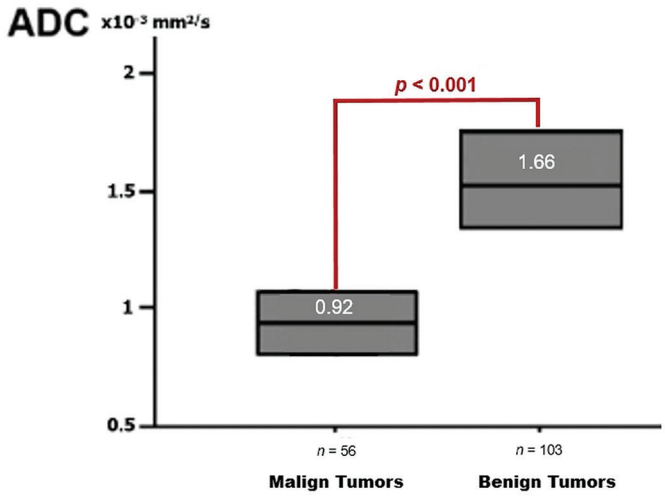

Figure 2. Median ADC values for benign and malignant breast tumors.

ADC, apparent diffusion coefficient

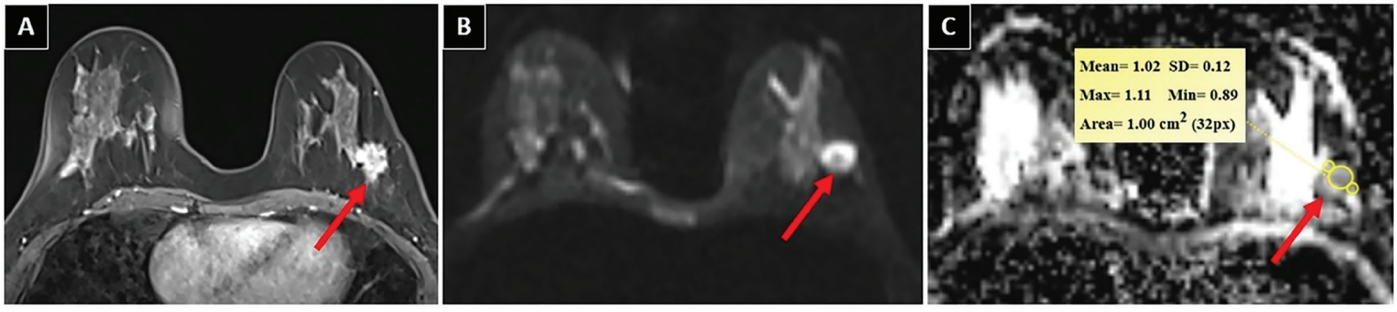

Figure 3. Invasive ductal carcinoma in a 48-year-old female patient. A) An irregularly contoured mass with significant contrast enhancement is noted in the upper outer quadrant of the left breast on post-contrast breast MR image (red arrow). B) The lesion exhibits hyperintensity on diffusion-weighted imaging (red arrow). C) The ADC value obtained from ROI measurement of the lesion on ADC maps is 1.02 ×10-3.mm²/s.

ADC, apparent diffusion coefficient; MR, magnetic resonance; ROI, region of interest, SD, standard deviation.

1.08×10^{-3} mm²/s, P = 0.03). No significant association was found between HER2 status and median ADC values. Furthermore, in the independent assessment, lower median ADC values were observed in patients with a high Ki-67 index (P = 0.015). The triple-negative breast cancer (TNBC) subtype had the highest median ADC value (1.13 × 10^{-3} mm²/s) compared with other molecular tumor subtypes.

An evaluation of the axillary lymph nodes was conducted in 26 patients with malignant tumors. Median ADC values of ipsilateral pathologically proven metastatic nodes were significantly lower than those in contralateral benign lymph nodes (0.78 versus 1.82×10^{-3} mm²/s; P < 0.001, Figure 4). Figure 5 shows a metastatic axillary lymph node.

DISCUSSION

In this retrospective study, we demonstrated that diffusion-weighted MRI and quantitative ADC measurements can effectively distinguish between benign and malignant breast lesions, while also providing valuable information about tumour biology and axillary lymph node status.

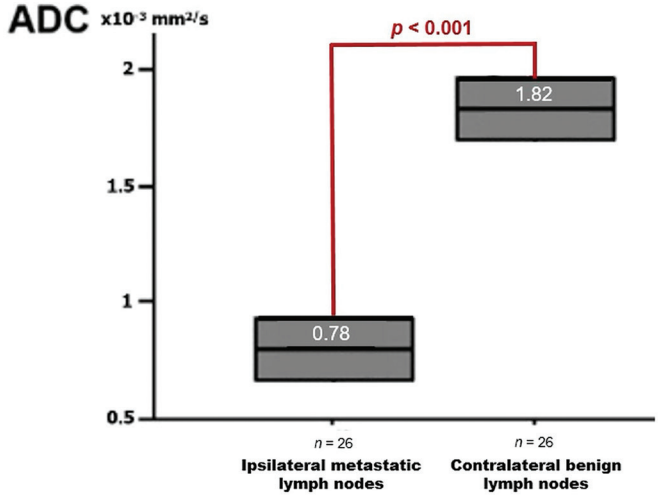

Figure 4. Median ADC values for benign and malignant axillary lymph nodes.

ADC, apparent diffusion coefficient

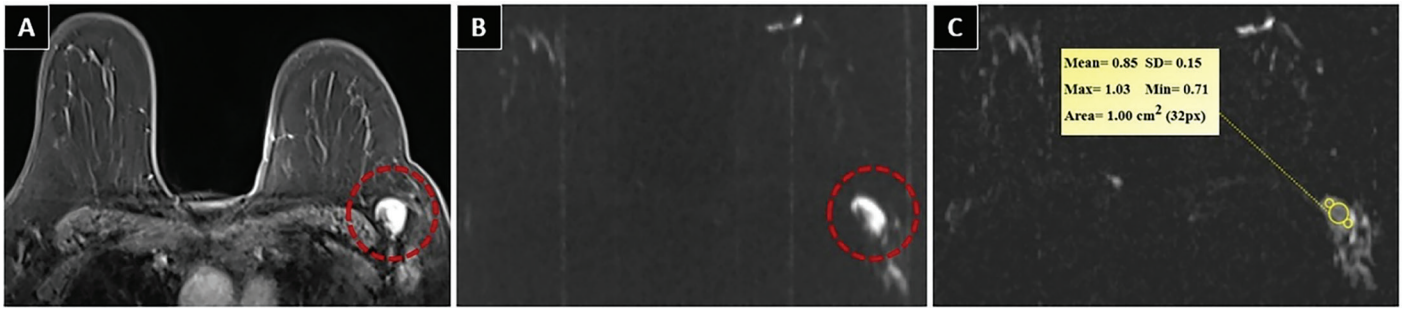

Figure 5. Metastatic left axillary lymphadenopathy in a 51-year-old female patient. A) The post-contrast breast MR image shows lymphadenopathy with a thickened and markedly enhanced cortex in the left axilla (red circle). B) The lesion exhibits hyperintensity on diffusion-weighted imaging (red circle). C) The ADC value obtained from ROI measurement of the cortex on ADC maps is 0.85 ×10−3 mm^2/s.

ADC, apparent diffusion coefficient; MR, magnetic resonance; ROI, region of interest, SD, standard deviation.

This study revealed that malignant breast tumors demonstrated markedly lower ADC values than benign lesions. The optimal ADC threshold value of 1.24 × 10^{-3} mm^2/s demonstrated excellent diagnostic performance, with 95.2% sensitivity and 89.1% specificity, aligning with other meta-analyses that indicate the high accuracy of DWI in breast tumor characterization.[6,10] This observation supports the established scientific rationale that increased cell density and reduced extracellular space restrict the movement of water molecules, thereby reducing ADC values.[10] In an early study on breast cancer diagnosis, Marini et al.[11] found a sensitivity of 80% and a specificity of 81% at a cut-off ADC value of 1.1 × 10^{-3} mm^2/s. In an alternative investigation, the ADC threshold value most similar to that in our study was determined for differentiating malignant from benign breast tumors, resulting in a proposed cut-off value of 1.23 × 10^{-3} mm^2/s.[12]

The main reason for selecting b values of 0 and 1000 in DWI is to increase the comparability of our results with those reported in the literature we cite on this subject.[2,5]

Beyond lesion characterisation, this study showed that ADC values can predict pathological biomarkers indicative of molecular features in malignant tumors. Hormone receptor-positive tumors showed markedly lower ADC values compared with hormone receptor-negative lesions. This phenomenon can be attributed to the comparatively elevated histopathological grade and increased cellularity commonly observed in luminal B type tumors. The results suggest that quantitative ADC measurements of lesions in patients with breast cancer can serve as a non-invasive method for grading and prognostic assessment.[8,13]

Moreover, our investigation found that malignancies with an elevated Ki-67 proliferation index had reduced ADC values, consistent with the biological mechanism whereby aggressive tumours with rapid cellular turnover exhibit increased diffusion restriction.[14,15] Conversely, no significant association was detected between HER2 status and ADC values. These data align with prior reports suggesting that HER2 status is not a reliable predictor of diffusion.[8,16]

Interestingly, the highest median ADC levels were observed among TNBC subtypes. While the literature indicates that TNBCs demonstrate an aggressive clinical course, it is highlighted that diffusion restriction diminishes due to the necrotic or heterogeneous microarchitecture of the tumors, leading to elevated ADC values. Aggressive tumors are expected to exhibit low ADC levels; nevertheless, the paradox seen in TNBCs is believed to stem from microarchitectural attributes. Areas of tumor necrosis signify a reduction in tumor cellularity, accompanied by enhanced diffusion, signal attenuation, and elevated ADC values on DWI.[8,17]

Another noteworthy finding concerns the evaluation of axillary lymph nodes and the proven benefit of DWI in axillary staging for breast cancer patients. The ADC values of pathologically proven metastatic lymph nodes were markedly lower than those of contralateral benign lymph nodes. This underscores the potential value of DWI in both the evaluation of the primary tumor and nodal staging. An increasing body of studies underscores that DWI is a non-invasive technique for evaluating lymph nodes, especially when the use of contrast agents is contraindicated or to guide targeted biopsies. Nevertheless, as highlighted in the literature, repeatability challenges in ADC measurements persist. Consequently, further comprehensive prospective research will be necessary to confirm the reliability of DWI in nodal staging.[9,18]

The strengths of the study include the use of a standardized imaging protocol, histological verification of all lesions, blinded evaluations by two observers with disagreements resolved by consensus, and the establishment of carefully defined, rigorous inclusion criteria. Moreover, a comprehensive evaluation of biomarker correlations and nodal analyses contributes to the existing literature. Nonetheless, there are numerous limitations. The retrospective design, modest single-center sample size, and manual ROI placement may limit the generalizability of our results. Additionally, only specific b-values were assessed, and advanced diffusion models, including intravoxel incoherent motion and diffusion kurtosis imaging, were not included. The lack of evaluation of inter-observer agreement is a limitation of our study. Another important limitation is the unequal numbers of patients across the IHC subgroups. Although most of our results are statistically significant, this situation may reduce statistical power. Ultimately, bias in lesion selection may arise from the exclusion of small lesions that are not detectable on DWI.

In clinical practice, we emphasize the significance of DWI as a biomarker for non-contrast imaging. The correlation between ADC and tumor aggressiveness supports the potential use of DWI in personalized oncology. Further investigations ought to encompass larger patient cohorts, integrate advanced diffusion models, and examine radiomics-based methodologies to enhance prognostic efficacy. Studies increasingly indicate that artificial intelligence technologies provide substantial for image construction and analysis in MRI.[19] Therefore, artificial intelligence technologies should also be included in future studies.

The study found that DWI and ADC enhance the evaluation of breast cancer. Breast malignancy, hormone receptor positivity, and proliferative activity are associated with lower ADC values. Additionally, ADC values may indicate nodal metastases. Notwithstanding its limitations, our findings suggest that DWI could be used in clinical practice as a safe, reliable biomarker if supported by large, multicenter trials.

Ethics

Ethics Committee Approval: The study received ethical approval from the Clinical Research Ethics Committee at Erzincan Binali Yıldırım University (protocol number: EBYU-KAEK-2024-17-008-412224, date: 05.12. 2024).

Informed Consent: Retrospective study. All patients have provided written informed consent for their data to be included in the MRI studies database and used in scientific research.

Footnotes

Author Contributions

Concept and Design – K.B.M., A.S.Ç.; Data Collection and/or Processing – A.S.Ç., M.F.Ö.; Analysis and/or Interpretation – K.B.M.; Literature Review – A.S.Ç.; Writing, Reviewing and Editing – K.B.M., A.S.Ç.

Conflict of Interest: The authors declare no conflict of interest.

Funding: The authors declared that this study has received no financial support.

REFERENCES

1. Gullo RL, Partridge SC, Shin HJ, Thakur SB, Pinker K. Update on DWI for breast cancer diagnosis and treatment monitoring. *AJR Am J Roentgenol*. 2024;222(1):e2329933. [CrossRef]
2. Meyer HJ, Martin M, Denecke T. DWI of the breast - possibilities and limitations. *Rofo*. 2022;194(9):966-974. [CrossRef]
3. Partridge SC, Amornsiripanitch N. DWI in the assessment of breast lesions. *Top Magn Reson Imaging*. 2017;26(5):201-209. [CrossRef]
4. Tsvetkova S, Doykova K, Vasilska A, et al. Differentiation of benign and malignant breast lesions using ADC values and ADC ratio in breast MRI. *Diagnostics (Basel)*. 2022;12(2):332. [CrossRef]
5. Pereira FP, Martins G, Figueiredo E, et al. Assessment of breast lesions with diffusion-weighted MRI: comparing the use of different b values. *AJR Am J Roentgenol*. 2009;193(4):1030-1035. [CrossRef]
6. Surov A, Meyer HJ, Wienke A. Can apparent diffusion coefficient (ADC) distinguish breast cancer from benign breast findings? A meta-analysis based on 13 847 lesions. *BMC Cancer*. 2019;19(1):955. [CrossRef]
7. Lo Gullo R, Sevilimedu V, Baltzer P, et al. A survey by the European Society of Breast Imaging on the implementation of breast diffusion-weighted imaging in clinical practice. *Eur Radiol*. 2022;32(10):6588-6597. [CrossRef]
8. Martincich L, Deantoni V, Bertotto I, et al. Correlations between diffusion-weighted imaging and breast cancer biomarkers. *Eur Radiol*. 2012;22(7):1519-1528. [CrossRef]
9. Cho P, Park CS, Park GE, Kim SH, Kim HS, Oh SJ. Diagnostic usefulness of diffusion-weighted mri for axillary lymph node evaluation in patients with breast cancer. *Diagnostics (Basel)*. 13(3):513. [CrossRef]
10. Baxter GC, Graves MJ, Gilbert FJ, Patterson AJ. A meta-analysis of the diagnostic performance of diffusion MRI for breast lesion characterization. *Radiology*. 291(3):632-641. [CrossRef]
11. Marini C, Iacconi C, Giannelli M, Cilotti A, Moretti M, Bartolozzi C. Quantitative diffusion-weighted MR imaging in the differential diagnosis of breast lesion. *Eur Radiol*. 2007;17(10):2646-2655. [CrossRef]
12. Tsushima Y, Takahashi-Taketomi A, Endo K. Magnetic resonance (MR) differential diagnosis of breast tumors using apparent diffusion coefficient (ADC) on 1.5-T. *J Magn Reson Imaging*. 2009;30(2):249-255. [CrossRef]
13. Razek AA, Gaballa G, Denewer A, Nada N. Invasive ductal carcinoma: correlation of apparent diffusion coefficient value with pathological prognostic factors. *NMR Biomed*. 2010;23(6):619-623. [CrossRef]
14. Zhang Y, Zhu Y, Zhang K, et al. Invasive ductal breast cancer: preoperative predict Ki-67 index based on radiomics of ADC maps. *Radiol Med*. 2020;125(2):109-116.[CrossRef]
15. Mori N, Ota H, Mugikura S, et al. Luminal-type breast cancer: correlation of apparent diffusion coefficients with the Ki-67 labeling index. *Radiology*. 2015;274(1):66-73. [CrossRef]
16. Iima M, Kataoka M, Honda M, Le Bihan D. Diffusion-weighted MRI for the assessment of molecular prognostic biomarkers in breast cancer. *Korean J Radiol*. 2024;25(7):623-633. [CrossRef]
17. Liu HL, Zong M, Wei H, et al. Added value of histogram analysis of apparent diffusion coefficient maps for differentiating triple-negative breast cancer from other subtypes of breast cancer on standard MRI. *Cancer Manag Res*. 2019;11:8239-8247. [CrossRef]
18. De Cataldo C, Bruno F, Palumbo P, et al. Apparent diffusion coefficient magnetic resonance imaging (ADC-MRI) in the axillary breast cancer lymph node metastasis detection: a narrative review. *Gland Surg*. 2020;9(6):2225-2234.[CrossRef]
19. Kantarcı M, Aydın S, Oğul H, Kızılgöz V. New imaging techniques and trends in radiology. *Diagn Interv Radiol*. 2025;31(5):505-517. [CrossRef]

ABCResearch

Arch Basic Clin Res 2026;8(1):53-58
DOI: 10.4274/ABCR.2025.25385

Research Article

What Magnetic Resonance Imaging Can Miss Around the Knee? Correlation of Imaging Results with Arthroscopic Findings

İhsaniye Süer Doğan[1], Teoman Bekir Yeni[2], Batuhan Gencer[3], Özgür Doğan[2]

[1]Clinic of Radiology, Ankara Etlik City Hospital, Ankara, Türkiye
[2]Clinic of Orthopaedics and Traumatology, Ankara Bilkent City Hospital, Ankara, Türkiye
[3]Department of Orthopaedics and Traumatology, Marmara University Pendik Training and Research Hospital, İstanbul, Türkiye

Cite this article as: Süer Doğan İ, Yeni TB, Gencer B, Doğan Ö. What magnetic resonance imaging can miss around the knee? Correlation of imaging results with arthroscopic findings. *Arch Basic Clin Res*. 2026;8(1):53-58.

ORCID IDs of the authors: İ.S.D., 0000-0002-7586-0537, T.B.Y., 0000-0002-2264-5489, B.G., 0000-0003-0041-7378, Ö.D. 0000-0002-5913-0411.

ABSTRACT

Objective: Magnetic resonance imaging (MRI) is a non-invasive and extensively used diagnostic tool for evaluating intra-articular knee pathologies. Nevertheless, the diagnostic concordance between MRI and arthroscopic findings remains a matter of debate. This study aimed to assess the correlation between MRI and arthroscopic findings in patients with intra-articular knee pathologies.

Methods: This retrospective study included 203 patients who underwent knee arthroscopy between 2020 and 2022 for suspected intra-articular pathology. MRI and intraoperative findings were compared for the anterior cruciate ligament, medial and lateral menisci, chondral lesions, and plica structures.

Results: The mean age of patients was 42.0 ± 12.87 years; 62.1% were male. MRI findings demonstrated a strong correlation with arthroscopy for anterior cruciate ligament injuries ($\kappa = 0.75$, $P < 0.001$) and a moderate correlation for medial meniscal tears ($\kappa = 0.60$, $P < 0.001$). However, reliability was weak to very weak for lateral meniscal tears and chondral lesions ($\kappa < 0.49$, $P < 0.05$); no significant reliability was observed for lateral femoral condyle cartilage ($\kappa = 0.03$, $P = 0.644$) or for the presence of plica ($\kappa = 0.01$, $P = 0.771$) between MRI and arthroscopic findings.

Conclusion: Although MRI is a valuable diagnostic tool for evaluating intra-articular knee pathologies, its correlation with arthroscopy was weak for detecting lateral meniscal injuries, chondral lesions, and the presence of plica. The use of MRI as the sole diagnostic tool may be inadequate, potentially resulting in failure to diagnose patients with persistent or unexplained knee symptoms. Although MRI plays an important role in the diagnosis of intra-articular knee pathologies, arthroscopy remains the definitive gold standard for confirming these lesions.

Keywords: Knee, MRI, arthroscopy, anterior cruciate ligament, meniscus, cartilage, plica

INTRODUCTION

The knee joint is one of the most frequently affected sites in musculoskeletal disorders presenting to primary care and orthopedic clinics.[1] Knee pain is a common problem in clinical practice and one of the primary causes of activity limitation in daily life. Over the past 20 years, the prevalence of knee pain has increased by nearly 65% and has resulted in approximately 4 million primary care visits each year.[2,3]

Anterior cruciate ligament (ACL) injuries are frequently observed in sports and may be caused by contact or non-contact mechanisms.[4] According to several studies, the annual incidence of ACL injuries has been reported as 25-78 per

Corresponding author: Batuhan Gencer, , **E-mail:** gencer.batuhan@gmail.com

Received: October 6, 2025 **Accepted:** October 27, 2025 **Publication Date:** January 26, 2026
Revision Requested: October 16, 2025

100.000 person-years. About 70% of these injuries are reported to occur, and ACL rupture is among the most common knee injuries requiring treatment in younger patients.[5,6] Meniscal tears have an average annual incidence of 60-70 per 100.000 population, with a consistent male predominance observed across all age groups, as reflected in a male-to-female ratio ranging from 2.5:1 to 4:1.[7,8] Furthermore, chondral lesions are relatively common among the pathologies observed during arthroscopy. While prevalence rates differ across studies, large series involving 25,124 arthroscopies documented chondral lesions in 60% of cases.[9]

Diagnosis of intra-articular knee pathologies begins with a meticulous clinical assessment, including the patient's history and a physical examination. When deemed necessary, these are followed by advanced imaging modalities to confirm and characterize the pathology. Magnetic resonance imaging (MRI) is a diagnostic imaging modality that provides high soft-tissue resolution, facilitating accurate visualization of intra-articular structures of the knee.[10] MRI is most frequently indicated in patients with possible injuries to the cruciate ligaments, menisci, and soft tissues. Although MRI has been documented to exhibit high diagnostic sensitivity, specificity, and accuracy, the true sensitivity and specificity of the test remain challenging to ascertain.[11] A considerable number of studies evaluating the accuracy of MRI are vulnerable to bias, possibly resulting in diagnostic tests showing inaccurately high sensitivity estimates.[12-14]

The primary objective of the present study was to evaluate the correlation between MRI-based diagnoses and arthroscopic findings of intra-articular knee lesions, with a view to providing a more precise and reliable diagnostic outcome.

MATERIAL AND METHODS

Study Population and Data Collection

The present retrospective study included patients who underwent knee arthroscopy at our institution between January 2020 and May 2022 for suspected meniscal pathology, ACL injury, or chondral lesions, with approval from the institutional Ethics Committee of Ankara Bilkent City Hospital Clinical Research (decision no.: E1-22-3070, date: 30.11.2022). All arthroscopies were performed at the same hospital by the same senior surgeon (Ö.D.), who had 15 years of experience in arthroscopic knee surgery, using standardized approaches and portals as described in the literature.[15] As part of our clinic's routine practice, the primary surgeon reviews all patients' MRI images and reports following the physical examination. Preoperative planning and surgical indications are then determined based on these evaluations. The indication for surgery was determined based on MRI and physical examination findings. All preoperative MRI scans were performed within six weeks of arthroscopic surgery.

The exclusion criteria were as follows:

- Patients diagnosed with oncological or infectious diseases,
- Patients who have previously undergone meniscus surgery,
- Patients who have previously suffered a fracture in the same knee,
- Patients for whom MRI data or intraoperative records were unavailable for any reason.

Initially, 220 patients were evaluated; 203 met the inclusion and exclusion criteria and were enrolled in the study. A retrospective review of the demographic, radiological, and intraoperative data of the included patients was conducted using the hospital's digital archive system.

Radiological and Clinical Evaluation

The same standard protocol was applied to all knee MRI examinations performed on a 1.5-T MR system (Signa Pioneer, GE Healthcare, ABD). Coronal, sagittal, and axial images were assessed using T1- and T2-weighted sequences with a 3 mm slice thickness. MRI examinations were reported by radiologists specializing in musculoskeletal imaging in the study hospital's Radiology Department; evaluations were performed based on these reports, which were recorded in the system. The radiologists responsible for reporting had no knowledge of the patients' clinical symptoms or surgical outcomes.

The MRI evaluation encompassed the ACL, the medial and lateral menisci, the articular cartilage of the medial and lateral femoral condyles and of the medial and lateral tibial plateaus, the patellofemoral joint, and the synovial plicae. Chondral damage detected on the MRI was graded according to the International Cartilage Repair Society (ICRS) criteria, which have been validated for use in this context.[16,17] The ICRS Grading System is a validated classification method used to evaluate the severity of cartilage damage. Cartilage of "Grade 0" is characterized by the absence of any discernible defects. The term "Grade 1" denotes superficial lesions, including cartilage softening and surface cracks and fissures. Grade 2 lesions involve cartilage loss of less than 50% of the total cartilage thickness. Grade 3 lesions are characterized by defects that traverse more than 50% of the cartilage thickness. However, these lesions do not extend to the subchondral bone. The presence of complete-thickness cartilage loss that extends into the subchondral bone is indicative of "Grade 4" lesions. A meniscal tear was

MAIN POINTS

- The reliability of magnetic resonance imaging (MRI) in detecting intra-articular knee pathologies varies significantly depending on the anatomical structure being evaluated.
- MRI demonstrates a moderate-to-strong correlation with arthroscopic findings for anterior cruciate ligament and medial meniscus injuries, but performs poorly in detecting damage to the lateral femoral condyle, lateral meniscus tears, and the medial plica.
- Although MRI remains a valuable non-invasive imaging modality, it should not be used in isolation; combining MRI results with thorough physical examination—and confirming uncertain cases via arthroscopy—ensures more accurate diagnosis.

defined on sequential MRI slices as an abnormal signal reaching the articular surface, loss of meniscal tissue, or a displaced fragment.[18,19] Accordingly, ACL injuries were classified as intact, partial, or complete. Medial meniscal status was categorized as intact, posterior root rupture, anterior root rupture, bucket-handle tear, or combined bucket-handle and root lesions. Lateral meniscal status was classified as intact, posterior root rupture, anterior root rupture, or discoid meniscal lesion.

Intraoperative assessment was based on documentation recorded in the operative theatre and routinely reviewed and approved by the most senior surgeon involved in the procedure. The surgeon had access to the MRI scans before the operation. The ICRS Grading System was again used to evaluate the severity of cartilage damage. The documentation of meniscal injuries was conducted in accordance with their anatomical location and the tear pattern, as determined by direct visualization and probing. In a similar manner, the ACL integrity was evaluated using a probe and subsequently categorized as intact, partially torn, or completely ruptured.

Statistical Analysis

The statistical analyses were performed using IBM® Statistical Package for the Social Sciences (SPSS) for Windows, version 26.0 (Armonk, NY: IBM Corp., USA). The Kolmogorov-Smirnov test was used to analyze whether the continuous data were normally distributed or skewed. Skewed continuous data were expressed as medians, interquartile ranges, and minimum-maximum values, while categorical data were presented as frequencies and percentages. To evaluate the reliability of the MRI and arthroscopic findings, Cohen's kappa coefficient was used. A *P* value less than 0.05 was considered statistically significant. The strength of the correlation coefficient (κ) was classified as follows: very weak (0.00-0.25), weak (0.26-0.49), moderate (0.50-0.69), strong (0.70-0.89), or very strong (0.90-1.00). Negative correlations were indicated by r values ($r < 0$).

RESULTS

The mean age of the 203 patients (77 females, 126 males) was 42 ± 12.87 years. The ACL was intact on MRI in 141 patients (69.5%); partial ACL rupture was predicted in 17 patients (8.4%) and complete ACL rupture was predicted in 45 patients (22.2%). Perioperatively, the ACL was found to be intact in 141 patients (69.5%), while partial rupture was observed in 15 patients (7.4%) and complete rupture was observed in 47 patients (23.2%). The demographic data and radiological characteristics of the patients are set out in Table 1, while operative characteristics are presented in Table 2.

A reliability analysis was conducted to assess the agreement between MRI and intraoperative findings. The MRI operation reliability was strong for ACL ruptures (κ = 0.75, $P < 0.001$) and moderate for medial meniscopathy (κ = 0.60, $P < 0.001$). However, reliability was weak to very weak for lateral meniscal tears and chondral lesions (κ < 0.49, $P < 0.05$ for each). The reliability between MRI findings and operative findings regarding the presence of plica and lateral femoral condyle cartilage lesion was not statistically significant (κ = 0.01, $P = 0.771$ and κ = 0.03, $P = 0.644$, respectively) (Table 3).

Table 1. Demographic Data and Radiological Characteristics of the Patients

		Number of patients (%)
Age	42 ± 12.87 (16-68)	
Gender	Female	77 (37.9%)
	Male	126 (62.1%)
Side	Right	106 (52.2%)
	Left	97 (47.8%)
Anterior cruciate ligament	Intact	141 (69.5%)
	Partial Rupture	17 (8.4%)
	Complete Rupture	45 (22.2%)
Medial meniscus	Intact	65 (32%)
	Posterior horn rupture	121 (59.6%)
	Anterior horn rupture	7 (3.4%)
	Bucket handle rupture	8 (3.9%)
	Bucket handle + root lesion	2 (1%)
Lateral meniscus	Intact	162 (79.8%)
	Posterior horn rupture	17 (8.4%)
	Anterior horn rupture	9 (4.4%)
	Bucket handle rupture	5 (2.5%)
	Discoid	10 (4.9%)
Medial femoral condyle cartilage lesion	Intact	161 (79.3%)
	Grade 1-2	2 (1%)
	Grade 3-4	40 (19.7%)
Lateral condyle cartilage lesion	Intact	194 (95.6%)
	Grade 1-2	1 (0.5%)
	Grade 3-4	8 (3.9%)
Medial tibial plateau cartilage lesion	Intact	179 (88.2%)
	Grade 1-2	0
	Grade 3-4	24 (11.8%)
Lateral tibial plateau cartilage lesion	Intact	202 (99.5%)
	Grade 1-2	0
	Grade 3-4	1 (0.5%)
Patellar cartilage lesion	Intact	145 (71.4%)
	Grade 1-2	22 (10.8%)
	Grade 3-4	36 (17.7%)
Plica existence	None	123 (60.6%)
	Notch	1 (0.5%)
	Suprapatellar	47 (23.2%)
	Medial	32 (15.8%)

Table 2. Operative Characteristics of the Patients

		Number of patients (%)
Anterior cruciate ligament	Intact	141 (69.5%)
	Partial rupture	15 (7.4%)
	Complete rupture	47 (23.2%)
Medial meniscus	Intact	70 (34.5%)
	Posterior horn rupture	105 (51.7%)
	Anterior horn rupture	11 (5.4%)
	Bucket handle rupture	12 (5.9%)
	Bucket handle + root lesion	5 (2.5%)
Lateral meniscus	Intact	143 (70.4%)
	Posterior horn rupture	30 (14.8%)
	Anterior horn rupture	12 (5.9%)
	Bucket handle rupture	3 (1.5%)
	Discoid	15 (7.4%)
Medial femoral condyle cartilage lesion	Intact	89 (43.8%)
	Grade 1-2	27 (13.3%)
	Grade 3-4	87 (42.9%)
Lateral condyle cartilage lesion	Intact	186 (91.6%)
	Grade 1-2	3 (1.5%)
	Grade 3-4	14 (6.9%)
Medial tibial plateau cartilage lesion	Intact	176 (86.7%)
	Grade 1-2	10 (4.9%)
	Grade 3-4	17 (8.4%)
Lateral tibial plateau cartilage lesion	Intact	194 (95.6%)
	Grade 1-2	2 (1%)
	Grade 3-4	7 (3.4%)
Patellar cartilage lesion	Intact	129 (63.5%)
	Grade 1-2	30 (14.8%)
	Grade 3-4	44 (21.7%)
Plica existence	None	146 (71.9%)
	Notch	40 (19.7%)
	Suprapatellar	7 (3.4%)
	Medial	10 (4.9%)

Table 3. Comparison of the Reliability of Radiological and Perioperative Observation

	Reliability		
	κ	*P*	Level of agreement
Anterior cruciate ligament	0.75	**< 0.001**	Strong
Medial meniscus	0.60	**< 0.001**	Moderate
Lateral meniscus	0.35	**< 0.001**	Weak
Medial femoral condyle cartilage lesion	0.32	**< 0.001**	Weak
Lateral femoral condyle cartilage lesion	0.03	0.644	None
Medial tibial plateau cartilage lesion	0.32	**< 0.001**	Weak
Lateral tibial plateau cartilage lesion	0.2	**< 0.001**	Very weak
Patellar cartilage lesion	0.27	**< 0.001**	Weak
Plica existence	0.01	0.771	None

κ, *P*, and level of agreement were calculated using Cohen's Kappa Variable.

DISCUSSION

MRI is a non-invasive procedure; arthroscopy is an invasive technique. Consequently, radiological imaging, in conjunction with physical examination, is considered an integral component of preoperative evaluation. While other studies have highlighted the validity of MRI for diagnosing knee lesions, our analysis focused on its reliability compared with arthroscopy and found it to be limited for identifying specific clinically important findings. In the present study, it was also observed that certain critical findings may be overlooked on MRI. While MRI findings were inconsistent with arthroscopic findings in cases of lateral femoral condyle lesions and the presence of plica (both potential causes of chronic knee pain), there was a high level of concordance between MRI and arthroscopy in detecting medial meniscus pathologies and ACL injuries.

MRI showed a strong correlation with intraoperative findings for ACL rupture (κ = 0.75, $P < 0.001$) and a moderate correlation for medial meniscopathy (κ = 0.60, $P < 0.001$). The strong correlation between MRI and arthroscopic findings in ACL and medial meniscal pathologies may be explained by well-defined imaging criteria, high anatomical visibility and biomechanical vulnerability of these structures. Numerous studies in the literature have also emphasized the adequacy of MRI for diagnosing ACL ruptures and medial meniscus tears.[18,20,21]

In the present study, arthroscopic evaluation revealed lateral femoral condyle cartilage damage classified as grade 1-2 in 3 patients (1.5%) and grade 3-4 in 14 patients (6.9%). However, MRI detected such lesions in only one patient (0.5%) with grades 1-2 and in eight patients (3.9%) with grades 3-4, suggesting a limitation in radiological detection. Consistent with our findings, Vaz et al.[21] reported that MRI is a satisfactory diagnostic tool for evaluating meniscal and ligamentous lesions of the knee; however, it does not clearly identify articular cartilage lesions. Von Engelhardt et al.[22] furthermore highlighted that the positive predictive value was low for all grades of articular cartilage lesions. In a separate study, Figueroa et al.[23] demonstrated that a significant proportion of cartilage lesions remained undetected at arthroscopy. Porter and Shadbolt[24] demonstrated that MRI exhibited a relatively poor correlation with arthroscopic grading of cartilage damage. In the study by Schnaiter et al.[25], the medial femoral joint surface was accurately evaluated in 81% of cases; 15% were overestimated and 4% were underestimated. With regard to the lateral cartilage,

classification was correct in 73% of cases, while 21% were overestimated and 6% were underestimated. An examination of the rationale underlying this relationship suggests that cartilage damage may have been exacerbated between the imaging procedure and the arthroscopy. Consequently, a lesion that is not visible on an initial MRI may become more apparent during arthroscopy. Furthermore, low-grade cartilage lesions are often superficial and may not produce significant signal changes on MRI, making them difficult to detect. Anatomically, the lateral femoral condyle exhibits a more convex and more inclined surface morphology than the medial condyle. This observation complicates full-thickness, perpendicular visualization of cartilage with conventional MRI sequences.

In our study, as shown in Tables 1 and 2, MRI demonstrated lower diagnostic reliability for lateral meniscal injuries compared with arthroscopic findings. Similarly, Esmaili Jah et al.[26] reported that the correlation between MRI and arthroscopy for lateral meniscus pathology was the weakest. Ben-Galim et al.[10] also reported similar findings, noting that the sensitivity of MRI differs between the medial and lateral menisci. As a result, lateral meniscal tears are often underdiagnosed, whereas medial tears tend to be overdiagnosed. Furthermore, Blake et al.[27] reported that MRI evaluation of the lateral meniscus is less sensitive, which may lead to diagnostic errors, including false-negative results. Therefore, the use of confirmatory arthroscopy may be beneficial. In our study, MRI findings did not correlate with arthroscopy findings regarding the presence of plicae. Plica findings were routinely evaluated in the initial MRI reports; no re-evaluation was performed as part of this study.

Study Limitations

The major strength of this study is its systematic assessment of multiple intra-articular structures of the knee, including the often-overlooked medial plica, by correlating MRI and arthroscopic findings. However, this study has several limitations, including its retrospective design, limited sample size, the fact that not all MRIs were evaluated by a single radiologist within a similar time frame, and the lack of standardized MRI-to-injury time intervals. Moreover, the primary surgeon's review of the preoperative MRI images for all patients may have introduced bias. However, preoperative evaluation of all imaging studies is an integral part of routine clinical practice, as it is essential for patient safety and successful surgical planning. Prospective randomized studies could help obtain results independent of this potential source of bias.

CONCLUSION

In conclusion, this study demonstrated that, while MRI remains a non-invasive and valuable diagnostic tool for assessing intra-articular knee lesions, its diagnostic reliability varies significantly depending on the structure being evaluated. Although MRI showed moderate-to-strong correlation with arthroscopic findings in ACL and medial meniscal injuries, MRI findings correlated poorly with arthroscopic findings in identifying lateral femoral condyle damage, lateral meniscal injuries, and medial plica. These findings emphasize that although MRI remains an essential non-invasive imaging tool, it should not be relied upon solely in cases of persistent or unexplained knee pain. Therefore, an integrated approach encompassing MRI evaluation alongside physical examination is recommended. Arthroscopy is considered the gold standard for definitive diagnosis of intra-articular knee lesions.

Ethics

Ethics Committee Approval: Ankara Bilkent City Hospital Clinical Research Ethics Committee decision number: E1-22-3070, date: 30.11.2022.

Informed Consent: Written and verbal informed consent were obtained from all patients for their data to be used in scientific research.

Footnotes

Author Contributions

Concept Design – İ.S.D., T.B.Y., B.G., Ö.D.; Data Collection or Processing – İ.S.D., T.B.Y., B.G., Ö.D.; Analysis or Interpretation – İ.S.D., Ö.D.; Literature Review –İ.S.D., T.B.Y., B.G., Ö.D.; Writing, Reviewing and Editing – İ.S.D., T.B.Y., B.G., Ö.D.

Declaration of Interests: The authors declared no conflicts of interest.

Funding: No funding.

REFERENCES

1. Gencer B, Doğan Ö, Çulcu A, et al. Internet and social media preferences of orthopaedic patients vary according to factors such as age and education levels. *Health Info Libr J.* 2024;41(1):84-97. [CrossRef]
2. Ülgen NK, Nazlıgül AS, Yiğit N, Erginoğlu SE, Akkurt MO. Epidemiologic patterns of musculoskeletal disorders by body region across 1.2 million orthopedic visits: a 15-year experience from a middle-ıncome country. *J Eval Clin Pract*. 2025;31(5):e70230. [CrossRef]
3. Baker P, Reading I, Cooper C, Coggon D. Knee disorders in the general population and their relation to occupation. *Occup Environ Med.* 2003;60(10):794-797. [CrossRef]
4. Dragoo JL, Castillo TN, Braun HJ, Ridley BA, Kennedy AC, Golish SR. Prospective correlation between serum relaxin concentration and anterior cruciate ligament tears among elite collegiate female athletes. *Am J Sports Med.* 2011;39(10):2175-2180. [CrossRef]
5. Doğan Ö, Çalışkan E, Gencer B. Clinical results of single bundle anterior cruciate ligament reconstruction with hamstring autograft. *Akdeniz Med J*. 2019;5:504-509. [CrossRef]
6. Doğan Ö, Gencer B, Süer Doğan İ. The effectiveness of anterior cruciate ligament reconstruction on the patellofemoral stability and patellar height. *Arch Curr Med Res*. 2023;4(2):94-101. [CrossRef]
7. Greis PE, Bardana DD, Holmstrom MC, Burks RT. Meniscal injury: I. Basic science and evaluation. *J Am Acad Orthop Surg*. 2002;10(3):168-176. [CrossRef]
8. Gu YL, Wang YB. Treatment of meniscal injury: a current concept review. *Chin J Traumatol.* 2010;13(6):370-376. [CrossRef]
9. Widuchowski W, Widuchowski J, Trzaska T. Articular cartilage defects: study of 25,124 knee arthroscopies. *Knee*. 2007;14(3):177-182. [CrossRef]

10. Ben-Galim P, Steinberg EL, Amir H, Ash N, Dekel S, Arbel R. Accuracy of magnetic resonance imaging of the knee and unjustified surgery. *Clin Orthop Relat Res.* 2006;447:100-104. [CrossRef]
11. Oei EH, Nikken JJ, Verstijnen AC, Ginai AZ, Myriam Hunink MG. MR imaging of the menisci and cruciate ligaments: a systematic review. *Radiology*. 2003;226(3):837-848. [CrossRef]
12. Jung JY, Yoon YC, Kwon JW, Ahn JH, Choe BK. Diagnosis of internal derangement of the knee at 3.0-T MR imaging: 3D isotropic intermediate-weighted versus 2D sequences. *Radiology*. 2009;253(3):780-787. [CrossRef]
13. Nishikawa H, Imanaka Y, Sekimoto M, Ikai H. Verification bias in assessment of the utility of MRI in the diagnosis of cruciate ligament tears. *AJR Am J Roentgenol*. 2010;195(5):W357-W364. [CrossRef]
14. Richardson ML, Petscavage JM. Verification bias: an under-recognized source of error in assessing the efficacy of MRI of the meniscii. *Acad Radiol*. 2011;18(11):1376-1381. [CrossRef]
15. Igdir V, Gencer B, Dogan O, Caliskan E, Orhan A, Demir Ozbudak S. The effects of remnant-preserving anterior cruciate ligament reconstruction on proprioception: a prospective comparative study. *Acta Orthop Traumatol Turc*. 2023;57(3):109-115. [CrossRef]
16. Brittberg M, Winalski CS. Evaluation of cartilage injuries and repair. *J Bone Joint Surg Am*. 2003;85-A Suppl 2:58-69. [CrossRef]
17. Smith GD, Taylor J, Almqvist KF, et al. Arthroscopic assessment of cartilage repair: a validation study of 2 scoring systems. *Arthroscopy*. 2005;21(12):1462-1467. [CrossRef]
18. De Smet AA, Tuite MJ. Use of the "two-slice-touch" rule for the MRI diagnosis of meniscal tears. *AJR Am J Roentgenol.* 2006;187:911-914. [CrossRef]
19. Milewski MD, Sanders TG, Miller MD. MRI-arthroscopy correlation: the knee. *J Bone Joint Surg Am*. 2011;93(18):1735-1745. [CrossRef]
20. Chang CY, Wu HT, Huang TF, Ma HL, Hung SC. Imaging evaluation of meniscal injury of the knee joint: a comparative MR imaging and arthroscopic study. *Clin Imaging*. 2004;28(5):372-376. [CrossRef]
21. Vaz CE, Camargo OP, Santana PJ, Valezi AC. Accuracy of magnetic resonance in identifying traumatic intraarticular knee lesions. *Clinics (Sao Paulo)*. 2005;60(6):445-450. [CrossRef]
22. von Engelhardt LV, Kraft CN, Pennekamp PH, Schild HH, Schmitz A, von Falkenhausen M. The evaluation of articular cartilage lesions of the knee with a 3-Tesla magnet. *Arthroscopy*. 2007;23(5):496-502. [CrossRef]
23. Figueroa D, Calvo R, Vaisman A, Carrasco MA, Moraga C, Delgado I. Knee chondral lesions: incidence and correlation between arthroscopic and magnetic resonance findings. *Arthroscopy*. 2007;23(3):312-315. [CrossRef]
24. Porter M, Shadbolt B. Accuracy of standard magnetic resonance imaging sequences for meniscal and chondral lesions versus knee arthroscopy. A prospective case-controlled study of 719 cases. *ANZ J Surg*. 2021;91(6):1284-1289. [CrossRef]
25. Schnaiter JW, Roemer F, McKenna-Kuettner A, et al. Diagnostic accuracy of an MRI protocol of the knee accelerated through parallel ımaging in correlation to arthroscopy. *Rofo*. 2018;190(3):265-272. [CrossRef]
26. Esmaili Jah AA, Keyhani S, Zarei R, Moghaddam AK. Accuracy of MRI in comparison with clinical and arthroscopic findings in ligamentous and meniscal injuries of the knee. *Acta Orthop Belg*. 2005;71(2):189-196. [CrossRef]
27. Blake MH, Lattermann C, Johnson DL. MRI and arthroscopic evaluation of meniscal injuries. *Sports Med Arthrosc Rev*. 2017;25(4):219-226.[CrossRef]

ABCResearch

Arch Basic Clin Res 2026;8(1):59-65
DOI: 10.4274/ABCR.2025.25372

Research Article

3D Printed Cutting Guide for Subtrochanteric Transverse Shortening Osteotomy in Total Hip Replacement for Crowe Type 4 Developmental Dysplasia

Murat Önder[1], Abdurrahman Aydın[2], Muhammed Mert[1], Muhammed Bilal Kürk[1], Berksu Polat[1], Alper Köksal[1]

[1]Clinic of Orthopaedics and Traumatology, Baltalimani Metin Sabancı Bone and Joint Diseases Training and Research Hospital, İstanbul, Türkiye
[2]Clinic of Orthopaedics and Traumatology, Düzce Akçakoca State Hospital, Düzce, Türkiye

Cite this article as: Önder M, Aydın A, Mert M, Kürk MB, Polat B, Köksal A. 3D printed cutting guide for subtrochanteric transverse shortening osteotomy in total hip replacement for Crowe type 4 developmental dysplasia. *Arch Basic Clin Res*. 2026;8(1):59-65.

ORCID IDs of the authors: M.Ö. 0000-0001-9965-7448, A.A. 0000-0002-5570-9493, M.M. 0000-0002-2552-8851, M.B.K., 0000-0001-8956-3819, B.P. 0000-0001-8082-4621, A.K. 0000-0002-0748-2749.

ABSTRACT

Objective: Subtrochanteric transverse femoral shortening osteotomy is a frequently employed technique to avoid potential complications in total hip arthroplasty with a high hip center. However, when performed freehand, the osteotomy may be associated with complications such as non-union, instability, and rotational deformities. Additional assistance is often required during prosthesis insertion and reaming procedures. In this study, we developed a simple, non-patient-specific 3D incision guide to improve the quality and outcomes of shortening osteotomy procedures.

Methods: Following design development in SolidWorks 2023, the 3D cutting guide was printed using an FLSUN T1 Ultra 3D printer. The cutting guide was printed with polylactic acid + filament (layer height 0.2 mm, infill 40%, nozzle 0.4 mm, 210 °C). The designed device has only been tested on a Sawbone synthetic foam cortical shell femur model using Wagner cone stems.

Results: Use of the non-patient-specific 3D cutting guide during subtrochanteric femoral shortening osteotomy in total hip arthroplasty with a high hip center resulted in a more precise osteotomy line, facilitated rotational adjustment, and reduced the overall duration of the prosthesis implantation procedure.

Conclusion: The non-patient-specific 3D cutting guide used in subtrochanteric transverse shortening osteotomy can enhance the quality of the osteotomy and minimize complications. Furthermore, owing to its circumferential design enveloping the femur, it may serve as a prophylactic splint, thereby reducing the risk of fissure formation during prosthesis implantation. Future clinical trials and further refinements of the cutting guide are expected to yield more favorable outcomes.

Keywords: Subtrochanteric femoral shortening osteotomy, Crowe type IV hip, 3D printed cutting guide, total hip arthroplasty

INTRODUCTION

Hip arthroplasty for osteoarthritis secondary to developmental dysplasia of the hip presents unique challenges compared with arthroplasty for primary hip osteoarthritis. The primary issue lies in the malpositioning of the femoral head away from its anatomical center.[1] Because the femoral head is located superior to the native acetabulum, the surrounding anatomical structures adapt to this altered development. Consequently, hip arthroplasty with shortening presents a number of challenges. In patients with leg length discrepancies of ≥ 4 cm, increased sciatic nerve tension, rotational abnormalities, and difficulties achieving reduction after prosthesis implantation have highlighted the need for femoral shortening osteotomy.[2-6]

The literature contains numerous descriptions of techniques for performing shortening osteotomies. In 1990, Paavilainen et al.[6] introduced femoral shortening osteotomy in conjunction with greater trochanteric advancement, reporting improvements in patients' gait patterns and reductions in pain scores.[7] Currently,

Corresponding author: Murat Önder, **E-mail:** muratonder89@gmail.com

Received: September 19, 2025 **Accepted:** December 1, 2025 **Publication Date:** January 26, 2026
Revision Requested: October 7, 2025

subtrochanteric osteotomy is the most commonly used shortening technique in high hip dislocations. This approach was initially described by Becker and Gustilo[8], using a double-chevron osteotomy. Subsequently, Reikeraas et al.[9] reported the use of a transverse derotational subtrochanteric osteotomy for femoral shortening in a series of 25 patients. In cases where femoral shortening is achieved via subtrochanteric transverse osteotomy, the geometry of the osteotomy surfaces of the proximal and distal fragments is critical for stable fixation along the osteotomy line. Moreover, the configuration of the cut enhances bone-to-bone contact between fragments, thereby reducing complications such as malunion and non-union. The rotational alignment between the two segments is also pivotal in determining postoperative gait and hip stability.[10-12]

No previous study has demonstrated a method for performing a subtrochanteric transverse osteotomy that ensures complete and congruent bone contact after shortening. Moreover, reports addressing strategies to prevent potential complications resulting from an inadequate osteotomy are limited. In the present study, we aimed to facilitate and optimize the execution of subtrochanteric transverse femoral shortening osteotomy by employing the cutting guide we developed. We also aimed to streamline the surgical procedure to reduce operative time and thereby avoid complications associated with prolonged operations.

The primary hypothesis of the study was that the use of an appropriately designed cutting device would shorten the surgical duration in high hip arthroplasty and enhance the congruence of bony contact between the proximal and distal fragments following the osteotomy. The secondary hypothesis was that the reduction in surgical duration afforded by guide-assisted procedures would decrease the need for blood transfusions.

MATERIALS AND METHODS

Following the initial design stage in SolidWorks, iterative improvements were made using trial cutting guides produced using FLSUN T1 Ultra 3 dimensional (3D) printer. The cutting guide was printed with polylactic acid + filament (layer height 0.2 mm, infill 40%, nozzle 0.4 mm, 210 °C). The designed device has only been tested on a Sawbone synthetic foam cortical shell femur model using Wagner cone stems. Since it is not used on living organisms, sterilization is not required. However, for use on living organisms, the device can be manufactured from titanium and sterilized in an autoclave. This allows the cutting guide to be reused.

MAIN POINTS

- The newly developed cutting guide facilitates the application of femoral shortening osteotomy in Crowe Type 4 hip dysplasia surgery.
- The device may reduce the risk of intraoperative complications by shortening surgical time.
- Experimental tests demonstrate that it improves osteotomy accuracy.

The cutting guide comprises two components that are secured together using a screw and bolt system. The upper and lower bone segments firmly stabilize the intermediate piece, analogous to a component enclosed between two opposing supports. The upper component features five cutting slots, each 1.27 mm thick and spaced 7.46 mm apart. The saw blade used for the osteotomy is 1.25 mm thick. This configuration is intended to prevent the saw blade from oscillating proximally or distally, thereby avoiding irregularities along the osteotomy line that could compromise the press-fit between the bone segments. In addition, the guide is equipped with holes—aligned in a straight line at the distal, proximal, and midline positions—that allow for the insertion of 2-mm Kirschner wires (K-wires).

These holes serve two purposes: first, they facilitate fixation of the guide to the bone; second, following the osteotomy, they provide immediate information regarding the rotational alignment of the proximal and distal fragments without requiring additional markings. Furthermore, the holes adjacent to the midline openings at the most distal and proximal positions are angled at 15 °. Based on our preoperative planning, this approach enables us to determine the required amount of derotation by referencing this area in patients who need it (Figure 1).

The lower component of the guide has a simpler design. Although it mirrors the design of the upper part, it does not include any cutting slots or K-wire insertion holes. The bone, interposed between the upper and lower components (again resembling a hot dog in a bun), is secured to the assembly by a bolt system, with two bolts placed at the proximal and distal ends.

Two advantages of this design were observed during the Sawbone trials. First, the absence of cutting slots in the lower component prevents the saw blade from coming into contact with medial structures, effectively serving as a protective retractor. Second, once the osteotomized segment is resected, controlling the proximal and distal fragments can be challenging. This device allows the two segments to be approximated and, following rotational alignment, to be compressed together in a sandwich-like configuration, effectively reconstituting a single, continuous femur. Consequently, the separate reaming procedures for the proximal and distal fragments, as well as the reduction process following trial stem placement, are simplified, thereby eliminating intraoperative instability and rotational issues (Figures 2, 3, 4, and 5).

The presence of a cutting gap at different levels of the guide allows additional cuts in patients with insufficient shortening after testing, without removing the guide. When the rotational alignment of the proximal and distal fragments is deemed appropriate, the K-wires placed at the "0" position of the cutting guide can be used to establish rotational reference points for the osteotomy. In the Sawbone trials, the Wagner Cone Prosthesis (Zimmer Biomet) was used.

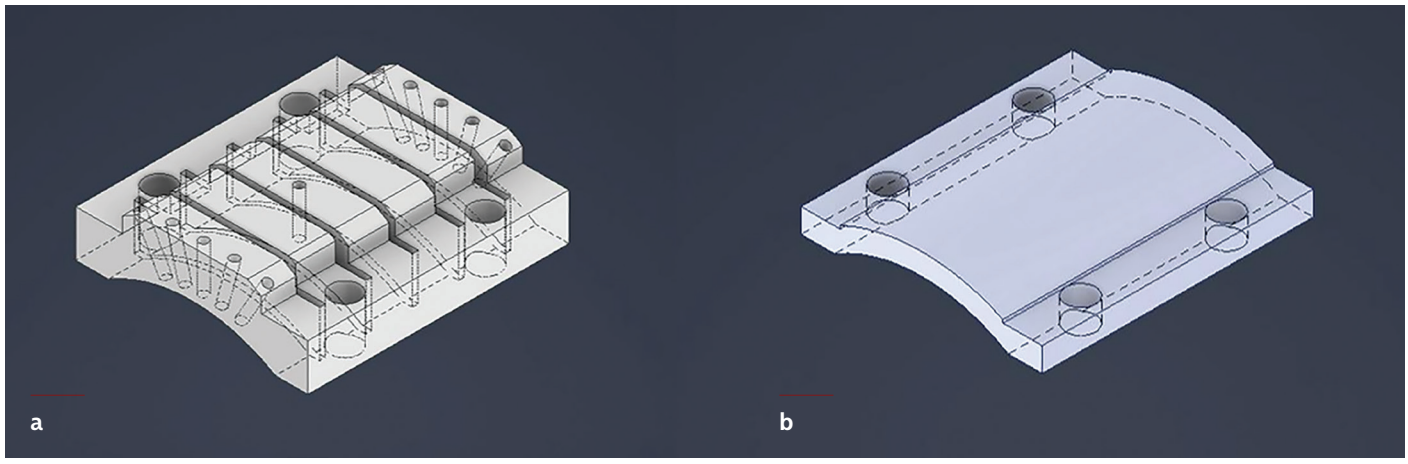

Figure 1. a, Upper part of the guide; b, Lower part of the guide

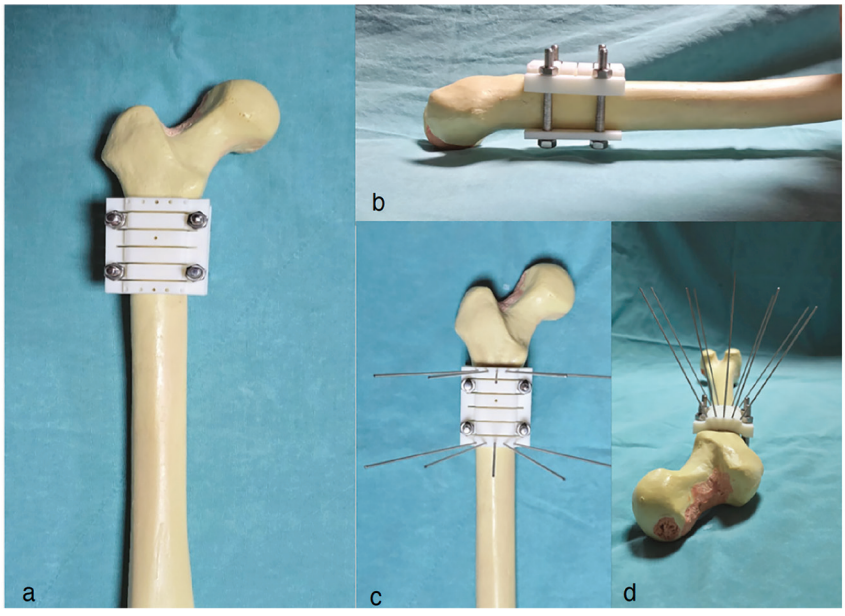

Figure 2. a, Anteroposterior view during positioning of the guide before the osteotomy; b, Lateral view of the guide during pre-osteotomy positioning; c, Image of the guide on the bone after placement of the rotational wires; d, Axial view of the guide after placing the rotational wires (demonstrating a 15° interval between the wires). Note: All wires are shown to clearly illustrate the angles.

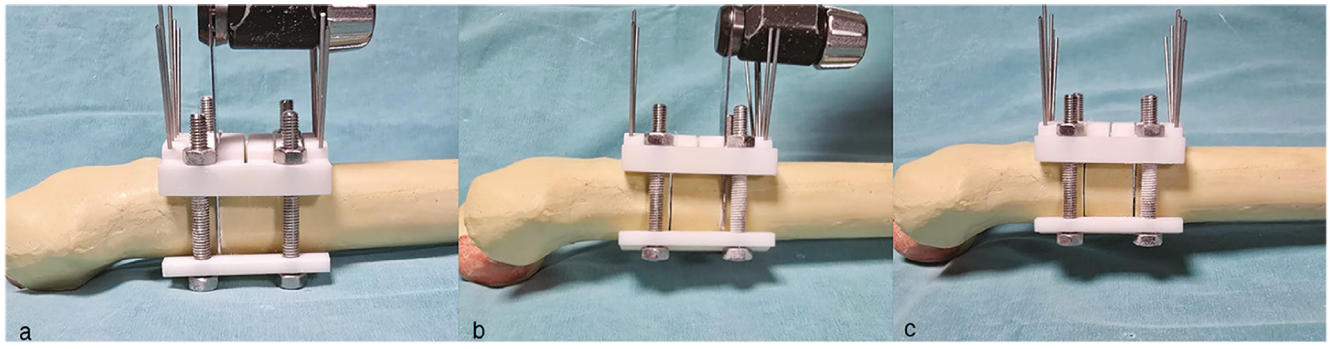

Figure 3. a, Proximal cut-of the fragment to be resected performed with the assistance of the guide; b, Distal cut-of the fragment to be resected performed with the assistance of the guide; c, Image showing the integrity of the resected fragment and the remaining bone following completion of the proximal and distal cuts.

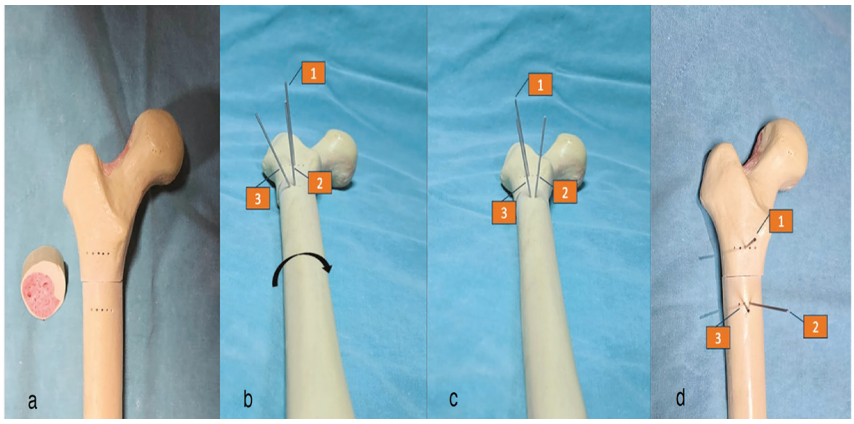

Figure 4. a, Image showing the congruity between the proximal and distal segments after the excised segment has been removed following the proximal and distal cuts; b–d, Demonstration of rotational adjustment on the Sawbone model using the K-wire insertion holes. In the neutral position, the first and second K-wires are aligned vertically; after internally rotating the distal fragment by 15°, the first and third K-wires come into opposition.

K-wires: Kirschner wires

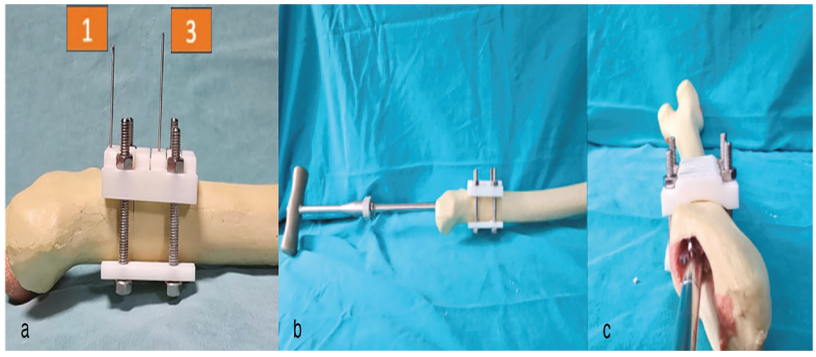

Figure 5. a, After achieving the desired rotational alignment of the proximal and distal fragments, the second K-wire is removed. The guide is passed over the wires on the proximal and distal fragments to secure proper alignment between them; b, With the assistance of the guide, the femur is stabilized prior to reaming; c, Reaming is performed on the femur, which has been consolidated into a single unit with the aid of the guide.

RESULTS

The guide was designed using SolidWorks 2023 and manufactured using an FLSUN T1 Ultra 3D printer. The 3D-printed osteotomy guide was positioned on a Sawbone so that it was aligned beneath the lesser trochanter and was secured with compression screws. For rotational orientation, K-wires were inserted through the designated holes in the guide, which demonstrated excellent stability when affixed to the bone. The saw used for the osteotomy was press-fit into the cutting slot of the guide, and no oscillation occurred during the cutting process. The bone segment produced after the osteotomy measured 2 cm, as planned, and the resulting surfaces were perfectly aligned.

Upon removal of the guide, the K-wire holes provided clear guidance regarding rotation. Following a 15° derotation, the proximal and distal segments were reassembled, the guide was repositioned, and no distraction was observed along the osteotomy line. Throughout the carving process, the guide remained well fixed to the bone; after prosthesis implantation and subsequent removal of the guide, no rotational instability was observed. The osteotomy line appeared to be perfectly aligned. Additionally, while the guide was in place, no fissure formation was detected during the carving and prosthesis implantation procedures Figure 6.

DISCUSSION

Currently, 3D cutting guides are used in many areas of orthopaedics.[13-22] One of the primary reasons for their widespread adoption in surgical procedures compared with the past is their increased accessibility and the fact that they no longer require large industrial facilities for production. The 3D-printed cutting guides can be produced specifically for individual patients or fabricated for one-time, general use.

Because the planned osteotomy is not complex, one of the most important features of the cutting guide we designed is that it can be produced as a single-use, non-patient-specific guide. In a study examining proximal femoral morphology in 51 hips from 45 patients with Crowe type IV dysplasia, the average femoral canal width—calculated from the mediolateral and

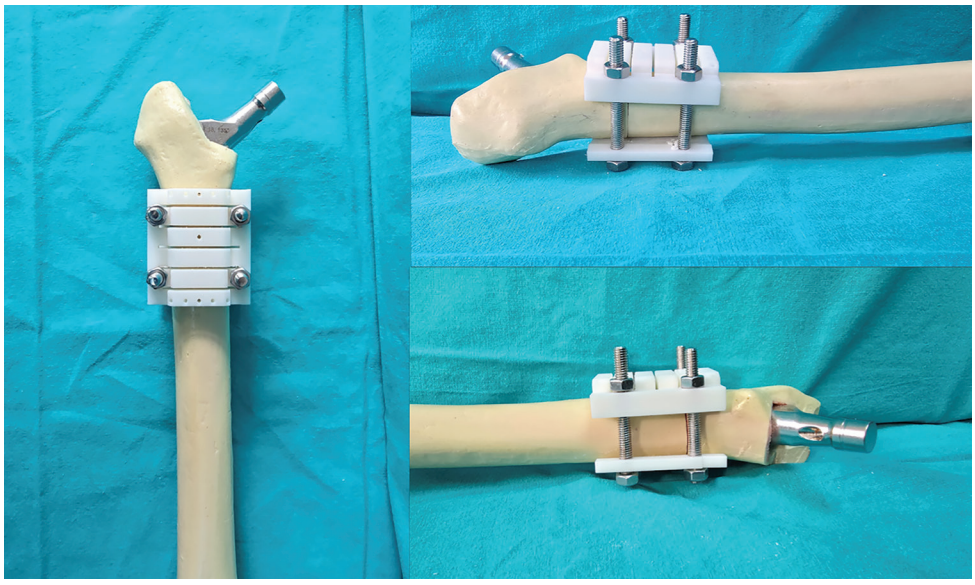

Figure 6. After reaming, the prosthesis is securely and smoothly implanted without removing the guide, as if placing it into an intact femur. Image showing the congruity and fixation between the fragments after prosthesis implantation.

anteroposterior dimensions—was approximately 2 cm in the widest patient, measured at a level 1-2 cm below the lesser trochanter.[1] Based on this information, the guide was oriented just distal to the lesser trochanter. The bone-contacting section of the guide was designed to be 3 cm wide with a slightly curved surface, ensuring that it is not patient-specific and is reusable. The ability to use a standardized guide without having to manufacture a separate one for each patient also provides a cost advantage. Numerous techniques have been described for subtrochanteric shortening osteotomy. One of the most common complications encountered with these procedures is inadequate union at the osteotomy site.[23,24] When osteotomies are performed freehand in a 3D context, achieving complete cortical contact is extremely challenging. Limited contact between bone ends has been reported to adversely affect union.[23,25] Huang et al.[26] reported that to maximize bone contact between the proximal and distal segments after osteotomy, the osteotomy level should be set approximately 1-1.5 cm below the lesser trochanter, which would promote union. Zadeh et al.[11] reported that, for a stable osteotomy, the portion of the femoral stem distal to the osteotomy should be at least 6 cm. Furthermore, if rotational correction is required following osteotomy, performing a freehand cut in the same plane becomes challenging, thereby hindering complete cortical contact between the proximal and distal fragments. Readjusting the bone ends with a saw would prolong operative time, increase bleeding, and make limb-length adjustment difficult because of excessive shortening. In the present study, evaluation of postoperative radiographs revealed that in all cases complete cortical contact was achieved along the osteotomy line on both anteroposterior and lateral views with no detectable gaps.

In hip arthroplasty performed on elevated hip surfaces, femoral anatomy differs from that of normal hips and includes rotational variations. In such hips, femoral anteversion is increased, and the greater trochanter is positioned more posteriorly.[27,28] Failure to adjust anteversion during surgery can cause recurrent anterior dislocations and result in the greater trochanter and abductor muscles remaining positioned posteriorly, thereby shortening the abductor lever arm and causing gait abnormalities and instability.[10-12,29] One of the most significant advantages of subtrochanteric transverse osteotomy is that the congruence between the cylindrical bone surfaces allows the proximal fragment to be rotated, thereby bringing the greater trochanter—and consequently the abductor muscles—into the proper anatomical position.[1,24,29] Under normal circumstances, various techniques exist for accurately adjusting the rotational alignment during a freehand osteotomy.[28] For example, some methods involve drilling holes with K-wires at the proximal and distal ends of the osteotomy or marking the bone intraoperatively with a surgical pen. However, such markings can disappear when additional bone resection is required or when the osteotomy surfaces need to be revised with a second cut. In particular, pen markings may easily be erased by intraoperative bleeding and fluids. This can necessitate repeating these steps, thereby increasing operative time and blood loss. In contrast, the K-wire holes positioned at 15 ° intervals along the proximal and distal edges of our cutting guide indicate the degree of rotational correction required and permit direct marking on the guide if an additional cut is required. This design facilitates easy and precise rotational adjustment.

Krych et al.[30] described the technique of total hip arthroplasty with subtrochanteric transverse shortening osteotomy in Crowe type IV hips and noted that, after resecting the femoral neck—and before proceeding with the shortening osteotomy—reaming should be performed. This step is critical for achieving a tight press-fit prosthesis in the distal fragment and contributes to the rotational stability of the implant and the osteotomy site.[30,31] Because our cutting guide securely approximates the distal and proximal femoral segments after the osteotomy—

effectively allowing them to function as a single continuous femur—it enables reaming to be performed post-osteotomy without requiring initial reaming. Consequently, this approach has the potential to reduce surgical duration and blood loss.

One of the most significant challenges encountered during femoral preparation in Crowe type IV hips is the occurrence of femoral fissures.[32,33] In a series of 28 Crowe type IV hip cases reported by Krych et al.[30], fissures developed in the distal region of the femoral osteotomy during prosthesis insertion in five of the patients. They stated that a prophylactic cable is routinely wrapped around the distal segment to prevent this from occurring.[30] Although this study was conducted using Sawbone models—thus precluding definitive conclusions—we believe that the way the cutting guide conforms to bone mimics the effect of a prophylactically applied cable and thus prevents fissure formation in the distal fragment. However, prophylactic cerclage wiring is still recommended to minimize fissure risk.

Infection remains one of the most significant complications of total hip arthroplasty. Numerous studies have demonstrated that prolonged surgical duration increases the risk of postoperative infection.[34-37] By employing the osteotomy cutting guide, the need for the pre-osteotomy reaming phase is eliminated, additional reaming of the distal segment is avoided, and the placement of trial stems and the reduction process are facilitated, resulting in a shorter surgical duration. This reduction in surgical duration may contribute to a lower infection rate.

Furthermore, a shorter surgical duration reduces the overall operating room usage, leading to decreased expenses related to electricity, materials, and personnel. In their study on high tibial osteotomy using a patient-specific 3D cutting guide, Pérez-Mañanes et al.[17] demonstrated that the reduction in surgical duration more than offset the cost of the guide, resulting in a net saving of €507 per procedure.[21] Although we have not yet quantified the exact economic benefit of our non-patient-specific, reusable cutting guide, it is evident that it offers substantial long-term cost savings.

Study Limitations

The main limitations of this study include that the device has not been tested in patients and that the biomechanical outcomes have not been evaluated using cadaveric specimens. Future multicenter, controlled studies with larger patient cohorts will be instrumental in elucidating these issues.

CONCLUSION

In Crowe type IV hip arthroplasty, the cutting guide that we developed for subtrochanteric transverse shortening osteotomy achieved complete cortical contact along the osteotomy surfaces during our Sawbone trials. We believe that the swift, practical execution of cutting and prosthesis-implantation procedures facilitated by the guide will lead to reduced surgical duration and a reduced need for blood transfusions. Additionally, the cutting guide's ability to act as a temporary cable to prevent fissure formation appears to be a key advantage.

Ethics

Ethics Committee Approval: Baltalimani Metin Sabanci Bone and Joint Diseases Education and Research Hospital Ethical Review Committee, İstanbul with decision no.: 188, date: 30.09.2024.

Informed Consent: No human participants or patient data were involved; ethical approval and informed consent were not required for this Sawbone model study.

Footnotes

Author Contributions

Concept Design – A.A., M.M., A.K.; Data Collection or Processing – M.Ö., M.B.K.; Analysis or Interpretation – M.Ö., A.A., B.P.; Literature Review – M.Ö., M.M., B.P.; Writing, Reviewing and Editing – M.Ö., A.A., A.K.

Declaration of Interest: The authors declared no conflicts of interest.

Funding: No funding.

REFERENCES

1. Yang Y, Liao W, Yi W, et al. Three-dimensional morphological study of the proximal femur in Crowe type IV developmental dysplasia of the hip. *J Orthop Surg Res*. 2021;16(1):621. [CrossRef]
2. Kiliçoğlu Oİ, Türker M, Akgül T, Yazicioğlu O. Cementless total hip arthroplasty with modified oblique femoral shortening osteotomy in Crowe type IV congenital hip dislocation. *J Arthroplasty*. 2013;28(1):117-125. [CrossRef]
3. Lewallen DG. Neurovascular injury associated with hip arthroplasty. *Instr Course Lect*. 1998;47:275-283. [CrossRef]
4. Lai KA, Shen WJ, Huang LW, Chen MY. Cementless total hip arthroplasty and limb-length equalization in patients with unilateral Crowe type-IV hip dislocation. *J Bone Joint Surg Am*. 2005;87(2):339-345. [CrossRef]
5. Dunn H, Hess W. Total hip reconstruction in chronically dislocated hips. *J Bone Joint Surg Am*. 1976;58(6).838-845. [CrossRef]
6. Paavilainen T, Hoikka V, Solonen KA. Cementless total replacement for severely dysplastic or dislocated hips. *J Bone Joint Surg Br*.1990;72(2):205-211. [CrossRef]
7. Paavilainen T, Hoikka V, Paavolainen P. Cementless total hip arthroplasty for congenitally dislocated or dysplastic hips. Technique for replacement with a straight femoral component. *Clin Orthop Relat Res*. 1993;(297):71-81. [CrossRef]
8. Becker DA, Gustilo RB. Double-chevron subtrochanteric shortening derotational femoral osteotomy combined with total hip arthroplasty for the treatment of complete congenital dislocation of the hip in the adult. Preliminary report and description of a new surgical technique. *J Arthroplasty*. 1995;10(3):313-318. [CrossRef]
9. Reikeraas O, Lereim P, Gabor I, Gunderson R, Bjerkreim I. Femoral shortening in total arthroplasty for completely dislocated hips: 3-7 year results in 25 cases. *Acta Orthop Scand*. 1996;67(1):33-36. [CrossRef]
10. Bjørdal F, Bjørgul K. The role of femoral offset and abductor lever arm in total hip arthroplasty. *J Orthop Traumatol*. 2015;16(4):325-330. [CrossRef]

11. Zadeh HG, Hua J, Walker PS, Muirhead-Allwood SK. Uncemented total hip arthroplasty with subtrochanteric derotational osteotomy for severe femoral anteversion. *J Arthroplasty*. 1999;14(6):682-688. [CrossRef]
12. McGrory BJ, Morrey BF, Cahalan TD, An KN, Cabanela ME. Effect of femoral offset on range of motion and abductor muscle strength after total hip arthroplasty. *J Bone Joint Surg Br*. 1995;77(6):865-869. [CrossRef]
13. Zhang YZ, Lu S, Chen B, Zhao JM, Liu R, Pei GX. Application of computer-aided design osteotomy template for treatment of cubitus varus deformity in teenagers: a pilot study. *J Shoulder Elbow Surg*. 2011;20(1):51-56. [CrossRef]
14. Dagneaux L, Canovas F. 3D printed patient-specific cutting guide for anterior midfoot tarsectomy. Foot Ankle Int 2019;41(2):211-215. [CrossRef]
15. Gasparro MA, Gusho CA, Obioha OA, Colman MW, Gitelis S, Blank AT. 3D-Printed cutting guides for resection of long bone sarcoma and intercalary allograft reconstruction. Orthopedics 2022;45(1):e35-e41. [CrossRef]
16. Bergemann R, Roytman GR, Ani L, et al. The feasibility of a novel 3D-Printed patient specific cutting guide for extended trochanteric osteotomies. *3D Print Med*. 2024;10(1):7. [CrossRef]
17. Pérez-Mañanes R, Burró JA, Manaute JR, Rodriguez FC, Martín JV. 3D surgical printing cutting guides for open-wedge high tibial osteotomy: do it yourself. *J Knee Surg*. 2016;29(8):690-695. [CrossRef]
18. Gigi R, Gortzak Y, Barriga Moreno J, et al. 3D-printed Cutting Guides for Lower Limb Deformity Correction in the Young Population. *J Pediatr Orthop*. 2022;42(5):e427-e434. [CrossRef]
19. Imhoff FB, Schnell J, Magaña A, et al. Single cut distal femoral osteotomy for correction of femoral torsion and valgus malformity in patellofemoral malalignment - proof of application of new trigonometrical calculations and 3D-printed cutting guides. *BMC Musculoskelet Disord*. 2018;19(1):215. [CrossRef]
20. Shi J, Lv W, Wang Y, et al. Three dimensional patient-specific printed cutting guides for closing-wedge distal femoral osteotomy. *Int Orthop*. 2019;43(3):619-624. [CrossRef]
21. Arnal-Burró J, Pérez-Mañanes R, Gallo-Del-Valle E, Igualada-Blazquez C, Cuervas-Mons M, Vaquero-Martín J. Three dimensional-printed patient-specific cutting guides for femoral varization osteotomy: Do it yourself. *Knee*. 2017;24(6):1359-1368. [CrossRef]
22. Mulford JS, Babazadeh S, Mackay N. Three-dimensional printing in orthopaedic surgery: review of current and future applications. *ANZ J Surg*. 2016;86(9):648-653. [CrossRef]
23. Oe K, Iida H, Nakamura T, Okamoto N, Wada T. Subtrochanteric shortening osteotomy combined with cemented total hip arthroplasty for Crowe group IV hips. *Arch Orthop Trauma Surg*. 2013;133(12):1763-1770. [CrossRef]
24. Rosenstein AD, Diaz RJ. Challenges and solutions for total hip arthroplasty in treatment of patients with symptomatic sequelae of developmental dysplasia of the hip. *Am J Orthop (Belle Mead NJ)*. 2011;40(2):87-91. [CrossRef]
25. Rollo G, Solarino G, Vicenti G, Picca G, Carrozzo M, Moretti B. Subtrochanteric femoral shortening osteotomy combined with cementless total hip replacement for Crowe type IV developmental dysplasia: a retrospective study. *J Orthop Traumatol*. 2017;18(4):407-413. [CrossRef]
26. Huang ZY, Liu H, Li M, Ling J, Zhang JH, Zeng ZM. Optimal location of subtrochanteric osteotomy in total hip arthroplasty for crowe type IV developmental dysplasia of hip. *BMC Musculoskelet Disord*. 2020;21(1):210. [CrossRef]
27. Yasgur DJ, Stuchin SA, Adler EM, DiCesare PE. Subtrochanteric femoral shortening osteotomy in total hip arthroplasty for high-riding developmental dislocation of the hip. *J Arthroplasty*. 1997;12(8):880-888. [CrossRef]
28. Charity JA, Tsiridis E, Sheeraz A, et al. Treatment of Crowe IV high hip dysplasia with total hip replacement using the Exeter stem and shortening derotational subtrochanteric osteotomy. *J Bone Joint Surg Br*. 2011;93(1):34-38. [CrossRef]
29. Dallari D, Pignatti G, Stagni C, et al. Total hip arthroplasty with shortening osteotomy in congenital major hip dislocation sequelae. *Orthopedics*. 2011;34(8):e328-e333. [CrossRef]
30. Krych AJ, Howard JL, Trousdale RT, Cabanela ME, Berry DJ. Total hip arthroplasty with shortening subtrochanteric osteotomy in Crowe type-IV developmental dysplasia: surgical technique. *J Bone Joint Surg Am*. 2010;92 Suppl 1 Pt 2:1761-1787. [CrossRef]
31. Masonis JL, Patel JV, Miu A, et al. Subtrochanteric shortening and derotational osteotomy in primary total hip arthroplasty for patients with severe hip dysplasia: 5-year follow-up. *J Arthroplasty*. 2003;18(3 Suppl 1):68-73. [CrossRef]
32. Togrul E, Ozkan C, Kalaci A, Gülşen M. A new technique of subtrochanteric shortening in total hip replacement for Crowe type 3 to 4 dysplasia of the hip. *J Arthroplasty*. 2010;25(3):465-470. [CrossRef]
33. Dale H, Hallan G, Espehaug B, Havelin LI, Engesæter LB. Increasing risk of revision due to deep infection after hip arthroplasty. *Acta Orthop*. 2009;80(6):639-645. [CrossRef]
34. Jämsen E, Varonen M, Huhtala H, et al. Incidence of prosthetic joint infections after primary knee arthroplasty. *J Arthroplasty*. 2010;25(1):87-92. [CrossRef]
35. Pulido L, Ghanem E, Joshi A, Purtill JJ, Parvizi J. Periprosthetic joint infection: the incidence, timing, and predisposing factors. *Clin Orthop Relat Res*. 2008;466(7):1710-1715. [CrossRef]
36. Thanni LO, Aigoro NO. Surgical site infection complicating internal fixation of fractures: incidence and risk factors. *J Natl Med Assoc*. 2004;96(8):1070-1072. [CrossRef]
37. Köksal A, Öner A, Çimen O, Aycan OE, Akgün H, Yapıcı F, Çamurcu Y. Femoral stem fractures after primary and revision hip replacements: a single-center experience. *Jt Dis Relat Surg*. 2020;31(1):557-563. [CrossRef]

ABCResearch

Arch Basic Clin Res 2026;8(1):66-70
DOI: 10.4274/ABCR.2025.25382

Research Article

Predictive Factors for Ureteral Stricture in Patients Undergoing Endoscopic Stone Surgery

Sezgin Yeni[1], Nurullah Ay[2]

[1]Department of First and Emergency Aid, Mudanya University Vocational School, Bursa, Türkiye
[2]Department of Nursing, Mudanya University Faculty of Health Sciences, Bursa, Türkiye

Cite this article as: Yeni S, Ay N. Predictive factors for ureteral stricture in patients undergoing endoscopic stone surgery. *Arch Basic Clin Res.* 2026;8(1):66-70.

ORCID IDs of the authors: S.Y. 0000-0001-5143-6507, N.A. 0000-0002-0122-5725.

ABSTRACT

Objective: To evaluate predictive factors for ureteral stricture in patients undergoing ureterorenoscopy (URS) for ureteral stones and to identify radiological and demographic parameters that may influence surgical access.

Methods: This retrospective study analyzed data from 197 patients who underwent URS between 2023 and 2025. After applying inclusion and exclusion criteria, 141 patients with available abdomino-pelvic computed tomography (CT) scans were included. Group 1 comprised 30 patients with ureteral strictures requiring passive dilatation with double-J stenting, whereas Group 2 included 111 patients with successful ureteral access and stone fragmentation. Demographic data [age, sex, body mass index (BMI)] and CT-based measurements renal pelvis anteroposterior (AP) diameter, proximal, mid, and distal ureteral AP diameters, distal coronal AP diameter, and stone size) were compared between groups.

Results: Distal ureteral transverse AP diameter (2.25 ± 0.28 mm vs 3.17 ± 0.55 mm, $P < 0.001$), distal coronal AP diameter (2.83 ± 0.43 mm vs 3.56 ± 0.42 mm, $P < 0.001$), and stone size (6.19 ± 2.48 mm vs 7.48 ± 2.06 mm, $P = 0.031$) were significantly lower in Group 1 than in Group 2. In addition, BMI was significantly higher in Group 1. Other CT parameters showed no significant differences.

Conclusion: Narrow distal ureteral diameters and smaller stone sizes measured on preoperative CT, along with higher BMI, were associated with failure of ureteral access at the initial URS session. Identifying these predictors preoperatively may guide patient counseling and surgical planningand reduce intraoperative complications.

Keywords: Ureteral stricture, URS, ureter stone, endoscopy

INTRODUCTION

Urolithiasis is a prevalent urological condition, affecting between 1% and 20% of the population, with prevalence varying according to geographic region.[1] Over the past two decades, substantial advancements have been made in minimally invasive techniques for the management of this condition, including ureterorenoscopy (URS), shock wave lithotripsy (SWL), and percutaneous nephrolithotomy.[2] In recent decades, advances in laser technology and URS have established URS as the standard treatment for ureteral stones.[3] The utilization of URS has increased as the surgical management of upper urinary tract stone disease shifts from predominantly non-invasive methods, such as SWL, toward more invasive approaches, notably flexible URS.[3] Despite its minimally invasive nature, URS can present significant technical challenges, particularly in cases involving ureteral strictures or narrow ureteral anatomy, which may hinder access to the calculi.[4]

When ureteral access cannot be achieved during the initial procedure, active balloon dilatation, or more commonly passive dilatation via placement of a double-J (DJ) stent followed by URS, is indicated. However, in cases of severe ureteral stenosis accompanied by stone obstruction, placement of a DJ stent may be infeasible. Consequently, this situation not only elevates patient morbidity and healthcare costs but also prolongs the

Corresponding author: Sezgin Yeni, **E-mail:** sezgin19yeni90@gmail.com

Received: October 16, 2025 **Accepted:** November 12, 2025 **Publication Date:** January 26, 2026
Revision Requested: November 5, 2025

duration of stone-related symptoms.[5] Moreover, in obstructive pyelonephritis, urgent urinary drainage is critical to prevent renal deterioration. If endoscopic DJ stent placement cannot be achieved, percutaneous nephrostomy remains the only viable alternative.[6] Taken together, these factors underscore the importance of identifying reliable predictors of difficult ureteral access, as early recognition can enhance clinical decision-making and optimize patient outcomes. Furthermore, it can facilitate the timely preparation of both patients and surgeons for potential percutaneous nephrostomy placement. Interestingly, smaller stones have also been associated with ureteral stricture, which may be explained by their tendency to lodge in already narrowed or fibrotic segments, where chronic irritation and limited luminal expansion promote further fibrosis and stricture formation.

Several studies have reported that factors such as young age, female sex, small ureteral diameter, and high body mass index (BMI) may predispose patients to ureteral stenosis and increase the risk of ureteral injury.[7] In recent years, preoperative measurement of ureteral and renal pelvic diameters using non-contrast computed tomography (NCCT) has gained popularity for predicting ureteral stenosis and potential surgical complications.[8] Nevertheless, evidence remains limited regarding which specific radiological and demographic parameters constitute the most significant risk factors for ureteral stenosis requiring stent placement.

The present study aims to evaluate the risk of ureteral stenosis by assessing preoperative CT-based ureteral measurements alongside other clinical and demographic factors in patients undergoing URS. Identifying these risk factors may facilitate better preoperative counseling and surgical planning. Moreover, primary nephrostomy placement instead of URS in high-risk patients—particularly those with infection or renal obstruction—may reduce morbidity and improve clinical outcomes.

MATERIAL AND METHODS

This study was approved by the Mudanya University Health Sciences Ethics Committee (reference no: E-40839601-50.04-62, date: 03.12.2024) and conducted in accordance with the Declaration of Helsinki (1975, revised 2008). Patient data were recorded and analyzed retrospectively.

MAIN POINTS

- Preoperative computed tomography findings, specifically narrow distal ureteral diameters, are strong predictors of difficult ureteral access during ureterorenoscopy.
- Higher body mass index is associated with an increased risk of requiring passive dilatation with double-J stent placement before definitive stone treatment.
- Smaller ureteral stones are paradoxically associated with higher rates of ureteral strictures, possibly due to inadequate luminal dilation.

Patient Selection

A total of 197 patients who underwent URS between January 2023 and January 2025 were evaluated. Of these, 141 patients with available abdomino-pelvic NCCT were included. Exclusion criteria were:

- Age < 18 years (n=1),
- Absence of preoperative CT data (n=51),
- URS performed for diagnostic purposes (n=4).

Group Classification

- Group 1 (n=30): Patients in whom the distal ureter could not be accessed because of a stricture and who underwent passive dilatation with DJ stent placement.
- Group 2 (n=111): Patients with successful ureteral access and stone fragmentation during the first URS session.

Data Collection

Demographic parameters: age, sex, BMI.

Radiological measurements on NCCT (1 mm slice interval):

- Renal pelvis anteroposterior (AP) diameter (mm)
- Proximal, mid, distal ureteral AP diameters (mm)
- Distal ureteral coronal AP diameter (mm)
- Stone diameter (mm)

Measurement Method

Transverse measurements of the renal pelvis, proximal ureter, mid-ureter, and distal ureter were obtained in all patients using NCCT with a slice thickness of 1 mm. Additionally, measurements were taken at the level of the distal ureter in the coronal plane. For consistency, the ureter was defined at the same anatomical level in each case, and measurements were performed on the corresponding section images. All radiological measurements were independently performed by an experienced urologist (S.Y.).

Surgical Technique

All procedures were performed by a single experienced surgeon (SY) using a 7.5 Fr Storz semirigid ureteroscope. A guidewire was advanced through the ureteral orifice. In cases without strictures, stones were accessed and fragmented using laser lithotripsy. When a distal ureteral stricture was present, a DJ stent was placed and URS was postponed for one month to allow passive dilatation before definitive stone treatment.

Statistical Analysis

Statistical analyses were performed using MedCalc statistical software (Mariakerke, Belgium). The results were expressed as mean ± standard deviation. The normality of data distribution was evaluated using the Kolmogorov-Smirnov test. Since the data were normally distributed, comparisons between groups were performed using the Student's t-test. *P* values were considered statistically significant.

RESULTS

A total of 141 patients were included. Thirty patients (21.3%) required DJ stenting for ureteral stricture (Group 1), while 111 patients (78.7%) underwent successful primary URS (Group 2) (Table 1). No significant differences were observed between the groups in terms of age and gender. However, BMI was significantly higher in Group 1 patients than in those Group 2 ($P = 0.049$; Table 1).

- Distal ureteral AP diameter was significantly lower in Group 1 (2.25 ± 0.28 mm) than in Group 2 (3.17 ± 0.55 mm; $P < 0.001$) (Table 2).
- Distal coronal AP diameter was also lower in Group 1 (2.83 ± 0.43 mm) than in Group 2 (3.56 ± 0.42 mm; $P < 0.001$) (Table 2).
- Stone size was smaller in Group 1 (6.19 ± 2.48 mm) than in Group 2 (7.48 ± 2.06 mm; $P = 0.031$).
- BMI was significantly higher in Group 1 ($P < 0.05$).
- Other parameters (renal pelvis AP, proximal-mid ureter AP, stone proximal location) showed no significant differences.

DISCUSSION

To date, no studies have addressed the measurement of ureteral diameters in patients undergoing prestenting for ureteral stenosis. Our findings suggest that narrower distal ureteral diameters on preoperative CT scans and higher BMI are associated with failure to obtain ureteral access during initial URS, necessitating DJ stenting. Additionally, small stones were associated with ureteral stenosis, suggesting that failure of these stones to pass may indicate ureteral stenosis. Interestingly, in our study, smaller stones were paradoxically associated with ureteral stenosis and failure of initial URS. This may be explained by the inability of even small stones to pass through a pre-existing narrow distal ureter. While some studies report that larger stones are more likely to cause obstruction and stricture formation, others have observed paradoxical findings, suggesting that stone size alone may not fully predict ureteral patency.[9,10] These discrepancies highlight the importance of considering ureteral anatomy and preexisting narrowing in addition to stone characteristics when planning an intervention. Furthermore, recent evidence indicates that increased ureteral wall thickness is associated with both decreased spontaneous passage of ureteral stones and a higher risk of ureteral stricture after URS.[11] These findings support our observation that ureteral anatomy, including distal ureteral narrowing, plays a critical role in predicting procedural success and long-term outcomes.

Table 1. Comparison of Demographic Characteristics Between Groups

	Group 1 (n=30)	Group 2 (n=111)	*P* value
Age	42.2 ± 6.2	39.9 ± 7.4	0.578
Male	29 (96.6%)	93 (83.9%)	0.145
Female	1 (3.4%)	18 (16.1%)	0.217
BMI	27.6±3.4	26.0±2.5	**0.049***

A Student's t-test was used. *P values < 0.05 > are considered statistically significant and are shown in bold.
BMI, body mass index.

Table 2. Comparison of Tomographic Measurement Data Between the Two Groups

	Group 1 (n=30)	Group 2 (n=111)	*P* value
Renal Pelvis AP	14.41 ± 5.54	14.90 ± 8.46	0.788
Proximal ureter AP	6.35 ± 2.34	6.70 ± 2.20	0.551
Mid ureter AP	3.99 ± 1.51	4.47 ± 1.79	0.260
Distal ureter AP	2.25 ± 0.28	3.17 ± 0.55	**< 0.001***
Distal ureter (Cor)	2.83 ± 0.43	3.56 ± 0.42	**< 0.001***
Stone size	6.19 ± 2.48	7.48 ± 2.06	**0.031***

Student's t-test was used. *P value 0.05 is considered statistically significant and is bolded.
AP, anteroposterior; Cor, coronal.

These findings are consistent with previous literature emphasizing the role of ureteral anatomy in determining URS outcomes. Narrow distal ureters have been consistently associated with an increased risk of stricture formation and technical difficulties during URS.[12,13] Similarly, higher BMI has been associated with more complex surgical rerouting and anatomic reorientation, potentially complicating surgical access.[13] This association may be explained by increased retroperitoneal fat and altered ureteral angulation, which can complicate endoscopic navigation. Additionally, obesity may affect patient positioning and limit the working space for instrumentation, potentially increasing operative difficulty. A meta-analysis has shown that older age and obesity are associated with a higher risk of ureteral stricture.[7] Our study expands on these observations by quantitatively linking the distal ureteral diameter to failure of initial URS, providing objective, imaging-based parameters that may predict procedural difficulty.

In this study, no significant differences were observed between the two groups in the diameters of the renal pelvis, proximal ureter, and mid-ureter as measured on CT scans. However, both AP and coronal measurements showed that distal ureteral diameters were significantly smaller in patients in Group 1 than in patients in Group 2. This suggests that distal ureteral narrowing plays a central role in determining initial ureteral accessibility. Distal ureteral stricture present in the majority of unsuccessful or non-accessible URS procedures. Our findings highlight the potential clinical utility of standardizing these measurements to provide patients with clearer preoperative information regarding the likelihood of ureteral stricture.

As the diameter of ureteral stones decreases, the incidence of ureteral stenosis and of failed URS increases.[9] The present results reinforce this observation, indicating that even small calculi may fail to pass through a narrowed ureter. Clinically, 2-4-mm stones causing significant obstructive uropathy often fail to pass despite 2-4 weeks of conservative management and medical expulsive therapy.[10] The decision to proceed with surgical intervention is based on a comprehensive evaluation of the stone's size, location, degree of hydronephrosis, as well as the patient's clinical symptoms. Our data suggest that in such cases the ureter is often too narrow to be accessed during the

initial URS attempt, requiring prior ureteral stenting to facilitate access.[14] Incorporating ureteral diameter measurements into the preoperative assessment may therefore enable earlier surgical planning, avoiding unnecessary delays in stone passage, relieving obstruction, and improving patient outcomes.

The standard treatment for ureteral obstruction caused by stones is URS combined with laser lithotripsy.[15] However, in patients presenting with infection secondary to renal obstruction, timely renal drainage is imperative due to the elevated risk of urosepsis.[16] In such cases, the most commonly employed interventions are DJ stent placement or percutaneous nephrostomy.[17] Based on our results, when managing patients with stone-related hydronephrosis and urosepsis, particularly those with a narrow ureteral diameter on CT, proceeding with percutaneous nephrostomy may be more appropriate to optimize both clinical outcomes and patient safety. This consideration is underscored by the increased technical challenges associated with DJ stent placement in the presence of ureteral obstruction and stenosis, factors that may elevate the risk of intraoperative complications.

From a clinical standpoint, our study emphasizes that preoperative identification of patients at higher risk of stricture allows for improved surgical planning. Surgeons may anticipate the need for staged procedures, prepare for DJ stenting, and provide patients with realistic expectations regarding outcomes.[18] Additionally, careful manipulation in patients predicted to have narrow ureters may reduce the risk of iatrogenic ureteral injury.[19]

Study Limitations

Limitations of this study include its retrospective design, single-center setting, and a relatively small number of stricture cases. Nonetheless, the prospective data collection and the standardized surgical approach by a single surgeon strengthen its validity. Our findings should therefore be interpreted as hypothesis-generating and should encourage larger multicenter studies to validate these predictors and to incorporate them into preoperative risk stratification models.

CONCLUSION

Preoperative CT parameters, specifically distal ureteral AP and coronal diameters, along with BMI and stone size, significantly predict the likelihood of failed ureteral access during URS. Surgeons should consider these factors in preoperative planning to minimize complications, improve patient counseling, and optimize treatment strategies. However, prospective multicenter validation studies are warranted to confirm these findings and enhance their generalizability.

Ethics

Ethics Committee Approval: This study was approved by the Mudanya University Health Sciences Ethics Committee (reference no.: E-40839601-50.04-62, date: 03.12.2024)

Informed Consent: Informed consent was obtained from all individual participants included in the study.

Footnotes

Author Contributions

Concept Design – S.Y.; Data Collection or Processing – S.Y.; Analysis or Interpretation – S.Y., N.A.; Literature Review – S.Y.; Writing, Reviewing and Editing – S.Y., N.A.

Declaration of Interests: The authors declare no conflict of interest regarding the publication of this paper.

Funding: The authors declare no financial support or funding.

REFERENCES

1. Scales CD Jr, Smith AC, Hanley JM, Saigal CS; urologic diseases in America Project. Prevalence of kidney stones in the United States. *Eur Urol*. 2012;62(1):160-165. [CrossRef]
2. Türk C, Petřík A, Sarica K, et al. EAU guidelines on urolithiasis. *European Association of Urology*., 2020; 87. [CrossRef]
3. Geraghty RM, Jones P, Somani BK. Worldwide trends of urinary stone disease treatment over the last two decades: a systematic Review. *J Endourol.* 2017;31(6):547-556. [CrossRef]
4. Savić S, Vukotić V, Lazić M, Savić N. Stenting versus non-stenting following uncomplicated ureteroscopic lithotripsy: comparsion and evaluation of symptoms. *Vojnosanit Pregl.* 2016;73(9):850-856. [CrossRef]
5. De Coninck V, Keller EX, Somani B, et al. Complications of ureteroscopy: a complete overview. *World J Urol*. 2020;38(9):2147-2166. [CrossRef]
6. Yamamoto Y, Fujita K, Nakazawa S, et al. Clinical characteristics and risk factors for septic shock in patients receiving emergency drainage for acute pyelonephritis with upper urinary tract calculi. *BMC Urol.* 2012;12:4. [CrossRef]
7. Utraadi AK, Patil SR, Kumar N. The non-accessible ureter: can history, gender, age, BMI, radiology and stone size predict the requirement of pre-stenting in narrow ureters. National Journal, 2024; 9(2):77. [CrossRef]
8. Tran TY, Bamberger JN, Blum KA, et al. Predicting the impacted ureteral stone with computed tomography. *Urology*. 2019;130:43-47. [CrossRef]
9. Senel S, Uzun E, Ceviz K, et al. Predictive factors for difficult ureter in primary kidney stone patients before retrograde intrarenal surgery. *Cent European J Urol*. 2024;77(2):280-285. [CrossRef]
10. Ahmadi A, Al Rashed AA, Hasan O, et al. Challenges of retrograde ureteroscopic procedures in overweight patients. *Cureus*. 2023;15(10):e47815. [CrossRef]
11. Ekici O, Gul A, Zengin S, Boyaci C, Kilic M. The impact of ureteral wall thickness on spontaneous passage and development of long-term ureteral stricture in patients with ureteral stone. *J Coll Physicians Surg Pak*. 2023;33(1):97-102. [CrossRef]
12. Byrne MHV, Georgiades F, Light A, et al. Impact of COVID-19 on the management and outcomes of ureteric stones in the UK:

a multicentre retrospective study. *BJU Int*. 2023;131(1):82-89. [CrossRef]

13. Bhanot R, Jones P, Somani B. Minimally invasive surgery for the treatment of ureteric stones - state-of-the-art review. *Res Rep Urol*. 2021;13:227-236. [CrossRef]
14. Mckay A, Somani BK, Pietropaolo A, et al. Comparison of primary and delayed ureteroscopy for ureteric stones: a prospective non-randomized comparative study. *Urol Int*. 2021;105(1-2):90-94. [CrossRef]
15. Tran TY, Hernandez Bustos N, Kambadakone A, Eisner B, Pareek G. Emergency ureteral stone treatment score predicts outcomes of ureteroscopic intervention in acute obstructive uropathy secondary to urolithiasis. *J Endourol*. 2017;31(9):829-834. [CrossRef]
16. Kamei J, Nishimatsu H, Nakagawa T, et al. Risk factors for septic shock in acute obstructive pyelonephritis requiring emergency drainage of the upper urinary tract. *Int Urol Nephrol*. 2014;46(3):493-497. [CrossRef]
17. Anıl H, Şener NC, Karamık K, et al. Comparison of percutaneous nephrostomy and ureteral DJ stent in patients with obstructive pyelonephritis: a retrospective cohort study. *J Invest Surg*. 2022;35(7):1445-1450. [CrossRef]
18. Hubert KC, Palmer JS. Passive dilation by ureteral stenting before ureteroscopy: eliminating the need for active dilation. *J Urol*. 2005;174(3):1079-1080; discussion 1080. [CrossRef]
19. Gild P, Kluth LA, Vetterlein MW, Engel O, Chun FKH, Fisch M. Adult iatrogenic ureteral injury and stricture-incidence and treatment strategies. *Asian J Urol*. 2018;5(2):101-106. [CrossRef]

ABCResearch

Arch Basic Clin Res 2026;8(1):71-75
DOI: 10.4274/ABCR.2025.25388

Research Article

The Role of Serum Zinc, Iron, Magnesium, and Selenium Levels in the Pathogenesis of PFAPA Syndrome

Fatma Atalay, Murat Yaşar

Department of Otorhinolaryngology, Head and Neck Surgery, Kastamonu University Faculty of Medicine, Kastamonu, Türkiye

Cite this article as: Atalay F, Yaşar M. The role of serum zinc, iron, magnesium, and selenium levels in the pathogenesis of PFAPA syndrome. *Arch Basic Clin Res*. 2026;8(1):71-75.

ORCID IDs of the authors: F.A. 0000-0002-0344-1982, M.Y. 0000-0003-3300-4430.

ABSTRACT

Objective: To investigate the potential role of zinc, iron, magnesium, and selenium in the pathogenesis of Periodic Fever, Aphthous Stomatitis, Pharyngitis, Adenitis (PFAPA) syndrome.

Methods: A retrospective analysis was conducted of 26 children diagnosed with PFAPA and 31 age- and sex-matched healthy controls. Serum levels of zinc, iron, magnesium, and selenium were retrieved from hospital records and compared between the groups.

Results: Magnesium levels were 2.03 ± 0.14 mg/dL in the PFAPA group and 1.99 ± 0.13 mg/dL in the control group. The difference was not statistically significant (P = 0.308). Median iron levels (25^{th}-75^{th} percentiles) were 52.5 µg/dL (22.0-81.5) in the PFAPA group and 61.1 µg/dL (42.5-89.0) in the control group; the difference was not significant (P = 0.226). Zinc levels were similar: 86.24 ± 11.18 mcg/L in the PFAPA group and 87.26 ± 10.06 mcg/L in the control group (P = 0.720). However, median selenium levels differed significantly: 38.9 mcg/L (34.2-50.0) in the PFAPA group versus 48.0 mcg/L (43.0-55.5) in the control group (P = 0.002). Each one-unit increase in selenium levels increased the odds of disease by approximately 8.6%, and this association was statistically significant (odds ratio = 1.086, 95% confidence interval: 1.019-1.157, P = 0.011).

Conclusion: In conclusion, this study demonstrates that low selenium levels are associated with PFAPA syndrome in children. No significant relationships were observed between zinc, iron, or magnesium levels and the disease. Given the effects of selenium on the immune system and inflammation, we hypothesize that selenium deficiency may contribute to the pathogenesis of PFAPA.

Keywords: Periodic fever, autoinflammatory, selenium, zinc, magnesium

INTRODUCTION

Periodic Fever, Aphthous Stomatitis, Pharyngitis, Adenitis (PFAPA) syndrome, characterized by periodic fever, aphthous stomatitis, pharyngitis, and cervical adenitis is an autoinflammatory disease first described by Marshall et al.[1] in 1987.[2] PFAPA is the most widespread cause of periodic fever in childhood, although the true incidence is unknown.[3] There is no specific laboratory finding or diagnostic test for the syndrome.[2] Although the clinical manifestations have been well described, the lack of a disease-specific laboratory finding makes diagnosis difficult. Diagnosis is therefore based on clinical criteria, with the modified Marshall criteria most frequently employed. According to these criteria, periodic fever attacks commencing before five years of age, aphthous stomatitis without upper respiratory tract infection, pharyngitis or cervical lymphadenitis, being asymptomatic between attacks, exclusion of cyclic neutropenia, and normal growth and development are regarded as diagnostic.[4]

Zinc, iron, magnesium, and selenium are elements with important functions. Zinc is an essential trace element for biological processes and serves as a cofactor for more than 300 enzymes involved in protein synthesis and repair systems. It is also involved in cellular signaling at all levels and plays an

Corresponding author: Fatma Atalay, **E-mail:** fatmatalay_88@hotmail.com

Received: October 21, 2025 **Accepted:** November 3, 2025 **Publication Date:** January 26, 2026

important role in immune system regulation.[5] Although the principal function of iron is the transport of O_2 by hemoglobin, it is also an important cofactor for several enzymes and plays a critical role in the immune system and in defense against infection.[6] Selenium is an important micronutrient for human health, particularly through its effects on thyroid metabolism, the cardiovascular system, and the immune system. It is involved in the activation, proliferation, and differentiation of cells that direct immune responses and contributes to immune regulation by preventing excessive responses that could lead to autoimmunity or chronic inflammation.[7] Finally, magnesium is an important element in the regulation of metabolism and homeostasis in all tissues. It regulates ion channel activity, acts as a second messenger in signal transmission, contributes to the production of adenosine triphosphate, and influences immunological functions by affecting immune cells.[8]

PFAPA syndrome has long been recognized. Several potential etiological factors have been investigated, including infectious agents, immunological mechanisms, and genetic predisposition; however, the disease's etiopathogenesis and genetic basis remain unclear.[9] The purpose of this study was to investigate the potential role of zinc, iron, magnesium, and selenium, all of which are involved in immune function, in the pathogenesis of PFAPA.

MATERIAL AND METHODS

Approval for the study was obtained from the Kastamonu University Clinical Research Ethics Committee prior to commencement (decision no.: 2023-KAEK-106, date: 13.09.2023). All procedures in studies involving human participants are carried out in accordance with institutional ethical standards (Kastamonu Ethical Committee) and with the 1964 Declaration of Helsinki. Informed consent was not obtained because the study was conducted retrospectively.

This retrospective study included 26 patients diagnosed with PFAPA who were under follow-up at the Kastamonu Training and Research Hospital Ear, Nose, and Throat Clinic (Türkiye) between 01.09.2021 and 01.09.2023, and 31 age- and sex-matched healthy controls. Test results obtained during the follow-up periods were retrieved retrospectively from the hospital records, and zinc (70-115 mcg/L), iron (16-129 µg/dL), magnesium (1.7-2.3 mg/dL), and selenium (46-143 mcg/L) levels were recorded. The obtained data were then compared with data from the healthy control group. Patients with acute bacterial infection, autoimmune diseases, or anemia were excluded.

MAIN POINTS

- Serum selenium levels were significantly lower in children with Periodic Fever, Aphthous Stomatitis, Pharyngitis, Adenitis (PFAPA) syndrome compared to healthy controls.
- Each unit increase in selenium concentration was associated with an 8.6% lower risk of PFAPA, suggesting a potential protective role for selenium.
- No significant differences were observed in serum zinc, iron, and magnesium levels between PFAPA patients and controls.
- Low selenium levels may contribute to immune dysregulation and excessive inflammatory responses in the pathogenesis of PFAPA.
- Selenium supplementation may represent a therapeutic approach, but further prospective studies are required.

Statistical Analysis

Normality of the study data distribution was assessed using histograms, Q-Q plots, and the Shapiro-Wilk test. Quantitative variables were compared between the groups using the Mann-Whitney U test and paired samples t-test, while relationships between categorical variables were evaluated using the chi-square test. Univariate logistic regression analysis was applied to evaluate potential risk factors affecting the disease. The analysis results were reported as odds ratios (ORs) with 95% confidence interval (CI). *P* values < 0.05 were considered statistically significant. Statistical analyses were performed using IBM SPSS Statistics for Windows, version 22.0 (IBM Corp., Armonk, NY, USA).

RESULTS

The mean ages of the PFAPA and control groups were 7.12 ± 2.25 and 6.97 ± 2.34 years, respectively; no significant difference was observed between them (*P* = 0.810). In terms of gender distribution, girls comprised 46.2% and boys 53.8% of the PFAPA group, compared with 45.2% and 54.8% in the control group. No significant difference in gender distribution was observed between groups (*P* = 0.999).

Regarding biochemical parameters, magnesium levels were 2.03 ± 0.14 mg/dL in the PFAPA group and 1.99 ± 0.13 mg/dL in the control group. The difference was not statistically significant (*P* = 0.308). Median iron levels (25^{th}-75^{th} percentile) were 52.5 µg/dL (22.0-81.5) in the PFAPA group and 61.1 µg/dL (42.5-89.0) in the control group, the difference also being insignificant (*P* = 0.226). Zinc levels were also similar, at 86.24 ± 11.18 mcg/L in the PFAPA group and 87.26 ± 10.06 mcg/L in the control group (*P* = 0.720). However, median selenium levels differed significantly, at 38.9 mcg/L (34.2-50.0) in the PFAPA group and 48.0 mcg/L (43.0-55.5) in the control group (*P* = 0.002) (Figure 1). The groups' demographic characteristics and biochemical parameters are summarized in Table 1.

In univariate regression analysis, magnesium levels exhibited a protective effect against the disease; however, this association was not statistically significant (OR = 0.119, 95% CI: 0.002-6.966, *P* = 0.305). Similarly, no significant association was observed between iron levels and the disease (OR = 1.007, 95% CI: 0.992-1.022, *P* = 0.360). Zinc levels also exhibited no significant association (OR = 1.009, 95% CI: 0.960-1.062, *P* = 0.714). However, a significant relationship was observed between selenium levels and the disease. Each one-unit increase in selenium levels increased the odds of disease by approximately 8.6%, and this association was statistically significant (OR = 1.086, 95% CI: 1.019-1.157, *P* = 0.011) (Table 2).

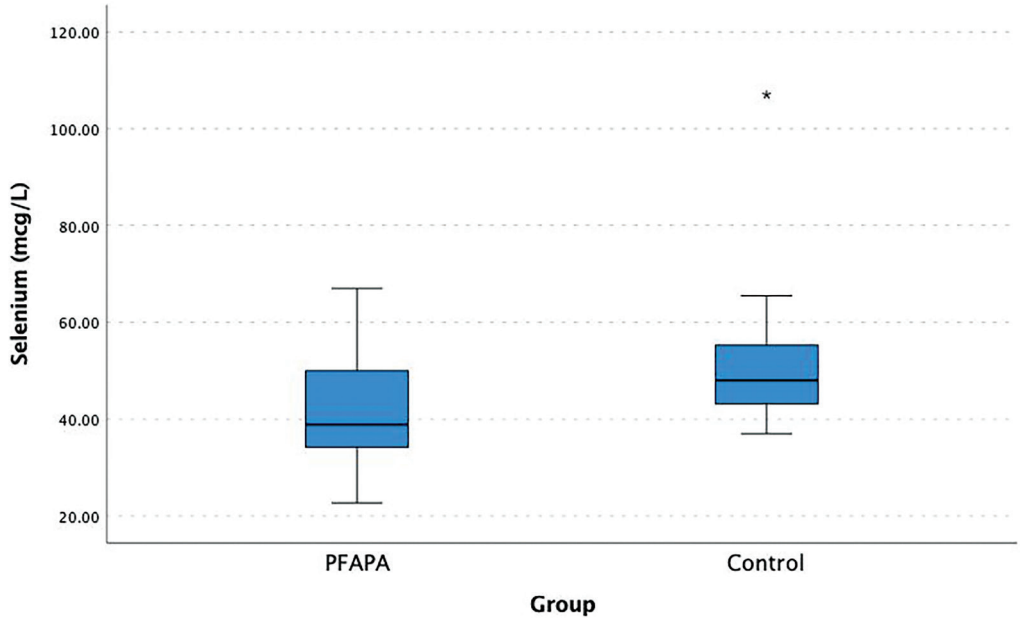

Figure 1. Box plot of selenium levels in the PFAPA and control groups.
PFAPA, periodic fever, aphthous stomatitis, pharyngitis, adenitis.

Table 1. The Groups' Demographic Characteristics and Biochemical Parameters

Variables	Group		*P*
	PFAPA (n=26)	Control (n=31)	
Age	7.12 ± 2.25	6.97 ± 2.34	0.810
Gender			
Female	12 (46.2)	14 (45.2)	0.999
Male	14 (53.8)	17 (54.8)	
Magnesium	2.03 ± 0.14	1.99 ± 0.13	0.308
Iron	52.5 (22.0-81.5)	61.1 (42.5-89.0)	0.226
Zinc	86.24 ± 11.18	87.26 ± 10.06	0.720
Selenium	38.9 (34.2-50.0)	48.0 (43.0-55.5)	**0.002**

Data expressed as n (%), mean ± standard deviation, and median (25^{th}-75^{th} percentile) values.
PFAPA, periodic fever, aphthous stomatitis, pharyngitis, adenitis.

Table 2. Analysis of Risk Factors Affecting the Disease

Variables	Univariate	
	OR (95% CI)	*P*
Magnesium	0.119 (0.002-6.966)	0.305
Iron	1.007 (0.992-1.022)	0.360
Zinc	1.009 (0.960-1.062)	0.714
Selenium	1.086 (1.019-1.157)	**0.011**

OR, odds ratio; CI, confidence interval.

DISCUSSION

Serum selenium levels in this study were significantly lower in children with PFAPA syndrome than in the control group, and an increase in selenium levels was associated with a reduced risk of the disease. This finding is consistent with the known anti-inflammatory and regulatory effects of selenium on the immune system and suggests that it may play a role in the etiopathogenesis of PFAPA syndrome.[7,10-12] Huang et al. [7] examined the role of selenium in inflammation and immunity and reported that selenium levels were important for initiating immunity and also played a role in regulating excessive immune responses and chronic inflammation. Similarly, Hariharan and Dharmaraj[10] emphasized the antioxidant and anti-inflammatory effects of selenoproteins and concluded that glutathione peroxidase assisted in controlling excessive free-radical production at the site of inflammation. Navarro Garcia et al.[11] emphasized selenium's neuroprotective and anti-inflammatory properties and showed that it may be beneficial in various inflammatory states. Osuna-Padilla et al.[12] also reported that selenium supplementation reduced immune activation and inflammation in individuals infected with human immunodeficiency virus.

PFAPA syndrome is an autoinflammatory disease of uncertain etiology.[13-15] Overactivation of the innate immune system and of proinflammatory cytokines has been implicated in the pathogenesis.[13] The low selenium levels observed in the present study suggest that either selenium requirements may have increased to counteract the heightened inflammatory response and oxidative stress in patients with PFAPA syndrome or that selenium deficiency may contribute to these inflammatory processes. Considering the role of selenium in immune regulation, low selenium levels may be either a cause or a result of the excessive immune response observed in PFAPA syndrome. This, in turn, suggests that selenium supplementation may represent a potential therapeutic approach for the management of the syndrome. However, more extensive prospective studies are now needed to confirm that hypothesis.

No significant associations were determined between zinc, iron, or magnesium levels and PFAPA syndrome in this study. However, in light of the general effects of these elements on the immune system and inflammation, their potential roles in the pathogenesis of PFAPA still merit investigation. Sanna et al.[5] examined the relationship between zinc and autoimmunity and reported that zinc deficiency can impair the function of immune cells and affect inflammatory responses. Although the principal function of iron is oxygen transport, it also plays a critical role in immune function and defense against infection.[6] Brock and Mulero[6] examined the cellular and molecular aspects of iron and reported that iron deficiency or excess can affect immune responses. No significant difference in iron levels between the two groups was detected in the present study. This suggests that iron plays no direct role in the pathogenesis of PFAPA. However, inflammatory conditions can affect iron metabolism.

Magnesium is an important element involved in the regulation of homeostasis and metabolism of all tissues. It also affects immune cells by regulating immune functions.[16] Maier et al. [8] reported that magnesium deficiency activated phagocytes and triggered inflammation by increasing cytokine production. Low magnesium levels have therefore been linked to various chronic inflammatory diseases. Although no significant difference in magnesium levels was observed in the present study, its role in PFAPA requires more detailed examination in light of the potent effects of magnesium on inflammation. In particular, vitamin D deficiency has been shown to be associated with PFAPA, and magnesium is an important cofactor in vitamin D metabolism.[17,18] Future studies should therefore assess the interaction between magnesium and vitamin D in the pathogenesis of PFAPA.

Study Limitations

The principal limitations of this study are its retrospective design and relatively small sample size. Although the low selenium levels represent an important finding, further prospective, randomized controlled studies are needed to establish whether this relationship is causal or consequential. Future studies should evaluate the effects of selenium supplementation on the frequency, severity, and duration of PFAPA syndrome and establish the safety and efficacy of such supplementation. In addition, the effects of other trace elements such as zinc, iron, and magnesium on inflammatory markers and cytokine profiles might be investigated. Further, more extensive studies investigating the role of genetic and immunological parameters and environmental factors are needed to better understand the etiopathogenesis of PFAPA syndrome.

CONCLUSION

In conclusion, this study shows that low selenium levels in children with PFAPA syndrome are related to the disease. No significant relationships were determined between zinc, iron, or magnesium levels and the disease. Considering the effects of selenium on the immune system and inflammation, we think that selenium deficiency may play a role in the pathogenesis of PFAPA.

Ethics

Ethics Committee Approval: Approval for the study was obtained from the Kastamonu University Clinical Research Ethical Committee (decision no.: 2023-KAEK-106, date: 13.09.2023).

Informed Consent: Retrospective study. Permission was obtained from hospital management to collect study data from the Information Management System.

Acknowledgements

We want to thank Mr. Carl Austin Nino Rossini for his valuable contribution.

Footnotes

Author Contributions

Concept Design – F.A.; Data Collection or Processing – F.A.; Analysis or Interpretation – F.A.; Literature Review – M.Y.; Writing, Reviewing and Editing – F.A., M.Y.

Declaration of Interests: The authors declare no conflict of interest regarding the publication of this paper.

Funding: The authors declare no financial support or funding.

REFERENCES

1. Marshall GS, Edwards KM, Butler J, Lawton AR. Syndrome of periodic fever, pharyngitis, and aphthous stomatitis. *J Pediatr*. 1987;110(1):43-46. [CrossRef]
2. Onur H, Onur AR. Diagnostic performance of routine blood parameters in periodic fever, aphthous stomatitis, pharyngitis, and adenitis syndrome. *J Clin Lab Anal*. 2023;37(11-12):e24934. [CrossRef]
3. Lazea C, Damian L, Vulturar R, Lazar C. PFAPA syndrome: clinical, laboratory and therapeutic features in a single-centre cohort. *Int J Gen Med*. 2022;15:6871-6880. [CrossRef]
4. Hausmann J, Dedeoglu F, Broderick L. Periodic fever, aphthous stomatitis, pharyngitis, and adenitis syndrome and syndrome of unexplained recurrent fevers in children and adults. *J Allergy Clin Immunol Pract*. 2023;11(6):1676-1687. [CrossRef]
5. Sanna A, Firinu D, Zavattari P, Valera P. Zinc status and autoimmunity: a systematic review and meta-analysis. *Nutrients*. 2018;10(1):68. [CrossRef]
6. Brock JH, Mulero V. Cellular and molecular aspects of iron and immune function. *Proc Nutr Soc*. 2000;59(4):537-540. [CrossRef]
7. Huang Z, Rose AH, Hoffmann PR. The role of selenium in inflammation and immunity: from molecular mechanisms to therapeutic opportunities. *Antioxid Redox Signal*. 2012;16(7):705-743. [CrossRef]
8. Maier JA, Castiglioni S, Locatelli L, Zocchi M, Mazur A. Magnesium and inflammation: advances and perspectives. *Semin Cell Dev Biol*. 2021;115:37-44. [CrossRef]
9. Yıldız M, Haslak F, Adrovic A, et al. Periodic Fever, Aphthous Stomatitis, Pharyngitis, and Adenitis Syndrome: a single-center experience. *Turk Arch Pediatr*. 2022;57(1):46-52. [CrossRef]
10. Hariharan S, Dharmaraj S. Selenium and selenoproteins: it's role in regulation of inflammation. *Inflammopharmacology*. 2020;28(3):667-695. [CrossRef]
11. Navarro Garcia E, Leon S, Alvarez Toledo N. Selenium's role in neuroprotection against stroke-induced inflammation. *Cureus*. 2024;16(1):e52205. [CrossRef]
12. Osuna-Padilla IA, Rodríguez-Moguel NC, Aguilar-Vargas A, et al. Zinc and selenium supplementation on treated HIV-infected individuals induces changes in body composition and on the expression of genes responsible of naïve CD8+ T cells function. *Front Nutr*. 2024;11:1417975. [CrossRef]
13. Rydenman K, Fjeld H, Hätting J, Berg S, Fasth A, Wekell P. Epidemiology and clinical features of PFAPA: a retrospective cohort study of 336 patients in western Sweden. *Pediatr Rheumatol Online J*. 2022;20(1):82. [CrossRef]
14. Tekin M, Toplu Y, Kahramaner Z, et al. The mean platelet volume levels in children with PFAPA syndrome. *Int J Pediatr Otorhinolaryngol*. 2014;78(5):850-853. [CrossRef]
15. Burton MJ, Pollard AJ, Ramsden JD, Chong LY, Venekamp RP. Tonsillectomy for periodic fever, aphthous stomatitis, pharyngitis and cervical adenitis syndrome (PFAPA). *Cochrane Database Syst Rev*. 2019;12(12):CD008669. [CrossRef]
16. Stefanache A, Lungu II, Butnariu IA, et al. Understanding how minerals contribute to optimal immune function. *J Immunol Res*. 2023;2023:3355733. [CrossRef]
17. Nalbantoğlu A, Nalbantoğlu B. Vitamin D deficiency as a risk factor for PFAPA syndrome. *Int J Pediatr Otorhinolaryngol*. 2019;121:55-57. [CrossRef]
18. Faydhi SA, Kanawi HMA, Al-Khatib T, Zawawi F. The association between vitamin D level and PFAPA syndrome: a systematic review. *Indian J Otolaryngol Head Neck Surg*. 2022;74(Suppl 3):5548-5555. [CrossRef]

ABCResearch

Arch Basic Clin Res 2026;8(1):76-79
DOI: 10.4274/ABCR.2025.25379

Research Article

Changes in Gastritis During the COVID-19 Pandemic: A Retrospective Comparative Study According to the Sydney Criteria

Orhan Çimen[1], Ferda Keskin Çimen[2]

[1]Department of General Surgery, Erzincan Binali Yıldırım University Faculty of Medicine, Erzincan, Türkiye
[2]Department of Medical Pathology, Erzincan Binali Yıldırım University Faculty of Medicine, Erzincan, Türkiye

Cite this article as: Çimen O, Keskin Çimen F. Changes in gastritis during the COVID-19 pandemic: a retrospective comparative study according to the Sydney criteria. *Arch Basic Clin Res*. 2026;8(1):76-79.

ORCID IDs of the authors: O.Ç. 0000-0001-9932-7465, F.K.Ç. 0000-0002-1844-0827.

ABSTRACT

Objective: This study aimed to evaluate whether the coronavirus disease-2019 (COVID-19) pandemic caused changes in the severity of gastritis, as assessed by the Sydney criteria, through a retrospective comparison of patients in the pre- and post-pandemic periods.

Methods: Pathology reports of 107 pre-pandemic patients until March 2019 and 96 post-pandemic patients until May 2023, who underwent upper gastrointestinal endoscopy for dyspeptic complaints and were diagnosed with gastritis were retrospectively analyzed. Gastritis severity was assessed according to the Sydney criteria. Percentages were calculated and compared.

Results: The pre-pandemic group included 62 women and 45 men (mean age 58.6 years). The post-pandemic group included 50 women and 46 men (mean age 57.6 years). No significant demographic differences were observed. According to the Sydney criteria, no permanent effect of COVID-19 on gastritis severity was identified.

Conclusion: Our study found no significant differences in gastritis severity between the periods before and after the COVID-19 pandemic. Larger prospective studies are required to further explore potential long-term effects.

Keywords: COVID, gastritis, Sydney criteria

INTRODUCTION

Gastritis is the term given to the inflammatory process that extends from the mucosa, the innermost of the histological layers of the stomach wall, to the serosa, the outermost layer. In this process, if neutrophils predominate, it is defined as acute gastritis; if mononuclear cells (lymphocytes, plasma cells, macrophages) are present together, it is defined as chronic gastritis. Another classification describes these processes as acute erosive gastritis and chronic atrophic gastritis, a terminology that is more commonly used in clinical practice.

In addition to improper nutrition, various chemical factors—such as the consumption of salicylate-containing medications—as well as certain bacterial infections or the toxins released during these infections, viral agents and their effects, and allergic reactions may lead to the development of gastritis. Another important factor is *Helicobacter pylori* (*H. pylori*) infection. In order to describe the histopathological reactions caused by *H. pylori* in the gastric mucosa and establish a common scientific language, the Sydney criteria were developed by pathology experts in 1990 and still remain significant today. In the updated 1994 version of the criteria, chronic inflammation, neutrophil activity, glandular atrophy (GA), intestinal metaplasia (IM), and *H. pylori* density are evaluated in a graded manner.

Cases of gastritis, which may occur together with many other diseases, have continued to be observed during the Coronavirus

Corresponding author: Orhan Çimen, **E-mail:** orhancimen24@hotmail.com

Received: November 17, 2025 **Accepted:** December 9, 2025 **Publication Date:** January 26, 2026

disease-2019 (COVID-19) pandemic as well. Gastritis is an inflammatory process of the gastric wall.[1-3] The Sydney criteria, developed in 1990 and updated in 1994, provide standardized assessment of gastritis histopathology.[4] The COVID-19 pandemic affected millions worldwide[5] and had physiological and emotional impacts, potentially influencing gastric pathology.[6] This study investigated whether there were changes in gastritis severity before and after the COVID-19 pandemic.[7,8]

MATERIAL AND METHODS

Our study is a retrospective observational study. Patients included in the study were those who presented to the General Surgery Department of Erzincan Binali Yıldırım University Mengücek Gazi Training and Research Hospital with complaints suggestive of gastric diseases in their anamnesis, and who were diagnosed with gastritis during upper gastrointestinal (GI) endoscopies performed by the General Surgery Department. The study included 107 patients from the pre-pandemic period up to March 2019 and 96 patients from the post-pandemic period up to May 2023 who underwent upper GI endoscopy due to dyspeptic complaints. Inclusion criteria for the study were patients who underwent endoscopy and biopsy and were diagnosed with gastritis histopathologically. The exclusion criterion was incomplete pathology data.

Biopsy results evaluated by the same pathologist were consistent with gastritis. Patients whose biopsy results differed from gastritis, particularly those indicating malignancy, were excluded from the study. Another criterion used in patient selection was timing. Patients who presented during the pandemic period were not included in the study. Based on the pandemic start date, patients who presented within the last year constitute the pre-pandemic group. Based on the pandemic end date, patients who presented within the last year constitute the post-pandemic group. Both groups were separately subjected to the Sydney Criteria. Developed by pathologists in 1990, the Sydney Criteria still retain their importance today. The criteria, updated in 1994, attempt to define the severity of gastritis by considering chronic inflammation, neutrophil activity, GA, IM, and Helicocacter pylori (H. Pylori) density in gastric biopsies. Accordingly, each parameter is expressed in four grades, numbered 0, 1, 2, and 3, representing increasing severity from 0 (no severity) to 3 (most severe), as determined by the pathologist. For this reason, another criterion applied in patient selection was that only patients whose biopsies were evaluated by the same pathologist were included in the study.

MAIN POINTS

- One of the most common stomach diseases is gastritis, and most studies in the literature related to the Coronavirus disease-2019 (COVID-19) pandemic focus on the pandemic period.
- This study was planned to investigate the post-pandemic effects.
- Our study observed that the COVID-19 pandemic did not affect the severity of gastritis according to the Sydney Criteria.

Ethical Approval

The study received ethical approval from the Non-Interventional Clinical Research Ethics Committee of Erzincan Binali Yıldırım University with decision number: 470098, dated 31.07.2025.

Statistical Analysis

Percentages were calculated for each Sydney criteria parameter. Group comparisons were performed using descriptive statistics.

The percentage method was used because it is easy and understandable. Patients in two main groups, pre-pandemic and post-pandemic, were classified.

And each group classified according to the Sydney criteria, with each parameter evaluated separately and gastritis severity increasing from 0 to 3. Percentage ratios were then calculated and compared.

RESULTS

Pre-pandemic group: 62 female, 45 male, mean age 58.6 years. Post-pandemic group: 50 females and 46 males (mean age 57.6 years). No significant demographic differences were noted.

The distribution of pre-COVID-19 gastritis patients, according to the Sydney criteria, is shown in Table 1.

Table 2 shows the distribution of patients with post-COVID-19 gastritis according to the Sydney criteria.

According to the Sydney criteria, in the Activation Criterion, 52.3% showed no cases before COVID-19, while the group with 3 positive cases (3.7%) was observed to be the least frequent group. Similarly, according to the Sydney criteria, in the post-COVID-19 period, 55.2% showed no cases, while the group with 3 positive cases (0%) was observed to be the least frequent group. Our study observed that the COVID-19 pandemic did not affect the Activation Criterion.

According to the Sydney criteria, in the Chronic Inflammation Criterion, in the pre-COVID-19 period, 49.5% showed the most cases in the group with 2 positive cases (53 patients), while the group with 0 positive cases (0.9%) was observed to be the least frequent group. According to the Sydney criteria for Chronic Inflammation, in the post-COVID-19 period, the highest percentage (39.6%) was found in the 2-positive group, while the 0-positive patient group had no patients, as in the pre-COVID-19 period. Our study observed that the COVID-19 pandemic did not affect the Chronic Inflammation Criterion.

According to the Sydney criteria for *H. pylori*, in the pre-COVID-19 period, the highest percentage (57.9%) was found in the 0-positive group, comprising 62 patients, while the 4-positive patient group had the lowest percentage (3.7%). According to the Sydney criteria for *H. pylori*, in the post-COVID-19 period, the highest percentage (70.8%) was found in the 0-positive group, comprising 68 patients, while the 5-positive patient group had the lowest percentage (5.2%). Our study observed that the COVID-19 pandemic did not affect the *H. pylori* Criterion.

Table 1. Distribution of Pre-COVID-19 Gastritis Patients According to the Sydney criteria (n=107)

Parameter	0	1	2	3	Total (%)
Activation	56 (52.3%)	35 (32.7%)	12 (11.2%)	4 (3.7%)	107 (100%)
Chronic inflammation	1 (0.9%)	33 (30.8%)	53 (49.5%)	20 (18.7%)	107 (100%)
H. pylori	62 (57.9%)	15 (14.0%)	26 (24.4%)	4 (3.7%)	107 (100%)
Metaplasia	86 (80.4%)	11 (10.3%)	8 (7.5%)	2 (1.9%)	107 (100%)
Atrophy	106 (99.1%)	0 (0.0%)	1 (0.9%)	0 (0.0%)	107 (100%)

H. pylori, Helicobacter pylori.

Table 2. Distribution of Post-COVID-19 Gastritis Patients According to the Sydney criteria (n=96)

Parameter	0	1	2	3	Total (%)
Activation	53 (55.2%)	33 (34.4%)	10 (10.4%)	0 (0.0%)	96 (100%)
Chronic inflammation	0 (0.0%)	28 (29.2%)	38 (39.6%)	30 (31.2%)	96 (100%)
H. pylori	68 (70.8%)	9 (9.4%)	14 (14.6%)	5 (5.2%)	96 (100%)
Metaplasia	76 (79.2%)	16 (16.7%)	4 (4.2%)	0 (0.0%)	96 (100%)
Atrophy	95 (99.0%)	1 (1.0%)	0 (0.0%)	0 (0.0%)	96 (100%)

H. pylori, Helicobacter pylori.

According to the Sydney criteria for metaplasia, in the pre-COVID-19 period, the highest percentage (80.3%) was found in the 0-positive group, comprising 62 patients, while the lowest percentage (2 patients) was observed in the 3-positive group.

According to the Sydney criteria for metaplasia, in the pre-COVID-19 period, the highest percentage (80.4%) was found in the 0-positive group, comprising 86 patients, while the lowest percentage (2 patients) was observed in the 3-positive group. According to the Sydney criteria for metaplasia, in the post-COVID-19 period, the highest percentage (79.2%) was found in the 0-positive group, comprising 76 patients, while no positive patients were observed in the 3-positive group.

Our study observed that the COVID-19 pandemic did not affect the metaplasia criterion.

According to the Sydney criteria, in the pre-COVID-19 period, the Atrophy Criterion was observed to be most prevalent in the 0-positive group (99%), with only 1 patient in the 2-positive group, and no patients in the 1-positive and 3-positive patient groups. Similarly, in the post-COVID-19 period, the Atrophy Criterion was observed to be most prevalent in the 0-positive group (99%), with only 1 patient in the 1-positive group, and no patients in the 2-positive and 3-positive patient groups. Our study observed that the COVID-19 pandemic did not affect the Atrophy Criterion.

DISCUSSION

The development of gastritis is multifactorial and includes diet, medications, infections, and emotional stress.[1-3] COVID-19 was suspected to affect the GI system.[8-10] Some studies reported that patients with GI symptoms had worse respiratory outcomes.[10,11] Others emphasized that COVID-19 may progress asymptomatically.[12,13]

It is noteworthy that a considerable portion of the existing literature was conducted exclusively during the pandemic period and, therefore, did not encompass both the pre- and post-pandemic intervals. In several of these studies, the most frequently reported GI symptoms were abdominal pain, nausea, and diarrhea.

In the present study, inclusion criteria were restricted to patients who underwent upper GI endoscopy specifically due to upper GI symptoms, from whom biopsy samples were obtained, and who subsequently received a histopathological diagnosis of gastritis. In this way, individuals who may have experienced the disease but had not yet received a formal diagnosis were inadvertently incorporated into the sample. The intention was to capture a broader population-level effect rather than an isolated individual impact. We consider that one potential explanation for the absence of significant differences between the pre-pandemic and post-pandemic groups according to the Sydney criteria may be the inclusion of such potentially undiagnosed individuals. Unlike previous studies.[8,9] our retrospective analysis comparing pre- and post-pandemic patients showed no significant changes in gastritis severity according to the Sydney criteria.[4]

Study Limitations

This study has several limitations. First, because the research was retrospective, data were obtained from archived endoscopy reports and pathology records. This carries the risk of incomplete documentation, measurement inconsistencies, and potential information bias. Although the Sydney classification was used to standardize gastritis assessment, interobserver variability could not be completely eliminated.

Second, due to restrictions applied during the COVID-19 pandemic, indications for endoscopy changed, with priority given to symptomatic or urgent cases. This may have caused selection bias within the sample and led to uncontrolled

differences in clinical characteristics between the pre-pandemic and post-pandemic groups.

Third, the study was conducted at a single center with a limited sample size. Therefore, the generalizability of the findings to other regions or diverse patient populations is restricted. Additionally, factors known to influence the severity of gastritis—such as *H. pylori* infection, non-steroidal anti-inflammatory drug use, proton pump inhibitor therapy, smoking, stress level, dietary habits, and comorbid conditions—could not be fully controlled.

Fourth, the pre-pandemic and post-pandemic periods were restricted to specific intervals. Thus, the dynamic and phase-dependent effects of the pandemic on gastritis could not be comprehensively evaluated. Furthermore, the relatively short observation period prevented the assessment of long-term morphological changes in the gastric mucosa.

Finally, due to the observational and retrospective design of the study, causal inferences regarding the impact of the COVID-19 pandemic on gastritis severity cannot be made. The results reflect associations and trends between the two periods rather than direct causality.

Future multicenter, prospective studies with larger sample sizes and more detailed control of lifestyle and infection-related variables will contribute to a clearer and more generalizable understanding of the pandemic's effect on gastritis.

CONCLUSION

According to the Sydney criteria, COVID-19 did not cause persistent changes in gastritis severity. Larger series are needed to confirm these findings.

Ethics

Ethics Committee Approval: Ethical approval obtained from Erzincan Binali Yıldırım University Non-Interventional Clinical Research Ethics Committee (decision no.: 470098, date: 31.07.2025.)

Informed Consent: Retrospective study. Permission was obtained from hospital management to collect study data from the Information Management System.

Footnotes

Author Contributions

Concept Design – O.Ç., F.K.Ç.; Data Collection or Processing – O.Ç., F.K.Ç.; Analysis or Interpretation – O.Ç., F.K.Ç.; Literature Review – O.Ç., F.K.Ç.; Writing, Reviewing and Editing – O.Ç., F.K.Ç.

Acknowledgements

The authors would like to thank Erzincan Binali Yıldırım University Faculty of Medicine for their institutional support and all colleagues who contributed to the endoscopy and pathology units during the study period.

Conflict of Interest: The authors declare that they have no conflict of interest related to this study.

Funding: No external funding was received for this study.

REFERENCES

1. Dixon MF, Genta RM, Yardley JH, Correa P. Classification and grading of gastritis. The updated Sydney system. International Workshop on the Histopathology of Gastritis, Houston 1994. *Am J Surg Pathol*. 1996;20(10):1161-1168. [CrossRef]
2. Price AB. The Sydney system: histological division. *J Gastroenterol Hepatol*. 1991;6(3):209-222. [CrossRef]
3. Sipponen P, Price AB. The Sydney system for classification of gastritis 20 years ago. *J Gastroenterol Hepatol*. 2011;26 Suppl 1:31-34. [CrossRef]
4. Stolte M, Meining A. The updated Sydney system: classification and grading of gastritis as the basis of diagnosis and treatment. *Can J Gastroenterol*. 2001;15(9):591-598. [CrossRef]
5. World Health Organization. Coronavirus disease (COVID-19) pandemic. Geneva: WHO; 2020. [CrossRef]
6. Cheung KS, Hung IFN, Chan PPY, et al. Gastrointestinal manifestations of SARS-CoV-2 infection and virus load in fecal samples from a Hong Kong Cohort: systematic review and meta-analysis. *Gastroenterology*. 2020;159(1):81-95. [CrossRef]
7. Yong SJ. Long COVID or post-COVID-19 syndrome: putative pathophysiology, risk factors, and treatments. *Infect Dis (Lond)*. 2021;53(10):737-754. [CrossRef]
8. D'Amico F, Baumgart DC, Danese S, Peyrin-Biroulet L. Diarrhea during COVID-19 infection: pathogenesis, epidemiology, prevention, and management. *Clin Gastroenterol Hepatol*. 2020;18(8):1663-1672. [CrossRef]
9. Pan L, Mu M, Yang P, et al. Clinical characteristics of COVID-19 patients with digestive symptoms in Hubei, China: a descriptive, cross-sectional, multicenter study. *Am J Gastroenterol*. 2020;115(5):766-773. [CrossRef]
10. Jin X, Lian JS, Hu JH, et al. Epidemiological, clinical and virological characteristics of 74 cases of coronavirus-infected disease 2019 (COVID-19) with gastrointestinal symptoms. *Gut*. 2020;69(6):1002-1009. [CrossRef]
11. Han C, Duan C, Zhang S, et al. Digestive symptoms in COVID-19 patients with mild disease severity: clinical presentation, stool viral RNA testing, and outcomes. *Am J Gastroenterol*. 2020;115(6):916-923. [CrossRef]
12. Oran DP, Topol EJ. Prevalence of asymptomatic SARS-CoV-2 infection: a narrative review. *Ann Intern Med*. 2020;173(5):362-367. [CrossRef]
13. Byambasuren O, Cardona M, Bell K, Clark J, McLaws ML, Glasziou P. Estimating the extent of asymptomatic COVID-19 and its potential for community transmission: systematic review and meta-analysis. *J Assoc Med Microbiol Infect Dis Can*. 2020;5(4):223-234. [CrossRef]

ABCResearch

Arch Basic Clin Res 2026;8(1):80-89
DOI: 10.4274/ABCR.2025.23207

Research Article

Classification of Potential Risk Factors for Maxillary Sinus Membrane Perforation Using Cone-Beam Computed Tomography

Nazan Koçak Topbaş[1], Esin Alpöz[2], Hayal Boyacıoğlu[3]

[1]Department of Oral and Maxillofacial Radiology, Mersin University Faculty of Dentistry, Mersin, Türkiye
[2]Department of Oral and Maxillofacial Radiology, Ege University Faculty of Dentistry, İzmir, Türkiye
[3]Department of Statistics, Ege University Faculty of Science, İzmir, Türkiye

Cite this article as: Koçak Topbaş N, Alpöz E, Boyacıoğlu H. Classification of potential risk factors for maxillary sinus membrane perforation using cone-beam computed tomography. *Arch Basic Clin Res*. 2026;8(1):80-89.

ORCID IDs of the authors: N.K.T. 0000-0002-3717-2098, E.A. 0000-0001-6654-9715, H.B. 0000-0003-0887-0302.

ABSTRACT

Objective: To determine the frequency of anatomic variations, pathologies, and physiological alterations in the maxillary sinus, and to identify the most common combinations in which these risk factors coexist and may predispose to perforation of the maxillary sinus membrane. The relationship between the most common potential risk factor and patients' age, gender, and dental status was also evaluated.

Methods: Radiographic examinations of the anatomic variations, pathologies, and physiological alterations in 500 maxillary sinuses from 376 patients were classified under 16 headings using cone beam computed tomography images, and their coexistence was evaluated. For each evaluated sinus, every pathology, physiological alteration, and anatomic variation observed was recorded. A Mann-Whitney U test was conducted to assess the effect of age, sex, and dental status on the most common potential risk factor.

Results: The average mucosal thickening was 3.64 mm. Pathological mucosal thickenning was the most common pathology in the maxillary sinus (67.2%). The rates of mucosal thickening, septa-mucosal thickening, interruption of the medial sinus wall, and pneumatization-septa-mucosal thickening were 30.8%, 29.2%, 7.6%, 6.2%, respectively. Pathological mucosal thickenning was the most common in partially edentulous, males, aged 36-53 years ($P < 0.05$).

Conclusion: The most common anatomic variations, physiological alterations, and pathologies in the maxillary sinus were pathological mucosal thickening, septa, interruption of the medial sinus wall, and pneumatization. The most coexisting combinations were mucosal thickening-septa and pneumatization-septa-mucosal thickening. In addition to these combinations, partially edentulous patients of 36-53 age group may be considered as sinus membrane perforation risk.

Keywords: Anatomy, cone-beam computed tomography, maxillary sinus, membrane perforation, sinus floor augmentation

INTRODUCTION

The maxillary sinus epithelium is ciliated and captures foreign materials, carrying them to the ostium via spiral movements. The drainage ostium of the maxillary sinus is located in the anterior one-third of the ethmoid infundibulum, between the processus uncinatus and the lamina papyracea. When pathology is present, ciliary wave motion is disrupted, and foreign substances cannot be expelled from the ostium. For mucociliary drainage to function normally, ostia and mucociliary transport pathways must remain patent.[1]

Implant placement in the posterior atrophic maxilla can be a challenging surgical procedure because of insufficient bone height due to maxillary sinus expansion. Maxillary sinus floor elevation procedures are often necessary for implant treatment planning in the presence of insufficient bone height.[2] During these procedures, two distinct complications may arise from

Corresponding author: Nazan Koçak, **E-mail:** nazannkocak@gmail.com

Received: September 29, 2025
Revision Requested: October 3, 2025
Last Revision Received: May 9, 2024
Accepted: October 15, 2025
Publication Date: January 26, 2026

anatomical variations, physiological alterations, or pathologies. The most common of these is maxillary sinus membrane perforation, which occurs in 20-60% of cases; the second most common is bleeding.[3] Generally, inadequate surgical planning or maneuvers are the major cause of membrane perforation.[4] Although maxillary sinus floor elevation procedures cause these complications, the high survival rates of implants placed in grafted sinuses make this method advantageous.[5] Therefore, a thorough knowledge of the anatomy, physiology and possible variations of the maxillary sinus to minimize the risk of potential complications associated with the surgical procedure is important to improve success of the procedures.[6]

Numerous studies have investigated risk factors for maxillary sinus pathologies and sinus membrane perforation. It has been reported that the membrane perforation rate is inversely proportional to maxillary sinus mucosal thickness. In addition, the cortical thickness of the lower border of the maxillary sinus has been inversely associated with membrane perforation. Odontogenic and periodontal infections affect the cortical border. The principal factors related to the maxillary sinus are the presence and height of septa, residual ridge height, thickness of the lateral sinus wall, antrum width, and the extent and condition of mucosal thickening.[7-9] The parameters determined in this study such as pneumatization, septa, exostosis, pathological mucosal thickening, polypoid lesion, interruption of the sinus floor, interruption of the medial sinus, lateral wall bone thickening, antroliths, fluid retention, foreign bodies, interruption of the lateral sinus wall, ectopic tooth in the sinus, root in the sinus may directly or indirectly cause perforation of the sinus membrane or spread of existing infection during or after sinus surgery.

However, no study has evaluated the distribution of multiple pathologies, variations, and physiological alterations in the sinus in relation to their coexistence. Also to our knowledge relationship between the most common potential risk factor and patients's age, gender, and dental status has not been evaluated yet. The hypothesis of our study was that the risk of sinus membrane perforation would increase as the prevalence of coexisting anatomic variations, physiological alterations, and pathologies in a single sinus increased. Morover the importance of maxillofacial surgeons' and radiologists' knowledge on the most common potential risk factor and subsequent coexistence combinations is emphasized.

MAIN POINTS

- Pathological mucosal thickening alone was a strong risk factor for maxillary sinus membrane perforation.
- The presence of multiple coexisting risk factors may further increase the likelihood of maxillary sinus membrane perforation.
- Cone beam computed tomography examination is essential for major surgical procedures.

MATERIAL AND METHODS

Study Samples

This retrospective study included cone-beam computed tomography (CBCT) images of the maxillary posterior regions of 2,500 patients, retrieved from the archives of the Faculty of Dentistry of Ege University, for whom data on sex, age, and indications for scanning were available. The Clinical Research Ethics Committee of the Medical Faculty of Ege University approved this study (approval no: 14-7.1/6, date: 08.09.2014), and informed consent was obtained from all participants. Images with artefacts (e.g., beam hardening, noise, metal artefacts, and ring artefacts), images of individuals younger than 18 years (because the maxillary sinus continues to develop until age 18)[10], images with prosthetic restorations on the teeth, and unclear, low-quality, or incomplete images were excluded. A total of 500 images were included in the study.

To evaluate the age distribution of maxillary sinus pathologies, anatomic variations, and physiological alterations, patients were divided into four age groups: 18-35, 36-53, 54-71, and ≥ 72 years. The patients were further subdivided into three groups according to their dental status: dentate, partially edentulous, and totally edentulous.

CBCT Image Analysis

The CBCT images of all the patients were obtained using a Kodak 9000 3D device (Carestream Health, Rochester, NY, USA), with total filtration > 2.5 mm Al, a 5 × 3.7 cm field of view (FOV), a 76 µm isotropic voxel size, and 14-bit contrast resolution. The CBCT images were taken at 70 kVp (maximum of 10 mA) by positioning the patient perpendicular to the sagittal plane and parallel to the Frankfort horizontal plane. All CBCT images were retrospectively evaluated by a dentomaxillofacial radiologist with 5 years' experience, using Care stream 3D Imaging Software 3.1.9 (Carestream Health, Inc., Rochester, NY, USA). The anatomic variations, physiological alterations and maxillary sinus pathologies were evaluated on the axial, sagittal, and coronal sections of all the CBCT images, and the amounts of mucosal thickening were measured on the sagittal and coronal sections. Measurements were made along a straight line from the deepest point of curvature of the maxillary sinus floor to the point of greatest mucosal thickening (Figures 1 and 2). Measurements of this parameter were made separately in the right and left maxillary sinuses. All data were recorded and correlations between this variable were evaluated. To ensure consistency, the first author selected all images and measured maxillary sinus mucosal thickening. Fifty percent of these images (250 images) were randomly selected, re-marked, and re-measured. Coefficient of variation (CV) analysis was performed to determine the accuracy and reproducibility of the measurements. For this purpose, the first author re-measured the images two weeks after the initial measurements, and the first and second measurements were analyzed for 250 randomly selected dental CT images.

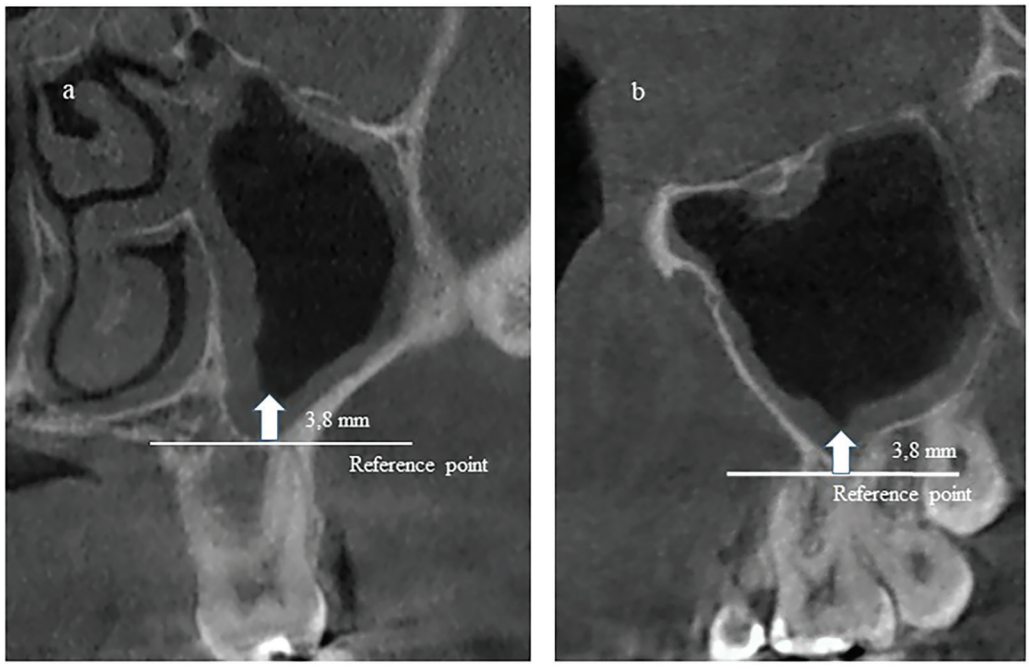

Figure 1. Detailed radiographic demonstration of mucosal thickening measurements. a) Coronal sections b) Sagittal sections.

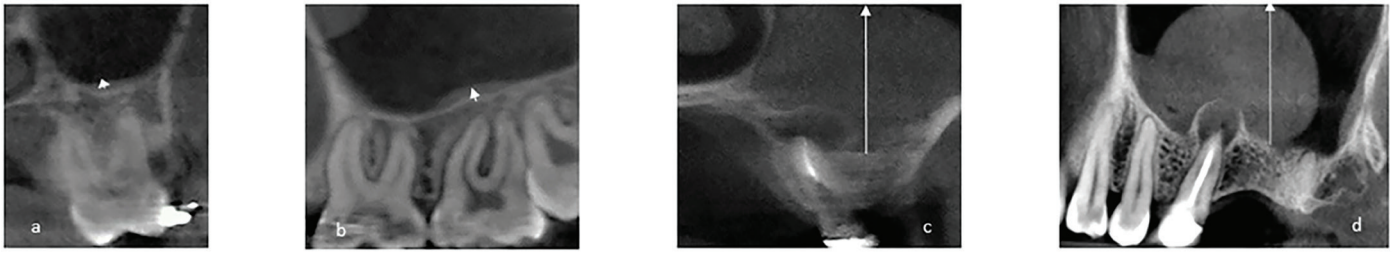

Figure 2. Radiographic demonstration of mucosal thickening measurements. a) Normal mucosal thickenning coronal sections, b) normal mucosal thickenning sagittal sections, c) pathologic mucosal thickenning coronal sections, d) pathologic mucosal thickenning coronal sections.

Study Variables

Assessment of Maxillary Sinus Anatomic Variations, Physiological Alterations and Pathologies

Anatomic variations identified were septa, exostoses, and lateral wall bone thickening. Physiological alterations were categorized as pneumatization and normal mucosal thickening. Pathologies identified included pathological mucosal thickening; polypoid lesions; interruption of the sinus floor and of the medial and lateral sinus walls; antroliths; fluid retention; foreign bodies; ectopic tooth in the sinus; and tooth root in the sinus.

The pathologies, physiological alterations, and anatomic variations in the maxillary sinus found on the coronal, sagittal, and axial sections of the CBCT images were classified as follows: 1) pneumatization (a), 2) septa (b), 3) exostoses (c), and 4) mucosal thickening > 0 mm; the presence of mucosal thickening greater than 0 mm was evaluated as a physiological alteration and a pathology. The presence or absence of mucosal thickening was evaluated.), normal mucosal thickenning (d) 5) pathological mucosal thickenning (e), 6) polypoid lesion (f) 7) interruption of the sinus floor (g), 8) interruption of the medial sinus wall (h-ı), 9) lateral wall bone thickening (i), 10) antroliths (j), 11) fluid retention (k), 12) foreign bodies (greft.etc) (l),13) interruption of the lateral sinus wall (m), 14) ectopic tooth in the sinus (n), 15) root in the sinus (o), (Figure 3). Since the presence of multiple pathologies, physiological alterations, and variations was thought to increase the risk of surgical complications, every pathology, physiological alteration, and variation observed in the sinus was recorded. Thus, only the presence or absence of the specified parameters was evaluated, and measurements were limited to pathological and normal mucosal thickening.

Evaluation of the Images

Measurements of Mucosal Thickenning

Maximum mucosal thickness was measured as the greatest distance from the sinus floor on the coronal and sagittal sections, and values greater than 0 mm were defined as mucosal thickening. Figures 2a, 2b, and 3d show the normal mucosal thickening measurements of the patients. In the

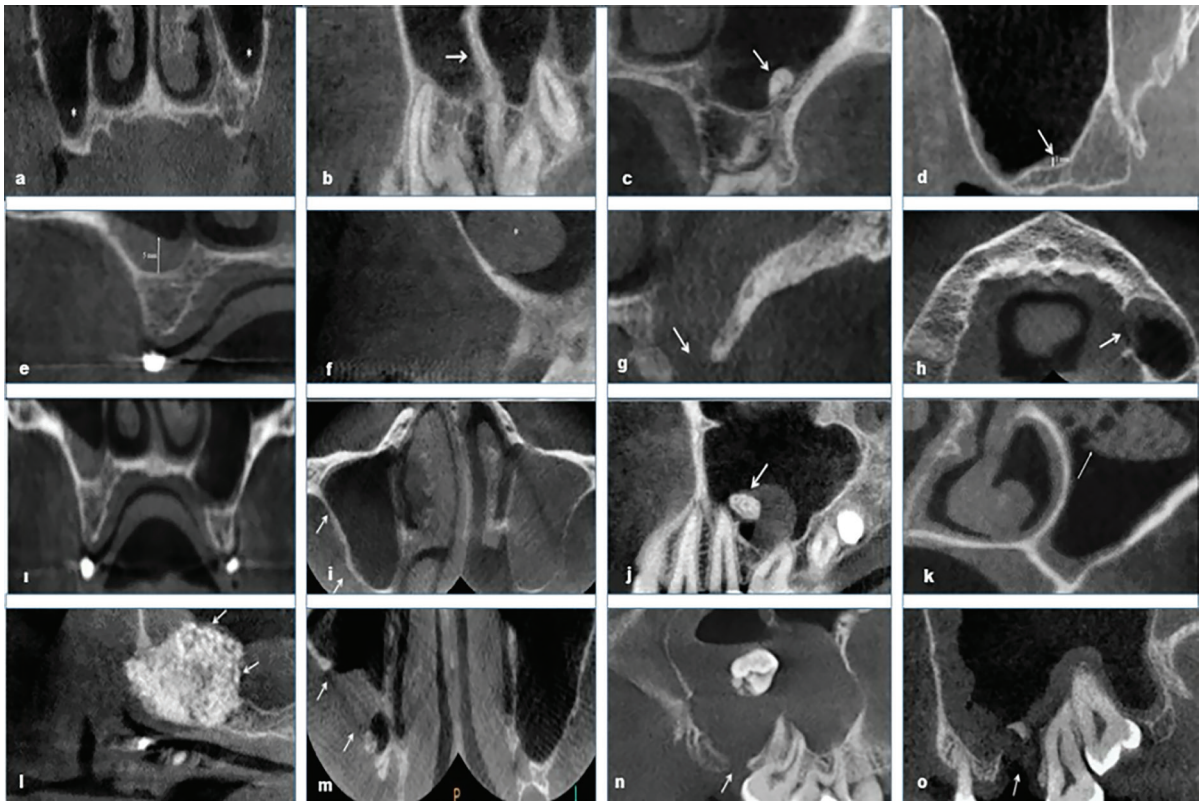

Figure 3. Radiographic demonstration of identified anatomical variations in the maxillary sinuses. a) Pneumatization, b) septa, c) exostoses, d) normal mucosal thickenning, e) pathological mucosal thickenning, f) polypoid lesion, g) interruption of the floor, h-ı) interruption of the medial wall, i) lateral bone wall thickening, j) antrolith, k) fluid retention, l) foreign body, m) interruption of the lateral wall, n) ectopic tooth, o) root.

current study, mucosal thickening of more than 2 mm was considered pathological (Figures 1a, 1b, 2c, 2d, 3e). Thus, the range of 0-2 mm represents physiological variation in mucosal thickness. Also, when a point in mucosal thickenning was measured more than 2 mm, it was evaluated as pathological mucosal thickenning.[7,11-12]

Types of Mucosal Thickenning

In all the patients, the types of mucosal thickenning were determined on the sagittal sections of CBCT images according to the classification criteria of Kocak et al.[13]: 1) normal (less than < 2 mm), 2) flat (flat, limited), 3) semipheric (polypoid), 4) mucocele-like (filling the sinus) or 5) mixed (both flat and polypoid). All types of mucosal thickening ≥ 2 mm were defined as pathological mucosal thickening.[11,12]

Mucosal Thickenning-Related Factors

Among the patients evaluated, mucosal-thickening-related factors were determined on sagittal CBCT sections according to Maillet et al.'s[14] classification criteria: 0) total edentulism; 1) stable, healthy mucosal thickening < 2 mm; 2) odontogenic sinusitis (i.e., mucosal thickening or polypoid pathology limited to a tooth); 3) non-odontogenic sinusitis (i.e., sinusitis occurring in the absence of an odontogenic origin; mucosal thickening not restricted to any one tooth); and 4) unknown origin (i.e., sinusitis for which the origin cannot be determined when more than one odontogenic factor is present; mucosal thickening not limited to any one tooth in the presence of a tooth with a defective restoration, a periapical lesion, any carious tooth, or a disrupted socket). Because mucosal thickening was evaluated with respect to odontogenic factors, totally edentulous patients were excluded from this analysis. Therefore, mucosal thickening in edentulous patients was evaluated to distinguish pathological from normal mucosal thickening.

Statistical Analysis

Descriptive statistics were used to summarize the distribution of maxillary sinus pathologies and anatomical variations. The Mann-Whitney U test was performed to evaluate the effects of age, sex, and dental status on the most common potential risk factor. A value of $P < 0.05$ was considered significant.

RESULTS

Demographic Data

Of the 2,500 CBCT images of the maxillary posterior region, 500 maxillary sinus images from 376 patients met the inclusion criterion. In the population analyzed, of the 376 patients, 177 were women (47%) and 199 were men (53%) with a mean age of 45.24 years (range: 18 to 90 years). Figure 4 presents the CBCT scanning indications among the 500 maxillary sinus cases: 256 (51.2%) sinuses in males and 244 (48.8%) sinuses in females.

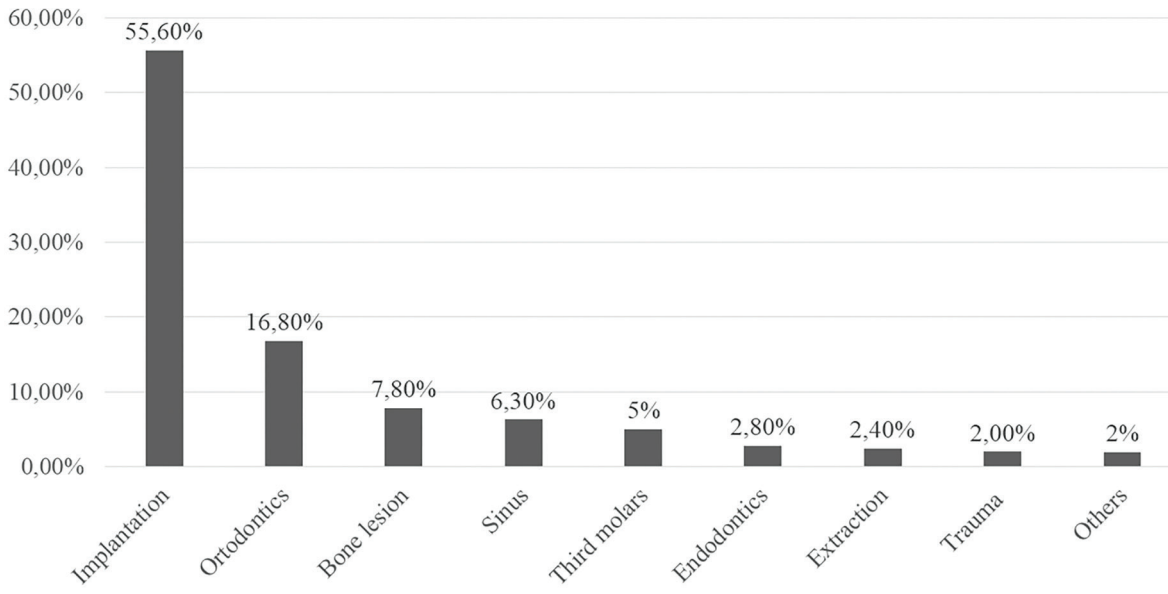

Figure 4. Distributions of the CBCT indications of the participants.

CBCT, cone-beam computed tomography.

The age distribution of the participants was as follows: 18-35 years (34.2%), 36-53 years (30.6%), 54-71 years (33.0%), and ≥ 72 years (2.2%). In the patient population, 45.6%, 33.6%, and 20.8% of cases were partially edentulous, dentate, and totally edentulous, respectively.

Study Variables

Assessment of Maxillary Sinus Anatomic Variations, Physiological Alterations and Pathologies

Interruption of the sinus floor, fluid retention, and both bony thickening and interruption of the lateral wall were conditions observed in association with other pathologies.

The most common potential risk factor was pathological mucosal thickening, with a rate of 67.2%. Then, frequently observed maxillary sinus pathologies, physiological alterations and anatomic variations were found as, mucosal thickenning (30.8%); septa and mucosal thickenning (29.2%); interruption of the medial sinus wall (7.6%); pneumatization, septa and mucosal thickenning (6.2%); sinus opacifying lesions (4.4%); and septa (3%) (Table 1). The CV for measurements of maxillary sinus mucosal thickening was found to be 0.91%.

Evaluation of the Images

Types of Mucosal Thickenning

The most common mucosal thickening type was flat (34.8%), followed by normal (32.8%), semipheric (11.6%), mixed (11.4%), and mucocele-like (9.4%) (Figure 5). The average mucosal thickenning was 3.64 mm.

Table 1. Pathologies and AVs With Distributions Above 1% in MS

AVs and pathological formations	Distribution %
No pathology and/or variation	3.6%
Septa	3%
Mucosal thickening	30.8%
Sinus opacifying lesion (retention cyst, polyp, etc.)	4.4%
Interruptionof the medial sinus wall	7.6%
Mucosal thickening and septa	29.2%
Septa and sinus opacifying lesion	1.8%
Pneumatization, septa, and mucosal thickening	6.2%
Septa, mucosal thickening, and antrolith	1%
Septa, mucosal thickening, and interruption of the medial sinus wall	1%

AVs, anatomic variations; MS, maxillary sinus

Mucosal Thickenning-Related Factors

The percentages of normal mucosal thickening (< 2 mm), non-odontogenic sinusitis, mucosal thickening of unknown origin, and odontogenic sinusitis were 29%, 19.4%, 18.6%, and 12%, respectively; 21% of the total edentulism cases were excluded from mucosal thickening-related factors. Pathological mucosal thickening was most common in partially edentulous individuals ($P = 0.001$), in males ($P = 0.005$), and in those aged 36-53 years ($P = 0.05$) (Table 2).

Table 2. Distributions of Normal and Pathological MT According to Age, Sex and Dental Status

		Normal MT	PMT	Total
Age	18-35	74 14.8%	97 19.4% *P* > 0.05	171 34.2%
	36-53	33 6.6%	120 24% *P* = 0.05	153 30.6%
	54-71	50 10%	115 23% *P* > 0.05	165 33%
	72-90	7 1.4%	4 0.8% *P* > 0.05	11 2.2%
Sex	Female	95 19%	149 29.8% *P* > 0.05	243 48.7%
	Male	69 13.8%	187 37.4% *P* = 0.005	257 51.3%
Dental Status	Dentate	73 14.6%	95 19% *P* > 0.05	168 33.6%
	Partially edentulous	64 12.8%	164 32.8% *P* = 0.001	228 45.6%
	Total edentulous	27 5.4%	77 15.4% *P* > 0.05	104 20.8%

MT, mucosal thickening; PMT, pathological mucosal thickening.

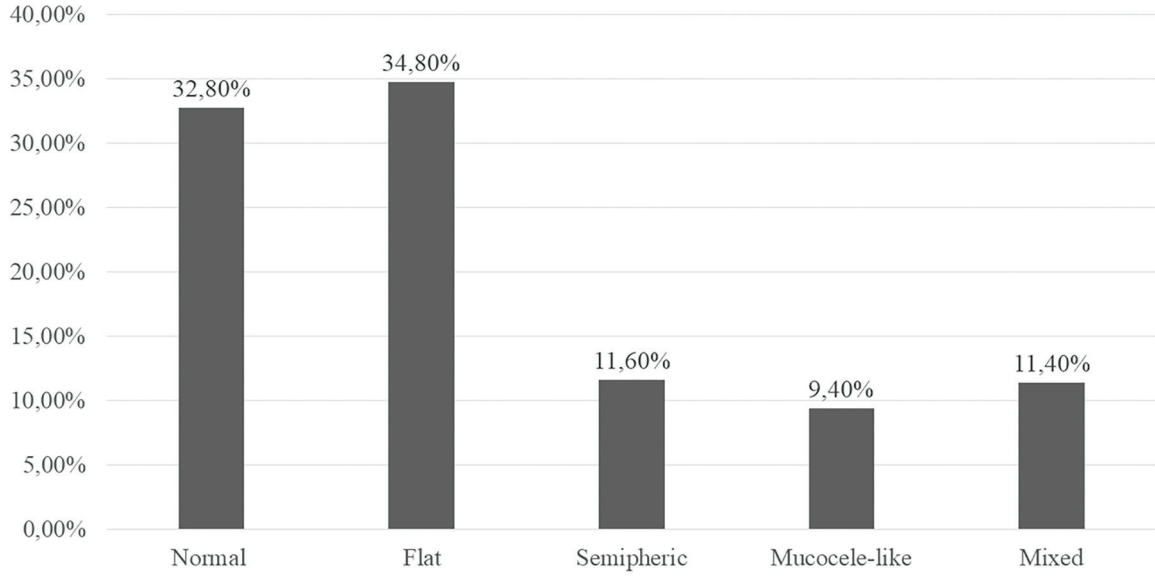

Figure 5. Distribution of the types of mucosal thickening in the maxillary sinuses of participants.

DISCUSSION

In the current study, the most frequently encountered maxillary sinus pathologies, physiological alterations, and anatomic variations are: pathological mucosal thickening, followed by mucosal thickening, septa, interruption of the medial sinus wall, pneumatization, and sinus opacifying lesions. When the maxillary sinus pathologies, physiological alterations and anatomic variations are analysed with respect to their coexistence; mucosal thickening and septa binary combination; interruption of medial wall and a combination of mucosal thickenning, septa and pneumatization was found to be most frequent respectively. Vogiatzi et al.[15] concluded that the most common maxillary sinus pathologies and anatomic variations were mucosal thickenning, septa and pneumatization in their systematic review. However Ata-Ali et al.[16] determined that, the most common pathologies and anatomic variations were mucosal thickening, sinusitis and sinus opacification in their systematic review.

The present study differs from that of previous studies due to the use of CBCT with a limited FOV, the use of different classification criteria based on the coexistence of anatomic variations and maxillary sinus pathologies, and the inclusion of a general population without specific indications (e.g. orthodontic, implant surgery or trauma patients).[17,18]

In the current study, the rate of pathological mucosal thickening was 67.2%, which is consistent with the result reported by Lana et al.[19] Differences in age groups, target populations, sample sizes, and classification probably explain the variation in reported incidence rates of pathological mucosal thickening in the literature (12%-67.2%).[7,17,19,20-23] In our study, the most up-to-date, commonly accepted classification system, pathological mucosal thickening > 2 mm, was used.[7,11,12,14,20,23]

Previous studies that evaluated the maxillary sinus reported mean mucosal thickening values ranging from 2.69 to 3.38 mm.[3,24] The average mucosal thickening was 3.64 mm (maximum: 6.24 mm, minimum: 1.04 mm) in our study. Investigators reported that mucosal thickenning may vary according to age and sex with increased mucosal thickenning found among those older than 40 years, with a male preponderance.[17,21] In the current study, pathological mucosal thickening was significantly higher in men (P = 0.005) and in participants aged 36-53 years (P = 0.05) than in females and other age groups, which is consistent with the literature.[17,21] The preponderance of pathological mucosal thickening in men may be explained by poorer oral hygiene and higher smoking rates compared with women.

A previous study demonstrated that the presence of chronic bacterial inflammation can lead to mucosal thickening of the maxillary sinus.[23] Although some studies have evaluated the relationship between periodontal bone loss and mucosal thickening[23,24], none have examined the relationship between dental status and mucosal thickening. In the current study, pathological mucosal thickening was most common among partially edentulous patients (P = 0.001), demonstrating a correlation between dentition and mucosal thickening.

The maxillary sinus is at risk of bacterial, fungal, viral, or odontogenic infections because of its anatomic position. Untreated odontogenic inflammation may cause sinusitis by extending into the maxillary sinus.[20] Therefore, imaging of the maxillary sinus is important for preventing inflammation-related complications, as well as for diagnosis and treatment planning.[3] A previous study reported that implant therapy and tooth extraction were potential causes of mucosal thickening.[25] Studies on the effects of mucosal thickenning emphasized that mucosal thickenning caused by dental factors contributed to the development of odontogenic sinusitis and that mucosal thickenning was associated with periodontal destruction.[14,23,24] Radiological images alone are not sufficient to confirm maxillary sinus pathology and anatomic variations, and clinical and radiological findings should be evaluated together, especially in the sinusitis diagnosis.[7]

CBCT is considered as an radiologic gold standard for implant planning, prior to implant procedures to determine the coexistence of maxillary sinus pathologies and anatomic variations and to prevent potential complications.[26] In the current study, implant planning (55.6%) was the primary reason for CBCT scanning, similar to the findings of Rege et al.[21]. Various imaging methods, including panoramic radiography, combined with CT and magnetic resonance imaging have been used to evaluate maxillary sinus pathologies.[17,18,27] Studies comparing the effectiveness of various radiographic methods for evaluating anatomic variations and pathologies of the maxillary sinus found that CBCT was the superior method.[17] In a previous study comparing panoramic radiography with CBCT, panoramic radiography failed to detect mucosal thickening < 3 mm.[18] CBCT allows detection of anatomic and pathological structures because it provides high spatial resolution and employs isotropic voxels.[2,17] Decreasing FOV and voxel size, the sensitivity and accuracy of CBCT images increases. Therefore, a smaller FOV provides higher diagnostic accuracy.[28]

Sayar and Aydın[29] conducted their study on a smaller sample comprising approximately 230 sinuses and used a CBCT device with an imaging field of 23 × 17 cm. Contrary to the findings of our study, they reported septal deviation as the most common pathology (13.9%), whereas mucosal thickening was the least common (2.6%). In contrast, Yalcin and Akyol[30] evaluated 650 maxillary sinuses in 2019 using CBCT devices with FOV of 16 × 5 cm, 16 × 9 cm, and 16 × 16 cm and identified mucosal thickening as the most prevalent pathology (53.5%). Similarly, Dogan et al.[31], in a 2024 study analyzing 1.000 maxillary sinuses with a 13 × 16-mm FOV, found a 45.8% prevalence of pathological mucosal thickening. Kawai et al.[32] reported incidental radiodensities in 56.3% of 338 maxillary sinuses examined in 2019 using FOVs of 20 × 10 mm and 20 × 17 mm. In our study, pathological mucosal thickening was observed in 67.2% of cases when a CBCT device with a significantly smaller FOV of 5 × 3.7 cm was used. The variation in findings across these studies may be attributed to differences in pathology-defining criteria, methodological approaches, and, particularly, the size of the FOV used during imaging.

Bone volume/height in the posterior maxilla is affected by a number of different factors; many factors such as age, gender, race, sinus pneumatization, trauma history and extraction of adjacent teeth, periodontitis, osteoporosis, edentulous period, multiple tooth extraction are the causes of atrophic alveolar ridge.[12,33] Risk assessment for maxillary sinus perforation includes factors such as sinus membrane thickness, septal presence and orientation, residual bone height, smoking status, sinusitis, and gingival biotype.[34,35]

Maxillary sinus membrane perforation is the most common complication encountered during lateral maxillary sinus floor elevation procedures and is associated with multiple factors. Prospective clinical studies reported in the literature identify age, presence of edentulous areas, lateral wall thickness, residual bone height, membrane thickness, smoking, presence of septa, and presence of mucous retention cysts as the most commonly reported factors associated with increased risk. Strategies to reduce risk in implant surgery vary depending on the physician's knowledge and skills, the technique applied, the surgical instruments and devices used, and treatment planning. Schneiderian membrane perforation, which is closely related to the anatomical variations of the maxillary sinus, can occur when local stress exceeds the membrane's stretch potential. The choice of surgical approach and the clinical outcomes are affected by the tensile properties of the Schneiderian membrane. In addition to residual bone height, clinicians should consider the stress potential, which is affected by membrane health status, maxillary sinus contours, and the presence of antral septa, when evaluating the choice of surgical approach and clinical outcomes.[36]

The risk of sinus pathologies can be reduced through therapeutic interventions by ear, nose, and throat specialists. A thick Schneiderian membrane is required for a safe sinus-lift procedure; pathology weakens the membrane, making it vulnerable to perforation.[34-39] Although not all of these criteria were included in our study, they were included as predictive factors. The limitations of our study include the small FOV of our CBCT device, its archival design, and the inability to evaluate multiple factors simultaneously. In addition to age, gender, and dental status, factors such as smoking, systemic disease status, and previous sinus surgery should also be included in the sample.

The study design is retrospective, and archival radiographic records were analyzed to derive conclusions and insights.[40] Prospective studies may be considered to confirm the findings and further investigate potential risk factors.[41] Using our study methodology as the basis for clinical prospective studies of membrane-perforation risk, and observing changes in maxillary sinus mucosa thickness and sinusitis risk over time, will provide a more comprehensive understanding of the study.

CONCLUSION

In this study, potential risk factors were identified as pathological mucosal thickening (67.2%), mucosal thickening (30.8%), septa-mucosal thickening (29.2%), non-odontogenic sinusitis (19.4%), mucosal thickening of unknown origin (18.6%), odontogenic sinusitis (12%), interruption of the medial sinus wall (7.6%), pneumatisation–septa–mucosal thickening (6.2). Particular attention should be paid to the presence of these factors. Membrane perforation, which is closely associated with anatomical variations of the maxillary sinus, can occur when local tension exceeds the membrane's stretch potential. In this regard, the presence of more than one pathology during sinus lift procedures may further increase the risk of local, tension-related perforations and susceptibility to infection. Patient-specific factors should be carefully evaluated before surgical procedures, and detailed imaging should be performed using CBCT to minimize potential complications.

Ethics

Ethics Committee Approval: This study was approved by the Clinical Research Ethics Committee of the Medical Faculty of Ege University (approval no.: 14-7.1/6, date: 08.09.2014).

Informed Consent: Informed consent was obtained from all individual participants included in the study.

Acknowledgments

We sincerely thank patients of Ege University, Faculty of Dentistry, who voluntarily participated in our study.

Footnotes

Author Contributions

Concept Design – E.A.; Data Collection or Processing – N.K.T., E.A.; Analysis or Interpretation – H.B.; Literature Review - N.K.T.; Writing, Reviewing and Editing – N.K.T.

Declaration of Interests: The authors declared no conflicts of interest.

Funding: The authors declare no financial support or funding.

REFERENCES

1. Whyte A, Boeddinghaus R. The maxillary sinus: physiology, development and imaging anatomy. *Dentomaxillofac Radiol.* 2019;48(8):20190205. [CrossRef]
2. Bornstein MM, Seiffert C, Maestre-Ferrín L, et al. An analysis of frequency, morphology, and locations of maxillary sinus septa using cone beam computed tomography. *Int J Oral Maxillofac Implants.* 2016;31(2):280-287. [CrossRef]
3. Danesh-Sani SA, Loomer PM, Wallace SS. A comprehensive clinical review of maxillary sinus floor elevation: anatomy, techniques, biomaterials and complications. *Br J Oral Maxillofac Surg.* 2016;54(7):724-730. [CrossRef]
4. von Arx T, Fodich I, Bornstein MM, Jensen SS. Perforation of the sinus membrane during sinus floor elevation: a retrospective study of frequency and possible risk factors. *Int J Oral Maxillofac Implants.* 2014;29(3):718-726. [CrossRef]
5. Pjetursson BE, Tan WC, Zwahlen M, Lang NP. A systematic review of the success of sinus floor elevation and survival of implants inserted in combination with sinus floor elevation. *J Clin Periodontol.* 2008;35(8 Suppl):216-240. [CrossRef]

6. Schriber M, von Arx T, Sendi P, Jacobs R, Suter VG, Bornstein MM. evaluating maxillary sinus septa using cone beam computed tomography: is there a difference in frequency and type between the dentate and edentulous posterior maxilla? *Int J Oral Maxillofac Implants*. 2017;32(6):1324-1332. [CrossRef]
7. Tassoker M. What are the risk factors for maxillary sinus pathologies? A CBCT study. *Oral Radiol*. 2020;36(1):80-84. [CrossRef]
8. Al-Dajani M. Incidence, Risk factors, and complications of schneiderian membrane perforation in sinus lift surgery: a meta-analysis. *Implant Dent*. 2016;25(3):409-415. [CrossRef]
9. Kocak N, Alpoz E, Boyacıoglu H. Morphological assessment of maxillary sinus septa variations with cone-beam computed tomography in a Turkish population. *Eur J Dent*. 2019;13(1):42-46. [CrossRef]
10. Lorkiewicz-Muszyńska D, Kociemba W, Rewekant A, et al. Development of the maxillary sinus from birth to age 18. Postnatal growth pattern. *Int J Pediatr Otorhinolaryngol*. 2015;79(9):1393-400. [CrossRef]
11. Amid R, Kadkhodazadeh M, Moscowchi A, Nami M. Effect of schneiderian membrane thickening on the maxillary sinus augmentation and implantation outcomes: a systematic review. *J Maxillofac Oral Surg*. 2021;20(4):534-544. [CrossRef]
12. Kim JH, Min EJ, Ko Y, Kim DH, Park JB. Change in maxillary sinus mucosal thickness in patients with preoperative maxillary sinus mucosal thickening as assessed by otolaryngologists: a retrospective study. *Medicina (Kaunas)*. 2023;59(10):1750. [CrossRef]
13. Kocak N, Alpoz E, Boyacioglu H. Evaluation of the effect of apical lesion on mucosal thickening and thickness of apical bone using limited cone-beam computed tomography. *Niger J Clin Pract*. 2018;21(8):954-959. [CrossRef]
14. Maillet M, Bowles WR, McClanahan SL, John MT, Ahmad M. Cone-beam computed tomography evaluation of maxillary sinusitis. *J Endod*. 2011;37(6):753-757. [CrossRef]
15. Vogiatzi T, Kloukos D, Scarfe WC, Bornstein MM. Incidence of anatomical variations and disease of the maxillary sinuses as identified by cone beam computed tomography: a systematic review. *Int J Oral Maxillofac Implants*. 2014;29(6):1301-1314. [CrossRef]
16. Ata-Ali J, Diago-Vilalta JV, Melo M, et al. What is the frequency of anatomical variations and pathological findings in maxillary sinuses among patients subjected to maxillofacial cone beam computed tomography? A systematic review. *Med Oral Patol Oral Cir Bucal*. 2017;22(4):e400-e409. [CrossRef]
17. Ritter L, Lutz J, Neugebauer J, et al. Prevalence of pathologic findings in the maxillary sinus in cone-beam computerized tomography. *Oral Surg Oral Med Oral Pathol Oral Radiol Endod*. 2011;111(5):634-640. [CrossRef]
18. Shiki K, Tanaka T, Kito S, et al. The significance of cone beam computed tomography for the visualization of anatomical variations and lesions in the maxillary sinus for patients hoping to have dental implant-supported maxillary restorations in a private dental office in Japan. *Head Face Med*. 2014;10:20. [CrossRef]
19. Lana JP, Carneiro PM, Machado Vde C, de Souza PE, Manzi FR, Horta MC. Anatomic variations and lesions of the maxillary sinus detected in cone beam computed tomography for dental implants. *Clin Oral Implants Res*. 2012;23(12):1398-1403. [CrossRef]
20. Shanbhag S, Karnik P, Shirke P, Shanbhag V. Association between periapical lesions and maxillary sinus mucosal thickening: a retrospective cone-beam computed tomographic study. *J Endod*. 2013;39(7):853-857. [CrossRef]
21. Rege IC, Sousa TO, Leles CR, Mendonça EF. Occurrence of maxillary sinus abnormalities detected by cone beam CT in asymptomatic patients. *BMC Oral Health*. 2012;12:30. [CrossRef]
22. Cağlayan F, Tozoğlu U. Incidental findings in the maxillofacial region detected by cone beam CT. *Diagn Interv Radiol*. 2012;18(2):159-163. [CrossRef]
23. Lu Y, Liu Z, Zhang L, et al. Associations between maxillary sinus mucosal thickening and apical periodontitis using cone-beam computed tomography scanning: a retrospective study. *J Endod*. 2012;38(8):1069-1074. [CrossRef]
24. Goller-Bulut D, Sekerci AE, Köse E, Sisman Y. Cone beam computed tomographic analysis of maxillary premolars and molars to detect the relationship between periapical and marginal bone loss and mucosal thickness of maxillary sinus. *Med Oral Patol Oral Cir Bucal*. 2015;20(5):e572-e579. [CrossRef]
25. Cao Z, Yuan J. Changes in maxillary sinus mucosal thickening following the extraction of teeth with advanced periodontal disease: a retrospective study using cone-beam computed tomography. *Biomed Res Int*. 2021;2021:6688634. [CrossRef]
26. Shankar MS, Pal B, Rai N, Patil DP. CBCT as an emerging gold standart for presurgical planning in implant restorations. *J Indian Acad Oral Med Radiol*. 2013;25(1):66-70. [CrossRef]
27. Dong Y, Zhou B, Wang CS, Huang Q, Cui SJ, Li YC, Wang XY. [CT and MRI diagnosis of lesions in unilateral maxillary sinus]. *Zhonghua Er Bi Yan Hou Tou Jing Wai Ke Za Zhi*. 2013;48(11):895-900. [CrossRef]
28. Salemi F, Shokri A, Maleki FH, et al. Effect of field of view on detection of condyle bone defects using cone beam computed tomography. *J Craniofac Surg*. 2016;27(3):644-648. [CrossRef]
29. Sayar G, Aydın, K. Evaluation of maxillary sinus pathologies with cone beam computed tomography. *Yeditepe J Dent*. 2018;14(2);7-12. [CrossRef]
30. Yalcin ED, Akyol S. Relationship between the posterior superior alveolar artery and maxillary sinus pathology: a cone-beam computed tomography study. *J Oral Maxillofac Surg*. 2019;77(12):2494-2502. [CrossRef]
31. Dogan ME, Uluısık N, Yuvarlakbaş SD. Author correction: retrospective analysis of pathological changes in the maxillary sinus with CBCT. *Sci Rep*. 2024;14(1):18236. [CrossRef]
32. Kawai T, Tanaka R, Yeung AWK, von Arx T, Bornstein MM. Frequency and type of incidentally detected radiodensities in the maxillary sinus: a retrospective analysis using cone beam computed tomography (CBCT). *Clin Oral Investig*. 2019;23(3):1091-1099. [CrossRef]
33. Clarot S, Christensen BJ, Chapple AG, Block MS. Prediction of residual alveolar bone height in the posterior maxilla after dental extractions. *J Oral Maxillofac Surg*. 2022;80(3):517-524. [CrossRef]
34. Prajapati S, Ninneman S, Zarrabi I, Daubert D, Wang IC, Hsu YT. Risk factors and longitudinal regenerative outcomes of sinus membrane perforation during lateral window sinus floor elevation: a retrospective analysis up to 9 years. *J Periodontol*. 2023;94(8):1045-1054. [CrossRef]
35. Testori T, Yu SH, Tavelli L, Wang HL. Perforation risk assessment in maxillary sinus augmentation with lateral wall technique. *Int J Periodontics Restorative Dent*. 2020;40(3):373-380. [CrossRef]
36. Lyu M, Xu D, Zhang X, Yuan Q. Maxillary sinus floor augmentation: a review of current evidence on anatomical factors and a decision tree. *Int J Oral Sci*. 2023;15(1):41. [CrossRef]
37. Hsu YT, Rosen PS, Choksi K, Shih MC, Ninneman S, Lee CT. Complications of sinus floor elevation procedure and management

strategies: a systematic review. *Clin Implant Dent Relat Res*. 2022;24(6):740-765. [CrossRef]

38. Zhang L, Zhou C, Jiang J, et al. Clinical outcomes and risk factor analysis of dental implants inserted with lateral maxillary sinus floor augmentation: a 3- to 8-year retrospective study. *J Clin Periodontol*. 2024;51(5):652-664. [CrossRef]
39. Nemati M, Khodaverdi N, Hosn Centenero SA, Tabrizi R. Which factors affect the risk of membrane perforation in lateral window maxillary sinus elevation? A prospective cohort study. *J Craniomaxillofac Surg*. 2023;51(7-8):427-432. [CrossRef]
40. Shenvi EC, Meeker D, Boxwala AA. Understanding data requirements of retrospective studies. *Int J Med Inform*. 2015;84:76-84(1). [CrossRef]
41. Gatti F, Gatti C, Tallarico M, Tommasato G, Meloni SM, Chiapasco M. Maxillary sinus membrane elevation using a special drilling system and hydraulic pressure: a 2-year prospective cohort Study. *Int J Periodontics Restorative Dent*. 2018;38(4):593-599. [CrossRef]

ABCResearch

Arch Basic Clin Res 2026;8(1):90-91
DOI: 10.4274/ABCR.2025.25393

Review

Pulmonary Ischemia-Reperfusion Injury

Funda Öz

Department of Thoracic Surgery, Erzincan Binali Yıldırım University, Erzincan, Türkiye

Cite this article as: Öz F. Pulmonary ischemia-reperfusion injury. *Arch Basic Clin Res*. 2026;8(1):90-91.

ORCID IDs of the authors: F.Ö. 0000-0002-1224-0226.

ABSTRACT

Pulmonary ischemia-reperfusion (I/R) injury is recognized as a key factor in the development of primary graft dysfunction and remains a major cause of perioperative morbidity and mortality in both lung transplantation and thoracic surgical procedures. This type of injury encompasses several pathological mechanisms, including oxidative stress, inflammation, and fibrosis. Literature indicates that I/R injury begins with tissue hypoxia, reperfusion-induced oxidative stress is closely linked to disruption of the endothelial barrier, contributing to early edema formation and impaired pulmonary compliance. Followed by the excessive generation of reactive oxygen species, and further progresses through an amplified inflammatory response. These observations highlight the essential role of antioxidants in both preventing and managing I/R injury across various tissues and organs.

Keywords: Antioxidant, pulmonary ıschemia, reperfusion

INTRODUCTION

Ischemia-reperfusion (I/R) injury refers to secondary organ and tissue damage that occurs following the restoration of blood flow (reperfusion) to ischemic tissue.[1] Ischemia, in contrast, refers to a state in which issue blood flow is partially diminished or entirely halted by various underlying factors, leading to an inadequate delivery of molecular oxygen (O^2) or a complete absence of oxygen within the affected tissues.[2] As is well known, I/R injury can occur in nearly all organs and tissues.[3] The sequence of ischemia followed by reperfusion can occur during numerous surgical interventions, such as lung transplantation.[4] Notably, pulmonary I/R injury is regarded as a leading factor in the development of primary graft dysfunction after lung transplantation and remains a significant contributor to perioperative morbidity and mortality in thoracic surgical practice.[5] It is well established that reperfusion causes more severe tissue damage than ischemia alone.[6] Matrix remodeling, angiogenesis, and fibrosis.[7]

Neutrophil-mediated inflammatory amplification further accelerates epithelial and microvascular injury, influencing postoperative respiratory outcomes. The primary mechanism underlying reperfusion injury is related to the reoxygenation that occurs during reperfusion. During this process, the xanthine oxidase accumulated throughout ischemia converts hypoxanthine to xanthine in the presence of an excessive supply of O^2, leading to the generation of abundant reactive oxygen species (ROS).[6,8] ROS, which act as key mediators during reperfusion, attack membrane lipids and promote the generation of harmful lipid peroxidation products, including aldehydes and malondialdehyde.[6] Among the most extensively studied ROS are the superoxide anion (O^2), hydroxyl radical, hydrogen peroxide, hypochlorous acid, and peroxynitrite, which is derived from nitric oxide.[2] In lung tissue, excessive ROS generation occurs both during ischemia and following reperfusion.[9] Endothelial cells and type II pneumocytes play a major role in the generation of ROS in the lungs. Moreover, the mechanisms of oxidative injury induced by ischemia and hypoxia in the lungs are known to differ from each other.[3] It has been proposed that oxidative stress during pulmonary ischemia can occur independently of adenosine triphosphate depletion.[3,10]

Another mechanism of I/R injury involves the increase in intracellular calcium levels during ischemia, which activates phospholipase A_2. This activation enhances the production of arachidonic acid from membrane phospholipids, leading to the activation of cyclooxygenase-2 (COX-2) and the subsequent release of proinflammatory prostaglandins and reactive oxygen

Corresponding author: Funda Öz, **E-mail:** ozfunda86@gmail.com

Received: November 19, 2025 **Accepted:** December 10, 2025 **Publication Date:** January 26, 2026
Revision Requested: December 4, 2025

species (ROS). Pharmacologic strategies, including antioxidant therapy and modulation of inflammatory signaling pathways, are increasingly being explored to mitigate pulmonary dysfunction.

As evidenced by the literature, I/R injury is a pathological condition initiated by a lack of oxygen in the tissue, progresses with the generation of ROS, and expands through inflammatory responses.[6] Therefore, the treatment of pulmonary I/R injury requires an integrated and multidisciplinary approach encompassing surgical, anesthetic, and pharmacological strategies.[5] It has been suggested that antioxidant therapy may be beneficial in preventing tissue damage caused by increased oxidant production. Protective ventilation approaches and controlled reperfusion techniques have demonstrated promise in reducing perioperative lung injury.

Antioxidants not only inhibit the formation of free radicals but also contribute to the recovery of tissues affected by oxidative damage, neutralize reactive intermediates, and promote the reduction of oxidized biomolecules.[11] Consequently, while oxidant parameters increase during I/R injury in various tissues and organs, antioxidant parameters tend to decrease. This indicates that antioxidants play a very important role in the prevention and treatment of tissue and organ I/R injury.

MAIN POINTS

- Pulmonary ischemia-reperfusion injury represents a major pathophysiological mechanism underlying primary graft dysfunction in lung transplantation and remains a critical determinant of perioperative clinical outcomes.
- Excessive generation of reactive oxygen species during reperfusion initiates a cascade of oxidative and inflammatory events, leading to structural and functional deterioration of pulmonary tissue.
- A coordinated approach integrating surgical refinement, anesthetic optimization, and targeted antioxidant strategies is essential for mitigating pulmonary ischemia-reperfusion-associated tissue injury.

Ethics

Informed Consent: N/A.

Footnotes

Declaration of Interests: The authors declare no conflict of interest regarding the publication of this paper.

Funding: The authors declare no financial support or funding.

REFERENCES

1. Robins M, Falkson SR, Goldfarb J, Wyatt HA. Hyperbaric treatment of ischemia reperfusion injury. 2024 Feb 12. In: StatPearls [Internet]. Treasure Island (FL): *StatPearls Publishing*; 2025. [CrossRef]
2. Süleyman H, Özçiçek A. Molecular mechanism of ischemia reperfusion injury. *Arch Basic Clin Res.* 2020; 2(1): 25-27. [CrossRef]
3. Kisaoglu A, Borekci B, Yapca OE, Bilen H, Suleyman H. Tissue damage and oxidant/antioxidant balance. *Eurasian J Med.* 2013;45(1):47-49. [CrossRef]
4. Chen-Yoshikawa TF. Ischemia-reperfusion injury in lung transplantation. *Cells*. 2021;10(6):1333. [CrossRef]
5. Berzenji L, Hendriks JMH, Verleden SE, et al. Lung ischemia-reperfusion injury in lung transplant surgery: where do we stand? *Antioxidants (Basel)*. 2025;14(11):1295. [CrossRef]
6. Yapca OE, Borekci B, Suleyman H. Ischemia-reperfusion damage. *Eurasian J Med.* 2013;45(2):126-127. [CrossRef]
7. Zhang M, Liu Q, Meng H, et al. Ischemia-reperfusion injury: molecular mechanisms and therapeutic targets. *Signal Transduct Target Ther*. 2024;9(1):12. [CrossRef]
8. Li C, Jackson RM. Reactive species mechanisms of cellular hypoxia-reoxygenation injury. *Am J Physiol Cell Physiol*. 2002;282(2):C227-C241. [CrossRef]
9. Kelly RF. Current strategies in lung preservation. *J Lab Clin Med*. 2000;136(6):427-440. [CrossRef]
10. Eckenhoff RG, Dodia C, Tan Z, Fisher AB. Oxygen-dependent reperfusion injury in the isolated rat lung. *J Appl Physiol (1985)*. 1992;72(4):1454-1460. [CrossRef]
11. Sorg O. Oxidative stress: a theoretical model or a biological reality? *C R Biol.* 2004;327(7):649-662. [CrossRef]